CHAPTER I

INTRODUCTION

Study of DNA and DNA Damage by Using NMR spectroscopy

Deoxyribonucleic acid (DNA) has been a very interesting and important compound for its unique biological function not only beginning at the time of its structural proposal by James D. Watson and Francis H. C. Crick in 1953, but from the origin of life on earth (Oliver, 1996; Watson and Crick, 1953). The three-dimensional structure of DNA bridged the gap between chemical and genetic information, in other words, chemistry and biology.

Chemically, DNA is a polyanion at neutral pH. It normally has two separate helical chains of nucleotides consisting of a phosphate, a sugar, and a base. The base comes from one of four bases: adenine [A], thymine [T], guanine [G], and cytosine [C]. The nucleotides assemble into the DNA double helix with hydrogen bonds via Watson-Crick base pairing: A to T and G to C (Figure 1-1 and 1-2). Generally, DNA is a molecule that has flexibility with structural deviations since the base can rotate about glycosidic bond to adopt different conformations: A, B, H and Z form DNA (Crawford et al., 1980; Nelson and Cox, 2000; Stryer, 1988). Hydrogen bonding plays an important role for stabilizing base pairs as Watson-Crick (Figure 1-2) or alternate mis-matched base pairs (Figure 1-3). Moreover, other factors in addition to hydrogen bonding influence the duplex stability, such as van der Waals interactions, hydrophobic effects, base-stacking interactions and charge-charge interactions.

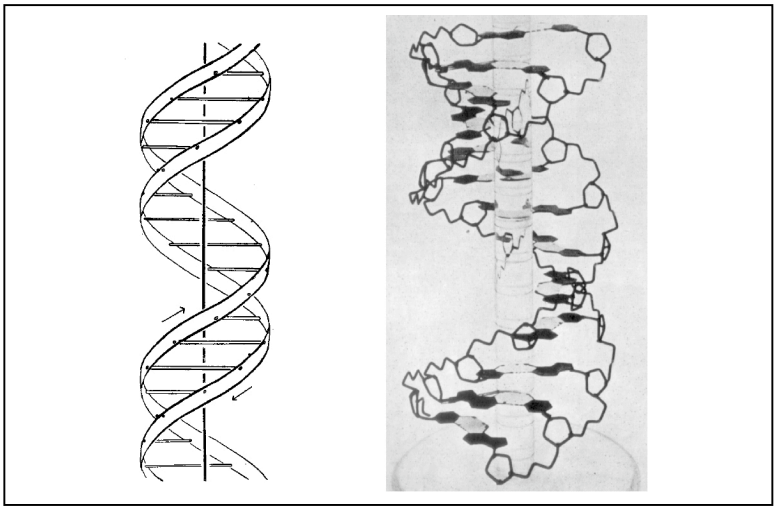

Figure 1-1. A diagrammatic figure and a 3-D model of deoxyribose nucleic acid.

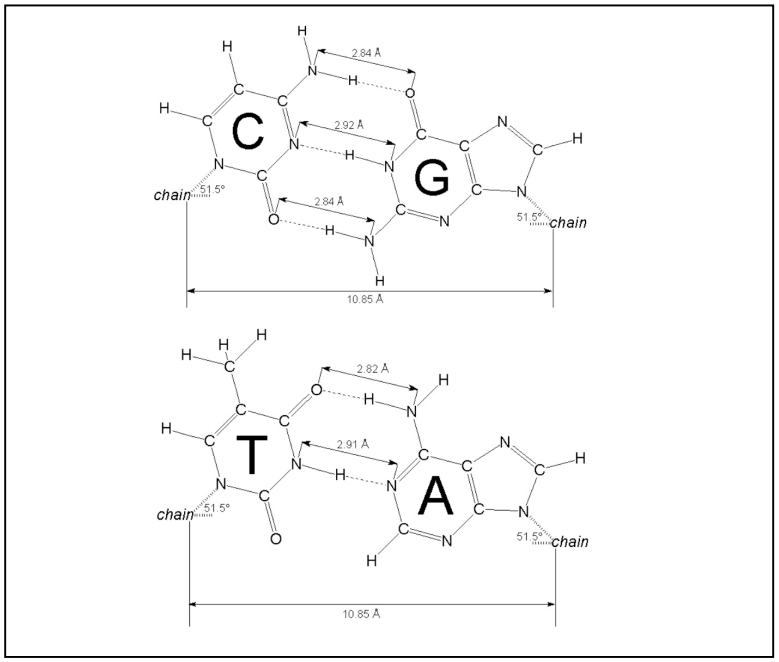

Figure 1-2. Watson- Crick base pairs maintained by Hydrogen bondings (dotted lines).

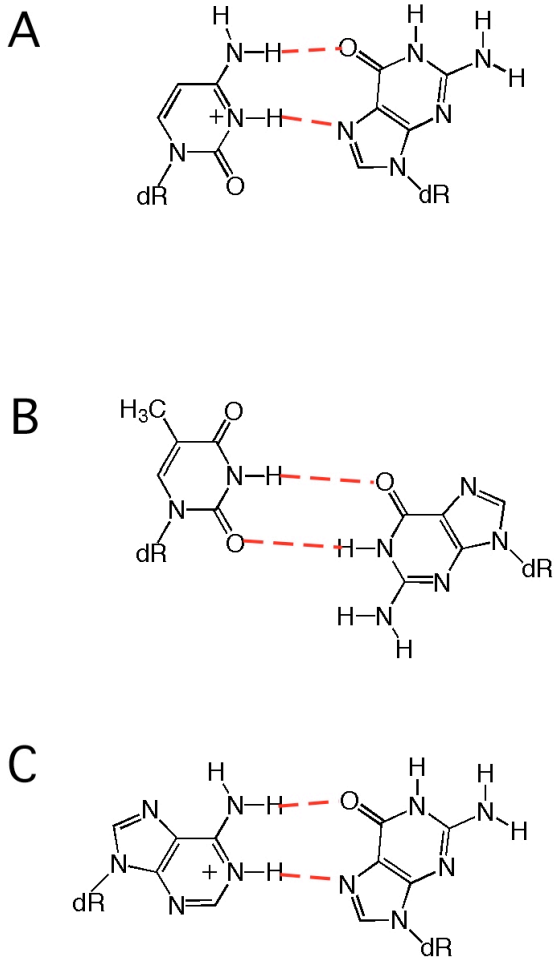

Figure 1-3. Examples of Mis-paired Bases: (A) G:C Hoogstein base pair; (B) G:T mismatch base pair; (C) G:A mismatch base pair.

Biologically, DNA serves as a storage unit for genetic material. DNA is transcribed into RNA, which is translated into a protein. The base sequence of a gene is related to the amino acid sequence of a polypeptide. Therefore, the scientific significance of DNA is of the highest importance as a biological information storage material. DNA is replicated by DNA polymerases. When a DNA polymerase misreads a base moiety, mutations can be happened. If errors occur during the replication, the DNA sequence can be changed. The changes of the gene lead to amino acid change in the protein based on the genetic code. Normally, the frequency of such errors is very low, but can be increased by DNA damage.

Damage to DNA can occur in the cell by radiation and chemicals. The modification of DNA can be affected by the sequence and the conformation of DNA. These alterations to DNA include mismatched base pairs, double-strand breaks, and chemically modified bases, such as the formation of covalent adducts with DNA bases.

It is known that DNA damage by many sources plays a major role in mutagenesis and carcinogenesis if not repaired (Scheme 1-1). The accumulation of mutations due to DNA damage-induced genomic instability is responsible for most cases of cancers. For instance, it has been suggested that exocyclic DNA adducts are involved in carcinogenesis, as they have been detected in target tissues of rodents treated with carcinogens (Chung, F. L. et al., 1996).

When DNA damage induces errors in polymerase replication, base substitution or frameshift mutation can occur (Foster et al., 1983; Refolo et al., 1987; Schnetz-Boutaud et al., ; Topal and Fresco, 1976). Base substitutions are the results of the insertion of an improper base. This leads to a change in the genetic

code as a whole. Frameshifts occur because of the addition or deletion of one or more bases, causing a series of misread codons. A high level of DNA damage without proper repair, results in detrimental effects on the cell via mutations (Nath, R.G. and Chung, 1994). Moreover, if one could decrease the level of DNA damage, a decline in cancer and other diseases might be expected (De Bont and van Larebeke, 2004).

Scheme 1-1. A schematic illustration of DNA damage induced cancer development (Kastan and Bartek, 2004).

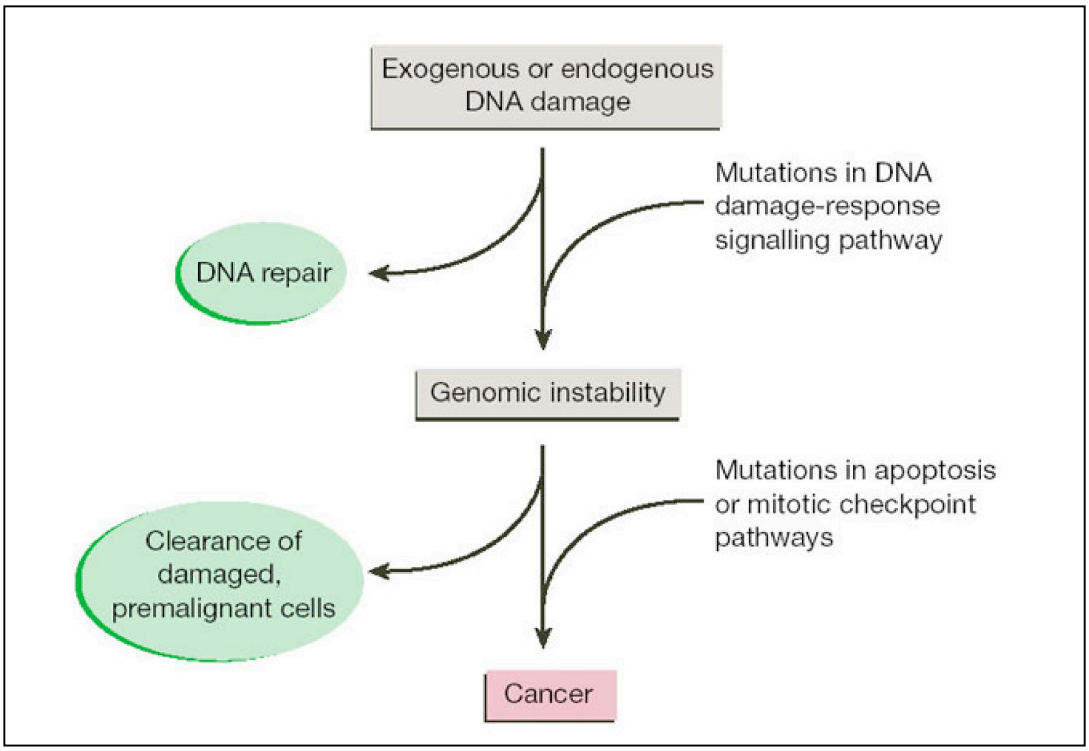

The structural information of DNA often has to be taken into account in connection with the functional consequences of DNA damage. Damage or structural alteration of DNA can block or slow down the replication process. It

has been a long range goal to correlate structural features with biochemical properties in the fields of mutagenesis and chemical carcinogenesis (Geacintov et al., 1997). For example, polycyclic aromatic hydrocarbons (PAH) diol epoxide-DNA adducts have been suggested to exhibit different mutagenic and tumorigenic activities based on their stereochemistry and conformations (Geacintov et al., 1997). The significance of DNA adduct lesion-induced mutagenesis during DNA replication has been recognized in connection with the stability of mismatches as possible intermediates (Lukin and de Los Santos, 2006).

The structural study of site-specific DNA adducts in oligodeoxynucleotides can provide insight at the molecular level of understanding in the genetic world, even if the structural information may be not fully explain the biological aspects of the DNA damage. To explain the structural attributions of DNA damage to the mutagenicity, structural studies at the atomic level are required. To do that, two techniques are being widely used: X-ray crystallography and NMR spectroscopy.

X-ray crystallography has a longer history in science. It is well know that the first structure of DNA was determined from X-ray diffraction data. X-ray crystallography has no molecular size limitations, and once a crystal is obtained the structural information of the molecule can be rapidly interpreted. It is a common and popular method for structural study. NMR spectroscopy is a powerful tool for studying the structure of oligonucleotides as well as other biomacromolecules. While X-ray crystallography always depends on the ability of a certain sequence of DNA to be crystallized, this is not necessary for NMR. NMR is also advantageous because the sample can be studied in solution at

physiological conditions, which cannot be done in X-ray technique. In many cases, NMR has been used as a main tool for acquiring the structural information on DNA and DNA damage. However, X-ray can provide useful information on systmes such as DNA replication in combination with polymerases, which may be beyond the scope of NMR due to the size limitation.

As of October 11, 2005, the number of X-ray generated structures was higher than that of NMR generated macromolecules. NMR is competitive, however, in the study of nucleic acids: 663 nucleic acids were deposited in the Protein Data Bank by NMR techniques in comparison to 843 by X-ray crystallography, of which many are the Dickerson dodecamer and other specific sequences that readily crystallize (Table 1-1). Another featured advantage of studying nucleic acids by NMR is that there is no sequence limitation like that in X-ray crystallography. A detailed NMR-based strategy for the study of DNA adducts is described later in this chapter.

Table 1-1. The number of structures solved by X-ray and NMR techniques, which are deposited in Protein Data Bank as of Oct 11, 2005.

		Molecule Type				
		Proteins, Peptides, and Viruses	Protein/Nucleic Acid Complexes	Nucleic Acids	Carbohydrates	Total
Exp. Tech.	X-ray Diffraction and other	26172	1236	843	11	28262
	NMR	4021	117	663	2	4803
	Total	30193	1353	1506	13	33065

Many endogenous sources can cause DNA damage by electrophilic attack, resulting in structural alterations. Several hundred DNA damages per cell per

day are generated by those endogenous agents (Lindahl, 2000). One of the salient electrophiles is the α,β-unsaturated aldehyde family. These compounds are product of both exogenous and endogenous sources, ranging from polluted materials (Izard et al., 1980; Treitman et al., 1980) to lipid peroxidation (Chung, F. L. et al., 1999; Marnett, L. J., 1999; Nath, R. G. and Chung, 1994). Scheme 1-2 illustrates the lipid peroxidation pathways from the oxidation of polyunsaturated fatty acid to the decomposition of endoperoxide into malondialdehyde, which exists mainly as β-hydroxyacrolein, one of the common α,β-unsaturated aldehydes. Some of the α,β-unsaturated aldehyde family are shown in Figure 1-4. In most cases, altered DNA bases in the form of exocyclic base adducts are reported as the major DNA damage from this family (Chung, F. L. et al., 1996; Nath, R. G. et al., 1994; Nath, R. G. and Chung, 1994; Smith, R. A. et al., 1990). While the α,β-unsaturated aldehydes can react with cytosine or adenine, the majority of DNA adducts come from the reaction with guanine to form exocyclic propano deoxyguanosine due to guanine's high nucleophilicity (Marnett, L. J. , 2000; Marnett, L. J. et al., 2003). The mechanism of the 1,N^2-propanodeoxyguanosine adduct via Michael addition followed by ring closure is shown in Figure 1-5.

Scheme 1-2. Lipid Peroxidation pathways (modified from (Marnett, L. J. , 1999))

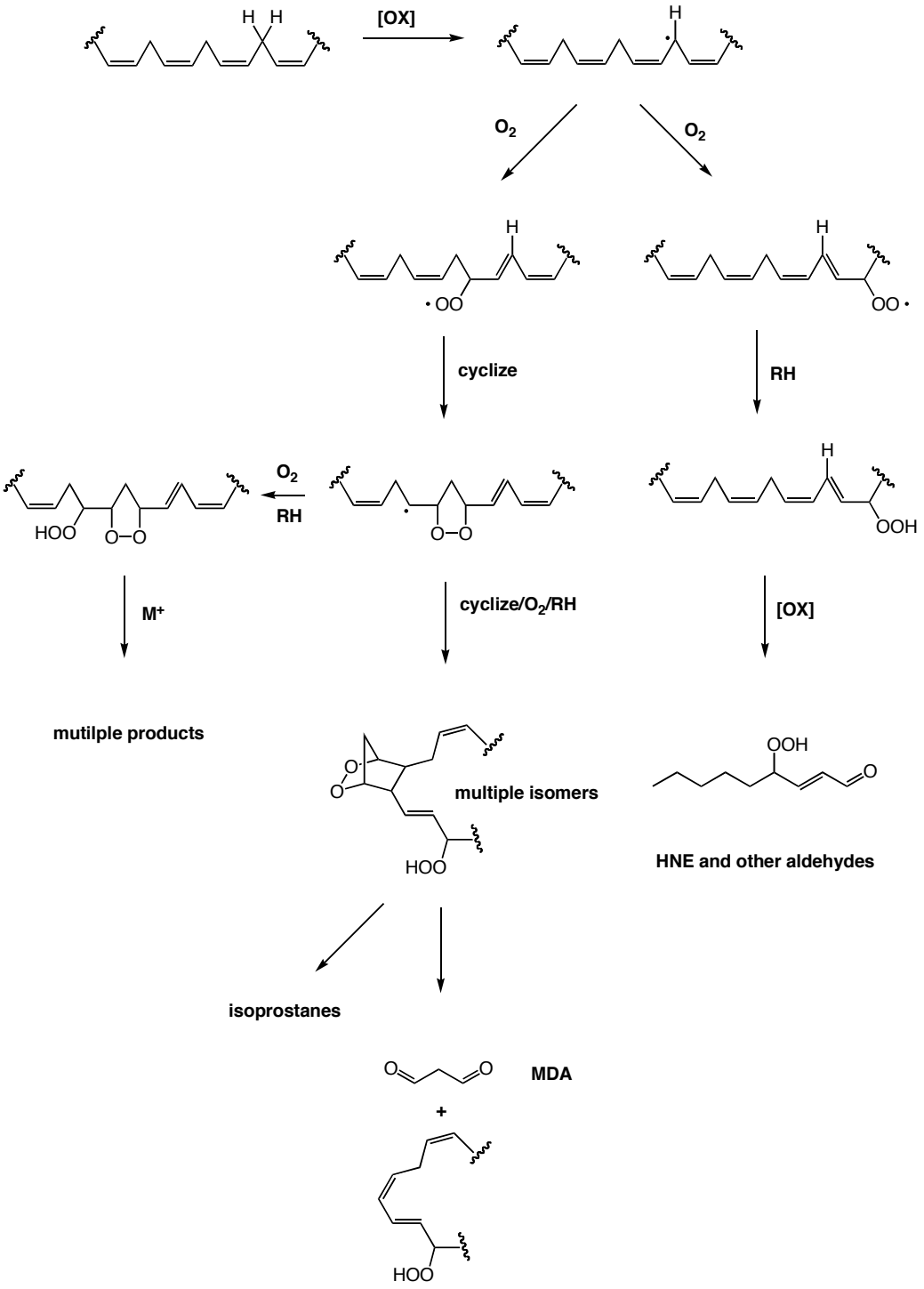

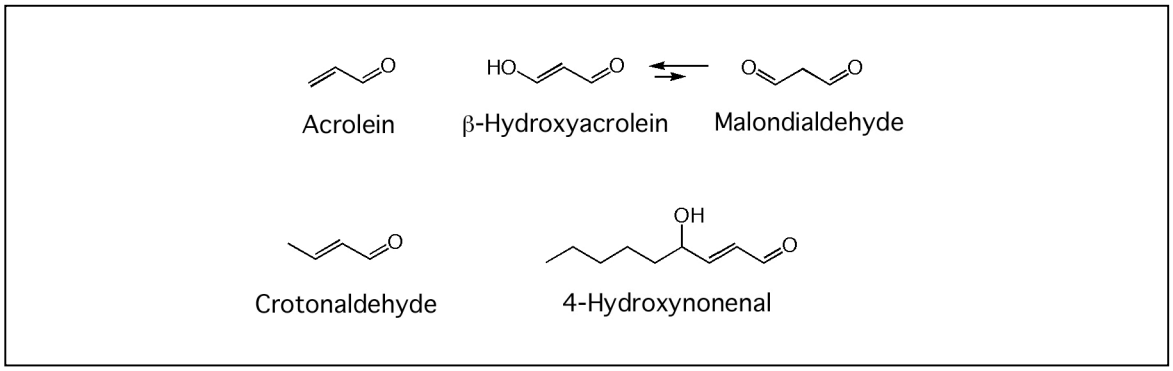

Figure 1-4. Some α,β-unsaturated aldehydes.

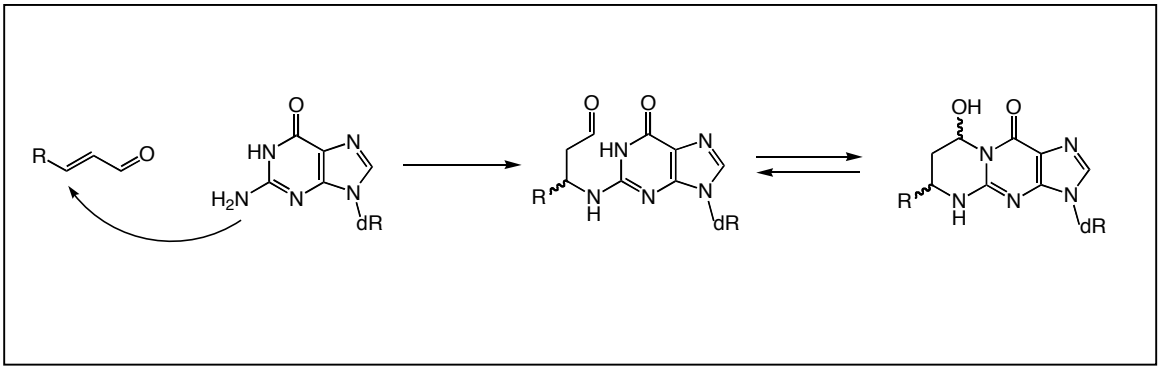

Figure 1-5. Formation of exocyclic propano-dG adduct by the reaction between α,β-unsaturated aldehyde and deoxyguanosine via Michael addition.

DNA Adducts of acrolein and crotonaldehyde

The family of α,β-unsaturated aldehydes is one of the main sources of exocyclic propano adducts that have relatively high prevalence in human DNA via exogenous and endogenous pathways such as from lipid peroxidation and tobacco smoking (Chung, F. L. and Hecht, 1983; Chung, F. L. et al., 1999; Chung, F. L. et al., 1984; Nath, R.G. and Chung, 1994; Treitman et al., 1980). They can react with DNA and covalently bind to it to form adducts that induce DNA mutations (Cajelli et al., 1987; Fernandes et al., 2005; Kanuri et al., 2002). An exocyclic propano adduct was thought to be responsible for the instability of duplex DNA due to its ability to block the normal Watson-Crick hydrogen bonding.

Figure 1-6 presents the two major acrolein-derived deoxyguanosine adducts via Michael addition to the N1 and N^2 positions of dG, followed by ring closure, which are distinguished by the location of the hydroxyl group. These adducts were detected in liver DNA from humans and rodents by ^{32}P-postlabeling methods using HPLC chromatography without carcinogen treatments (Chung, F. L. et al., 1999; Nath, R. G. et al., 1994; Nath, R. G. et al., 1996).

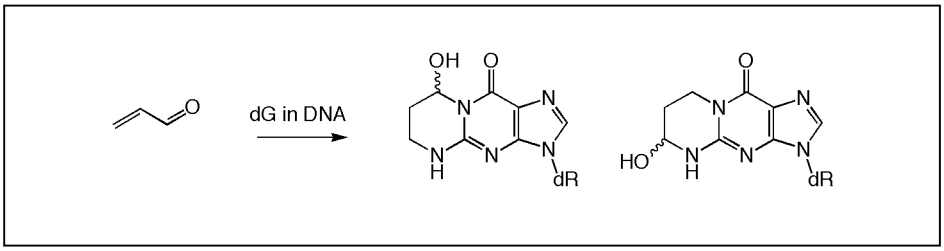

Figure 1-6. Major acrolein-derived dG adducts: γ-OH-PdG (left); α-OH-PdG (right)

Before a site-specifically synthesized DNA adduct was available (Khullar et al., 1999; Nechev et al., 2000), the stable 1,N^2-propanodeoxyguanosine (PdG) exocyclic adduct, in which the hydroxyl group had been removed, was used as a model of ring-closed exocyclic propano dG adducts like the malondialdehyde-derived PdG adduct (M_1dG) and acrolein-derived PdG adducts (OH-PdG)for mutagenic and structural studies (Benamira et al., 1992; Chung, F. L. et al., 1999; Moriya, M. et al., 1994). The PdG adduct induced G to T and G to A mutations as well as frame-shift mutations (Benamira et al., 1992; Burcham and Marnett, 1994; Moriya, M. et al., 1994).

From various structural studies, the PdG adduct was discovered to exist in a syn glycosidic bond conformation while forming a Hoogstein base pair opposite dC and dA at acidic conditions, and dG at physiological conditions (Figure 1-7) (Kouchakdjian et al., 1990; Weisenseel, J. P., Reddy, G.R., Marnett, L.J., & Stone, M.P., 2002; Weisenseel, J. P. et al., 1995).

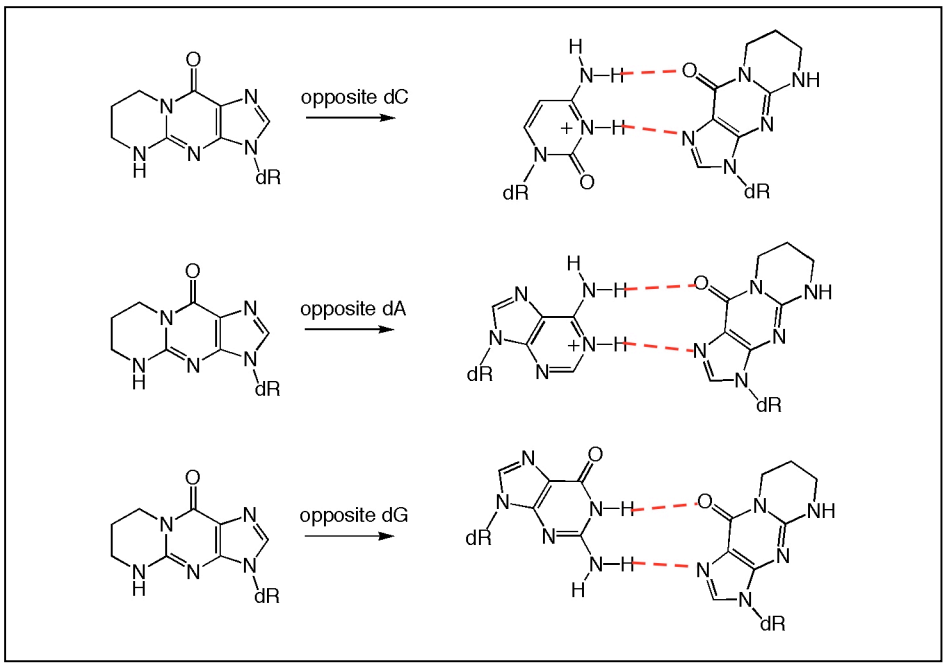

Figure 1-7. Base pairing of PdG adduct with different opposite bases with syn (PdG)•anti (base) Hoogstein base pairing: (Top) PdG:dC; (middle) PdG:dA in an acidic condition; (bottom) PdG:dG in a physiological condition.

Without further ring-opening, PdG adduct is still regarded as the best model for such ring closed exocyclic propano adducts. Furthermore, as a ring-closed adduct, PdG inhibiys replication and is therefore believed to be a strong block to the polymerase activity. As a ring-closed model of the M_1dG adduct, the PdG adduct is in a syn conformation, disrupting normal Watson-Crick hydrogen bonding and placing the exocyclic ring toward the major groove. In addition, the PdG adduct showed a high frequency of mutagenicity (Benamira et al., 1992; Velez-Cruz et al., 2005; Wolfle et al., 2005). The only discrepancy between the PdG and the M_1dG adducts comes from the fact that the latter can open the ring in a duplex environment placed specifically opposite dC (Figure 1-8). Recent progress has enabled M_1dG to be tested in a site-specifically synthesized DNA

sample. This sample showed frameshift mutations in bacteria and mammalian cells when positioned in a reiterated $(CpG)_4$ sequence but not in *Escherichia coli* and in COS-7 cells in a nonreiterated sequence with 2% frequency base substitutions (M_1dG to T and M_1dG to A) (VanderVeen, L. A. et al., 2003).

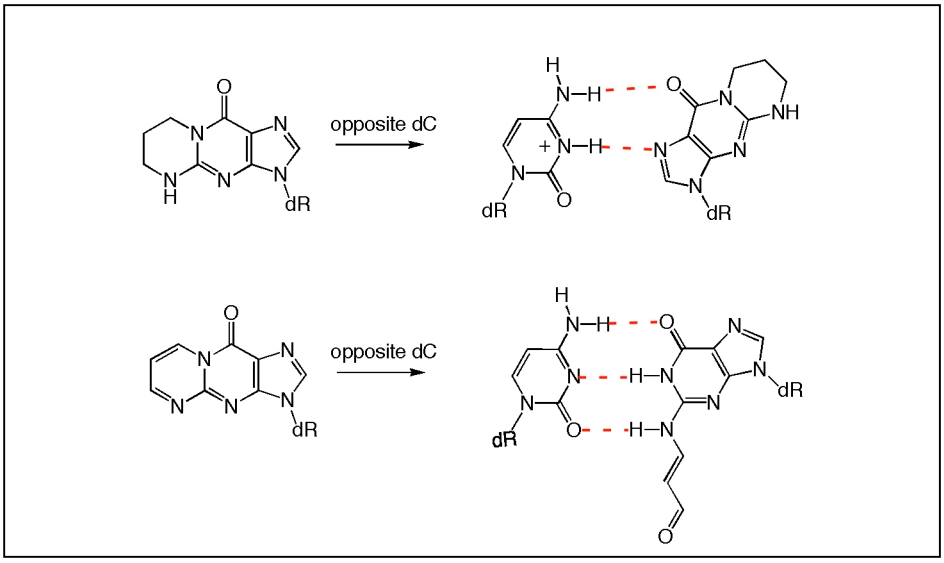

Figure 1-8. Different mechanisms between PdG and M_1dG adduct in duplex DNA by ring-opening process. PdG adduct with opposite dC in Hoogstein base pairing (top); M_1dG adduct with opposite dC conserves normal Watson-Crick pairing (bottom).

Acrolein, a mutagen and carcinogen (Chung, F. L. et al., 1999), is mutagenic in bacterial (Marnett, L.J. et al., 1985), mammalian (Smith, R. A. et al., 1990), and human (Curren et al., 1988; Kawanishi, M. et al., 1998) cells and carcinogenic in rats (Cohen et al., 1992 Jul 1). Crotonaldehyde is genotoxic and mutagenic in human lymphoblasts (Czerny et al., 1998) and fibroblast cells (Kawanishi, M. et al., 1998). It induces liver tumors in rodents (Chung, F. L. et al., 1986). The major adduct from both acrolein and crotonaldehyde was determined as the ring-closed exocyclic adduct via Michael type addition with

dG (Figure 1-6 and 1-9) (Chung, F. L. and Hecht, 1983; Chung, F. L. et al., 1984; Chung, F. L. et al., 1999; Eder et al., 1999). By treating the shuttle vector plasmids in human cells with acrolein or crotonaldehyde, they showed that the mutagenic spectrum consisted of base substitutions (G→T and G→A), deletion and insertion, and tandem substitution (Kawanishi, M. et al., 1998; Kawanishi, M. et al., 1998).

The acrolein adduct, based on the location of hydroxyl group, can be divided into 2 major adducts: α- and γ-OH-PdG adducts (Figure 1-6). The 3-(2-deoxy-β-D-erythro-pento-furanosyl)-5,6,7,8-tetrahydro-8-hydroxypyrimido[1,2-a]purin-10(3*H*)-one, γ-OH-PdG adduct, was detected in animal and human tissue (Chung, F. L. et al., 1999), suggesting its involvement in mutagenesis and carcinogenesis (Nath, R.G. and Chung, 1994). For the crotonaldehyde adduct, based on the stereochemistry of the methyl group on C_{α}, diasteromeric *R*- and *S*-α-methyl-γ-OH PdG adducts exist in a trans relationship between the methyl and hydroxyl groups (Figure 1-9) (Nath, R.G. and Chung, 1994; Nechev et al., 2001). These *R*- and *S*-α-CH_3-γ-OH-1,N^2-propano-2′-deoxyguanosine adducts are also formed through the reaction of acetaldehdye, a mutagen and potential human carcinogen (IARC, 1999), and the main metabolite from alcohol consumption, with deoxyguanosine (Lao and Hecht, 2005; Wang et al., 2000). Therefore, the importance of the crotonaldehyde-derived adduct, CPdG, has been increased due to the fact that diverse forms can be mutagenic and it can be formed easily with the help of other cellular components such as histones, the basic amino acids arginine or lysine, or polyamines at physiological conditions (Sako et al., 2003; Sako et al., 2002; Theruvathu et al., 2005). Figure 1-10 introduces the

possible mechanism of crotonaldehyde formation from acetaldehyde via the aldol condensation reaction (Theruvathu et al., 2005). The *R*- and *S*-CPdG adducts were detected in human and rodent tissues (Budiawan and Eder, 2000; Chung, F. L. et al., 1999). In humans, these probably result from various endogenous and exogenous exposures, including lipid peroxidation (Chung, F. L. et al., 1999; Nath, R. G. and Chung, 1994; Nath, R. G. et al., 1996), exposure to tobacco smoke (Izard et al., 1980; Treitman et al., 1980), and exposure to N-nitrosopyrrolidine (Chung, F. L. and Hecht, 1983; Hecht et al., 1999). Likewise for the M_1dG adduct, the question remained as to whether or not the ring can be triggered to open by the presence of an opposite dC in duplex DNA.

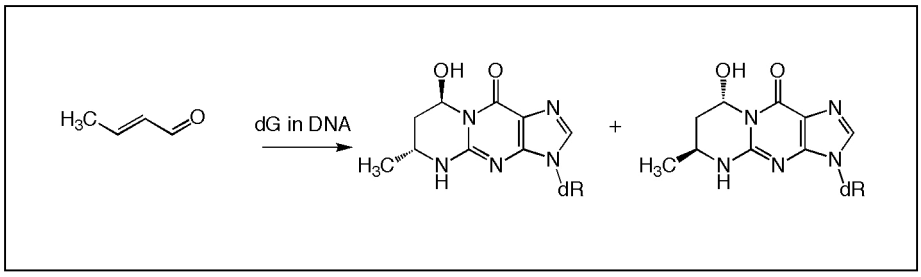

Figure 1-9. Major crotonaldehyde-derived dG adducts: *R*-α-CH_3-γ-OH-PdG (left); *S*-α-CH_3-γ-OH-PdG (right)

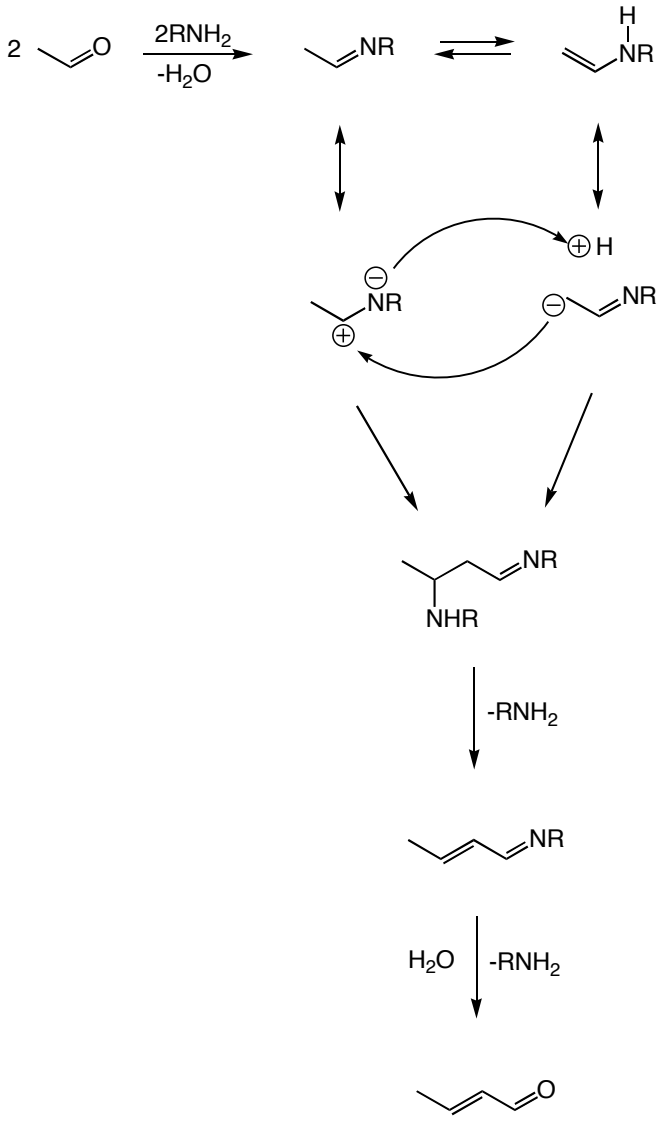

Figure 1-10. Proposed mechanism of the formation of crotonaldehyde via aldol type condensation reaction of acetaldehyde (modified from (Theruvathu et al., 2005)).

Although it has been known that these compounds are mutagenic, the relationship between their structures and toxicity has remained elusive. Recently, the ring-opening mechanism of the acrolein adduct (γ-OH-PdG) was reported by NMR studies (de los Santos, C. et al., 2001) to be similar to that of the M_1dG adduct (Mao, H. et al., 1999). In both cases, the ring opening process was considered as one of the main reasons for low mutagenicity, as it keeps the integrity of duplex DNA by keeping the Watson-Crick hydrogen bonds. De los Santos *et al.* concluded that the hydrated aldehyde is a ring-opened major species that is in equilibrium with a minor aldehyde species. The possibility of the ring-opened species was postulated to be responsible for less mutagenicity due to the fact that there was a conservation of Watson-Crick hydrogen bonding compared to the ring-closed species like the PdG adduct, which is deprived of normal Watson-Crick hydrogen bonding and that shows high mutagenicity (Benamira et al., 1992; Hashim and Marnett, 1996; Yang, I. Y. et al., 2002). The PdG adduct was also shown to inhibit the human Y family polymerases' extension activity (Wolfle et al., 2005) .

It was also hypothesized that the reactive aldehyde species of the M_1G adduct leads to actual mutagenic lesion by stabilizing a slipped mispairing intermediate of frameshift mutagenesis (VanderVeen, L. A. et al., 2003). In addition, the cross-linked form was submitted as a feasible adducted form by the γ-OH-PdG adduct but not by α-OH-PdG adduct incapable of opening the ring. Chemical trapping experiments provided evidence for the formation of interstrand cross-links and suggested that the generation of a cross-link was sequence dependent: where the 5′-CpG-3′ but not the 5′-GpC-3′ sequences were

capable of forming interstrand cross-links (Kozekov et al., 2003). Because of the fact that all other species such as aldehydes, hydrated aldehydes, and cross-links exist in equilibrium, monitoring the composition of the equilibrium mixtures *in situ* is of considerable interest. Indeed, NMR spectroscopy enabled the chemistry of these adducts to be monitored in DNA, *in situ*. In light of the interchain cross-linking study by Kim et al., the existence of carbinolamine cross-links was detected by ^{15}N HSQC, NOESY-HSQC, and TOCSY-HSQC experiments (Kim, H. Y. et al., 2002).

Many carcinogens and drugs such as cisplatin, mitomycin C, and psoralen can generate DNA interstrand cross-links. Those cross-links are thought to induce recombination by inhibiting replication and are reported to cause futile repair synthesis in mammalian cell (Mu et al., 2000). Therefore the biological significance of these DNA interstrand cross-links has been increased as well as DNA-polypetide and DNA-protein cross-links. Acrolein is a known mutagenic compound, and can derive γ-OH-PdG adduct that can form an interstrand cross-link. Understanding the chemistry of both acrolein and crotonaldehyde-derived dG adducts may provide much insight, ultimately, into DNA mutagenesis and repair processes. Furthermore there has been a controversy about the major cross-link forms based upon the data from chemical trapping and mass spectrometery experiments showing that other possible forms could be detected. As is considered in the chemistry of this adduct, the carbinolamine cross-link should exist in equilibrium with the imine and, possibly, the pyrimidopurinone cross-links as shown in Scheme 1-3.

Scheme 1-3. Equilibrium Chemistry of the γ-OH-PdG Adduct in the 5'-CpG-3' Sequence Context in Duplex DNA. γ-OH-PdG(2) undergoes ring-opening to form aldehyde(3) and hydrated diol aldehyde (4), and aldehyde(3) can react with opposite dG to form interstrand cross-link carbinolamine(4), imine(5) and pyrimidopurinone(6) in equilibrium.

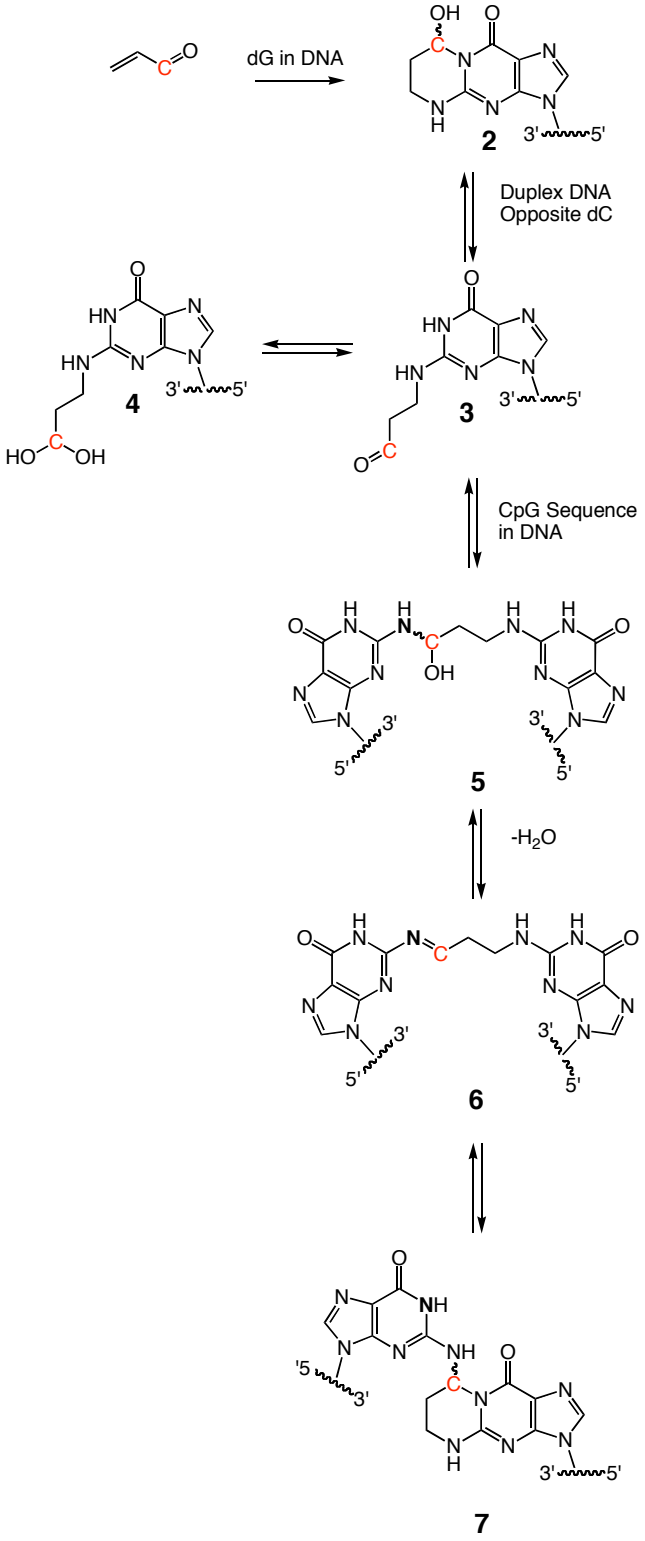

Crotonaldehyde has an extra methyl group in comparison to acrolein, and is genotoxic and mutagenic in human lymphoblasts (Czerny et al., 1998). Depending on the stereochemistry of the methyl group, it forms a pair of ring-closed propano diasteromers via Michael type addition: *R*- and *S*-α-CH_3-γ-OH-1, N^2-propano-2'-deoxyguanosine adducts (*R*-CPdG and *S*-CPdG) (Figure 1-9). Both *R*-CPdG and *S*-CPdG were detected in human and rodent tissues (Budiawan and Eder, 2000; Chung, F. L. et al., 1999). Like the acrolein adduct, they were assumed to undergo the ring-opening process with the presence of an opposite dC in duplex DNA. In the 5'-CpXpA-3' sequence context (X= *R*-CPdG and *S*-CPdG), the ring of the exocyclic adducts was believed to be open and thus to form N^2-(3-oxopropyl)-dG aldehydes in the minor groove facilitating DNA interstrand cross-linking (Scheme 1-4). The formation of the cross-link resulted in enantioselective generation, where the *R*- stereoisomer cross-links but the *S*- does not. The formation of cross-links of the *R*-CPdG adduct was kinetically slower and occurred less than that of the acrolein adduct (Kozekov et al., 2003).

The chemical trapping method was utilized to identify the cross-links by $NaCNBH_3$ reduction. It indicated the presence of saturated three-carbon interstrand N^2,N^2-dG linkages. Moreover, the γ-OH-PdG adduct formed cross-links with the N-terminal amine of the small peptide KWKK (Kurtz and Lloyd, 2003). In general, the imine was observable by NMR spectroscopy in organic solution but not in *in vitro* metabolic experiments due to the rapid decomposition of the carbinolamine to a primary amine and acetone (Shetty and Nelson, 1985). The relatively stable imine metabolites of trifluoromethyl-substitued propranolol analogs were investigated by ^{19}F NMR and mass spectrometry (Upthagrove and

Nelson, 2001). The Schiff base is one of the important intermediates in biochemical processes and its biological function and significance has been reported (Dickopf et al., 1995; Erskine et al., 1999; Longstaff and Rando, 1987; Sonar et al., 1994; Williams and David, 1998). Therefore, it was not anticipated that the spectroscopically stable carbinolamine cross-link species from α,β-unsaturated aldehyde-derived-dG adducts in duplex DNA would be detected. NMR studies indicated that the carbinolamine cross-link is a major interstrand cross-link whereas the imine was below the level of detection (Cho, Y. J. et al., 2005; Kim, H. Y. et al., 2002). However, the chemistry of both acrolein and crotonaldehdye-derived dG adducts still suggested that three kinds of cross-links are possible: carbinolamine, imine and pyrimidopurinone (Scheme 1-3 & 1-4).

Even though the ^{15}N related NMR data provided evidence for a significant amount of carbinolamine cross-links, questions remained as to why other species do not exist or exist in such small amounts in comparison to the amount of carbinolamine species. To answer this issue, various types of experiments had been tried for crotonaldehyde-derived dG adducts. Like the acroelin adduct study, an enzyme digestion study supported the existence of the pyrimidopurinone type cross-link. In a mass spectrometry study, all three species were shown, but the imine or the pyrimidorpurinone type cross-links were proposed to be more favorable than the carbinolamine cross-link. The chemical reduction study supported the chain linked cross-link such as imine and possibly carbinolamine. However, it was hard to distinguish between those species.

Heteronuclear NMR experiments for the γ-OH-PdG adduct clearly supported the presence of the carbinolamine cross-link. The possible answer for this controversial issue may depend on the condition of the sample in each experiment. For example, enzyme digestion and mass spectrometer forces cause the disruption of DNA, thus if the duplex environment and conformation is one of the chief factors for supporting the carbinolamine cross-link, it might be a reasonable explanation for the discrepancy of experimental data. Because NMR is a non-invasive tool, it was used as the main tool for achieving structural information *in situ*.

To better understand and define the major cross-link, it was essential to acquire a separated and conformationally pure sample. The physical separation trials for cross-link by HPLC were not sufficient to obtain stable cross-links and to carry out structural study. An advantage of using NMR is that we can use specifically labeled samples to carry out various heteronuclear NMR experiments to abstract structural information. The site-specifically labeled samples (^{13}C on C_γ and ^{15}N on N^2-dG) were provided by the labs of Drs. Harris and Rizzo, which enabled various heteronuclear NMR experiments to be carried out.

As a cross-linked species was unable to be separated for use as a model of interstrand carbinolamine cross-link in the 5′-CpG-3′ sequence, the fully reduced cross-link could be used alternatively for structural analyses. Due to the absence of a hydroxyl group at C_γ, while it keeps the sp^3 carbon conformation the same as that of the carbinolamine cross-link, it could be a good model for solving structural questions about carbinolamine type cross-links in duplex DNA. Previously, this kind of reduced cross-link was recognized as a model of an

imine type cross-link. However, maintaining the sp^3 conformation is more like the carbinolamine cross-link than the Schiff base type cross-link, which possesses the sp^2 conformation on the gamma carbon at physiological conditions.

Scheme 1-4. Equilibrium Chemistry of the *R*- and *S*-α-CH_3-γ-OH-PdG Adducts in the 5'-CpG-3' Sequence in Duplex DNA.

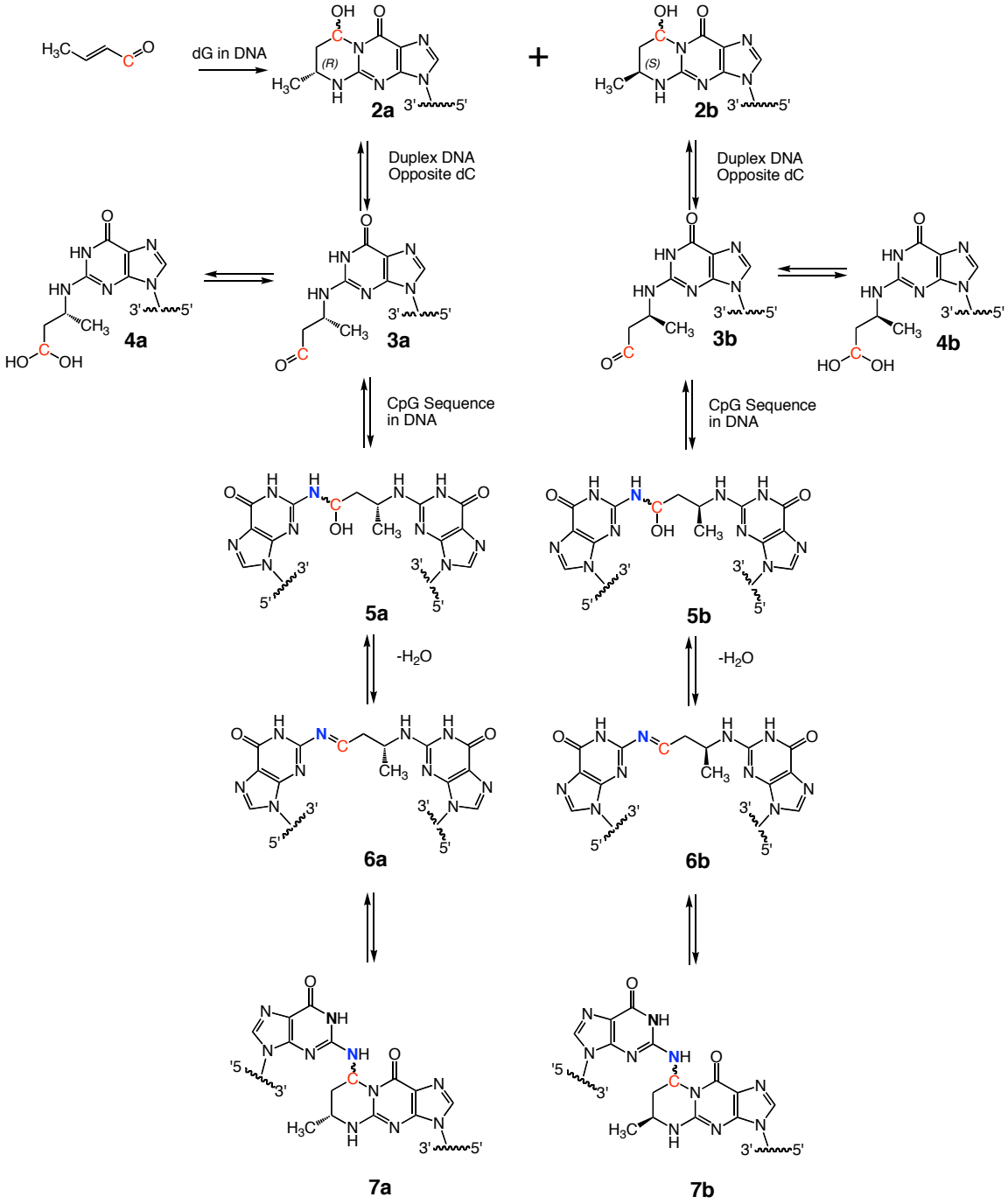

Synthesis of Modified Oligodeoxynucleotides

Synthesis of oligodeoxynucleotides containing site-specific ^{13}C in both acrolein and crotonaldehyde, and ^{15}N-deoxyguanosine are described in detail in Chapter II. The synthesis of the fully reduced cross-linked duplex is shown in Scheme 1-5. The fully reduced crotonaldehyde cross-links were used for the structural study as a real model of a carbinolamine type cross-link. Instead of an aldehydic moiety, the cross-linking reaction was forced by the reduction of the aldehyde into an amino group, which was annealed with a complementary sequence containing 2-fluoro-O^6-[(trimethylsilyl)ethyl]-2′-deoxyinosine at the G^{19} position site specifically at 45 °C. While the reaction was carried out, the methyl stereochemistry was conserved. Both fully reduced *R*- and *S*-crotonaldehyde cross-linked duplexes were provided by the labs of Drs. Harris and Rizzo and were utilized for further NMR analysis. Chapter VI and VII are concerned with NMR elucidation of the fully reduced *R*- and *S*-crotonaldehyde-derived cross-linked duplex, respectively.

Scheme 1-5. Synthetic scheme of the fully reduced *R*-crotonaldehyde cross-link.

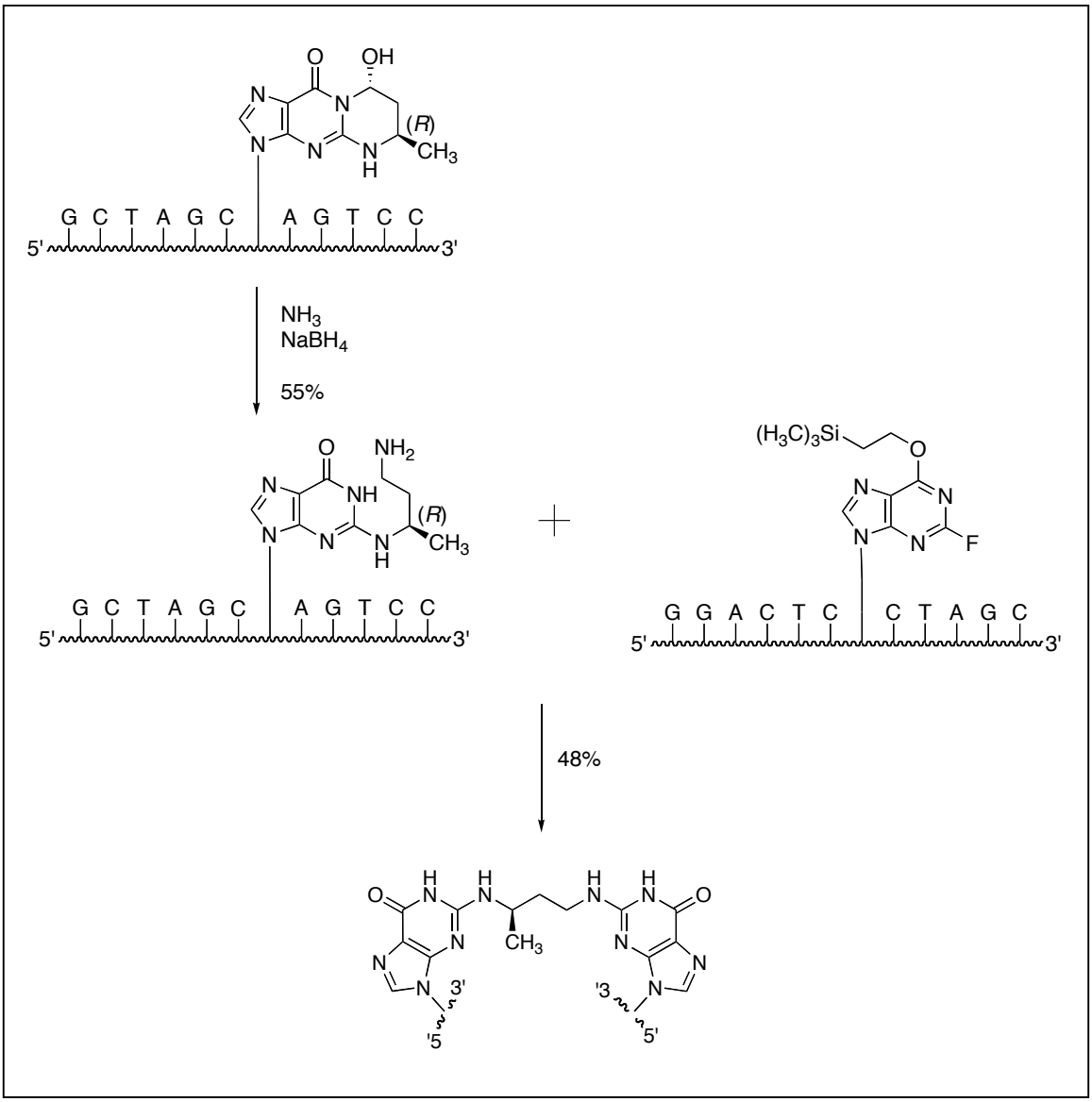

Structural Studies of Oigonucleotides by NMR Spectroscopy

Nuclear magnetic resonance spectroscopy is a powerful tool that can be used to acquire the solution structures of DNA and protein. In the following section, a brief description of the general methods of multi-dimensional and heteronuclear NMR techniques for the structural analysis of oligonucleotides

containing site-specific labeled adduct is discussed. More complicated NMR techniques share the same fundamental NMR theory.

Two dimensional Nuclear Overhauser Effect Spectroscopy (NOESY) spectra provide essential data on the distance information between protons. Theoretically, within about 5 Å, pairs of protons will display an NOE cross-peak proportional to $1/r^6$ where r is the interproton distance. The intensity volume of the cross-peak can be used for the estimation of the interproton distance. For collecting NOESY data, a D_2O environment is preferred for providing better digital resolution by using a narrow sweep width (SW). A deuterated water environment also offers simplicity by exchanging imino and amino protons for deuterium. As distance restraints are the main restraints for NMR derived structural determination, it is important to acquire a high quality and well processed NOESY spectrum.

In the case of oligodeoxynucleotides, there are typically characteristic fingerprint regions of the proton chemical shifts that are easily identified, which are arose due to the non-covalent environment such as base aromatic, anomeric and sugar protons. Those specific proton regions are presented in Figure 1-11. Among them is the NOESY walk region, which allows for assignments to be made based upon the stable base sequences. The rationale for the NOESY walk is illustrated in Figure 1-12. The complete NOESY walk can be achieved via base protons (H8/H6) to anomeric protons (H1′), H2′/H2″, or H3′ protons. In this way, one can expand the assignments to the rest of the proton resonances except the imino and amino peaks, which are observable in a NOESY in water environment.

The 2D NOESY in water can provide significant information on base stacking and pairing. If all bases are stacked well as a stable duplex, one can also make a complete NOESY walk in the imino proton region that represents the connectivity between the imino protons of dG's and T's. In addition, the amino protons of dC couple to the imino proton of dG and the H2 proton of dA forms a strong cross-peak with imino proton of dT. All information can be useful by yielding more empirical restraints for the refinement process.

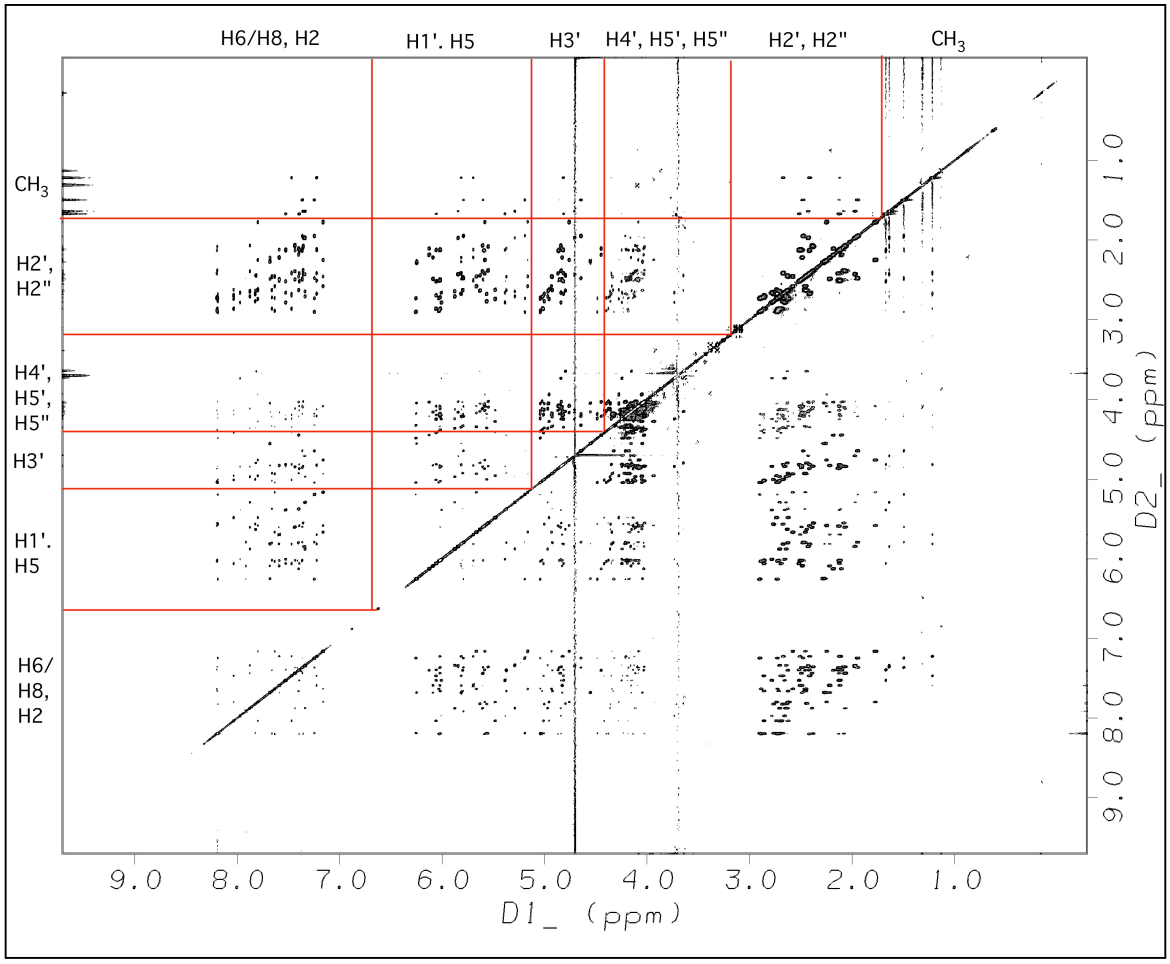

Figure 1-11. A typical 2D NOESY spectrum of a 12-mer oligonucleotide, 5'-(GCTAGCGAGTCC)-3'•5'-(GGACTCGCTAGC)-3'.

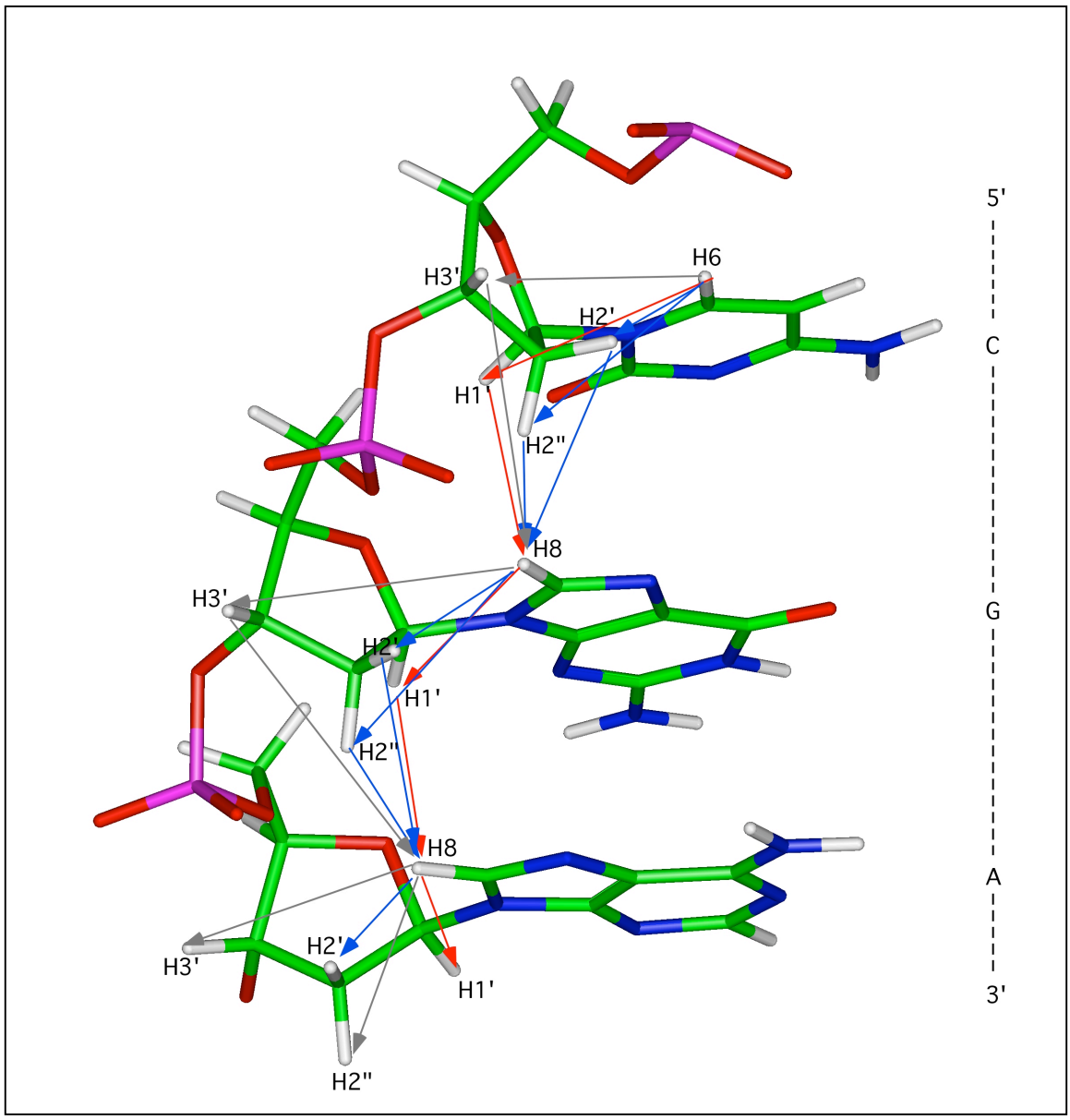

Figure 1-12. Sequential assignment pattern of an oligodeoxynucleotide by NOESY spectroscopy. NOESY walk can be accomplished between aromatic protons and anomeric protons (red arrow), H2′ and H2′′ protons (blue arrow), and H3′ protons (gray arrow).

While NOESY spectra indicate proton-proton dipolar (through-space) couplings, Correlated Spectroscopy (COSY) related experiments exhibit the scalar (J, through-bond) couplings between neighboring protons. When two

protons are connected through two or three chemical bonds (J=0-18 Hz), it will give rise to cross-peaks present in a 2D COSY spectrum. COSY spectra show much simpler cross-peak patterns than those in NOESY spectra, as it does not yield cross-peaks for those neighboring protons within a short distance that are not covalently bonded. It can be a useful method for the assignments of protons as the H5 and H6 of cytosine, H2′ and H2′′ and H3′ and H4′ of the sugar pucker and, especially, adduct site protons. Like the NOESY walk, the sugar proton connectivity can be drawn in a COSY spectrum. The H1′ will have cross-peaks to the H2′ and H2″ protons, and H2′ will have a cross-peak to H3′. A more detailed example is presented in Chapter VI (Figure 6-8) and VII (Figure 7-8). Furthermore, the double quantum filtered COSY, DQF-COSY can offer the coupling constant (J) values of sugar puckers, which is useful information for determining the geometry of the sugar ring needed for empirical restraints in rMD calculations. Indeed, those empirical values can be useful for the refinement.

While the COSY experiment presents the scalar couplings of neighboring protons through 1-3 bonds, longer through-bond spin systems can be detected in a total correlated spectroscopy, TOCSY spectrum. The magnetization can be transferred through multiple bonds with a longer spin lock process. The TOCSY spectrum appears more complex than a COSY spectrum but is simpler than a NOESY spectrum. Therefore, it can be very useful when confronted with adduct protons peaks in the populated cross-peaks area such as sugar proton coupling regions. It can therfore confer more information of interesting protons that are only connected through bonds.

The advantage of using a site-specifically labeled adduct sample is that it permits heteronuclear NMR experiments to be carried out. Since both ^{15}N and ^{13}C nuclei are NMR active with low abundance (^{13}C at 1.11% and ^{13}N at 0.36%), the chemistry of the isotopically labeled DNA adduct can be monitored by heteronuclear NMR experiments. A heteronuclear single quantum coherence (HSQC) experiment is the basic technique for detecting the proton signal directly and the heteroatom signal indirectly, directly attached to the proton. A coupling constant value (J) of 90 Hz (between H-N) and 125-200 Hz (between H-C) is applied. The HSQC spectrum shows the chemical shifts of the proton in the direct dimension and the heteroatom (^{15}N or ^{13}C) in the indirect dimension without having a diagonal peak. In general, these HSQC type experiments are routinely used for universally labeled protein samples for the assignments of the amide protons in peptides. Unlike those protein samples, the isotopically labeled DNA adduct sample would be expected to show clear and simple spectra based on the number of different chemical species. In particular, the correlation between the proton and the heteroatom or heteroatoms of the cross-link would be clearly revealed by the site-specifically, isotopically labeled sample on the gamma position of the carbon or N^2 of dG. Therefore, much simpler but equally useful NMR data than those from typical uniformly labeled sample can be obtained, which provide important clues as to which species exist *in situ* in duplex DNA. Figure 1-13 displays the pictorial explanation of those heteronuclear NMR experiments that were performed for this study.

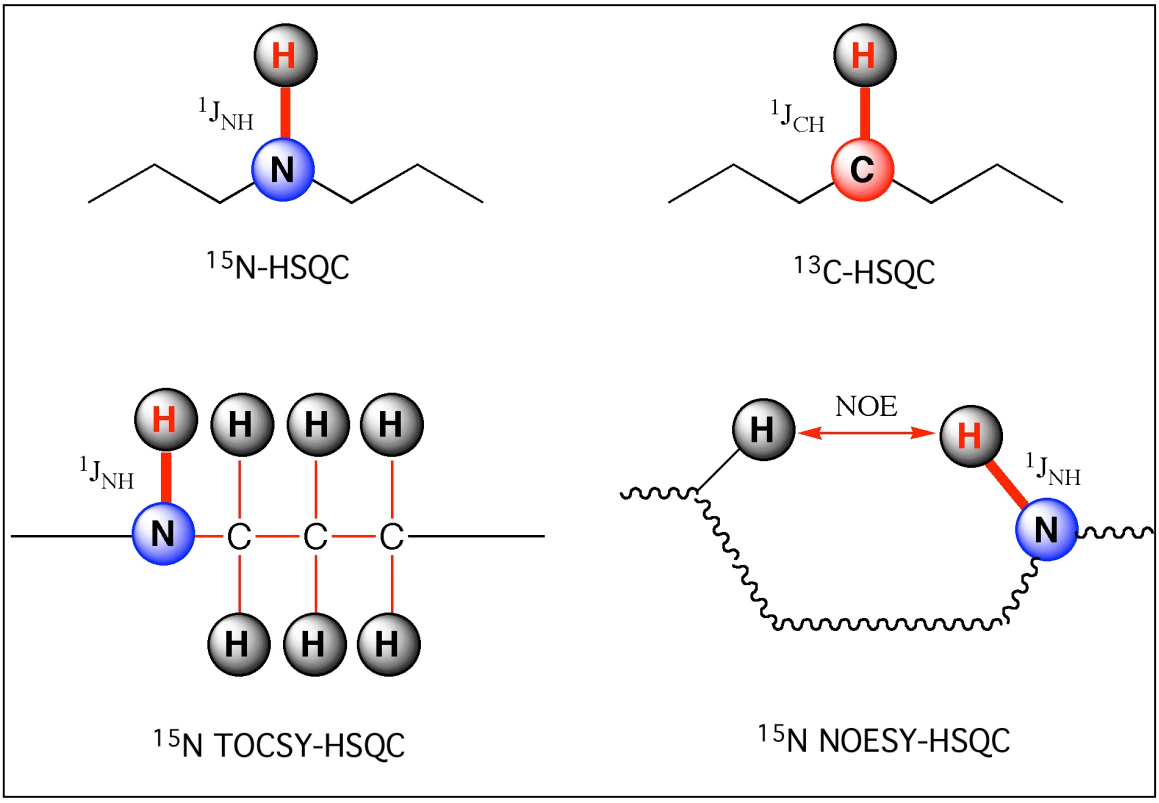

Figure 1-13. Heteronuclear NMR experiments. A Circle stands for NMR active nucleus and red lined bond or red arrow meant magnitization trasfer from the proton (red) attached to either ^{15}N or ^{13}C.

One of caveats for applying ^{15}N-HSQC type experiments is that there is no way to detect imine species, one of the possible candidates to be tested, due to the lack of a proton directly attached to ^{15}N. To tackle this problem, direct detection of imine ^{13}C was carried out using a probe with inner-coil ^{13}C geometry was carried out. This probe can detect the ^{13}C signal directly regardless of the existence of protons attached the ^{13}C. ^{1}H-^{13}C HSQC type experiments were also feasible since each candidate possesses a proton directly connected to ^{13}C, although its chemical shifts can be much closer to water peak (~4.7 ppm). To quantify each species, an inverse-gated decoupling pulse program was applied

(Figure 1-14). While collecting the FID in the carbon channel, the proton coupling was minimized by pulsing the proton channel using Waltz 16 decoupling. It reflects the avoidance of NOE effects during the acquisition time and can help to measure the ratio of ^{13}C relatively.

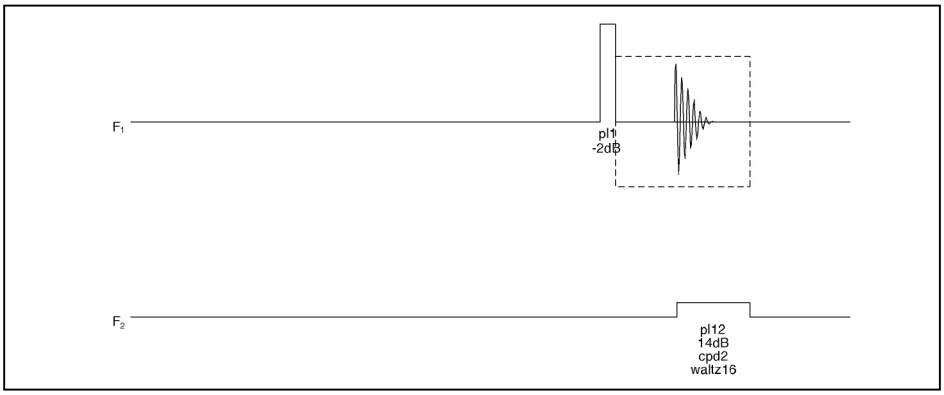

Figure 1-14. Inverse-gated decoupling pulse sequence: F_1 carbon channel; F_2 proton channel.

A site-specifically labeled sample allowed the use of more complex NMR experiments, such as NOESY-HSQC and TOCSY-HSQC, which provide more structural information for the cross-link. The former can show a NOESY spectrum only from the HSQC filtered proton, the latter shows a TOCSY spectrum from the HSQC filtered proton as shown in Figure 1-13. Site-specifically labeled acrolein- and crotonaldehyde-derived dG adducts in duplex DNA were examined by the same methods that were tested previously for the γ-OH-PdG adduct.

Other multi-dimensional experiments such as triple resonance experiments could also be carried out. The HCN and HNC type NMR experiments were applied for the confirmation of a cross-link species (Figure 1-

15). Those results are described in a related following chapter for the cross-link sample (Chapter IV).

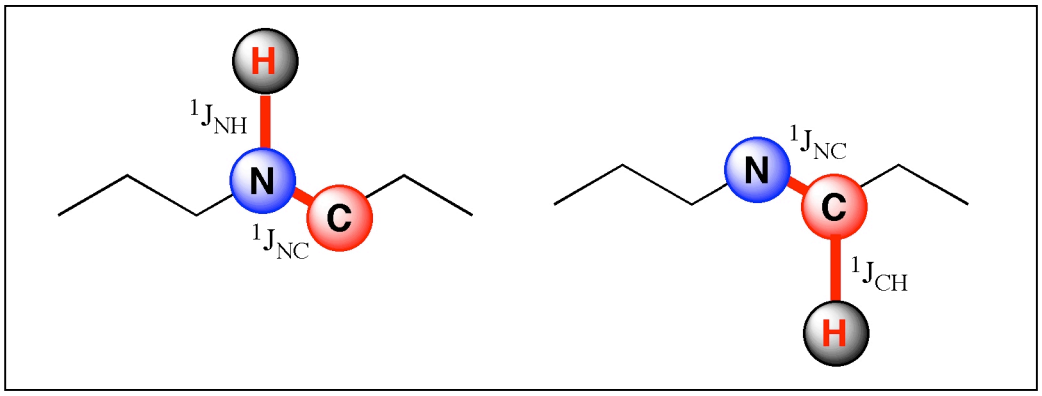

Figure 1-15. A schematic view of the nuclei observed in triple resonance experiments: HNC (left) and HCN (right).

Structural Refinement of DNA

Once satisfactory NMR spectra are collected and analyzed, a 3-Dimensional structure that satisfies the NMR data can be acquired by employing restrained molecular dynamics (rMD) calculations. Because of experimental uncertainties, the NMR restraints vary in allowed values. Therefore computational calculations create an ensemble of several structures where each structure reflects the input restraints equally well.

The typical procedure for refining oligodeoxynucleotide structure is outlined in scheme 1-6. At the initial step, the assignments must be completed. Once all possible protons of DNA are assigned properly, the volume of the peaks can be converted into the distance. For converting cross-peak volumes to distance restraints, the iterative relaxation matrix approach is applied by running Matrix Analysis of Relaxation for Discerning the Geometry of an Aqueous

Structure (MARDIGRAS). Torsion angle and distance restraints can be specified into empirical restraints from DQF-COSY and NOESY data, respectively (Figure 1-16).

Scheme 1-6. Strategy for the NMR-generated structural refinement of the oligodeoxynucleotides.

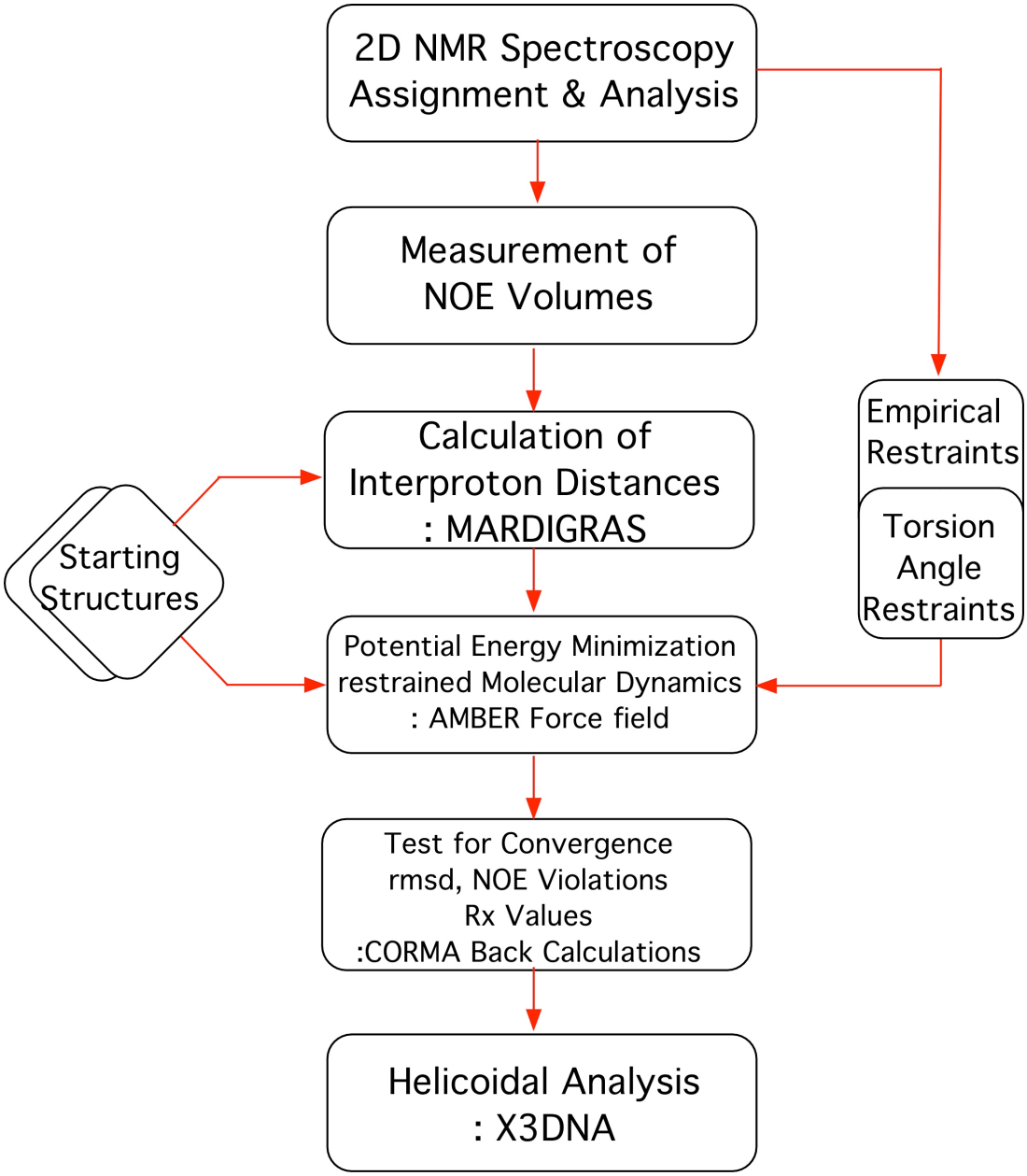

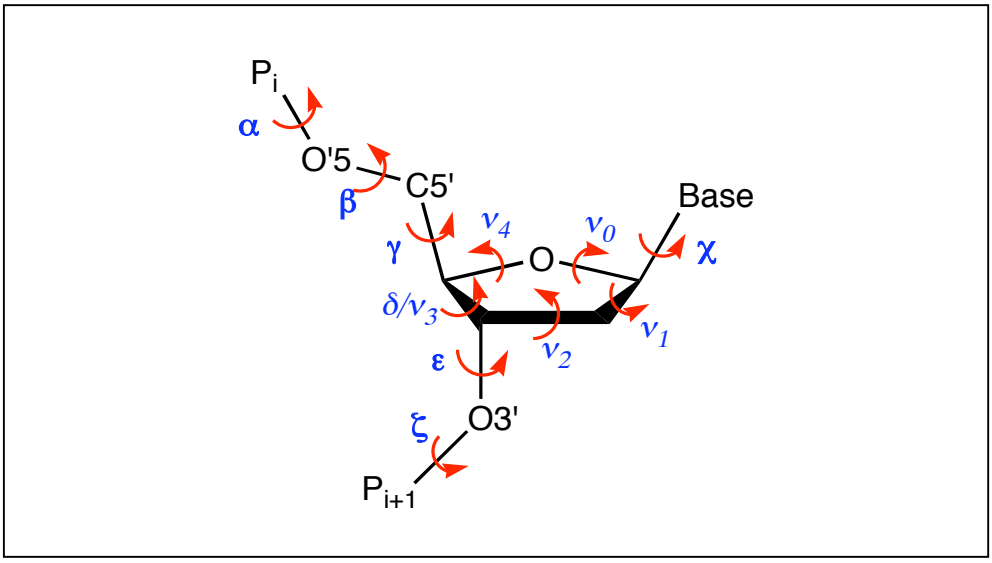

Figure 1-16. The backbone torsion angles in the mononucleotide in an oligodeoxynucleotide.

Prior to rMD calculations in AMBER, a non-standard base must have its own topology file: a coordinate file with its own library file that contains the atomic charges. Restrained electrostatic potential (RESP) charges can be calculated by running the GAUSSIAN 98 program. The Hartree Fock 6-31 G* method is recommended to develop those atomic charges. Finally, the unit of the adduct including the phosphate group should be kept to have –1 in total charge unless it had a charge on the adduct site.

Two starting structures, A-DNA and B-DNA, should be built and all restraints need to be applied while simulated annealing simulation is performed. Simulated annealing protocol heats the initial starting structures to high target temperature (600 K), and then slowly cools down to either room temperature or 0 K (Smith, J. A. et al., 2000). This process is used to search a wide range of conformational changes in the vicinity of the starting structure, and then find the

most stable conformation with regard to the input restraints. The root mean square deviation (RMSD) of the structures presents the preciseness of calculations. If the final structures converged well, those calculations can be finished. Otherwise, until obtaining a good convergence, those rMD calculations need to be repeated while modifying restraints with respect to NMR data. Determining not only A- or B-form DNA, but also the adduct conformation is always an important aspect by rMD calculations. The final result may possibly suggest to us the biological effects by structural information as well as defining the most feasible structure at physiological conditions. The final structure can be examined by the CORMA program for agreement between experimental intensities and theoretical values. The R_1^x value is defined in the formula below.

$$R_1^x = \frac{\sum (I_O^{1/6} - I_c^{1/6})}{\sum I_o^{1/6}}$$

The final refined structure can be analyzed in detail using the X3DNA program.

Dissertation Statement

The objectives of this dissertation are 1) to explore the structural difference of both acrolein- and crotonaldehyde-derived γ-OH-PdG adducts existing in duplex DNA (5′-CpG-3′ sequence), 2) to monitor each species by using isotopically labeled samples and various NMR techniques and 3) to investigate and elucidate each species: cross-link, aldehyde, hydrated aldehyde, and ring-closed by using NMR and restrained molecular dynamics calculations. Those studies will provide structural insight into these particular DNA adducts.

The underlying central hypothesis of this dissertation is that site-specific adducts of acrolein and crotonaldehyde *in situ* lie at the interface between chemistry and biology, and the structures and functions of these adducts. Although the biological role of each species is still in question, the chemical and structural differences of these adducts may give rise to different effects on DNA that can be strongly correlated with biological facts (mutagenicity).

The following chapters will present the structural studies of the acrolein- and crotonaldehyde-derived dG adducts in the 5′-CpG-3′ sequence. In Chapter II, the materials and methods are described. Chapter III details the monitoring the acrolein γ-OH-PdG DNA adduct *in situ* using ^{13}C and ^{15}N NMR. The carbinolamine cross-link formation and its detection are addressed. Chapter IV describes the monitoring the chemistry of diastereomeric crotonaldehyde 1,N^2-deoxyguanosine exocyclic adducts. Stereoselective formation of cross-link and detection of different species are discussed. Chapter V focuses on the structural study of an opened species by *S*-crotonaldehyde-derived dG adduct. Since all species are in equilibrium, it was not possible for the cross-link to be separated.

Therefore, the fully reduced cross-links from crotonaldehydes were used for more structural analyses in detail. Chapter VI states the structural study of the fully reduced *R*-crotonaldehyde cross-link. The NMR derived solution structures were examined. Chapter VII is concerned with the NMR study of the fully reduced *S*-crotonaldehyde cross-link. The thermodynamic stability of the cross-link by the methyl stereochemistry is addressed. The structural features are discussed as well as a recent heteronuclear NMR study for suggesting a kinetic basis for the lack of interstrand cross-link formation by this adduct.

Finally, the conclusion of the works in this dissertation and the future direction relevant to this project are discussed in Chapter VIII.

CHAPTER II

MATERIALS AND METHODS

Oligodeoxynucleotide Synthesis

The unmodified oligodeoxynucleotides were purchased from the Midland Certified Reagent Co. (Midland, TX) and purified by anion exchange chromatography. All modified oligodeoxynucleotides were provided by the laboratories of Professors Thomas M. Harris and Carmelo J. Rizzo. The synthesis of the ^{13}C- and ^{15}N-labeled adducted oligodeoxynucleotides was accomplished using a postoligomerization strategy previously employed for related modified oligodeoxynucleotides (Kozekov et al., 2003; Nechev et al., 2001; Nechev et al., 2001). This involved the incorporation of an electrophilic base, 2-fluoro-*O*6-(2-trimethylsilylethyl)-2'-deoxyinosine (DeCorte et al., 1996), into an oligodeoxynucleotide using standard phosphoramidite chemistry followed by displacement of the fluoro group by an amine analogue of the mutagen via a nucleophilic aromatic substitution reaction. A vicinal diol unit was used as a surrogate for the aldehyde group, which was cleaved with sodium periodate after the adduction reaction to give the desired modified oligodeoxynucleotide. The syntheses of the ^{13}C- and ^{15}N-labeled amino diols, 4-amino-2-^{13}C-butane-1,2-diol and 4-^{15}N-amino-2-butane-1,2-diol, are shown in Scheme 2-1 and 2-2.

The synthesis of the ^{13}C-labeled amino diol began with the conversion of alcohol, *tert*-butyl *N*-(2-hydroxyethyl)carbamic acid, to the corresponding mesylate followed by displacement with ^{13}C-labeled potassium cyanide (Scheme 2-1). Reductuion of the nitrile, *N*-*tert*-butyl [2-(^{13}C-cyano)ethyl]carbamic acid,

with DiBAl-H at low temperature followed by hydrolysis gave the labeled aldehyde, *N*-(*tert*-butylcarbamoyl)-3-amino-1-^{13}C-propanal. Wittig olefination followed by treatment with osmium tetroxide installed the vicinal diol unit. Deprotection of the amino group then provided the desired amino diol, 4-amino-2-^{13}C-butane-1,2-diol, with the ^{13}C-label in the proper location (Liu, Y.-S. et al., 1998).

The synthesis of the ^{15}N-labeled amino diol is outlined in Scheme 2-2. The hydroxyl group of alcohol, (*4R*)-4-(2-hydroxy-ethyl)-2,2-dimethyl-1,3-dioxolane, was converted to the corresponding mesylate, which was diplaced by potassium ^{15}N-phthalimide in DMF. Treatment with hydrazine and purification by ion-exchange chromatography gave the desired 4-^{15}N-amino-2-butane-1,2-diol.

The specifically labeled adducted oligodeoxynucleotides were prepared according to Scheme 2-3. Reaction of oligodeoxynucleotide containing the 2-fluoro-O^6-(2-trimethyl-silylethyl)-2′-deoxyinosine with either the ^{13}C- and ^{15}N-labeled aminodiol under nucleophilic aromatic substituion conditions gave specifically adducted oligodeoxynucleotide. Periodate oxidation of the vicinal diol unit gave the corresponding aldehyde, which exists in the ring-closed form in single-stranded DNA.

The site-specific incorporation of an $^{15}N^2$-dG label in the complementary strand involved the incorporation of the 2-fluoro-O^6-(2-trimethylsilylethyl)-2′-deoxyinosine nucleotide into the desired position using phosphoramidite chemistry (DeCorte et al., 1996; Harris et al., 1991; Kozekov et al., 2003; Kozekov et al., 2001). This oligodeoxynucleotide was then deprotected using 6M $^{15}NH_4OH$ which also displaced the fluoro group. Removal of the O^6-(2-trimethylsilyethyl) protecting group using 5% acetic acid afforded the site-specifically ^{15}N-labeled

oligodeoxynucleotide. The concentrations of the single-stranded oligodeoxynucleotides were determined from calculated extinction coefficients at 260 nm.

For the synthesis of ^{13}C-labeled crotonaldehyde adducts, the similar strategy was applied. A vicinal diol unit was used as a surrogate for the aldehyde group (Scheme 2-4); it was cleaved with sodium periodate after the adduction reaction to give the desired modified oligodeoxynucleotide. A significant advantage of this strategy was that access to both stereoisomers in the resulting adducted oligodeoxynucleotides was obtained by individually reactiong the (*R*)- and (*S*)-steroisomers of the amines with the same oligodeoxynucleotide containing the 2-fluoroinosine base (Scheme 2-5).

The synthesis of the ^{13}C-labeled amino diols is shown in Scheme 2-4. Commercially available (*S*)-2-amino-1-propanol was N-protected as the corresponding Boc derivative. The hydroxyl group was then converted to the mesylate and displaced with ^{13}C-labeled potassium cyanide to give nitrile. Reduction of the nitrile to the aldehyde was followed by Wittig methylenation to olefin in acceptable overall yield. Treatment of the olefin with osmium tetroxide gave diol as a mixture of stereoisomers. Because the diol was eventually cleaved to the aldehyde, the stereochemistry of the diol was of no consequence. Deprotection gave 4*S*-amino-pentane-1,2-diol. The antipodal 4*R*-enantiomer was prepared by an identical sequence starting from commercially available (*R*)-2-amino-1-propanol.

Scheme 2-1. Synthesis of the 4-Amino-2-^{13}C-butane-1,2-diol. a. (tBuCO)$_2$O, NaOH, b) MsCl, Et$_3$N, 70% c) K^{13}CN, DMSO, 40° C, 70% for two steps d) DiBAl-H, CH_2Cl_2, -78° C, 30% e) $Ph_3P^+CH_3$ I^-, t-BuO$^-$K$^+$, THF, 65% f) OsO_4, NMO, THF, H_2O, 69% g) Amberlyst-15 H^+, 91% (By Rizzo & Harris lab).

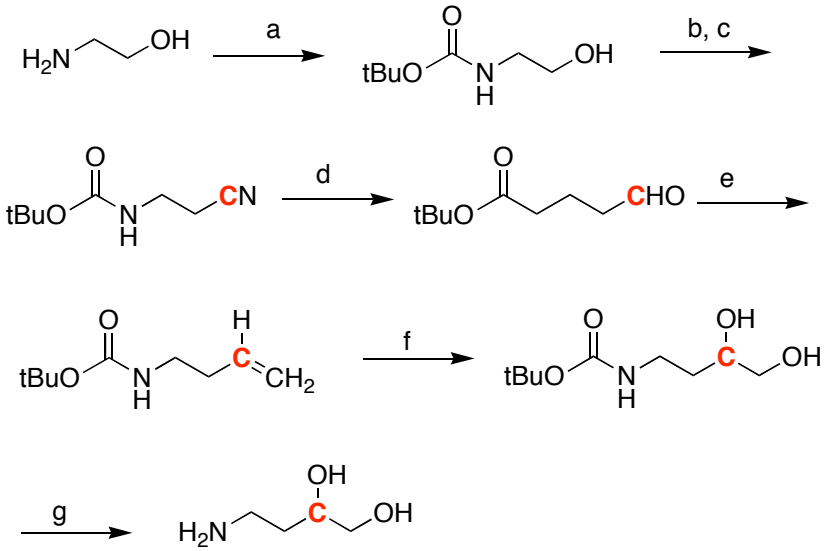

Scheme 2-2. Synthesis of 4-^{15}N-Amino-2-butane-1,2-diol (By Rizzo & Harris lab).

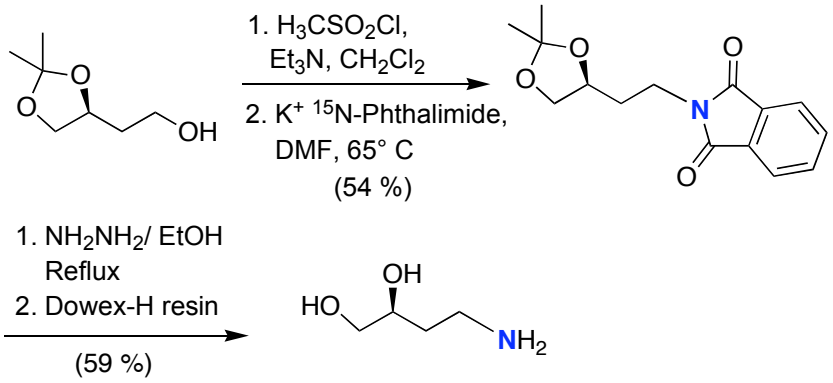

Scheme 2-3. Synthesis of Oligodeoxynucleotides Containing Site-Specific ^{15}N, ^{13}C Isotopes (By Rizzo & Harris lab).

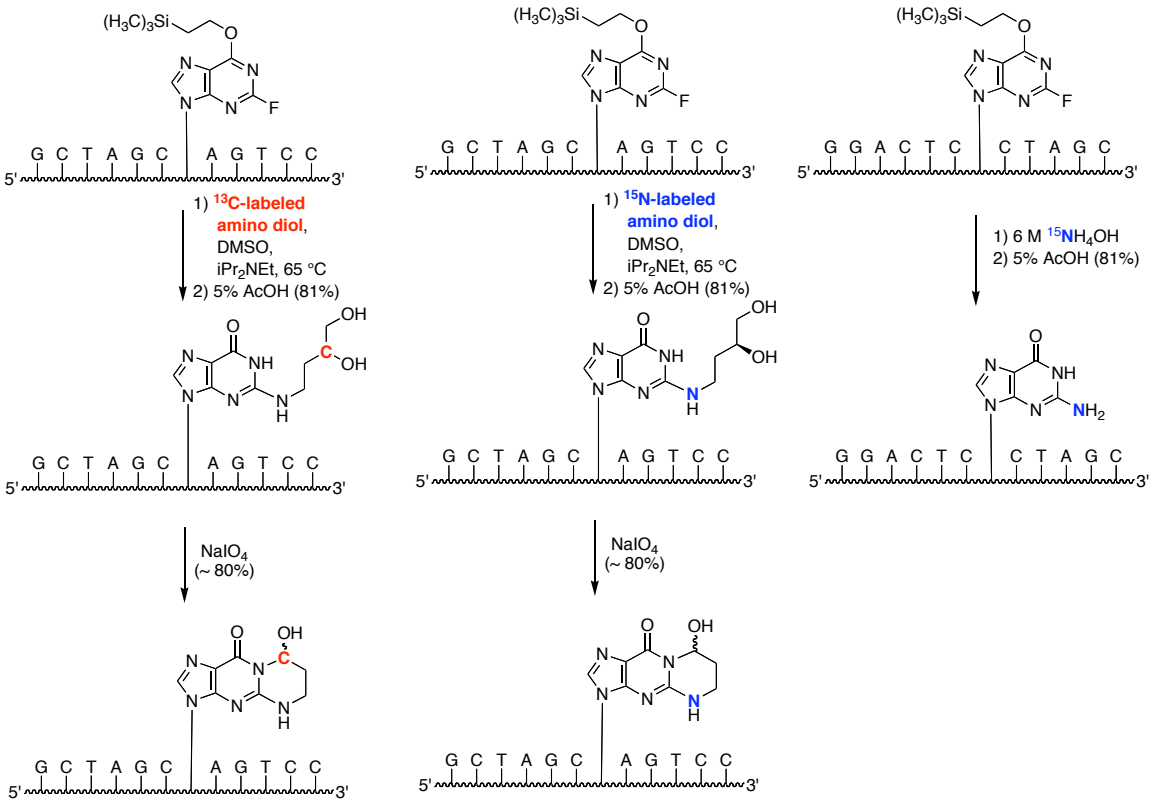

Scheme 2-4. Preparation of the stereoisomeric ^{13}C-labeled amino diols used for site-specific synthesis of adducts in oligodeoxynucleotides. Reagents: (a) $(Boc)_2O$, 1 M NaOH, overnight, 81.5%, (b) MsCl, Et_3N, CH_2Cl_2, rt, 2 hr; $K^{13}CN$, DMSO, 40 °C, 15 hr, 69% over 2 steps, (c) DIBAH, CH_2Cl_2, -78 °C, 32%, (d) Me_3PCH_2Cl,t-BuOK, THF, 70%, (e) OsO_4, NMP, THF/t-BuOH/H_2O, 76%, (f) Amberlist-H, CH_2Cl_2/CH_3OH; 4 M NH_3 in CH_3OH, 91% (By Rizzo & Harris lab).

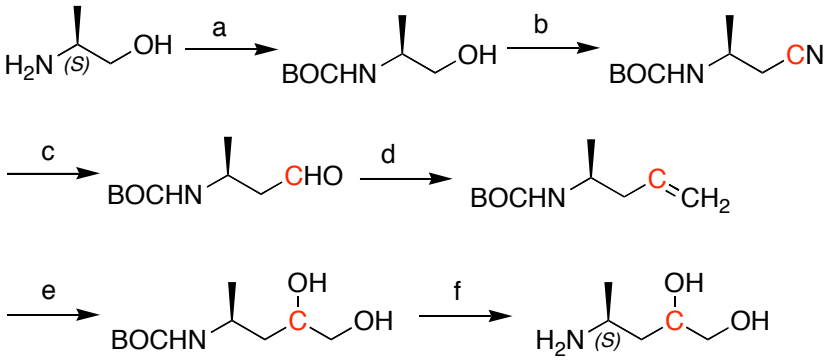

Scheme 2-5. Site-specific synthesis of the ^{13}C-labeled oligodeoxynucleotides containing stereoselective crotonaldehyde adducts (By Rizzo & Harris lab).

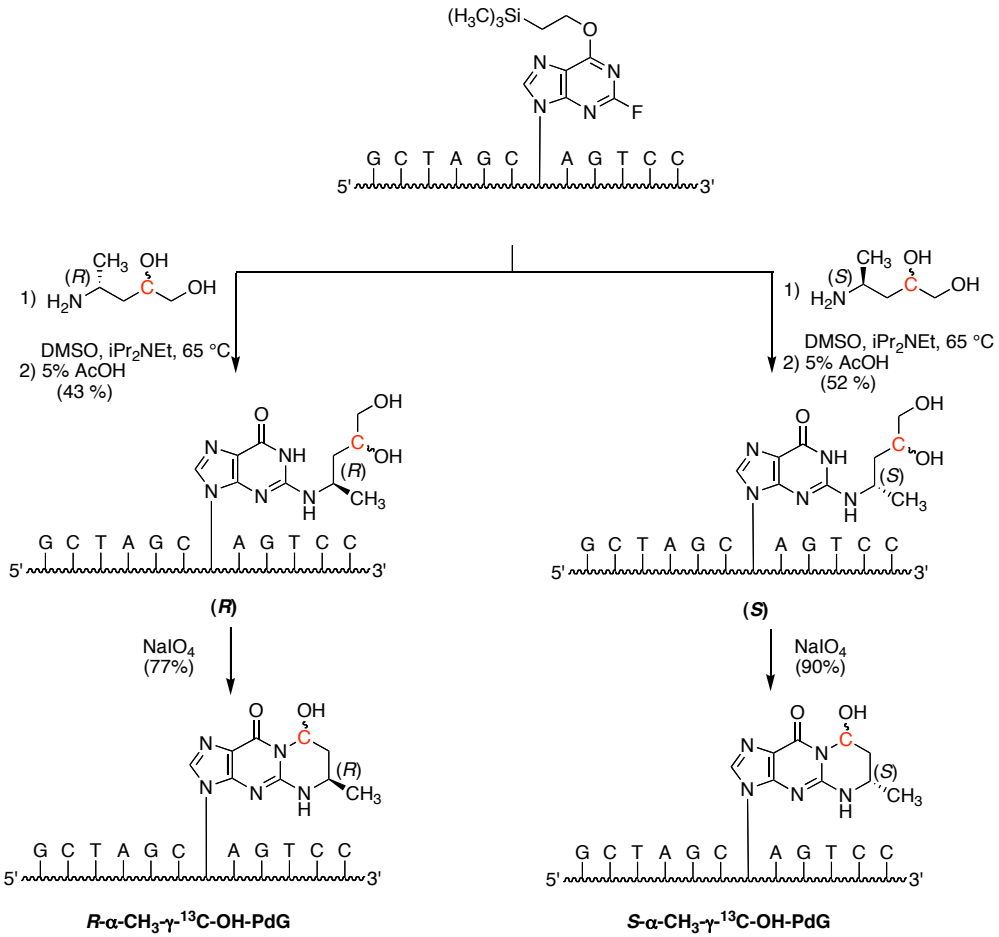

Sample Preparation

The modified oligodeoxynucleotide 5′-d(GCTAGCGAGTCC)-3′, X= Adducted dG (γ-^{13}C-OH PdG, *R*-α-CH_3-^{13}C-OH-PdG, and *S*-α-CH_3-^{13}C-OH-PdG) and its complementary strand 5′-d(GGACTCGCTAGC)-3′, 5′-d(GGACTCTCTAGC)-3′, or 5′-d(GGACTCACTAGC)-3′ were annealed respectively in a buffer consisting of 10 mM NaH_2PO_4, 0.1M NaCl, and 50 μM Na_2EDTA at pH 7.0. Unless otherwise indicated, the same buffer condition was utilized for all duplexes samples. In the case of the mixture of single strand and duplex DNA, the duplex was eluted from DNA Grade Biogel hydroxylapatite (Bio-Rad Laboratories, Hercules, CA) with a gradient from 10 to 200mM NaH_2PO_4, pH 7.0. Between each steps, the duplex was lyophilized, resuspended in 1 mL of H_2O and then desalted using Sephadex G-25. The purity of the duplex was analyzed using a PACE 5500 (Beckman Instruments, Inc., Fullerton, CA) instrument. Electrophoresis was conducted using an eCAP ssDNA 100-R kit applying 12,000 V for 30 min. The electropherogram was monitored at 254 nm. MALDI-TOF mass spectra were measured on a Voyager-DE (PerSeptive Biosystems, Inc., Foster City, CA) instrument in negative reflector mode. The matrix contained 0.5 M 3-hydrosypicolinic acid and 0.1 M ammonium citrate.

For the fully reduced sample, both *R* and *S* crotonaldehyde-dG adduct were reduced fully by sodiumborohydride forcing to generate reduced interchain cross-links as shown in Figure 1-7.

NMR Spectroscopy

The modified duplex was prepared at a concentration of 2 mM for acrolein adduct, 1 mM for each crotonaldehyde adducts and 1.8 mM for other reduced samples in 0.3 mL or 0.25 mL of 9:1 H_2O:D_2O containing 10 mM NaH_2PO_4, 0.1 M NaCl, 50 μM Na_2EDTA at pH 7.0 for observing exchangeable protons and amino protons of which is attached to labeled ^{15}N. The sample was exchanged three times with 99.96% D_2O and dissolved in 99.996% D_2O for observing non-exchangeable protons. Those samples were placed into a micro-NMR tube (Shigemi Glass, Inc., Allison Park, PA). NMR experiments were carried out at ^{1}H frequencies of 500.13, 600.13 or 800.23 MHz (^{13}C frequencies of 125 or 150 MHz and ^{15}N frequencies of 50 MHz) on Bruker spectrometers. One-dimensional ^{13}C NMR was conducted with a probe with inner-coil ^{13}C geometry using inverse-gated ^{1}H Waltz16 decoupling. Typical acquisition parameters were 16 K total data points, with a digital resolution of 1.3 Hz/pt, 12K scans, and a relaxation delay of 8 s. The ^{13}C HSQC experiments were performed using standard ^{1}H-detected pulse programs with States-TPPI phase cycling and watergate water suppression (Piotto et al., 1992). Typical experimental parameters were 8 scans, 512 FIDs, each of 2K points. The ^{13}C sweep width was varied from 20 to 180 ppm. The ^{15}N HSQC spectra (Sklenar et al., 1993) were recorded with 8/180 scans per increment, using State-TPPI phase cycling, a delay time 1/2 $^{1}J_{N-H}$ of 5.56 ms, 1536 complex data points for 10,000 Hz in the acquisition dimension and 256 points in the indirect dimension, covering 10,136.8 Hz, centered at 100 ppm. A relaxation delay of 1.5 s was used. ^{15}N was fully decoupled during the acquisition time. The ^{15}N TOCSY-HSQC experiments (Talluri, 1996) were recorded applying States phase cycling, 60 ms isotropic

mixing time applied with a 10,000 Hz dipsi spin lock pulse sequence optimized for a 90 Hz $^{1}J_{N-H}$ coupling. Complex data points (1536) for 10,000 Hz in the acquisition dimension and 128 points in the indirect dimension, covering 1,000.0 Hz centered around 106 ppm, were measured. A relaxation delay of 1.2 s was used and ^{15}N was fully decoupled during the acquisition time. The ^{15}N NOESY-HSQC experiments (Mori et al., 1995; Talluri, 1996) were recorded applying State phase cycling with a 150 ms mixing time, and were optimized for a 90 Hz $^{1}J_{N-H}$ coupling. Complex data points (1536) for 10,000 Hz in the acquisition dimension and 128 points in the indirect dimension, covering 1,000 Hz centered at 106 ppm, were measured. A relaxation delay of 1.5 s was used, and ^{15}N was fully decoupled during the acquisition time.

Two dimensional ^{1}H NOESY spectra of nonexchangealbe protons were recorded using TPPI phase cycling with mixing times of 60, 80, 150, 250, and 350 ms. These were recorded with 2048 complex data points in the acquisition dimension and 1024 real data points in the indirect dimension covering 9615.385 Hz. For each t1 increment, 32 scans were averaged with presaturation of the HDO resonance. The relaxation delay was 2 s. The data in the t_1 dimension were zero-filled to five a matrix 2K × 2K real points. While collecting data, in the case of *S*-COPdG, ^{13}C decoupling was applied in both dimensions. Two dimensional exclusive COSY (E-COSY), magnitude COSY, and double quantum-filtered ^{1}H correlation COSY (DQF-COSY) spectra were collected with 2048 complex points in the acquisition dimension and 512 points covering 6009.615 Hz and then zero-filled to 1024 points. For each t_1 increment, 64 or 84 scans were averaged with presaturation of the HDO resonance. A squared sine-bell apodization was applied in both dimensions. Two dimensional water NOESY spectra for

exchangeable protons were collected in H_2O:D_2O (95:5) solution using Watergate water suppression. The spectra were acquired at 13 °C using States-TPPI phase cycling in the cryogenic probe with mixing times of 200 and 250 ms. A squared sine-bell with 72 ° shift apodization was applied in d_2 dimension while cosine-squared bell apodization was applied in d_1 dimension. 1536 real data points in d_2 dimension and 512 points in d_1 dimension were used with 92/128 scans. A relaxation delay of 1 s was used. The ^{1}H chemical shifts were referenced to water. Both ^{13}C and ^{15}N chemical shifts were referenced indirectly (Chemistry, 1998; Markley et al., 1998; Wishart et al., 1995). The NMR data were processed on Silicon Graphics Octane workstations using the program FELIX 2000 (Accelrys, Inc., San Diego, CA), XWIN NMR or NMRPipe (Delaglio et al., 1995).

Molecular modeling

Modeling was performed on Silicon Graphics Octane workstations using the program AMBER 8.0 (Case et al., 2002). Classical B-DNA was used as a reference structure to create starting structures for potential energy minimization (Arnott and Hukins, 1972). DNA structures were constructed using the BUILDER module of INSIGHT II (Accelrys, Inc., San Diego, CA). The ANTECHAMBER program was used, and the atom types were based on AMBER atom types for parametrization. Atomic charges were calculated by using GAUSSIAN98 (Frisch et al., 1998) Hartree-Fock calculations with 6-31G* basis set, followed by an atom-centered fit of the electrostatic surface potential with the RESP program. The Appendix A contains the parameterization of the carbinolamine, pyrimidopurinone, N^2-(3-oxo-1(*S*)-methyl-propyl)-dG adduct, and fully reduced cross-link for the AMBER 8.0 forcefield. Potential energy

minimization was carried out with the SANDER program, using the generalised Born continuum solvent model (Bashford and Case, 2000; Tsui and Case, 2000) and the AMBER 8.0 force field.

Distance and Torsion Angle Restraints

Non-exchangeable interproton distances were acquired by running MARDIGRAS (Borgias and James, 1990; Liu, H. et al., 1996) from NOESY spectra. Footprints were drawn around cross-peaks for the NOESY spectrum measured at a mixing time of 250 ms to define the size and shape of individual cross-peaks, using the program FELIX2000. Identical footprints were transferred and fit to the cross-peaks obtained at the other two mixing times. Determined cross-peak intensities were combined with intensities generated from complete relaxation matrix analysis of a starting DNA structure to generate a hybrid intensity matrix. The program MARDIGRAS (v. 5.2) was used to refine the hybrid matrix by iteration to optimize the agreement between the calculated and the experimental NOE intensities. The molecular motion was assumed to be isotropic. The noise level was set at the weakest cross-peak. The RANDMARDI procedure was used while evaluating uncertainties in the distance estimations (Gotfredsen et al., 1996 Nov-Dec; Liu, H. et al., 1995 Dec). To generate hybrid intensity matrices, two starting models, A-form (IniA) and B-form (IniB) structures, were used. A total of 50 RANDMARDIGRAS runs were performed with 2, 3, and 4 ns isotropic correlation times. The minimum number of the best resolved cross-peaks were used for the calculations. The cytosine H5-H6 interproton distance of 2.46 Å was used as a reference. In addition, some distance restraints from cross-peaks of water NOESY and longer mixing time NOESY were added by rough estimation

based on peak intensity. In most case, the lower bounds were set at 1.8 Å, however, in the case of the reduced *S*-crotonaldehyde cross-link, two boundaries were imposed with different classes. In the case of torsion angle restraints, Pseudorotation phase angle (***P***) were estimated from COSY and NOESY spectra as described elsewhere (Kim, S. G. et al., 1992; Van De Ven and Hilbers, 1988). The intensities of the H2′-H3′, H2″-H3′, and H3′-H4′ multiplets help to constrain sugar pucker in the restricted ranges since the intensities of the corresponding cross-peaks depend directly on the magnitude of the coupling constants. If H2′-H4′ NOESY cross-peak is more intense than H2″-H4′ cross-peak, ***P*** values greater than 126°. For $\boldsymbol{P} \geq 144^{\circ}$, the intensity of H1′-H4′ should be less than that of H1′-H2′ cross-peak (Kim, S. G. et al., 1992). The pseudorotation and amplitude ranges were converted to the five dihedral angles ν_0 to ν_4. Most cases in here, the minimum number of torsion angle restraints were used. Hydrogen bonding constraints were included including terminal base pairs in the calculation, which are consistent with NOESY spectra in water.

Restrained Molecular Dynamics Calculations

Classical A-DNA and B-DNA were used as starting structures. The adduct was constructed using the BUILDER module of INSIGHT II (Accelrys Inc., San Diego, CA). Without experimental restraints, 250 steps using steepest descent energy minimization followed by 250 steps of conjugate gradient minimization were performed in the SANDER module of AMBER 8 on a Silicon Graphics computer to relieve any bad van der Waals contacts with a constant dielectric. The restraint energy function included terms describing distances

and dihedral restraints as square-well potentials. The Generalized Born solvent model was used for rMD SA calculations with 0.1 M salt concentration, and the SHAKE algorithm was on for the fixed hydrogen bond length (Bashford and Case, 2000; Tsui and Case, 2000).

Calculations were initiated by coupling to a heating bath rapidly up to 600 K and maintained for first 5 ps, followed by steady cooling to 100 K over 15 ps for equilibrium dynamics. During the final 5 ps of cooling, the temperature was reduced to 0 K. The force constants were scaled up during 5 ps of the heating period and maintained during the rest of time. Coordinate sets were archived every 0.2 ps, and 10 structures from the last 5 ps were averaged in total. An average structure was subjected to 500 iterations of conjugate gradient energy minimization to obtain the final structure. For the fully reduced *R*-crotonaldehyde cross-link sample, the lower and upper distance bounds were all set calculated from MARDIGRAS with 30 kcal/mol•A force constants for class1 and hydrogen bonding constraints. Throughout the calculations, the force constants 2, 3, 4, and 5 were set to 25, 20, 15, 10 kcal/mol•A. For the fully reduced *S*-crotonaldehyde cross-link sample, the lower and upper distance bounds were all set calculated from MARDIGRAS with 50 kcal/mol•A force constants for class1 and hydrogen bonding constraints. Throughout the calculations, the force constants 2, 3, 4, and 5 were set to 45, 40, 35, 30 kcal/mol•A. The empirical restraints were set to 35 kcal/mol•A unless otherwise noticed. The weight of force constants were increased from 0.1 to 1.5 over the first 3 ps and reduced back to 1.0 over the rest of calculations. Until acquiring

the nice convergence from the starting structures, those values slightly modified in each cases.

Once the final structure was derived from rMD calculations, from which the Complete Relaxation Matrix Analysis (CORMA)(v. 5.2) was utilized for the back calculation of theoretical ^{1}H NOE intensities (Keepers and James, 1984). For all of the analyses, isotropic correlation time τ_c = 3 ns was used. A sixth root residual (R_1^x) factor was calculated for each final structure to measure the fit of the NOESY data to the final structure: Basically, it measures the relative error between the calculated from the final structure and observed NOE intensities from the real sample. Helicodial parameters were examined using 3DNA (Lu and Olson, 2003).

CHAPTER III

SPECTROSCOPIC CHARACTERIZATION OF INTERSTRAND CARBINOLAMINE CROSS-LINKS FORMED IN THE 5′-CpG-3′ SEQUENCE BY THE ACROLEIN-DERIVED γ-OH-1,N^2-PROPANO-2′-DEOXYGUANOSINE DNA ADDUCT[†]

Introduction

The major acrolein-derived dG adduct, γ-OH-PdG adduct, was studied by using NMR with site-specifically labeled samples. The adduct exhibits an array of chemistry in DNA, which includes the formation of cyclic hydroxylated 1,N^2-propanodeoxyguanosine (OH-PdG) adduct, and DNA interchain cross-links (Scheme 1-2). DNA-peptide (Kurtz and Lloyd, 2003) and DNA-protein cross-links (Sanchez et al., 2003) are also formed. The 3-(2-deoxy-β-D-erythro-pentofuranosyl)-5,6,7,8-tetrahydro-8-hydroxypyrimido[1,2a]purin-10(3H)-one, γ-OH-PdG adduct (Chung, F. L. et al., 1999; Nath, R. G. et al., 1996) was detected in animal and human tissue (Chung, F. L. et al., 1999), suggesting its involvement in mutagenesis and carcinogenesis (Nath, R. G. and Chung, 1994). When placed into duplex DNA opposite dC at neutral pH, it opens spontaneously to aldehyde, in equilibrium with diol (de los Santos, C. et al., 2001).

The presence of aldehyde in duplex DNA leads to the potential for formation of both DNA-DNA and DNA-protein cross-links. Kozekov et al. (Kozekov et al., 2003; Kozekov et al., 2001) trapped a trimethylene cross-link upon insertion of γ-OH-PdG adduct into an oligodeoxynucleotide duplex at a 5'-

[†] Reproduced in part with permission from *J. Am. Chem. Soc*. **2005**, 127, 17686-17696. Copyright 2005 American Chemical Society.

CpG-3' sequence, followed by $NaCNBH_3$ treatment. This implied the presence of cross-linked imine, in equilibrium with cross-linked carbinolamine, and cross-linked pyrimidopurinone. Enzymatic digestion of the cross-linked DNA afforded cross-linked pyrimidopuinone (Kozekov et al., 2003). In contrast, ^{15}N HSQC NMR detected the presence of carbinolamine **4** *in situ*, in the 5'-CpG-3' sequence (Kim, H. Y. et al., 2002). The interstrand carbinolamine, imine, and pyrimidopurinone cross-links formed in 5'-CpG-3' sequences exist in equilibrium (Scheme 1-2) and monitoring the composition of the equilibrium mixture *in situ* is of considerable interest. All three cross-linked species may contribute to the mutagenic spectrum of acrolein, and interfere with DNA replication.

This chapter extends upon the earlier NMR studies (Kim, H. Y. et al., 2002). The site-specific introduction of a ^{13}C label at the γ carbon of acrolein, and of a ^{15}N label at N^2-dG of γ-OH-PdG, enabled the equilibrium chemistry of γ-OH-PdG adduct to be monitored, *in situ*. The results reveal that the previously detected (Kim, H. Y. et al., 2002) carbinolamine is in fact the major cross-linked species present in duplex DNA, *in situ*. At equilibrium, the amounts of imine crosslink and pyrimidopurinone cross-link remain below the level of detection. Molecular modeling suggests carbinolamine cross-link maintains Watson-Crick hydrogen bonding at both of the tandem C•G base pairs, with minimal distortion of the duplex.

Results

Epimerization of γ-OH-PdG. The single-stranded 5'-d(GCTAGCXAGTCC)-3' γ-^{13}C-OH-PdG oligodeoxynucleotide was examined

using ^{13}C HSQC NMR (Figure 3-1). At 37 ^{o}C two γ-^{13}C resonances were observed, at δ 71.3 ppm. The corresponding ^{1}H resonances were observed at δ 6.12 and 6.01 ppm. These two resonances were assigned as the *R*- and *S*-epimers of cyclic adduct, embedded in oligodeoxynucleotide. No resonance for γ-^{13}C aldehyde or hydrated aldehyde was observed, suggesting that, at equilibrium, the levels of these ring-opened species remained below the spectroscopic limit of detection.

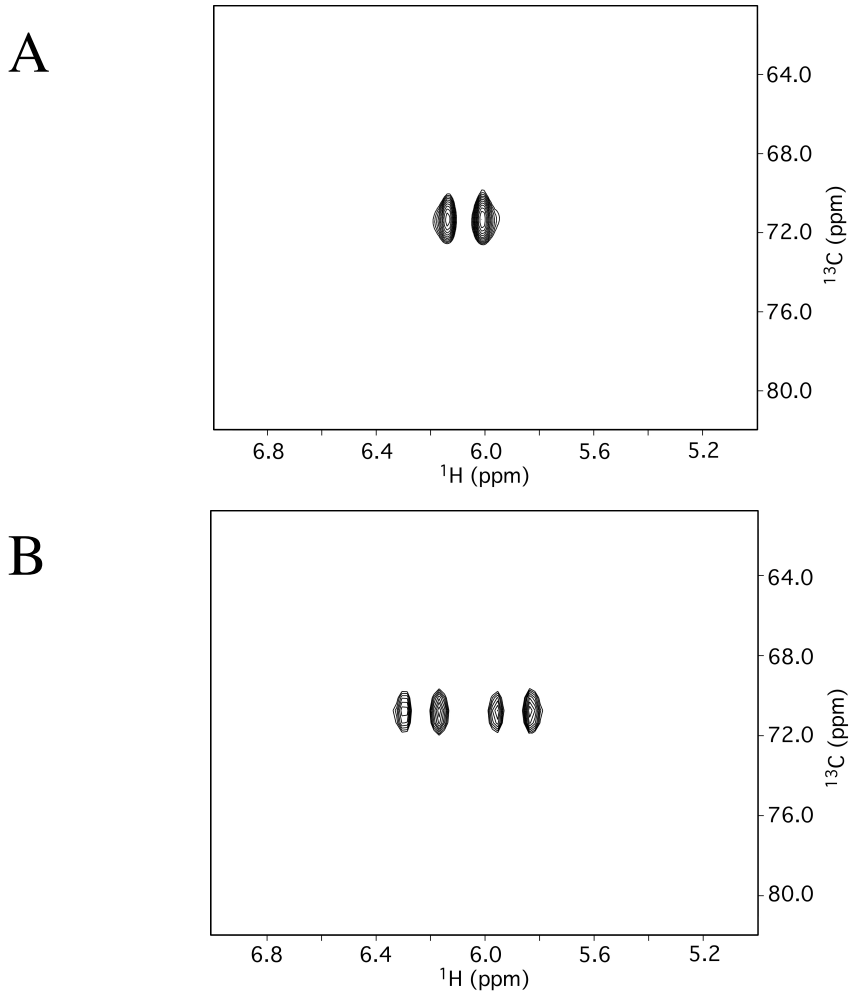

Figure 3-1. (A) ^{1}H-decoupled ^{13}C HSQC spectrum of single-stranded oligodeoxynucleotide 5′-d(GCTAGCXAGTCC)-3′; X= γ-^{13}C-OH PdG adduct; (B) ^{1}H-coupled ^{13}C HSQC spectrum.

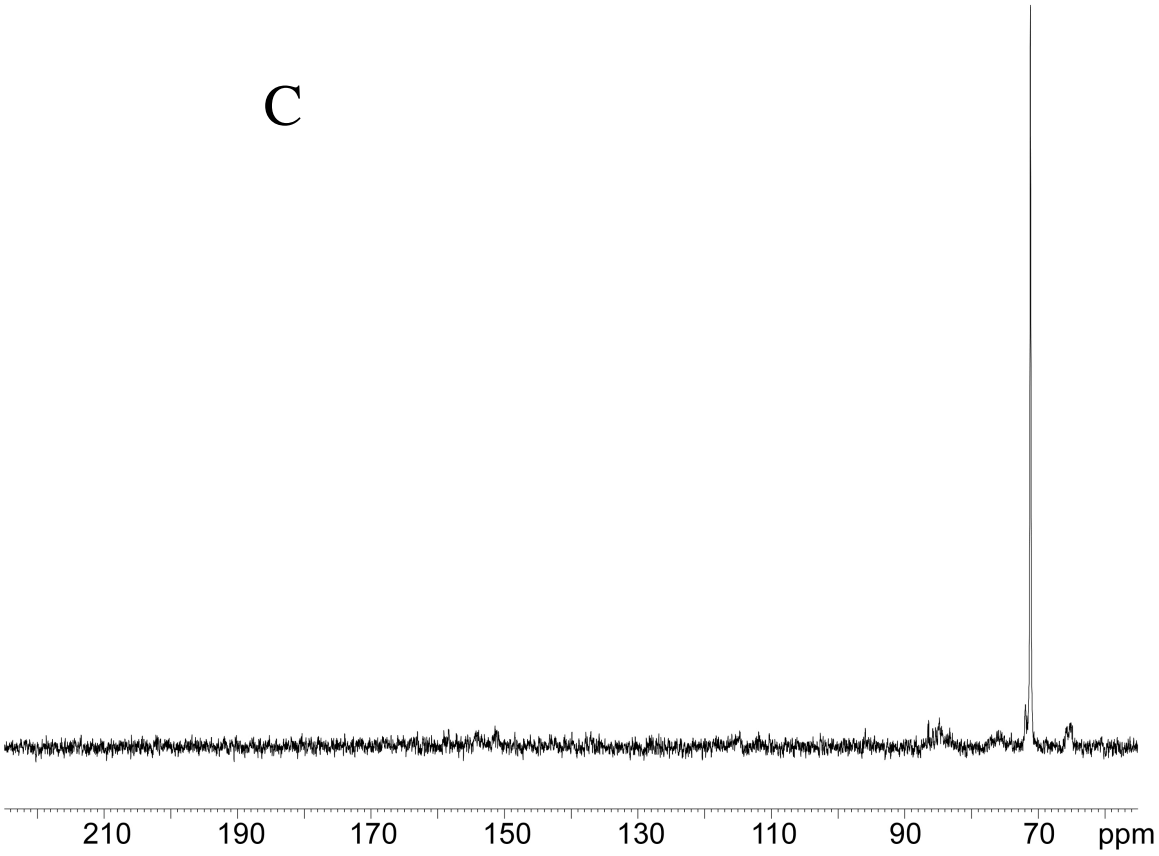

Figure 3-1 (continued) (C) ^{13}C spectrum of single-stranded oligodeoxynucleotide 5′-d(GCTAGCXAGTCC)-3′; X= γ-^{13}C-OH PdG adduct

Equilibrium Chemistry of the γ-OH-PdG Adduct in Duplex DNA. The single-stranded 5'-d(GCTAGCXAGTCC)-3' γ-^{13}C-OH-PdG oligodeoxynucleotide was annealed with the complementary strand to form the duplex 5'-d(GCTAGCXAGTCC)-3'•5'-d(GGACTCGCTAGC)-3' at pH 7, in which APdG adduct was placed opposite dC, and the sample was allowed to equilibrate at 37 °C (Figure 3-2). After 6 days, no further spectroscopic changes were observed. At equilibrium, the γ-^{13}C resonance in duplex DNA appeared as a mixture of three species. Furthest downfield, at approximately 207 ppm, was a resonance assigned as γ-^{13}C aldehyde. A second γ-^{13}C resonance, assigned as hydrated aldehyde (Ramu et al., 1995), was observed at approximately 90 ppm. The third resonance, assigned as carbinolamine cross-link, was observed at 76 ppm. The two diastereomers of carbinolamine were not resolvable in the ^{13}C spectrum. The secure assignment of the cross-linked resonance as carbinolamine and not pyrimidopurinone was accomplished by annealing ^{15}N-labeled oligodeoxynucleotide with the complementary strand at pH 7. An ^{15}N-HSQC filtered NOESY spectrum revealed the presence of an NOE between X^7 $^{15}N^2H$ and the imino proton X^7 N1H, consistent with a carbinolamine assignment, but not a pyrimidopurinone, for the cross-linked species (Figure 3-3). Supporting evidence for the assignment of carbinolamine was derived from a triple resonance HCN experiment conducted after annealing ^{13}C-labeled oligodeoxynucleotide with ^{15}N-labeled complementary strand (data not shown). Cross-link formation resulted in bonding between the ^{15}N and ^{13}C isotopes. A correlation was observed between the 76 ppm γ-^{13}C resonance and a ^{15}N resonance at 106 ppm, establishing that carbininolamine cross-link observed in the ^{13}C experiments (Figure 3-2) arose from the same chemical species observed in ^{15}N HSQC experiments, and assigned as carbinolamine (Kim, H. Y. et al., 2002). The ~5 ppm ^{13}C chemical shift difference of carbinolamine as compared to cyclic adduct

was consistent with the expectation that the γ-^{13}C nuclei in APdG adduct and carbinolamine cross-link, both of which were bonded to hydroxyl groups, should exhibit similar chemical shifts.

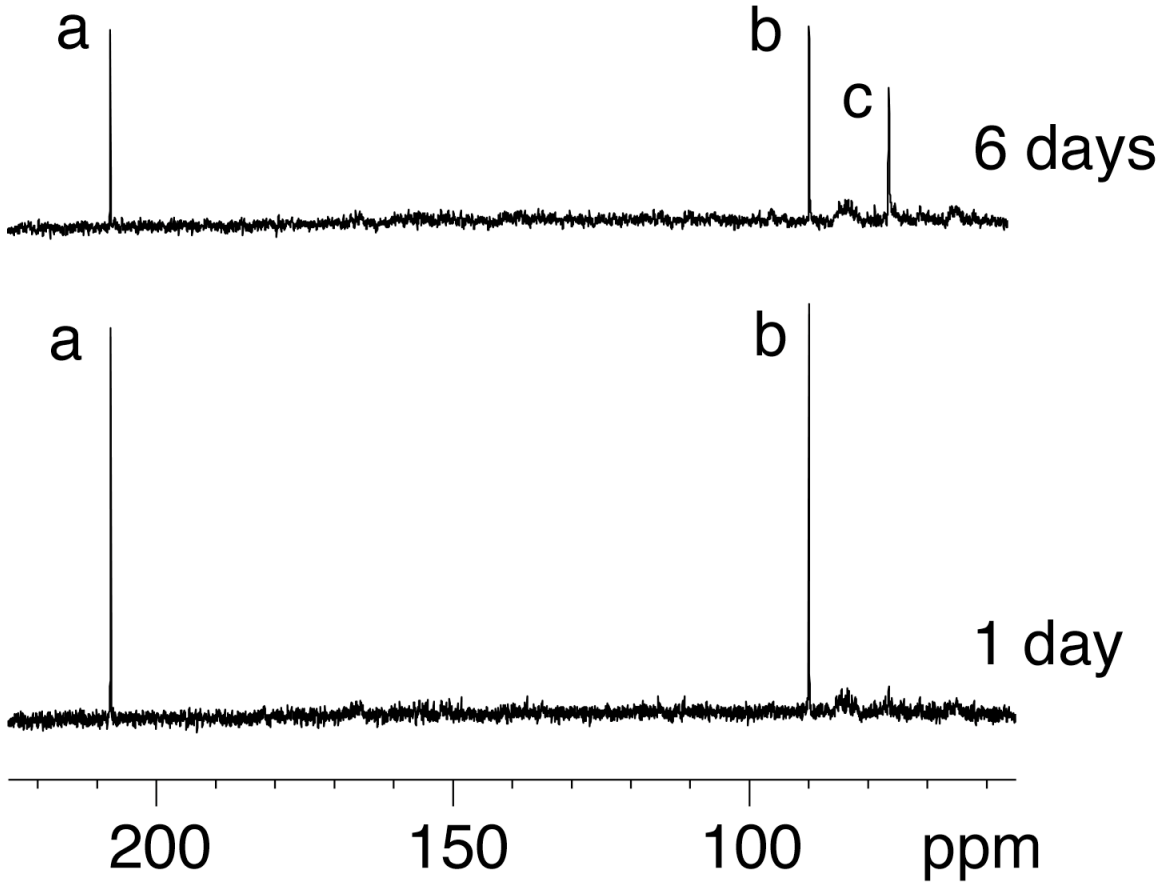

Figure 3-2. ^{13}C spectrum of oligodeoxynucleotide annealed with its complement to yield the duplex 5′-d(GCTAGCXAGTCC)-3′•5′-d(GGACTCGCTAGC)-3′, X= γ-^{13}C-OH PdG adduct. The bottom spectrum was collected in the first day after annealing the duplex. The top spectrum was collected after 6 days at 37 ºC. Assignments of resonances: (a) aldehyde; (b) hydrated-aldehyde; (c) carbinolamines

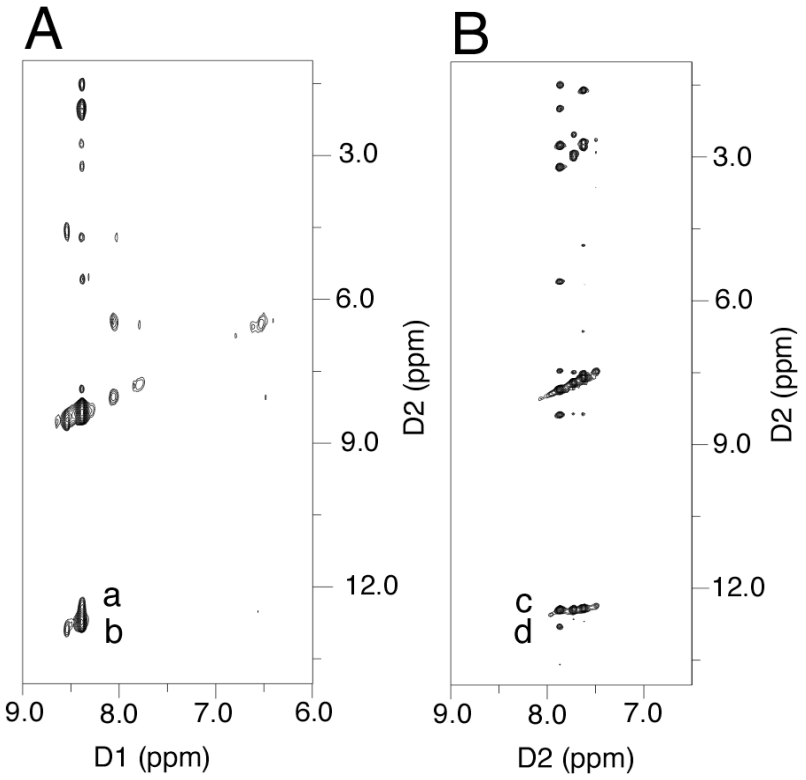

Figure 3-3. ^{15}N-NOESY HSQC spectra indicate that both base pairs in the 5′-CpG-3′ γ-OH-PdG induced interstrand cross-link remain intact. (A) ^{15}N-NOESY HSQC spectrum for $^{15}N^2$-dG labeled oligodeoxynucleotide annealed with its complement to yield the duplex 5′-d($G^1C^2T^3A^4G^5C^6\underline{X}^7A^8G^9T^{10}C^{11}C^{12}$)-3′•5′-d($G^{13}G^{14}A^{15}C^{16}T^{17}C^{18}\underline{Y}^{19}C^{20}T^{21}A^{22}G^{23}C^{24}$)-3′, X^7 = γ-OH-PdG adduct; Y = $^{15}N^2$-dG. Cross-peaks (a) Y^{19} $^{15}N^2$H→X^7 N1H (weak); (b) Y^{19} $^{15}N^2$H→ Y^{19} N1H (strong). (B) ^{15}N-NOESY HSQC spectrum for γ-OH-$^{15}N^2$-PdG labeled oligodeoxynucleotide annealed with its complement to yield the duplex duplex 5′-d($G^1C^2T^3A^4G^5C^6\underline{X}^7A^8G^9T^{10}C^{11}C^{12}$)-3′•5′-d($G^{13}G^{14}A^{15}C^{16}T^{17}C^{18}G^{19}C^{20}T^{21}A^{22}G^{23}C^{24}$)-3′, X^7 = γ-OH-$^{15}N^2$-PdG adduct. Cross-peaks (c) X^7 γ-OH-PdG $^{15}N^2$H→ X^7 γ-OH-PdG N1H (strong); (d) X^7 γ-OH-PdG $^{15}N^2$H→G^{19} N1H (weak).

Rate of Interstrand Crosslink Formation. An inverse-gated ^{13}C spectrum was obtained immediately upon annealing ^{13}C-labeled oligodeoxynucleotide with its complement. The γ-^{13}C resonances from aldehyde and hydrated aldehyde were detected, indicating that opening of APdG adduct was complete before the ^{13}C spectrum could be collected. The γ-^{13}C resonance assigned as carbinolamine cross-link was observed as a weak signal in the day 1 spectrum. It increased in intensity over a period of 6 days at 37 °C. The failure to observe a γ-^{13}C resonance in the 140-160 ppm spectral region, the range in which a resonance arising from γ-^{13}C imine would be anticipated, indicated that the amount of imine in equilibrium with carbinolamine was below the level of detection by ^{13}C NMR. This placed an upper limit on the amount of imine crosslink in equilibrium with carbinolamine crosslink, estimated to be ≤ 5%. At longer acquisition times, the natural abundance ^{13}C spectrum of the duplex oligodeoxynucleotide was observed.

Figure 3-4 shows the inverse-gated ^{13}C spectrum of the equilibrated sample as a function of temperature. At lower temperature, the intensity of the resonance arising from hydrated aldehyde increased, concomitant with a decrease in intensity of the resonance arising from aldehyde. At 37 °C, a 1:1 aldehyde: hydrated aldehyde ratio was observed, while a 1:2 aldehyde: hydrated aldehyde ratio was observed at 25 °C. Below the T_m of the duplex, the integrated area of the resonance arising from carbinolamine cross-link did not vary. It did, however, undergo line broadening as temperature was lowered. Above 65 °C thermal denaturation of the duplex oligodeoxynucleotide occurred and only the resonance arising from cyclic adduct was observed. No resonance arising from a transiently formed γ-^{13}C imine was detected through this range of temperature.

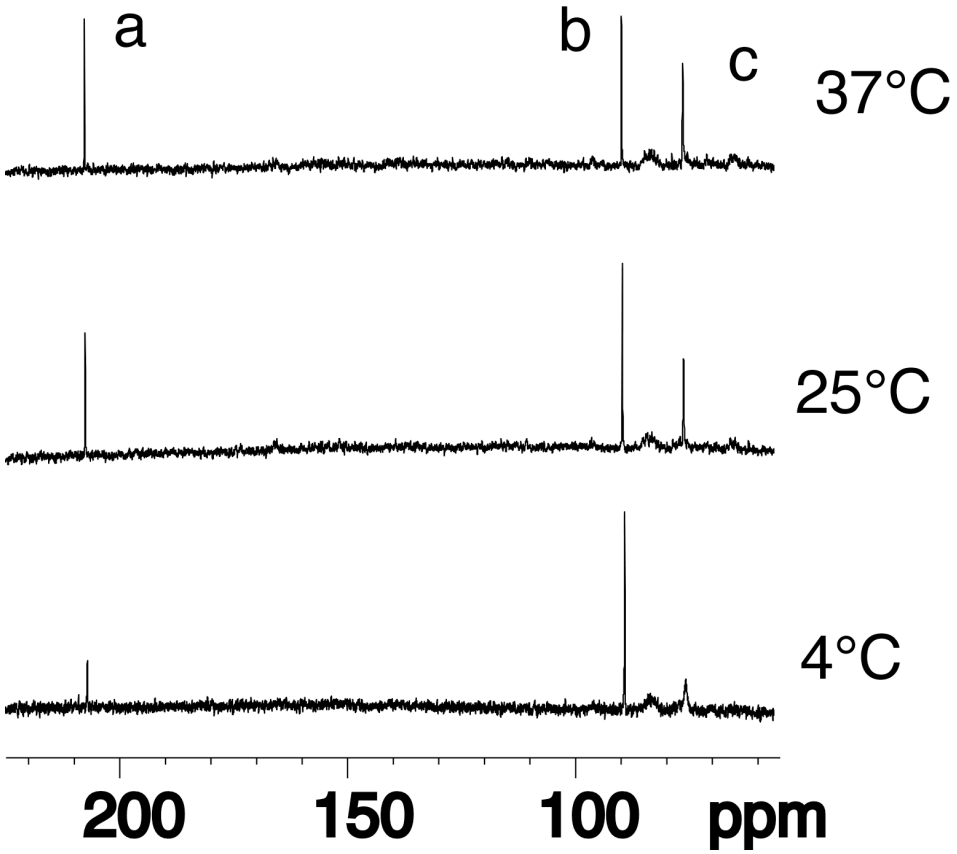

Figure 3-4. ^{13}C spectrum of oligodeoxynucleotide annealed with its complement to yield the duplex 5′-d(GCTAGCXAGTCC)-3′•5′-d(GGACTCGCTAGC)-3′, X= γ-^{13}C-OH PdG adduct, collected as a function of temperature. The bottom spectrum was collected at 4 °C, the middle spectrum, at 25 °C, and the top spectrum, at 37 °C. Assignments of resonances: (a) aldehyde; (b) hydrated-aldehyde; (c) carbinolamines.

Mispairing of T and dA Opposite the γ-OH-PdG Adduct. The acrolein γ-^{13}C-OH-PdG adducted oligodeoxynucleotide was annealed with the mismatched oligodeoxynucleotides placing a T opposite adduct in 5'-d(GCTAGCXAGTCC)-3'•5'-d(GGACTTGCTAGC)-3', and placing dA opposite adduct in 5'-d(GCTAGCXAGTCC)-3'•5'-d(GGACTAGCTAGC)-3', at pH 7. The degree of ring-opening to aldehyde and hydrated aldehyde was monitored by ^{13}C NMR (Figure 3-5). When placed opposite T, at equilibrium, a mixture of aldehyde, hydrated aldehyde, and cyclic adduct was observed. When placed opposite dA, no opening of cyclic adduct was observed.

Formation of DNA-Peptide Complexes by the γ-OH-PdG Adduct Placed Opposite to T and dA. Borohydride trapping probed for the presence of aldehyde in the mismatched duplex DNAs containing either dA or T opposite to cyclic adduct. The sing-strand oligodeoxynucleotide containing adduct was assayed as a reference. The 58-mer DNAs containing adduct were incubated with excess KWKK tetrapeptide in the presence of $NaCNBH_3$, and accumulation of the trapped DNA-peptide complexes was monitored using PAGE (Figure 3-6). In agreement with previous results (Kurtz and Lloyd, 2003), when adduct correctly paired with dC, it efficiently formed DNA-peptide complexes (data not shown). In reactions with single-stranded DNA, accumulation of DNA-peptide complexes was low (Figure 3-6) (Kurtz and Lloyd, 2003). When adduct was mispaired with T or dA, it also formed DNA-peptide complexes, albeit with different efficiencies. Specifically, initial rates of peptide cross-link formation

were 1.64, 0.14, and 0.27 fmol min^{-1} when cyclic adduct was mismatched opposite T, dA, or in single-stranded DNA, respectively.

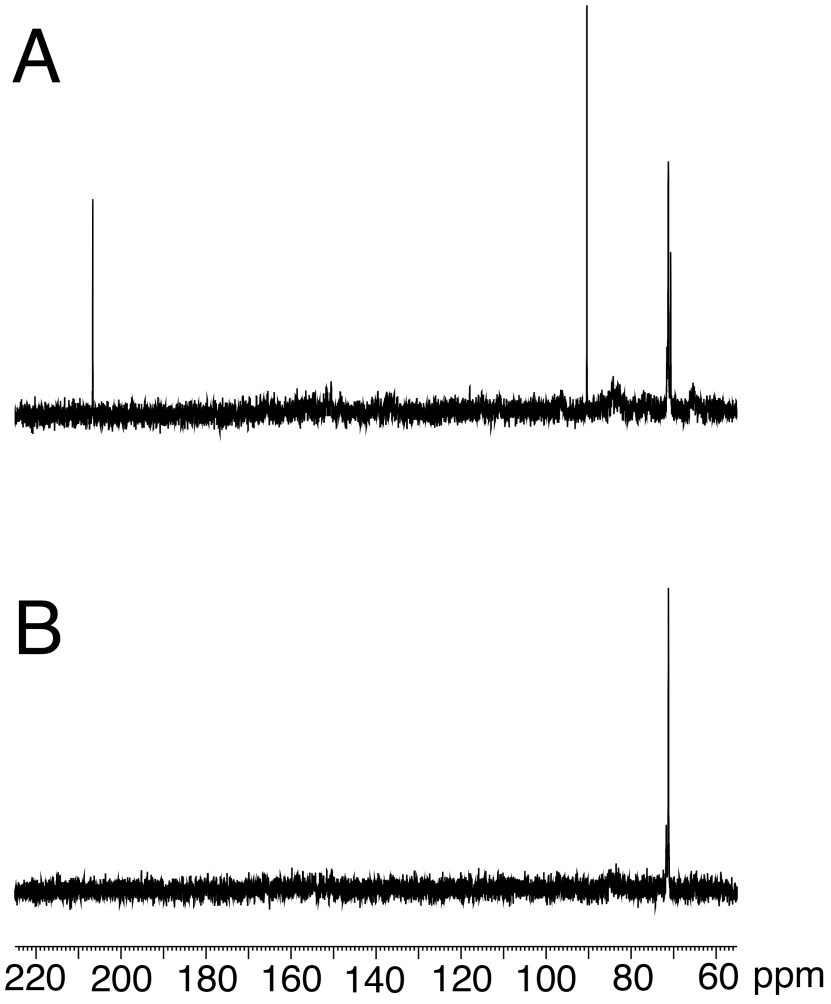

Figure 3-5. (A) ^{13}C spectrum of oligodeoxynucleotide annealed with its mismatched complement to yield the X•T duplex 5′-d(GCTAGCXAGTCC)-3′•5′-d(GGACTTGCTAGC)-3′, X= γ-^{13}C-OH PdG adduct. (B) ^{13}C spectrum of oligodeoxynucleotide annealed with its mismatched complement to yield the X•A duplex 5′-d(GCTAGCXAGTCC)-3′•5′-d(GGACTAGCTAGC)-3′, X= γ-^{13}C-OH PdG adduct.

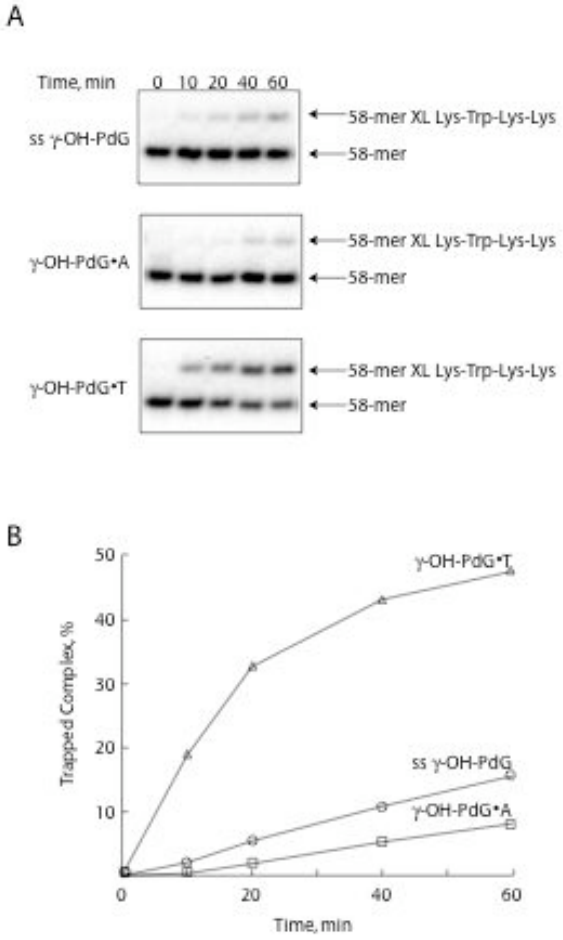

Figure 3-6. Accumulation of the trapped DNA-peptide complexes formed by OH-PdG modified oligodeoxynucleotides in single-stranded (ss γ-OH-PdG) and double-stranded DNAs containing either γ-OH-PdG•A or γ-OH-PdG•T mismatch. (A) PAGE analyses of the trapping reactions. The positions of the 58-mer oligodeoxynucleotides and the 58-mer oligodeoxynucleotides cross-linked with KWKK tetrapeptide are indicated. (B) Kinetic analyses of the accumkulation of the trapped complexes (By Lloyd lab).

Thermal Stability of the Interstrand Cross-Link. ^{15}N-labeled oligodeoxynucleotide was annealed with the complementary adducted oligodeoxynucleotide. A ^{15}N-NOESY-HSQC experiment (Mori et al., 1995; Talluri, 1996) revealed that the 5′ C•G base pair of the cross-link maintained Watson-Crick hydrogen bonding (Kim, H. Y. et al., 2002), which, as will be discussed below, was consistent with molecular modeling of carbinolamine. The T_m of the cross-linked duplex increased to 90 °C (Kozekov et al., 2003), in support of the molecular modeling studies and suggesting that carbinolamine stabilized the duplex with respect to thermal denaturation.

Molecular Modeling. Two diastereomers of the 5'-CpG-3' carbinolamine interstrand cross-link were modeled and compared to the corresponding unmodified oligodeoxynucleotide sequence. The model structures were subjected to potential energy minimization using the conjugate gradients algorithm in AMBER 8.0 (Figure 3-7). The potential energy minimization predicted that both diastereomers of carbinolamine cross-link maintained Watson-Crick hydrogen bonding at both of the tandem C•G base pairs involved in the interstrand cross-links. The modeling studies suggested that the sp^3 hybridization at the γ-carbon of the acrolein moieties allowed the cross-links to form without substantial perturbation of duplex structure. For the *S* diastereomer of the carbinolamine cross-link, the molecular modeling predicted the possibility of an additional hydrogen bond between the carbinolamine hydroxyl and N^3-dG of the 5' C•G base pair of the crosslink. In contrast, imine mandated sp^2 hybridization at the γ-carbon of the crosslink, which would require

breaking the Watson-Crick hydrogen bond between the amine proton of N^2-dG and O^2-dC of the 5' C•G base pair in the crosslink. Formation of either diastereomer of pyrimidopurinone cross-link prevented Watson-Crick hydrogen bonding at the 3' G•C base pair of the cross-link. It also disrupted Watson-Crick hydrogen bonding at the 5' C•G base pair of the cross-link, which, as noted above, was not consistent with ^{15}N-NOESY-HSQC NMR experiments revealing that the 5' C•G base pair of the cross-link was intact (Kim, H. Y. et al., 2002). The parameterization of the carbinolamine and the pyrimidopurinone cross-links, for the AMBER 8.0 forcefield, is provided in the Appendix A.

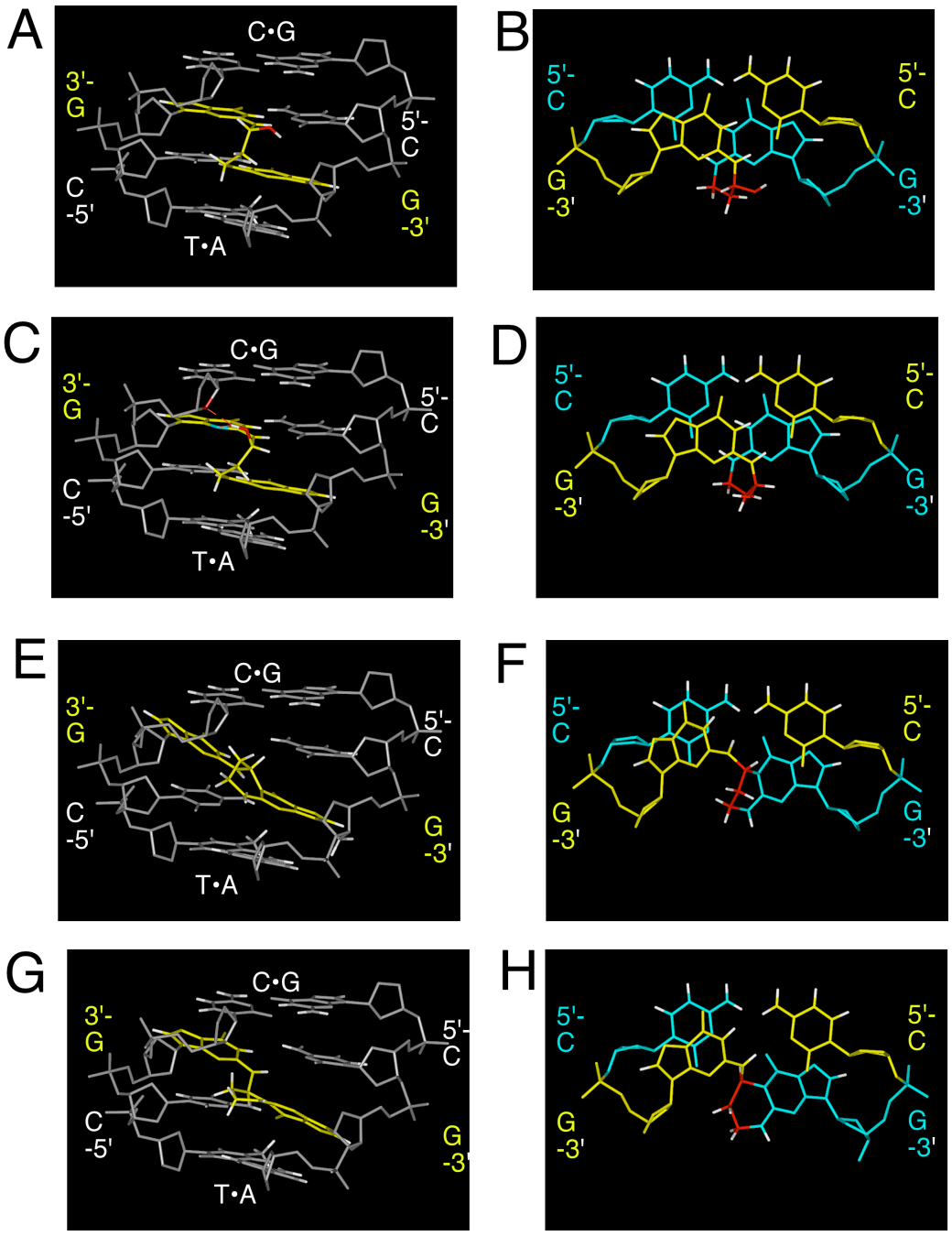

Figure 3-7. Molecular modeling studies acrolein-induced interstrand cross-linking in the 5′-CpG-3′ DNA sequence context. In all instances the 5′-flanking base pair to the 5′-CpG-3′ DNA sequence context is a C•G base pair; the 3′ flanking base pair is a T•A base pair. (A) *R*-diastereomer of carbinolamine cross-link, viewed from the minor groove. (B) *R*-diastereomer of carbinolamine cross-link, base stacking interactions. (C) *S*-diastereomer of carbinolamine cross-link, viewed from the minor groove. (D) *S*-diastereomer of carbinolamine cross-link, base stacking interactions. (E) *R*-diastereomer of pyrimidopurinone cross-link, viewed from the minor groove. (F) *R*-diastereomer of pyrimidopurinone cross-link, base stacking interactions. (G) *S*-diastereomer of pyrimidopurinone cross-link, viewed from the minor groove. (H) *S*-diastereomer of pyrimidopurinone cross-link, base stacking interactions.

Discussion

Epimerization of the γ-OH-PdG Adduct in the 5'-CpG-3' Sequence. In single-stranded DNA, γ-OH-PdG adduct existed as an equal mixture of two epimers. This suggested that in this 5'-CpXpA-3' single-stranded DNA sequence the two configurations of the γ-hydroxyl group were equally favored energetically. This was consistent with the notion that in the single-stranded DNA, there was little steric hindrance to either configuration due to the fact that the 1,N^2-cyclic ring faced away from the phosphodiester backbone. This contrasted with the situation in duplex DNA, in which the 1,N^2-cyclic ring of adduct clashed sterically with its complement and disrupted Watson-Crick hydrogen bonding. The failure to observe a γ-^{13}C resonance corresponding to ring-opened aldehyde in single-stranded DNA was consistent with the observation that at pH 7, cyclic adduct was favored as compared to ring-opened aldehyde. The data suggested that in single-stranded DNA, adduct spontaneously epimerizes, but slowly on the NMR time scale, without accumulation of aldehyde.

Ring Opening of the γ-OH-PdG Adduct in the 5'-CpG-3' Sequence. When placed into duplex DNA at pH 7 and 37 °C, with dC opposite γ-OH-PdG adduct, ring-opening yielded approximately equal amounts of aldehyde and hydrated aldehyde. De los Santos et al. reported two resonances for the H_γ proton of the ring-opened adduct, resonating at δ 9.58 ppm and δ 4.93 ppm, assigned as aldehyde and hydrated aldehyde (de los Santos, C. et al., 2001). The equilibrium ratio of aldehyde: hydrated aldehyde increased with temperature,

consistent with expectation. The presence of significant levels of aldehyde in the minor groove at pH 7 and 37 °C was significant with regard to its propensity for forming cross-links under physiological conditions.

Interstrand Cross-Link Exists as a Carbinolamine, *in situ*. It had been concluded that the interstrand acrolein cross-link must be comprised of an equilibrium mixture of carbinolamine, imine, and pyrimidopurinone. Carbinolamine was detected by ^{15}N HSQC NMR (Kim, H. Y. et al., 2002), and the presence of imine was inferred because the crosslink was reductively trapped in the presence of $NaCNBH_3$ (Kozekov et al., 2003; Kozekov et al., 2001). The present NMR studies show that the predominant form of the acrolein cross-link *in situ* is, in fact, carbinolamine. The amount of imine remained below the level of spectroscopic detection. Since the reduction of the interstrand cross-link occurred slowly in the presence of $NaCNBH_3$ (Kozekov et al., 2003; Kozekov et al., 2001), these data suggest that dehydration of carbinolamine to the reducible imine is rate limiting in duplex DNA. Enzymatic digestion of duplex DNA containing cross-link afforded a bis-deoxyguanosine conjugate, characterized by NMR as pyrimidopurinone arising from annelation of imine with N1-dG in the 5'-Cp*G*-3' sequence (Kozekov et al., 2003). The likely explanation is that the position of the equilibrium between carbinolamine, imine, and pyrimidopurinone depends on the conformational state of the DNA. Upon enzymatic degradation of duplex DNA, the equilibrium shifts to favor the pyrimidopurinone bis-nucleoside cross-link. The time required for cross-link to reach equilibrium at pH 7 and 37 °C was approximately 6 days, with approximately 40% cross-linking observed. These results corroborated studies in which the interstrand cross-linking reaction was

monitored by reverse-phase HPLC with gradient elution, using acetonitrile. In those studies, equilibrium was reached within 7 days, and cross-link was present at a level of approximately 50% (Kozekov et al., 2003).

DNA Duplex Maintains the Interstrand Carbinolamine Cross-Link. Molecular modeling provided a rationale as to why the carbinolamine interstrand cross-link predominated, *in situ*. It was predicted to conserve Watson-Crick hydrogen bonding at both of the tandem C•G base pairs, with minimal structural perturbation of the DNA duplex (Figure 3-7). The carbinolamine linkage maintained the N^2-dG amine proton, necessary for maintaining Watson-Crick hydrogen bonding at the 5'-side of the interstrand 5′-CpG-3′ cross-link. In addition, the carbinolamine hydroxyl group was predicted to be positioned such that it could allow an additional hydrogen bond at the 5'-side of the interstrand 5′-CpG-3′ cross-link. This provided an explanation as to both why elimination of water to form the reducible imine was disfavored in duplex DNA and why the reversible 5'-CpG-3' cross-link was extraordinarily stable with respect to thermal denaturation (Kozekov et al., 2003). Thus, the formation of imine was predicted to require disruption of Watson-Crick hydrogen bonding at both tandem C•G base pairs, whereas thermal strand dissociation to release the interstrand cross-link required breaking an additional hydrogen bond at the 5'-side of the interstrand cross-link. This was consistent with observations that oligodeoxynucleotides containing cross-link, once isolated, were relatively stable under conditions that maintained duplex DNA structure. However, they reverted completely to the single-stranded oligodeoxynucleotides within 1 h in unbuffered H_2O, conditions that favored

duplex denaturation (Kozekov et al., 2001). The molecular modeling predicted that formation of pyrimidopurinone cross-link in duplex DNA required disruption of Watson-Crick hydrogen bonding at both tandem C•G base pairs. It resulted in a distorted conformation of the duplex, which was not consistent with the thermal stabilization of the duplex DNA afforded by the cross-link.

Mispairing of the γ-OH-PdG Adduct. In the nucleoside, or in the single-stranded oligodeoxynucleotide, equilibrium between cyclic adduct and the ring-opened aldehyde or hydrated aldehyde adducts favored ring-closed adduct at neutral pH (Figure 3-1); under basic conditions ring-opening was favored (de los Santos, C. et al., 2001). In duplex DNA, when APdG adduct was placed opposite dC at neutral pH, opening of APdG adduct to the aldehyde or hydrated aldehyde adducts was favored (de los Santos, C. et al., 2001); *vide supra* (Figure 3-2). It is thought that when paired opposite dC at neutral pH, the equilibrium shifts because the aldehyde or hydrated aldehyde adducts orient into the minor groove, conserving Watson-Crick hydrogen bonding (de los Santos, C. et al., 2001).

Chemically, γ-OH-PdG adduct is similar to the pyrimidopurinone M_1dG adduct formed in DNA upon exposure to malondialdehyde (Basu et al., 1988; Marnett, L.J. et al., 1986; Reddy and Marnett, 1996; Seto et al., 1983; Seto et al., 1986) or base propenals (Dedon et al., 1998). When placed in duplex DNA opposite dC at neutral pH, M_1dG spontaneously opened to N^2-(3-oxopropenyl)-dG (OPdG) (Mao, H. et al., 1999). Similar to γ-OH-PdG adduct, it is thought that when paired opposite dC at neutral pH, the equilibrium between M_1dG and

OPdG favors the latter, because it orients into the minor groove, conserving Watson-Crick hydrogen bonding (Mao, H. et al., 1999; Mao, H. et al., 1999). However, in duplex DNA, the rate at which M_1dG converted to OPdG was negligible unless M_1dG was opposite dC in the complementary strand. When M_1dG was placed opposite T, rather than dC, OPdG did not form at a measurable rate, although OPdG itself was stable opposite T (Mao, H. et al., 1999). Likewise, when M_1dG was placed opposite a two-base bulge, conversion to OPdG was not observed (Schnetz-Boutaud et al., 2001). Riggins et al.(Riggins et al., 2004; Riggins et al., 2004) proposed that the N3-dC imine activates a molecule of water that then adds to the γ-carbon of M_1dG and catalyzes its conversion to OPdG.

Unlike M_1dG, the cyclic ring of γ-OH-PdG adduct is not conjugated with the purine ring of dG. Consequently, for γ-OH-PdG, the activation energy barrier with respect to interconversion between cyclic adduct and the aldehyde and hydrated aldehyde adducts is anticipated to be lower. The present results suggest that this is in fact the case. When γ-OH-PdG adduct was mispaired with T, an equilibrium mixture of cyclic adduct and the aldehyde and hydrated aldehyde adducts was observed (Figure 3-3), suggesting that the presence of dC in the complementary strand was no longer required to facilitate ring-opening.

When T was placed opposite APdG adduct, partial ring-opening was observed at equilibrium, indicating that opposite T, cyclic adduct and its ring-opened counterparts exhibit similar energetics in duplex DNA. It seems possible that when placed opposite T, the aldehyde and hydrated aldehyde adducts stabilize G•T wobble pairing. We surmise that γ-OH-PdG adduct re-orients into

the *syn* conformation about the glycosyl bond (Kim, H. Y. et al., 2002) when mispaired opposite T, placing the cyclic ring into the major groove, a position in which it does not clash sterically with the mispaired T. This may account for the observation that when placed opposite T, cyclic adduct and aldehyde and hydrated aldehyde adducts are in slow exchange on the NMR time scale. It is of interest to note that in the G•T wobble pair (Brown et al., 1985; Hare et al., 1986; Kalnik et al., 1988; Kennard, 1985; Kneale et al., 1985), the nucleophilic N1-dG imine of aldehyde adduct hydrogen bonds with O^2 of the mispaired T, positioning it to readily attack the carbonyl of aldehyde and re-cyclize to APdG adduct .

When dA was placed opposite APdG adduct, no ring-opening was observed at equilibrium, suggesting that, opposite A, the equilibrium in duplex DNA between APdG adduct and its ring-opened counterparts strongly favors the cyclic adduct. We surmise that when mispaired with dA, APdG adduct orients into the *syn* conformation about the glycosyl bond, thus placing the cyclic ring in the major groove and allowing the mispaired dA to hydrogen bond with the Hoogsteen edge of the modified dG in a G(syn)•A(anti) pair (Gao and Patel, 1988). In duplex DNA, the G(anti)•A(anti) (Kan et al., 1983 Jul; Patel, D. J. et al., 1984 Jul 3) and G(anti)•A(syn) (Hunter et al., 1986) mismatches have also been characterized as to structure. However, these conformations of the G•A mismatch utilize the N1-dG imine as a hydrogen bond donor, which is not possible for APdG adduct.

Formation of DNA-Peptide Complexes. Previous studies showed that γ-OH-PdG formed DNA–peptide cross-links mediated by aldehyde and the N-

terminal amines of peptides (Kurtz and Lloyd, 2003). These Schiff base intermediates were reduced by incubation with sodium cyanoborohydride. Thus, monitoring the formation of DNA–peptide complexes allows the presence of aldehydic DNA adduct to be probed. When APdG adduct was examined by ^{13}C HSQC NMR in single-stranded oligodeoxynucleotide (Figure 3-1), the two epimeric forms of the adduct were detected, but no aldehyde was observed. The presence of low levels of the aldehydic intermediate was inferred from the peptide trapping experiments (Figure 3-6), consistent with the slow epimerization of APdG adduct in single-strand DNA (Kurtz and Lloyd, 2003). Similarly, when placed opposite dA in duplex DNA, the amount of aldehyde remained below the level the level of detection by ^{13}C NMR (Figure 3-5). Nevertheless, the presence of low levels of the aldehyde intermediate can be inferred from the result of peptide trapping experiments (Figure 3-6). These data are consistent with the epimerization of APdG adduct.

CHAPTER IV

STEREOSPECIFIC FORMATION OF INTERSTRAND CARBINOLAMINE DNA CROSS-LINKS BY CROTONALDEHYDE- AND ACETALDEHYDE-DERIVED α-CH_3-γ-OH-1,N^2-PROPANO-2′-DEOXYGUANOSINE ADDUCT IN THE 5′-CpG-3′ SEQUENCE[†]

INTRODUCTION

Crotonaldehyde is one of α,β-unsaturated aldehydes, and is known to be one of major sources of exocyclic propano adducts that have relatively high prevalence in human DNA via exogenous and endogenous pathways such as lipid peroxidation and tobacco smoking (Chung, F.-L. et al., 1999; Nath, Raghu G. and Chung, 1994; Nath, Raghu G. et al., 1996). Michael type addition can lead the crotonaldehyde into two diastereomeric propano adducts based on the stereochemistry of the methyl group on α position: *R*- and *S*-α-CH_3-γ-OH-1,N^2-propano-2′-deoxyguanosine adducts (Figure 1-9) (Chung, F. L. and Hecht, 1983; Chung, F. L. et al., 1999; Eder et al., 1999). In comparison to the acrolein adducts, it does not provide any α- hydroxyl attached propano adducts (Chung, F.-L. et al., 1999; Nechev et al., 2001). Acetaldehyde, a mutagen and potential human carcinogen (IARC, 1999), can also form the diastereomeric *R*- and *S*-α-CH_3-γ-OH-1,N^2-propano-2′-deoxyguanosine adducts (Lao and Hecht, 2005; Wang et al., 2000).

After learning the molecular flexibility via ring-opening process with the presence of an opposite dC of the acrolein adduct in duplex DNA (Cho, Y.-J. et

[†] Reproduced in part with permission from *Chem. Res. Toxicol.* **2006**, 19, 195-208. . Copyright 2006 American Chemical Society.

al., 2004; de los Santos, Carlos et al., 2001; Kim, H.-Y. H. et al., 2002), the follow-up questions were arisen to the crotonaldheyde adducts including the possibility of generation of cross-links due to the similarity between APdG and CPdG adducts except the additional methyl group. As following the acrolein study in Chapter III, site-specifically synthesized *R*- and *S*-crotonaldehyde adducts in the same sequence of oligonucleotides were used and examined in duplex DNA. We could follow the cross-linking chemistry as well as the distribution of each species as shown in Scheme 1-4, *in situ* (Cho, Y.-J. et al., 2004; Nechev et al., 2001).

This chapter describes the spectroscopic studies that prove the enantioselective cross-link generation by substituted methyl group as well as structural hypothesis for the carbinolamine interstrand DNA cross-links.

Results

Epimerization of *R*- and *S*-α-CH_3-γ-OH-PdG Oilgodeoxynucleotide Adducts. The single stranded 5′-d(GCTAGCXAGTCC)-3′, modified with either *R*- or *S*-α-CH_3-γ-OH-PdG adducts, was examined using ^{13}C HSQC NMR (Figure 4-1). At pH 7 and 15 ºC, a single cross-peak was observed for *R*-CH_3-γ-OH-PdG adduct at a ^{13}C chemical shift of 71.9 ppm and a ^{1}H chemical shift of 5.96 ppm. This cross-peak was assigned as the epimer in which the α-CH_3 and γ-OH groups are in the trans configuration. For *S*-α-CH_3-γ-OH-PdG adduct, two cross-peaks were observed at pH 7 and 15 ºC. The major cross-peak was observed at a ^{13}C chemical shift of 71.5 ppm and a ^{1}H chemical shift of 5.89 ppm, also assigned as the epimer in which the α-CH_3 and γ-OH groups were in the trans configuration. The minor cross-peak was observed at a ^{13}C chemical shift of 71.6 ppm and a ^{1}H

chemical shift of 6.12 ppm. It was assigned as the hydroxyl epimer at the γ -carbon in which the α- CH_3 and γ-OH groups were in cis configurations. In both instances, as temperature was increased to 37 °C, increasing amounts of the cis epimers appeared in the ^{13}C-HSQC spectra, as measured by comparative volume integrations of the two resonances as a function of temperature. For *R*-α-CH3-γ-OH-PdG adduct, the cis epimer cross-peak was observed at a ^{13}C chemical shift of 71.3 ppm, and a ^{1}H chemical shift of 6.10 ppm. No resonances for opened forms (aldehyde or hydrated aldehyde) were observed, suggesting that at equilibrium, the levels of these ring-opened species remained below the spectroscopic limit of detection.

To detect the transient presence of aldehyds, a series of peptide trapping experiments were performed. The single-stranded oligodeoxynucleotide 5′-d(GCTAGCXAGTCC)-3′ containing either *R*- or a *S*-α-CH_3-γ-OH-PdG adduct was treated with the peptide KWKK for 0-120 min in the presence of $NaCNBH_3$. Reaction mixtures were quenched at the designated time points by adding $NaBH_4$ to reduce the aldehyde substrate. A gel-shifted complex was observed by denaturing PAGE analysis and designated as DNA-peptide cross-link (Figure 4-2; 12-mer + KWKK), consistent with the transient presence of aldehydes in single-stranded DNA. The accumulation of this product banc was monitored over a 2 h time course (Figure 4-2), at 4, 15, 37, or 50 °C. Higher temperatures facilitated faster formation of the peptide-DNA conjugate. At 4 °C, there was little complex accumulation over the 2 h time course, whereas at 50 °C a substantial amount of complex accumulated over this time period. These results were consistent with the NMR data, in which the rate of epimerization of the *R*-

or *S*-α-CH_3-γ-OH-PdG adducts increased at higher temperatures in single-stranded DNA.

On the millisecond time scale of the NMR experiments, the two epimers of the γ-hydroxyl groups of the 1,N^2-dG adducts were in slow exchange. A series of ^{13}C HSQC spectra collected as a function of temperature enabled van't Hoff analysis (Figure 4-3). These studies revealed that, for the *R*-adduct, the value of Δ*H* for the cis to trans interconversion was –14 kcal/mol and the value of Δ*S* for the interconversion was –42 cal/mol•K. For the *S*-adduct, the value of Δ*H* for the cis to trans interconversion was –10 kcal/mol and the value of Δ*S* for the interconversion was –29 cal/mol K.

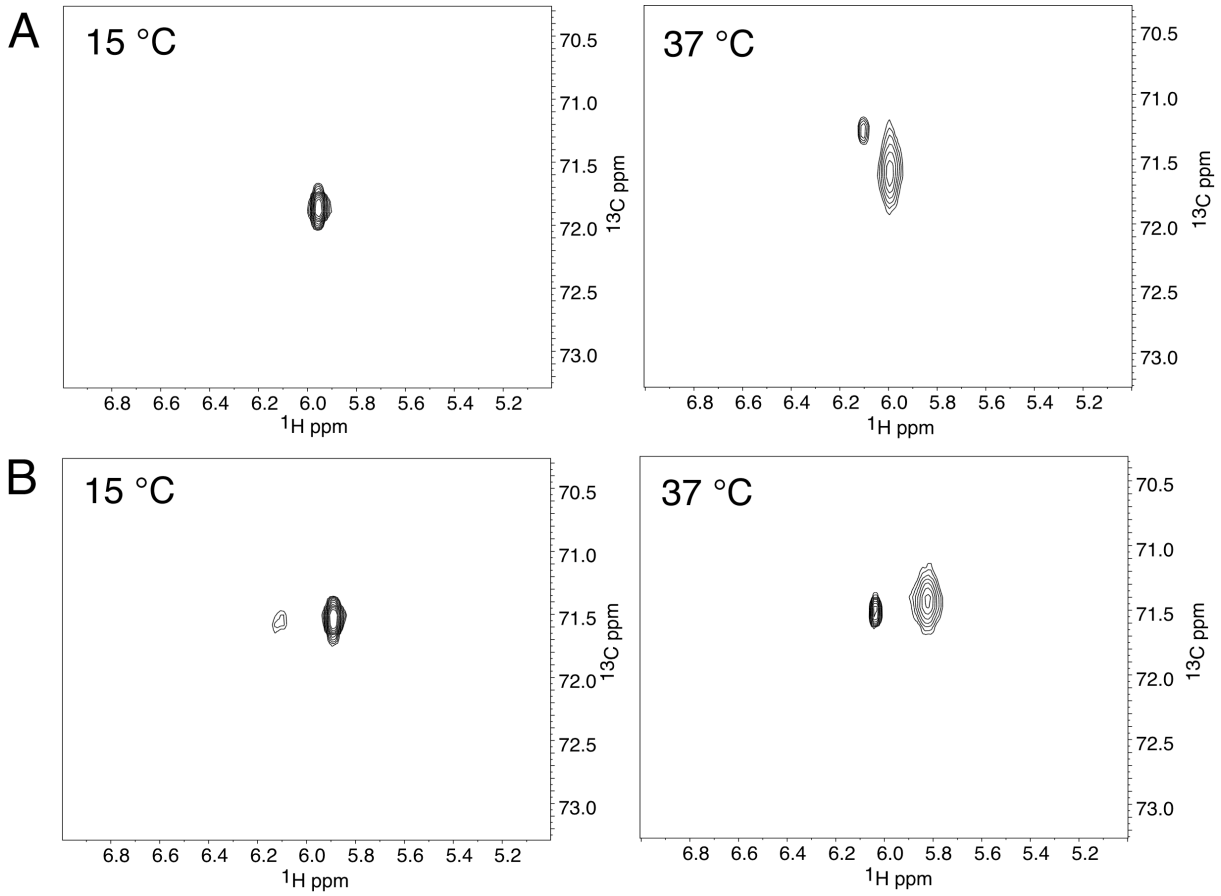

Figure 4-1. ^{13}C HSQC spectra of *R*-and *S*-α-CH_3-γ-OH-PdG adducts in the oligodeoxynucleotide 5′-d(GCTAGCXAGTCC)-3′ at 15 °C and 37 °C. A. *S*-α-CH_3-γ-OH-PdG adduct; B. *S*-α-CH_3-γ-OH-PdG adduct.

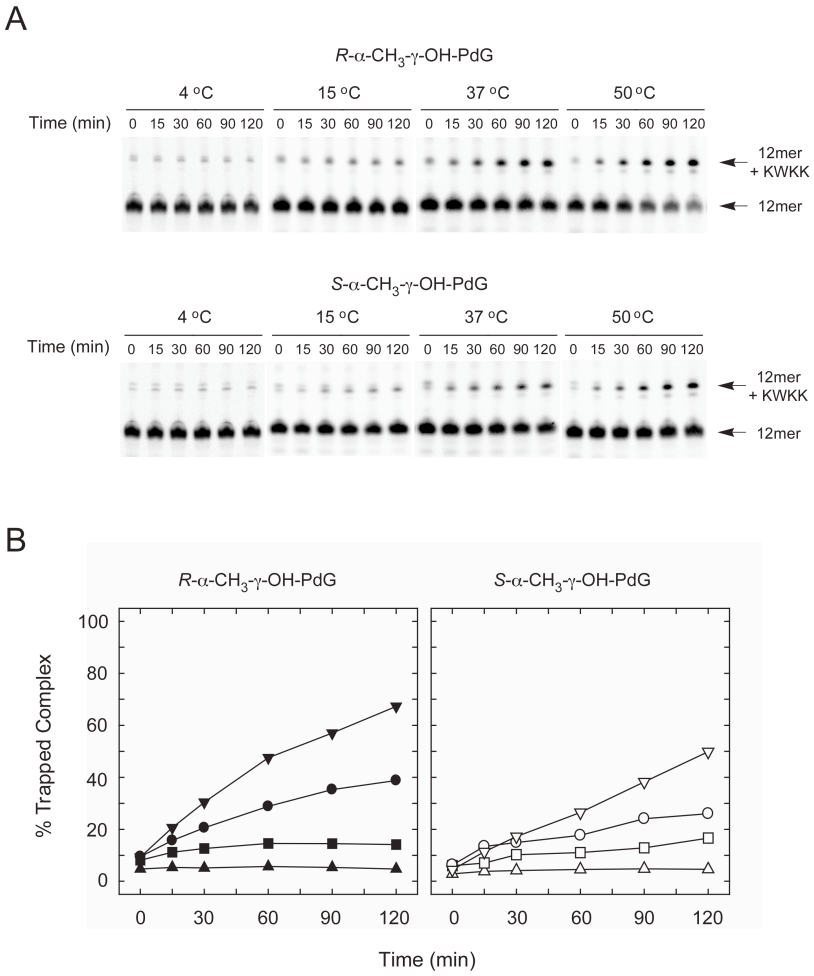

Figure 4-2. DNA—peptide cross-linking involving *R*- and *S*-α-CH_3-γ-OH-PdG adducts. **A.** For trapping reactions, single-stranded crotonaldehyde-adducted oligodeoxynucleotides (75 nM) were incubated with 1.0 mM KWKK the presence of 50 mM $NaCNBH_3$ at 4, 15, 37 or 50 °C. Reactions were carried out in 100 mM HEPES (pH 7.0) and 100 mM NaCl and were incubated for 0, 15, 30, 60, 90 or 120 min. Reactions were quenched at the end of the incubation period by the addition of 100 mM $NaBH_4$. Labels indicate the positions of the substrate 12-mer DNAs and the major reduced Schiff base conjugates (12-mer + peptide) following denaturing PAGE analysis. **B.** Kinetics of trapped conjugate formation are plotted over the 2 h time course at 4 °C (*R*-α-CH_3-γ-OH-PdG, π; *S*-α-CH_3-γ-OH-PdG, ρ), 15 °C (*R*-α-CH_3-γ-OH-PdG, ′; *S*-α-CH_3-γ-OH-PdG, ≤), 37 °C (*R*-α-CH_3-γ-OH-PdG, □; *S*-α-CH_3-γ-OH-PdG, □), and 50 °C (*R*-α-CH_3-γ-OH-PdG, θ; *S*-α-CH_3-γ-OH-PdG, σ) (By Lloyd lab).

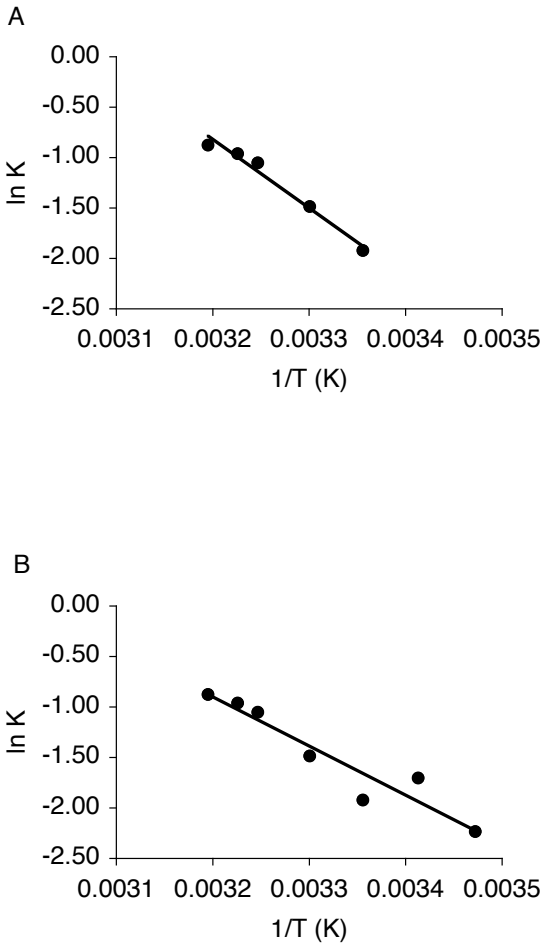

Figure 4-3. van't Hoff analysis of the epimerization of *R*-and *S*-α-CH_3-γ-OH-PdG adducts in the oligodeoxynucleotide 5′-d(GCTAGCXAGTCC)-3′. A. *R*-and *R*-α-CH_3-γ-OH-PdG adduct $\Delta H_{cis \rightarrow trans}$ = -14 kcal/mol; $\Delta S_{cis \rightarrow trans}$= -42 cal/molK. B. *S*-α-CH_3-γ-OH-PdG adduct. $\Delta H_{cis \rightarrow trans}$ = -10 kcal/mol; $\Delta S_{cis \rightarrow trans}$= -29 cal/molK.

Equilibrium Chemistry of the *R*-α-CH_3-γ-OH-PdG Adduct in Duplex DNA. The *R*-α-CH_3-γ-OH-PdG adduct was placed opposite dC in 5′-d(GCTAGCXAGTCC)-3′•5′-d(GGACTCGCTAGC)-3′ at pH 7, and the sample was allowed to equilibrate at 37 °C. An inverse-gated ^{13}C spectrum was obtained immediately upon annealing the duplex. The γ-^{13}C resonances from aldehyde and hydrated aldehyde were detected, indicating that opening of *R*-CPdG occurred before the ^{13}C spectrum could be collected. At pH 7, however, opening of the crotonaldehyde-derived 1,N^2-dG adduct to aldehyde and hydrated aldehyde was incomplete. After 20 days, no further spectroscopic changes were observed. At equilibrium, the γ-^{13}C resonance appeared as a mixture of four species (Figure 4-4). Furthest downfield, at 208 ppm, was a resonance assigned as γ-^{13}C aldehyde. A second γ-^{13}C resonance, assigned as hydrated aldehyde, was observed at 90 ppm. The third resonance, identified as carbinolamine cross-link, was observed at 73 ppm. This resonance increased in intensity over a period of 20 days at 37 °C. The two γ-hydroxyl diastereomers of cross-link were not resolvable in the ^{13}C spectrum, but were resolved using ^{1}H and ^{15}N NMR, as will be discussed below. The failure to observe a γ-^{13}C resoncance in the 140- 160 ppm spectral region, the range in which a resonance arising from γ-^{13}C imine would be anticipated, indicated that the amount of imine in equilibrium with carbinolamine in a duplex was below the level of detection by ^{13}C NMR. This placed an upper limit on the amount of 5′-CpG-3′ imine cross-link in equilibrium with carbinolamine cross-link estimated to be not more than 5 %. A fourth resonance, assigned as cyclic adduct (*R*-CPdG), was observed at 72 ppm. The ~1 ppm ^{13}C chemical shift difference of carbinolamine as compared to *R*-CPdG was

consistent with the expectation that the γ-^{13}C nuclei, in both cases, of which were bonded to hydroxyl groups, should exhibit similar chemical shifts.

Confirmation of the assignment of carbinolamine cross-link came from a series of ^{15}N HSQC, ^{15}N NOESY-HSQC, and ^{15}N TOCSY-HSQC experiments (Figure 4-5). The ^{15}N HSQC experiment revealed cross-peaks corresponding to the anticipated diastereomers of carbinolamine cross-link. The stronger of these two cross-peaks exhibited a ^{15}N chemical shift of 106 ppm and a ^{1}H chemical shift of 8.4 ppm. This cross-peak exhibited a 90 Hz coupling constant. The weaker of the two cross-peaks were observed at a ^{15}N chemical shift of 96 ppm and a ^{1}H chemical shift of 8.7 ppm. Two additional weaker cross-peaks in the ^{15}N HSQC spectrum were assigned as arising from noncross-linked oligodeoxynucleotide, in which $^{15}N^{2}$-dG-labeled base pair C^{6}•Y^{19} retained Watson-Crick hydrogen bonding. The cross-peak at 8.0 in the ^{1}H dimension was assigned as arising from the hydrogen-bonded amino proton, whereas that at 6.5 in the ^{1}H dimension arose from the nonhydrogen-bonded amino proton. An additional minor ^{15}N HSQC, labeled as peak e in Figure 4-5a, remained unidentified.

The ^{15}N-HSQC-filtered TOCSY experiment (Figure 4-5) established that the ^{1}H signal at 8.35 ppm, assigned as Y$^{19}N^{2}$H in carbinolamine cross-link, exhibited scalar coupling to protons of the cross-link crotonaldehyde moiety. The signal observed at 5.79 ppm indicated coupling to H_{γ} of the crotonaldehyde cross-link. Cross-peaks at 1.5 and 2.2 ppm were observed to $H_{\beta',\beta''}$ crotonaldehyde cross-link protons. No cross-peaks were observed for the minor diasteromer of the carbinolamine cross-link, presumably due to its low abundance.

A ^{15}N HSQC-filtered NOESY experiment (Figure 4-5) revealed that for the major diastereomer of cross-link, the Y^{19} *N*^{2}H→Y^{19} N1H NOE was observed at 12.8 ppm, in the expected chemical shift range for this imino proton involved in Watson-Crick hydrogen bonding. For the major diastereomer, NOEs were observed from Y^{19} *N*^{2}H to H_{α}, $H_{\beta',\beta''}$, H_{γ}, and the methyl protons of the crotonaldehyde cross-link. For the minor diastereomer of crosslink, the Y^{19} *N*^{2}H →Y^{19} N1H NOE was observed at 13.0 ppm, also in the expected chemical shift range for a Watson-Crick hydrogen-bonded imino proton.

The assignment of carbinolamine cross-link was corroborated by a triple resonance HNC experiment, in which the complementary strand of the duplex was site-specifically labeled with $^{15}N^{2}$-dG at the cross-linked dG residue (Figure 4-6). This experiment exploited the fact that cross-link formation resulted in bonding between the $^{15}N^{2}$-dG and the γ-^{13}C isotopes. A correlation was observed between the 73 ppm γ-^{13}C resonance and a ^{15}N resonance at 106 ppm, establishing that these resonances arose from the same chemical species observed in ^{15}N-HSQC experiments, and assigned as carbinolamine. No correlation was observed between the signal arising from the minor diastereomer observed at 96 ppm in the ^{15}N HSQC spectrum, and ^{13}C, presumably because of the low abundance of the minor diastereomer of cross-link observed in the ^{15}N HSQC experiments.[1]

[1] Furthermore, the ratio of each species is dependent on the temperature and the pH changes. In general, ring-closed form was favored at an acidic condition or higher temperature. At the higher temperature (65°C), the transition from the carbinolamine to the exocyclic adducts was detectable by HSQC experiments while the existence of imine was not (data not shown).

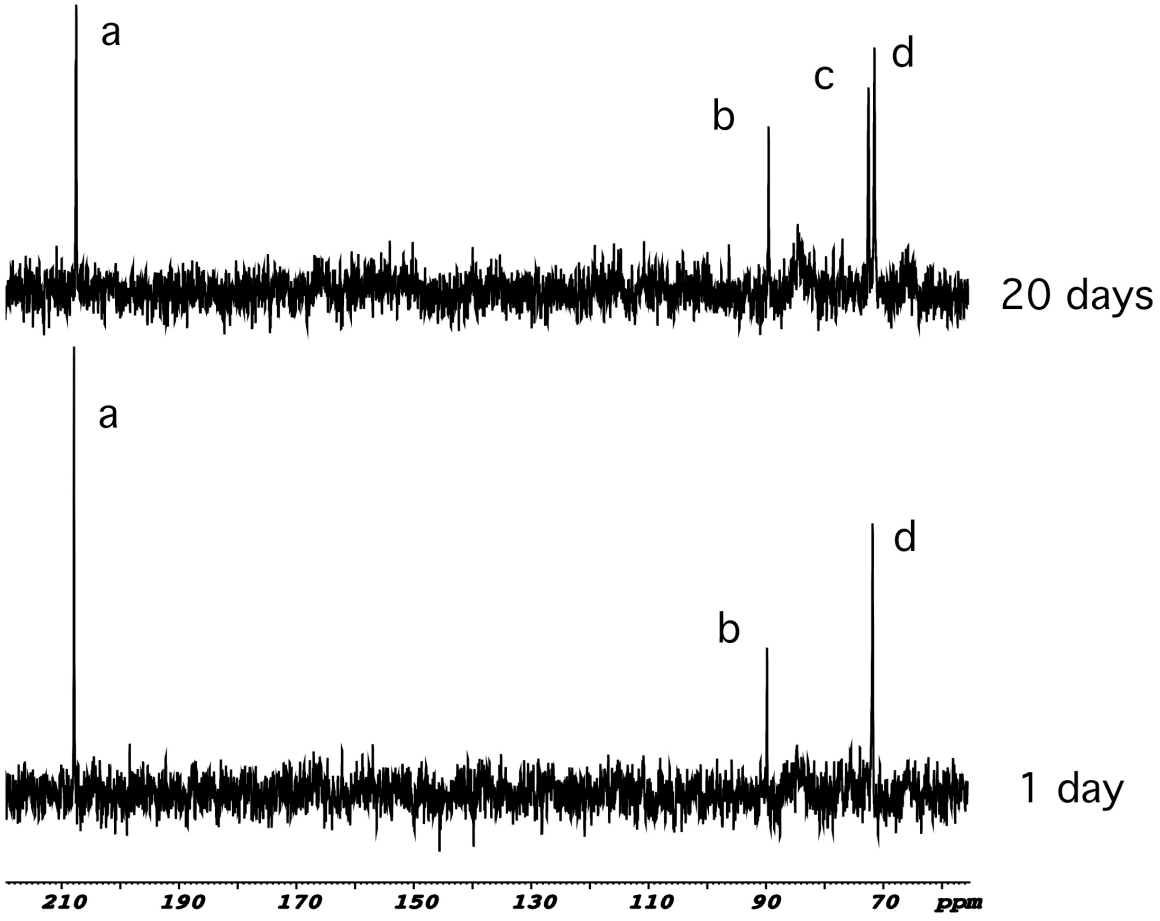

Figure 4-4. ^{13}C NMR spectra of oligodeoxynucleotide annealed with its complement to yield the duplex 5′-d(GCGAGCXAGTCC)-3′•5′-d(GGACTCGCTAGC)-3′, X= *R*-α-CH_3-γ-^{13}C-OH-PdG adduct. The bottom spectrum was collected in the first day after annealing the duplex. The top spectrum was collected after 6 days at 30 °C. Assignments of resonances: a, aldehyde; b, hydrated-aldehyde; c, carbinolamines; d, cyclic adduct.

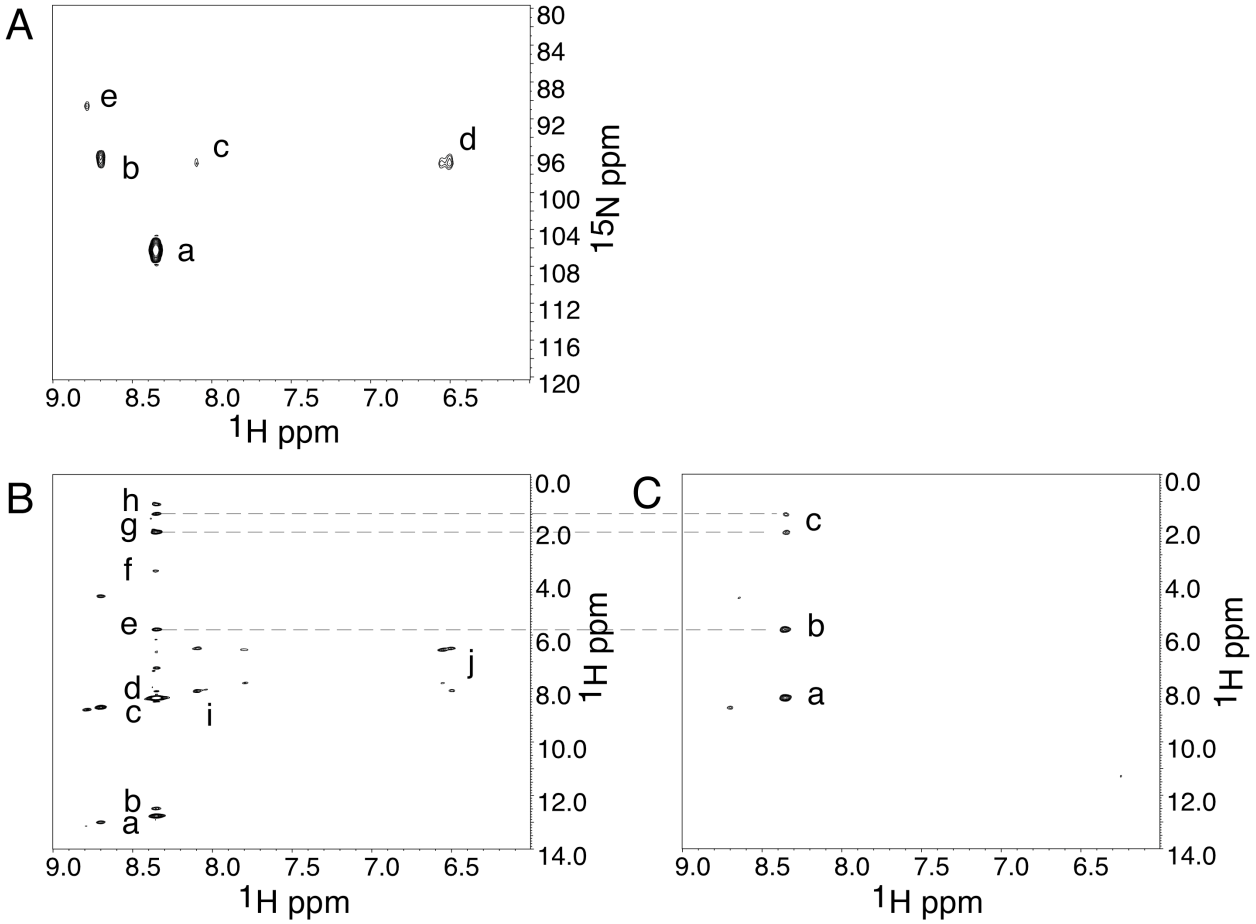

Figure 4-5. A . ^{15}N HSQC spectrum of *R*-α-CH_3-γ-OH-PdG in the oligodeoxynucleotide 5'-d(GCTAGCXAGTCC)-3'•5'-d(GGACTCYCTAGC)-3'. Cross-peaks: a, major stereoisomer of the carbinolamine cross-link; b, minor stereoisomer of the carbinolamine cross-link; c and d, hydrogen- and nonhydrogen-bonded $^{15}N^2$H protons of non-cross-linked base pair C^6•Y^{19}; e, unidentified cross-peak. **B.** ^{15}N NOESY HSQC spectrum. Cross-peaks: a, Y^{19} $^{15}N^2$H→Y^{19} N1H; b, Y^{19} $^{15}N^2$H→X^7 N1H; c, Y^{19} $^{15}N^2$H autocorrelation; d, Y^{19} $^{15}N^2$H→X^7 N^2H; e, Y^{19} $^{15}N^2$H→H_g; f, Y^{19} $^{15}N^2$H→H_a; g, Y^{19} $^{15}N^2$H→$H_{b'b''}$; h, Y^{19} $^{15}N^2$H→a-CH_3; I and j, hydrogen-and nonhydrogen-bonded $^{15}N^2$H protons of noncross-linked pair C^6•Y^{19}. **C.** ^{15}N TOCSY HSQC spectrum. Cross-peaks: a, autocorrelation peak for major stereoisomer of carbinolamine cross-link; b, coupling to H_g; and c, couplings to $H_{b',b''}$, two resonances.

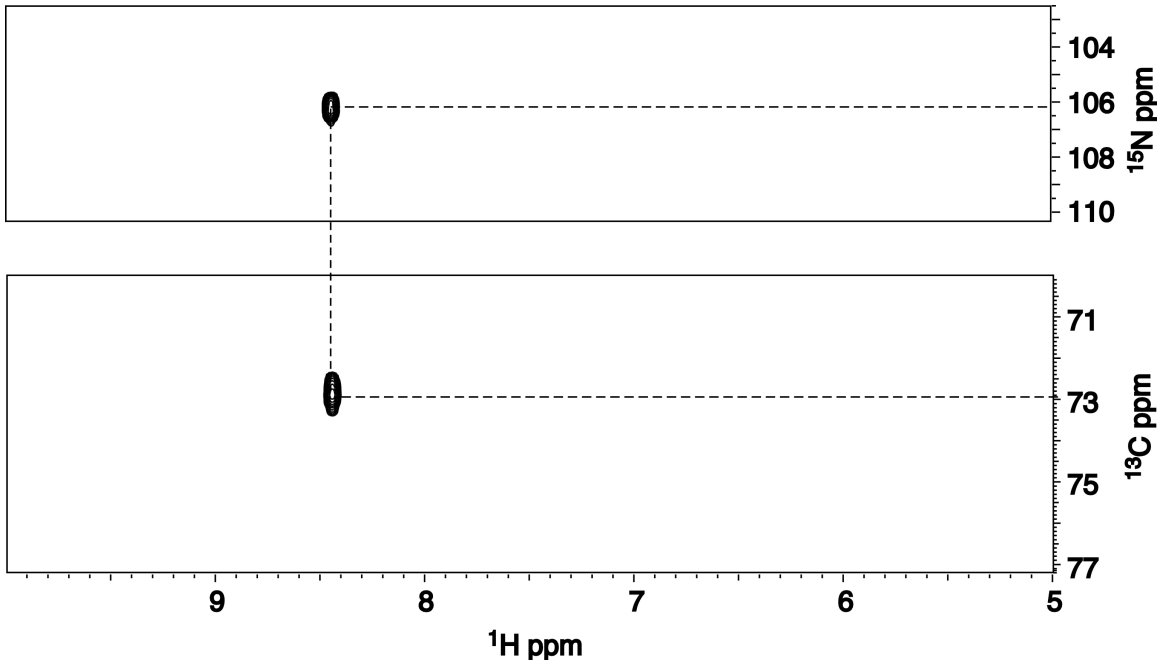

Figure 4-6. Triple resonance $^{1}H^{15}N^{13}C$ spectrum of *R*-α-CH_3-γ-OH-PdG in the oligodeoxynucleotide 5'-d(GCTAGCXAGTCC)-3'•5'-d(GGACTCYCTAGC)-3', confirming the presence of cross-linked carbinolamine.

Equilibrium Chemistry of the *S*-α-CH_3-γ-OH-PdG Adduct in Duplex DNA. The *S*-α-CH_3-γ-^{13}C-OH-PdG adduct differed from the *R*-α-CH_3-γ-^{13}C-OH-PdG adduct. At equilibrium, only low levels of interstrand cross-links were observed in the 5′-CpG-3′ sequence, as demonstrated by reductive trapping with $NaCNBH_4$ (Kozekov et al., 2003). The *S*-α-CH_3-γ-^{13}C-OH-PdG adduct was placed opposite dC in 5′-d(GCTAGCXAGTCC)-3′•5′-d(GGACTCGCTAGC)-3′ at pH 7 and 37 °C. Similar to the *R*-α-CH_3-γ-^{13}C-OH-PdG adduct, the γ-^{13}C resonances from aldehyde and hydrated aldehyde were detected. Thus, opening of cyclic adduct occurred before the ^{13}C spectrum could be collected. At pH 7, opening of crotonaldehyde-derived 1,N^2-dG adduct to aldehyde and hydrated aldehyde was incomplete. After 20 days, both the *R*-α-CH_3-γ-^{13}C-OH-PdG and the *S*-α-CH_3-γ-^{13}C-OH-PdG exhibited similar quantities of the cyclic adducts in equilibrium with aldehyde and hydrated aldehyde, suggesting that the positions of the equilibria involving the cyclic adducts and their ring-opened converted products were independent of stereochemistry at C_α of the crotonaldehyde moiety. Significantly, however, and corroborating the reductive trapping experiments (Kozekov et al., 2003), ^{13}C NMR failed to detect carbinolamine cross-link, confirming that formation of the interstrand cross-link in the 5′-CpG′-3′ sequence was dependant upon stereochemistry at C_α of the crotonaldehyde moiety.

Figure 4-7 shows the ^{13}C NMR spectrum of the *S*-α-CH_3-γ-^{13}C-OH-PdG adduct when placed opposite dC in 5′-d(GCTAGCXAGTCC)-3′•5′-d(GGACTCGCTAGC)-3′ at 37 °C, at pH values of 4.7, 9.3, and 10.7. At pH 4.7, the equilibrium between cyclic adduct (1,N^2-dG adduct) and N^2-(3-oxopropyl)-dG (*S*-COPdG) aldehyde and its hydrate favored cyclic adduct. Increasing the

pH to 9.3 favored formation of *S*-COPdG aldehyde and its hydrate. At pH 10.7, denaturation of the oligodeoxynucleotide duplex occurred, and only cyclic adduct was observed.

Mispairing of T Opposite the *S*-α-CH_3-γ-OH-PdG Adduct. Figure 4-8 shows the ^{13}C NMR spectrum of the *S*-α-CH_3-γ-^{13}C-OH-PdG adduct when placed opposite T in 5′-d(GCTAGCXAGTCC)-3′•5′-d(GGACTTGCTAGC)-3′ at 37 °C and pH 7. Under these conditions, cyclic adduct was favored, with *S*-COPdG aldehyde and its hydrate remaining below the level of detection by ^{13}C NMR.

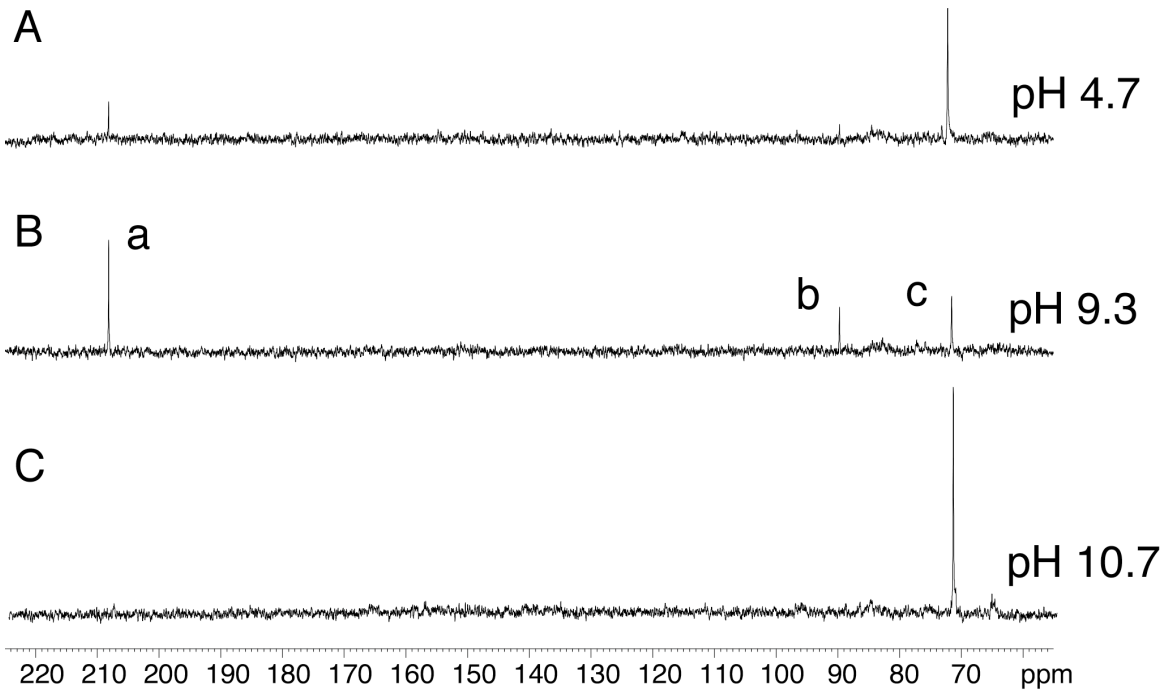

Figure 4-7. Chemical species arising from *S*-α-CH_3-γ-OH-PdG in the oligodeoxynucleotide 5'-d(GCTAGCXAGTCC)-3'•5'-d(GGACTCYCTAGC)-3' as a function of pH. A. pH 9.3, B. pH 10.7, and C. pH 4.7. Cross-peaks: a, aldehyde; b, hydrated aldehyde; and c, cyclic adduct.

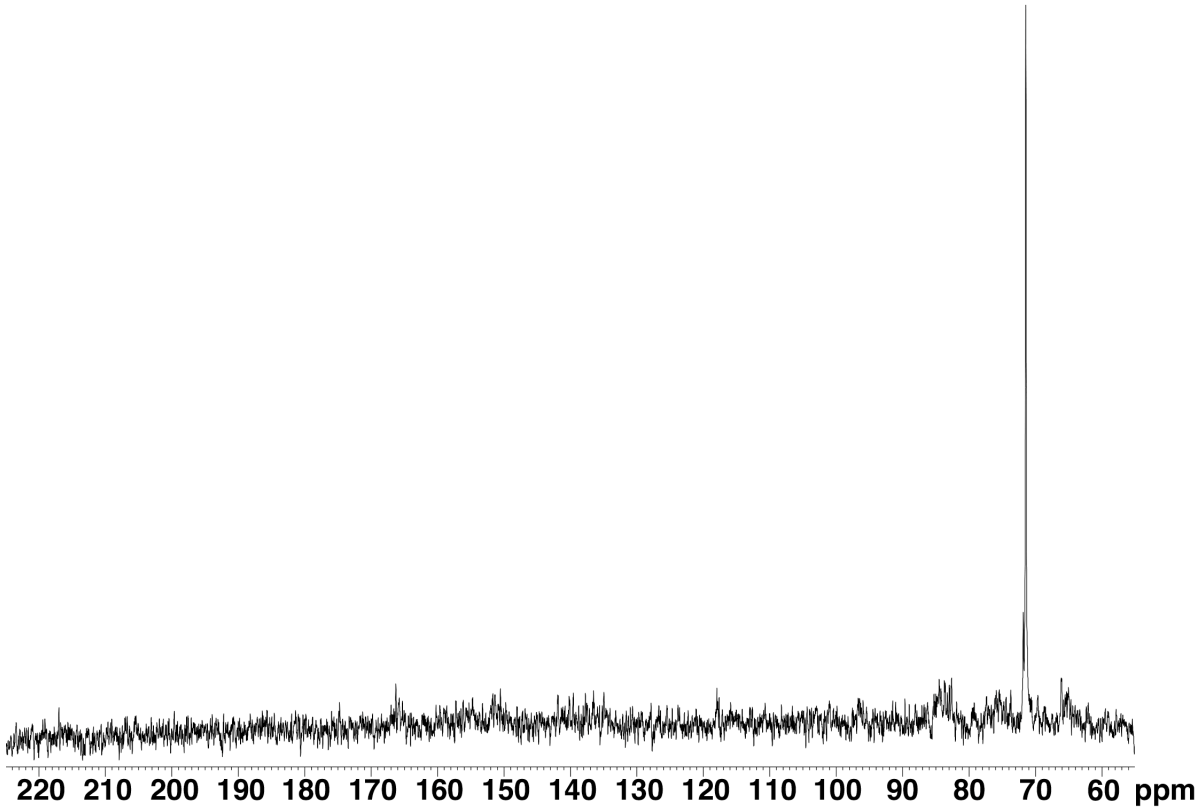

Figure 4-8. ^{13}C NMR of *S*-α-CH_3-γ-OH-PdG in the oligodeoxynucleotide 5'-d(GCTAGCXAGTCC)-3'•5'-d(GGACTTGCTAGC)-3'. Only cyclic adduct is observed.

Molecular Modeling. The two carbinolamine cross-links arising from interstrand cross-linking by *R*- and *S*-α-CH_3-γ-OH-PdG, respectively, were modeled in 5′-d(GCTAGCXAGTCC)-3′•5′-d(GGACTCGCTAGC)-3′. Starting conformations for the energy minimizations were built such that there were no bad steric contacts between the cross-links and the DNA duplex. The model structures were subjected to potential energy minimization using the conjugate gradients algorithm in AMBER 8.0 (Figure 4-9). The potential energy minimization suggested that for cross-link arising from *R*-CPdG, the methyl group projected into the minor groove, without disruption of duplex DNA structure. In contrast, the calculations suggested that for cross-link arising from *S*-CPdG, the methyl group interfered with the 3′-neighbor base pair A^8•T^{17}, presumably reducing the stability of the cross-linked duplex.

Additionally, the two COPdG aldehydes were modeled in the same sequence and compared to the corresponding AOPdG aldehyde, lacking the sterocenter at C_α of the AOPdG (Figure 4-10). The model structures were subjected to potential energy minimization using the conjugate gradients algorithm in AMBER 8.0. The potential energy minimization suggested that all OPdG aldehydes maintained Watson-Crick hydrogen bonding at both base pairs C^6•Y^{19} and X^7•C^{18} involved in the interstrand 5′-CpG-3′ cross-links. The modeling studies suggested that for the *R*-COPdG aldehyde, the C_α methyl group oriented within the minor groove in the 3′-direction from the adducted nucleotide X^7. This oriented the reactive aldehyde group into the 5′-direction, placing it proximate to the cross-linking target N^2-dG in base pair C^6•Y^{19}. The favored orientation of the corresponding acrolein-derived N^2-(3-oxopropyl)-dG

aldehyde was similar, placing the aldehyde group in the 5′-direction, proximate to the cross-linking target N^2-dG in base pair C^6•Y^{19}. In contrast, the modeling studies suggested that for the *S*-COPdG aldehyde, the C_α methyl group oriented within the minor groove in the 5′-direction from the adducted nucleotide X^7. This oriented the aldehyde group in the 3′-direction, placing it distal to the cross-linking target N^2-dG in base pair C^6•Y^{19}.

The two γ-hydroxyl diastereomers of the 5′-CpG-3′ carbinolamine cross-link arising from *R*-CPdG adduct were modeled and compared to the corresponding unmodified oligodeoxynucleotide sequence. The model structures were subjected to potential energy minimization using the conjugate gradients algorithm in AMBER 8.0 (Figure 4-11). The potential energy minimization predicted that both diasteromers of carbinolamine cross-link maintained Watson-Crick hydrogen bonding at both of the tandem C•G base pairs involved in the interstrand carbinolamine cross-links. The modeling studies suggested that the sp^3 hybridization at the γ-carbon allowed the cross-links to form without substantial perturbation of duplex structure. For the *S*-diastereomer of the carbinolamine cross-link, the molecular modeling predicted an additional hydrogen bonds between the carbinolamine hydroxyl and the N3-dG of the 5′ C•G base pair of the cross-link.[2] In contrast, the imine in cross-link mandated sp^2 hybridization of the amino group, which would require breaking the Watson-Crick hydrogen bond between the amine proton of N^2-dG and O^2-dC of the 5′-C•G base pair in the cross-link. Formation of either diastereomer of pyrimidopurinone cross-link prevented Watson-Crick hydrogen bonding at the

[2] The hydrogen bonds between carbinolamine hydroxyl and the oxygen in the sugar ring of C^{20} is also possibly suggested.

3′-G•C base pair of the cross-link. It also disrupted Watson-Crick hydrogen bonding at the 5′-C•G base pair of the cross-link. The parameterization of the carbinolamine and the pyrimidopurinone cross-links, for the AMBER 8.0 forcefield, are provided in Appendix A.

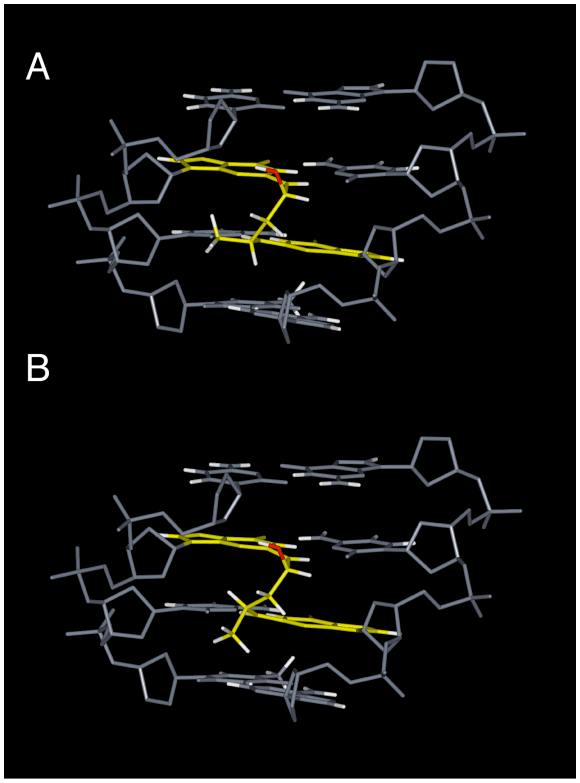

Figure 4-9. Molecular modeling of carbinolamine interstrand cross-links formed in the 5'-CpG-3' sequence by the *R*- and *S*-α-CH_3-γ-OH-PdG adducts **A.** Cross-link formed by *R* adduct. **B.** Cross-link formed by *S* adduct.

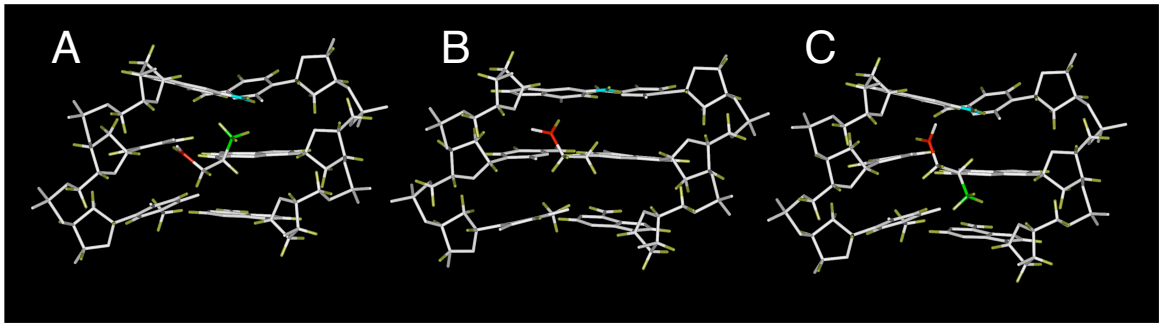

Figure 4-10. Molecular modeling of aldehydes formed in duplex DNA when adducts are placed opposite dC in the complementary strand. **A.** *S*-COPdG aldehyde arising from *S*-α-CH_3-γ-OH-PdG adduct, illustrating the 5'-minor groove orientation of the a -carbon methyl group. **B.** The N^2-(3-oxo-propyl)-dG aldehyde formed by the acrolein-derived g-OH-PdG adduct in duplex DNA. **C.** *R*-COPdG aldehyde arising from *R*-α-CH_3-γ-OH-PdG adduct, illustrating the 3'-minor groove orientation of the a-carbon methyl group.

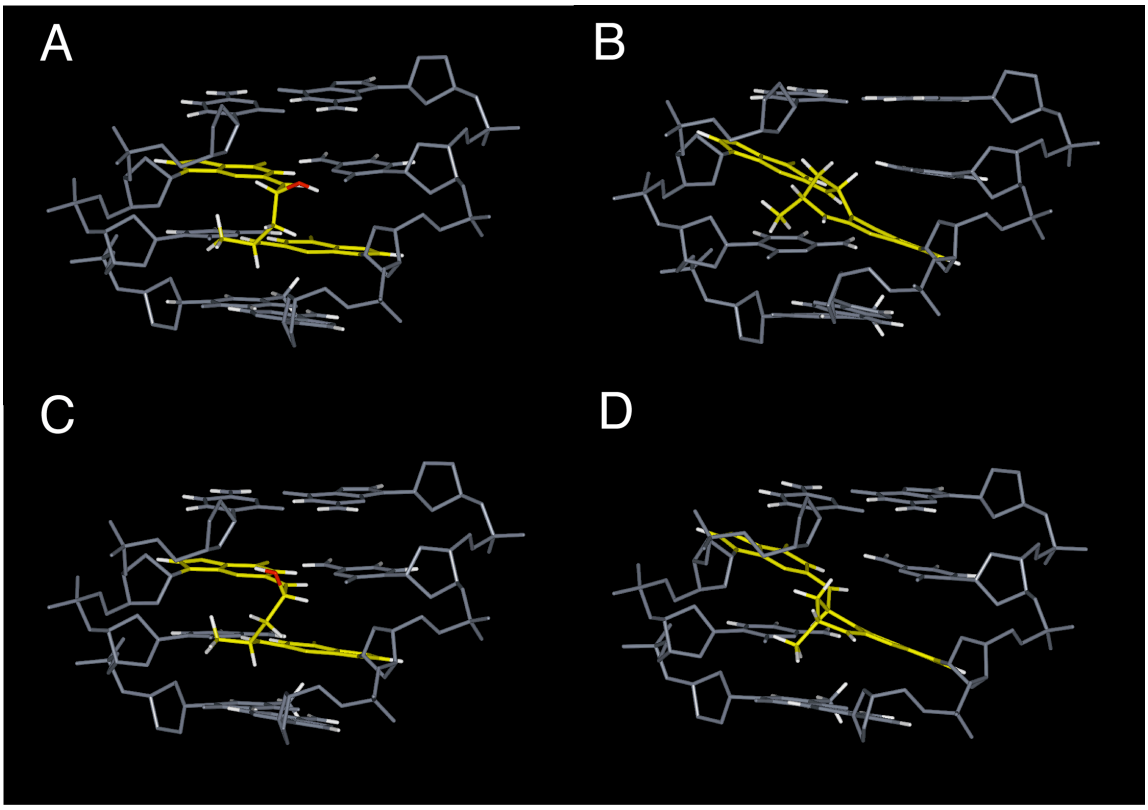

Figure 4-11. Molecular modeling of diastereomeric carbinolamine and pyrimidopurinone cross-links formed by *R*-COPdG aldehyde, arising from *R*-α-CH_3-γ-OH-PdG adduct. **A.** The *R*-diastereomer at the α-carbon of the carbinolamine cross-link. **B.** The *R*-diastereomer at the α-carbon of the pyrimidopurinone cross-link. **C.** The *S*-diasteromer at the α-carbon of the carbinolamine cross-link. **D.** The *S*-diastereomer at the α-carbon of the pyrimidopurinone cross-link.

Discussion

Epimerization of the Stereoisomeric *R*- and *S*-α-CH_3-γ-OH-PdG Adducts in the 5′-CpG-3′ Sequence. At equilibrium in single-stranded DNA, the *R*- and *S*-CPdG adducts existed as mixtures of diastereomers of the 1,N^2-dG adduct at C_γ, in slow exchange on the NMR time scale. In both instances, the trans orientation of the α-CH_3 and γ-OH groups predominated. This observation was consistent with previous observations in the NMR spectra of the nucleosides (Eder and Hoffman, 1992; Eder and Hoffman, 1993). This differed from the acrolein-derived γ-OH-PdG adduct lacking the CH_3 group at C_α, which exhibited equal amounts of both epimers.

The failure to observe a γ-^{13}C resonance corresponding to ring-opened aldehydes in single-stranded DNA was consistent with the observation that at pH 7 cyclic adducts were favored as compared to ring-opened aldehydes. The NMR data suggested that in single-stranded DNA, CPdG adducts spontaneously epimerized but slowly on the NMR time scale, without accumulation of aldehydes. Nevertheless, the peptide-trapping data revealed the transient presence of the aldehydes (Figure 4-2).

Ring Opening of the *R*- and *S*-α-CH_3-γ-OH-PdG Adducts in Duplex DNA in the 5′-CpG-3′ Sequence. For both the *R*- and *S*-CPdG adducts, the presence of duplex DNA was required for the stable formation of the aldehydes, as observed for the acrolein-derived γ-OH-PdG adduct (de los Santos, Carlos et al., 2001). In duplex DNA, the aldehydes, and their hydrates, similar to the acrolein γ-OH-PdG adduct (de los Santos, Carlos et al., 2001) and the

malondialdehyde M_1dG adduct (Mao, H. et al., 1999; Mao, H. et al., 1999), are accommodated in the minor grove of DNA, enabling maintenance of Watson-Crick hydrogen bonding at the adducted base pair. Significantly, in comparing the chemistry of the *R*- and *S*-CPdG adducts when placed into duplex DNA opposite dC at pH 7 with the corresponding acrolein-derived APdG (de los Santos, Carlos et al., 2001), ring opening of the *R*- and *S*-CPdG adducts to the aldehydes and the hydrated aldehydes was incomplete. As described previous chapter, when the APdG adduct was placed opposite dC in duplex DNA, equilibrium favored the ring-opened AOPdG aldehyde and its hydrate, to the extent that the APdG cyclic adduct was no longer detected (de los Santos, Carlos et al., 2001). The incomplete opening of the *R*- and *S*-CPdG adducts in duplex DNA, when placed opposite dC, might be explained by the fact that cyclic adducts position the methyl group to avoid steric clash with N3 of the adducted guanine. This becomes an issue upon formation of the COPdG aldehydes. The stabilization of cyclic adducts might also arise from the Thorpe-Ingold effect. For the *R*- and *S*-CPdG adducts in duplex DNA, the degree to which the cyclic adducts opened to the COPdG aldehydes increased significantly at pH 9.3 (Figure 4-7). In duplex DNA at pH 7, cross-link formed between the N-terminal peptide amine and the aldehyde rearragement products of the *R*- and *S*-CPdG adducts at 4 ^{o}C (Kurtz and Lloyd, 2003).

One factor with regard to the ring opening of the CPdG adducts to COPdG aldehyde in duplex DNA was the identity of the identity of the nucleotide opposite the CPdG adduct. When placed opposite to T in duplex DNA, the *S*-CPdG adduct did not undergo ring-opening to *S*-COPdG aldehyde (Figure 4-8), whereas the APdG adduct, when mispaired with T, existed as a

mixture of the cyclic APdG adduct and the ring-opened AOPdG aldehyde (Cho, Y.-J. et al., 2006). When mispaired with T, the M_1dG adduct remained as the cyclic form (Mao, H. et al., 1999). Similar to the acrolein-derived γ-OH-PdG adduct, the ratio of aldehyde to hydrated aldehyde for the crotonaldehyde-derived adducts increased with temperature.[3]

Role of Stereochemistry in Interstrand Cross-linking in the 5′-CpG-3′ Sequence Context. The presence of aldehydes in the minor groove at pH 7 and 37 °C was significant with regard to their potential for forming interstrand carbinolamine cross-links under physiological conditions in the 5′-CpG-3′ sequence. The present NMR studies corroborate the stereospecific preference for DNA interstrand cross-linking by the *R*-CPdG adduct, as opposed to the *S*-CPdG adduct (Kozekov et al., 2003). The time required for cross-link to reach equilibrium at pH 7 and 37 °C was approximately 20 days, with approximately 26% cross-linking observed by ^{13}C NMR.

To examine why interstrand cross-linking was much more extensive for the *R*-CPdG adduct than for the *S*-CPdG adduct in the 5′-CpG-3′ sequence context, a molecular modeling approach was employed (Figure 4-9). The modeling studies suggested that the low levels of cross-linking observed for the *S*-CPdG adduct in the 5′-CpG-3′ sequence can be attributed to the fact that the carbinolamine cross-link was of lower stability than that of cross-link from *R*-CPdG adduct, presumably due to the differential orientation of the CH_3 group at the α-carbon of the cross-link. Anecdotally, Lao and Hecht reported conducting

[3] The ratio of aldehyde to hydrate is different: more aldehydes than hydrates in the case of crotonaldehyde adducts due to, presumably, existence of methyl group.

molecular dynamics studies of pyrimidopurinone cross-links arising from *R*-and *S*-CPdG adducts, respectively, and reaching a similar conclusion, i.e., that the pyrimidopurinone cross-link arising from the *R*-CPdG adduct was of greater stability, due to a more favorable orientation of the α-carbon methyl group within the minor groove (Lao and Hecht, 2005). The modeling studeies also suggested that aldehyde, arising from *S*-CPdG adduct in duplex DNA, would not be oriented favorably for reaction with the cross-linking target N^2-dG in base pair $C^6 \bullet Y^{19}$ (Figure 4-10). NMR studies designed to examine these structural hypotheses are described in Chapter V.

Formation of an Interstrand Carbinolamine Cross-Link by the *R*-α-CH_3-γ-OH-PdG Adduct. At equilibrium in duplex DNA, the interstrand the *R*-α-CH_3-γ-OH-PdG cross-link comprises a mixture of carbinolamine, imine, and pyrimidopurinone. The presence of some of imine was inferred since the cross-link was reductively trapped in the presence of $NaCNBH_3$ (Kozekov et al., 2003). Lao and Hecht, using negative ion mode ESI-Q-TOF-MS analysis of a cross-linked oligodeoxynucleotide, observed m/z values corresponding to carbinolamine and either imine or pyrimidopurinone, with the lower m/z signal corresponding to imine or pyrimidopurinone predominating (Lao and Hecht, 2005). The present NMR studies suggested that the predominant form of the *R*-CPdG cross-link in situ is not imine. The amount of imine remained below the level of spectroscopic detection in duplex DNA. The reduction of cross-linked imine was slow in the presence of $NaCNBH_3$ (Kozekov et al., 2003), consist with

the notion that conversion of carbinolamine to the reducible imine was rate limiting in reductively trapping the cross-link in duplex DNA.

Similar to the acrolein-derived γ-OH-PdG interstrand cross-link (Cho, Y. J. et al., 2005), molecular modeling revealed that the carbinolamine linkage of cross-link maintained Watson-Crick hydrogen bonding at both of the tandem C•G base pairs (Figure 4-11). In contrast, dehydration of the carbinolamine cross-link to imine (Schiff base) cross-link, or cyclization of the latter to form pyrimidopurinone cross-link, required disruption of Watson-Crick hydrogen bonding at one or both of the tandem cross-linked C•G base pairs. The NMR studies supported this conclusion, suggesting intact Watson-Crick base pairing at the cross-linked X^7•C^{18} (Figure 4-5). In contrast, enzymatic digestion of duplex DNA containing cross-link afforded a bis-deoxyguanosine conjugate, characterized by a combination of mass spectrometry and NMR as pyrimidopurinone arising from annelation of imine with N1-dG in the 5′-Cp<u>G</u>-3′ sequence (Kozekov et al., 2003). The likely explanation is that the equilibrium between carbinolamine, imine, and pyrimidopurinone depends on the conformation state of the DNA. Enzymatic degradation of duplex DNA favors collapse of the carbinolamine cross-link to the pyrimidopurinone bis-nucleoside cross-link.

Structure-Biological Activity Relationships. Site specific mutagenesis in COS-7 mammalian cells using the single-stranded pMS2 shuttle vector (Fernandes et al., 2005) indicated that both *R*- and *S*-CPdG adducts yielded mutations at a 5-6% frequency. These were predominantly G→T transversions,

corroborating experiments utilizing a randomly modified shuttle vector and replicated in human cells (Kawanishi, M. et al., 1998). In the same mammalian site-specific mutagenesis system, the acrolein-derived γ-OH-PdG adduct showed a greater frequency of mutations, also predominantly G→T mutations (Kanuri et al., 2002). The propensity of cyclic adducts to undergo ring opening to the N^2-(3-oxopropyl)-dG aldehydes may facilitate lesion bypass, as reported for the acrolein-derived γ-OH-PdG adduct (Sanchez et al., 2003; VanderVeen, L. A. et al., 2001 ; Yang, I.-Y., Johnson, R., Grollman, A.P., & Moriya, M., 2002; Yang, I. Y. et al., 2002; Yang, I. Y. et al., 2001). On the other hand, in duplex DNA, incomplete conversion of crotonaldehyde-derived adducts to the opened forms, aldehydes and hydrated aldehydes, may result in more efficient block to DNA replication, possibly reducing their mutagenicity. The *R*- and *S*–CPdG adducts were reported to block trans-lesion synthesis by the Klenow (*exo-)* fragment of DNA polymerase I and DNA polymerase ε (Fernandes et al., 2005). The enzymes responsible for trans-lesion synthesis of the *R*- and *S*–CPdG adducts remain to be identified. However, Washingto et al. (Washington et al., 2004; Washington et al., 2004) showed that the Y-polymerase pol ι in conjunction with pol κ or Rev 1 in combination with pol ζ could efficiently bypass the acrolein-derived γ-OH-PdG adduct. Minko et al. showed that pol η could bypass the γ-OH-PdG to a lesser extent (Minko et al., 2003). It seems plausible that these error-prone polymerases might also bypass the *R*- and *S*–CPdG adducts.

CHAPTER V

ORIENTATION OF THE CROTONALDEHYDE-DERIVED N^2-(3-OXO-1(*S*)-METHYL-PROPYL)-DEOXYGUANOSINE DNA ADDUCT HINDERS INTERSTRAND CROSS-LINK FORMATION IN THE 5′-CpG-3′ SEQUENCE

Introduction

The conformation of the crotonaldehyde-derived N^2-(3-oxo-1(*S*)-methyl-propyl)-deoxyguanosine adduct in the oligodeoxynucleotide 5′-d(GCTAGCXAGTCC)-3′•5′-d(GGACTCGCTAGC)-3′; X= N^2-(3-oxo-1(*S*)-methyl-propyl)-dG (Scheme 5-1) is investigated. This adduct arises from opening of the cyclic N^2-(*S*-α-CH_3-γ-OH-1,N^2-propano-2')-dG adduct when placed opposite dC in duplex DNA. Generation of different cross-link was previously recognized based on the different stereochemistry of the α-methyl group of the crotonaldehyde-dG adduct in the 5′-CpG-3′ sequence (Chapter IV). For the lack of cross-link generation, it has been hypothesized based on molecular modeling studies in chapter IV. The orientation of methyl group may interfere with the reaction between aldehydic moiety of the adduct and amino group of the opposite 5′-side dG in a duplex. In other words, the metyl stereochemistry plays an important role that results in dramatically different amounts of interstrand cross-link by the different orientation of the methyl group of a ring opened species.

In this chapter, the previous hypothesis was examined by using NMR spectroscopy. The goal is to test this hypothesis if it is a feasible explanation with regard to generating cross-links, and restrained molecular dynamics calculations

were employed with NMR generated distance restraints for achieving the structure of an opened form of *S*-CPdG adduct in 5′-d(GCTAGCXAGTCC)-3′•5′-(GGACTCGCTAGC)-3′. The pH was maintained at 9.3 for maximizing the *S*-COPdG adduct in the 5′-CpG-3′ sequence.

Scheme 5-1. Oligonucleotide sequence (top) and the chemical structure of the N^2-(*S*-α-CH_3-γ-OH-1,N^2-propano-2′)-deoxyguanosine adducts and nomenclature.

5′-G^1 C^2 T^3 A^4 G^5 C^6 **X**^{7} A^8 G^9 T^{10} C^{11} C^{12}-3′
3′-C^{24}G^{23}A^{22}T^{21}C^{20}G^{19}C^{18}T^{17}C^{16}A^{15} G^{14} G^{13}-5′

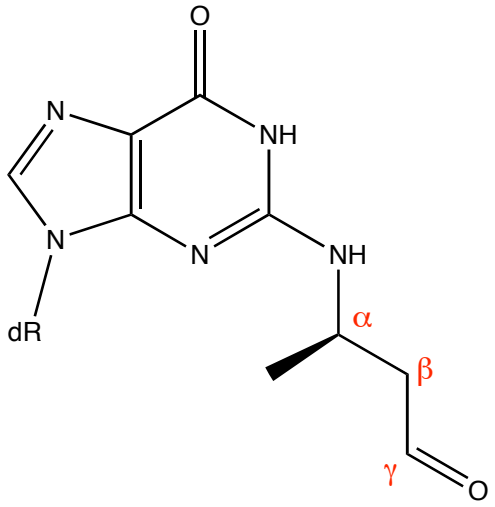

Results

When *S*-α-CH_3-OH-PdG adduct was placed opposite dC in 5'-d(GCTAGCXAGTCC)-3'•5'-d(GGACTCGCTAGC)-3' at 30ºC, the presence of aldehyde and hydrated aldehyde, in equilibrium with cyclic adduct, was immediately detected by NMR. Thus, opening of cyclic adduct occurred rapidly. At pH 7, the opening of the *S*-CPdG adduct to aldehyde and its hydrate was incomplete at equilibrium. At pH 9.3, equilibrium strongly favored the conversion of *S*-CPdG adduct to aldehyde and its hydrate; moreover, at pH 9.3 the duplex remained sufficiently stable for the present NMR studies. At pH 9.3, aldehyde exists in equilibrium with its hydrate; thus the NMR spectra show resonances arising from both species, as well as a trace of the cyclic adduct. The duplex oligodeoxynucleotide containing the *S*-stereoisomer of N^2-(3-oxopropyl)-dG aldehyde was sufficiently stable at pH 9.3 to provide excellent NMR data.

Assignment of nonexchangeable DNA protons. The sequential NOE connectivity between the aromatic and anomeric protons of the modified oligodeoxynucleotide duplex is shown in Figure 5-1. A complete NOE connectivity series was observed for both strands of the duplex. The completion of the NOESY walk in this region was indicative of a stable and ordered DNA conformation at pH 9.3 and 30 ºC. These assignments were extanded into other regions of ^{1}H NOESY spectrum to yield complete ^{1}H assignments for the H2', H2'', H3', and H4' protons (Patel, D.J. et al., 1987; Reid, 1987). The assignments of the non-exchangeable protons are detailed in Table 5-1.

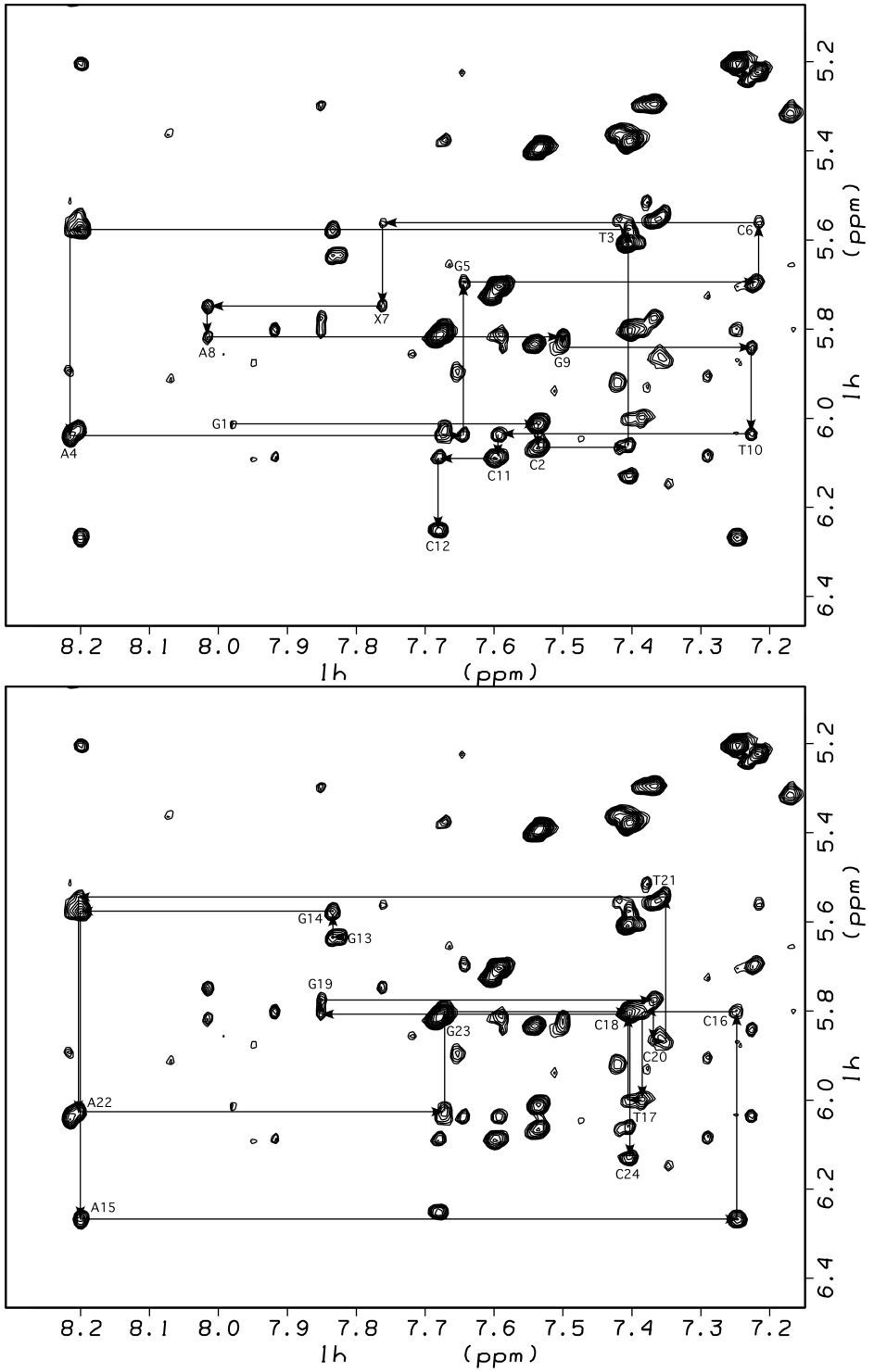

Figure 5-1. Expanded plot of a NOESY spectrum in D_2O buffer at a mixing time of 250 ms showing the sequential NOE connectivities for the *N*^{2}-(3-oxo-1(*S*)-methyl-propyl)-dG adduct at pH 9.3. The base positions are indicated at the intranucleotide cross-peaks of the aromatic proton to its own anomeric proton. (Top) Sequential NOE connectivities for nucleotides $G^1 \rightarrow C^{12}$. (Bottom) Sequential NOE connectivities for nucleotides $G^{13} \rightarrow C^{24}$.

Table 5-1. Chemical shifts (ppm) of non-exchangeable protons in the oligodeoxynucleotide 5'-d(GCTAGCXAGTCC)-3'•5'-(GGACTCGCTAGC)-3'.

BASE	H1′	H2′	H2″	H3′	H4′	H5′	H5″	H6/H8	Me/H5
G^{1}	6.01	2.67	2.79	4.85	4.25	3.74		7.98	
C^{2}	6.06	2.12	2.51	4.82	4.25	4.20	4.16	7.53	5.40
T^{3}	5.57	2.14	2.42	4.88	4.15	4.09	4.06	7.41	1.68
A^{4}	6.04	2.75	2.89	5.05	4.40	4.15	4.04	8.22	
G^{5}	5.69	2.46	2.61	4.95	4.35	4.20	4.18	7.65	
C^{6}	5.56	1.88	2.29	4.78				7.22	5.22
X^{7}	5.75	2.56	2.72	4.97	4.28	4.09	3.97	7.76	
A^{8}	5.82	2.61	2.81	4.99	4.13	4.20	3.97	8.02	
G^{9}	5.84	2.42	2.67	4.84	4.34	4.20	4.13	7.50	
T^{10}	6.04	2.12	2.51	4.85	4.22	4.17	4.10	7.22	1.23
C^{11}	6.09	2.22	2.49	4.83	4.21	4.17	4.09	7.59	5.70
C^{12}	6.25	2.25	2.29	4.56	4.17	4.05		7.68	5.81
G^{13}	5.64	2.45	2.64	4.80	4.16	3.65		7.82	
G^{14}	5.58	2.69	2.79	5.02	4.37	4.14	4.06	7.83	
A^{15}	6.27	2.74	2.91	5.06	4.50		4.19	8.20	
C^{16}	5.80	1.94	2.47	4.84	4.34	4.20	4.12	7.25	5.20
T^{17}	6.00	2.13	2.51	4.87				7.38	1.53
C^{18}	5.81	2.02	2.40	4.85	4.34	4.22	4.04	7.40	5.60
G^{19}	5.77	2.56	2.63	4.94	4.18	4.12	4.02	7.85	
C^{20}	5.86	1.99	2.42	4.86		4.11	4.04	7.37	5.30
T^{21}	5.54	2.08	2.37	4.84	4.17	4.10	4.03	7.35	1.65
A^{22}	6.03	2.73	2.88	5.04	4.39	4.13	4.03	8.21	
G^{23}	5.80	2.46	2.64	4.94	4.34	4.22	4.04	7.67	
C^{24}	6.13	2.11	2.19	4.45	4.22	4.04		7.40	5.38

X^{7} H_{α} (3.83); Me (0.99); H_{β}s (2.38); H_{γ} (9.60)

Exchangeable Protons. An expanded view of the far downfield region of the ^{1}H NOESY spectrum, showing the resonances arising from the Watson-Crick hydrogen bonded imino protons, is shown in Figure 5-2. For aldehyde adduct, the imino resonance arising from the C^6•G^{19} base pair was assigned at 12.7 ppm, the X^7•C^{18} base pair was assigned at 12.6 ppm, and the A^8•T^{17} imino resonance was assigned at 13.8 ppm, all within the anticipated chemical shift ranges. Imino proton resonances arising from the terminal base pairs G^1•C^{24} and C^{12}•G^{13} were not observed, presumably due to rapid exchange with solvent. The presence of a measurable amount of the diol adduct in equilibrium with aldehyde adduct was demonstrated by the presence of the cross-peak at 12.4 ppm. This resonance was assigned as arising from the X^7 imino proton of the geminal diol. Its identity was established by NOEs to the imino protons of the adjacent C^6•G^{19} and A^8•T^{17} base pairs. It also exhibited an NOE to the CH_3 protons of the crotonaldehyde adduct, the latter which was shifted approximately 0.1 ppm with respect to the crotonaldehyde CH_3 resonance arising from aldehyde. A complete set of sequential NOEs was observed for the oligodeoxynucleotide containing aldehyde, indicating the conservation of Watson-Crick hydrogen bonding at base pairs C^6•G^{19}, X^7•C^{18}, and A^8•T^{17}. Sequential assignment of the amino protons (Boelens et al., 1985) from base pairs C^2•G^{23}→C^{11}•G^{14} was obtained. Each of the peaks identified in the amino region exhibited a cross-peak with the appropriate imino proton as expected for Watson-Crick base pairing.

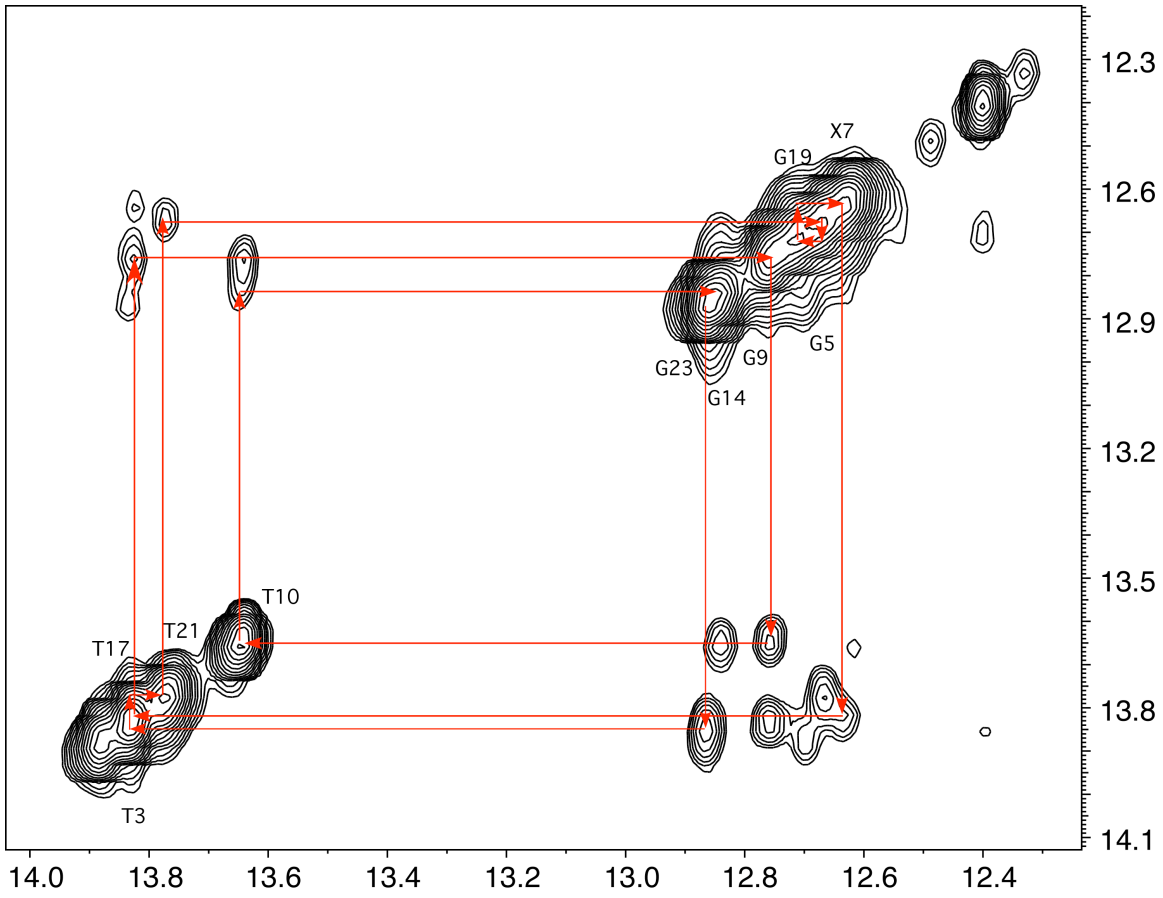

Figure 5-2. Expanded plot of a NOESY spectrum at a mixing time of 250 ms showing NOE connectivities for the imino protons for the base pairs from C^{2}•G^{23} to C^{11}•G^{14}.

***N*^{2}-(3-oxo-1(*S*)-methyl-propyl)-dG Adduct.** The adduct protons of adduct were assigned from a combination of ^{1}H COSY and NOESY experiments (Figure 5-3). The crotonaldehyde-derived CH_3 resonance was observed at 0.99 ppm. It exhibited a COSY cross-peak to a resonance at 3.83 ppm, assigned as arising from the H_α proton. The H_α proton exhibited an additional COSY cross-peak to a resonance at 2.38 ppm. Likewise, in the NOESY spectrum, the H_α proton also exhibited a cross-peak to the resonance at 2.38 ppm. Accordingly, this resonance was assigned as arising from a superposition of the $H_{\beta,\beta'}$ proton resonances. The H_γ aldehyde proton resonance was identified at 9.6 ppm. The aldehyde proton exhibited NOESY cross-peaks to $H_{\beta,\beta'}$, H_α, and CH_3 protons, and a COSY cross-peak to the $H_{\beta,\beta'}$ protons. The spectral linewidths of the adduct protons were comparable to those of the oligodeoxynucleotide, suggesting that the correlation times of these protons were similar to those of the overall duplex.

Chemical Shift Perturbations. Chemical shift differences between the aldehyde adduct and unmodified oligodeoxynucleotide are shown in Figure 5-4. These were localized at the adducted base pair X^7•G^{18}, and the 5'- and 3'-neighboring base pairs C^6•G^{19} and A^8•T^{17}, respectively. The largest perturbations were observed for the minor groove deoxyribose H1' resonances arising from the adducted nucleotide X^7, and A^8 in the modified strand, and nucleotides G^{18} and G^{19} in the complementary strand. Of these, the greatest perturbation was less than 0.3 ppm. The chemical shifts of the aromatic base protons were essentially unchanged.

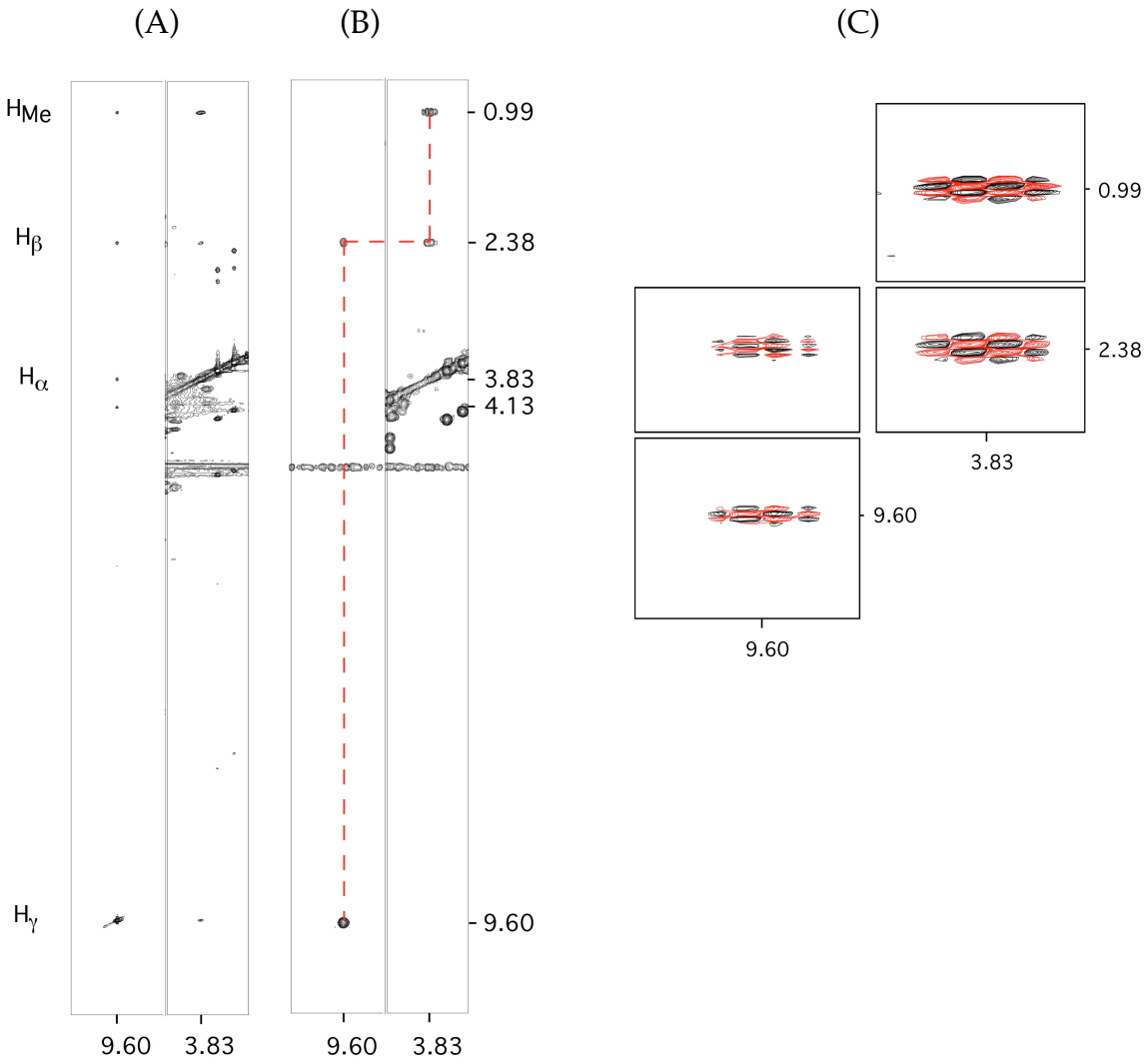

Figure 5-3. Expanded plots showing the assignments of the opened form resonances. (A) NOESY spectrum (B) magnitude COSY spectrum (C) E-COSY spectrum.

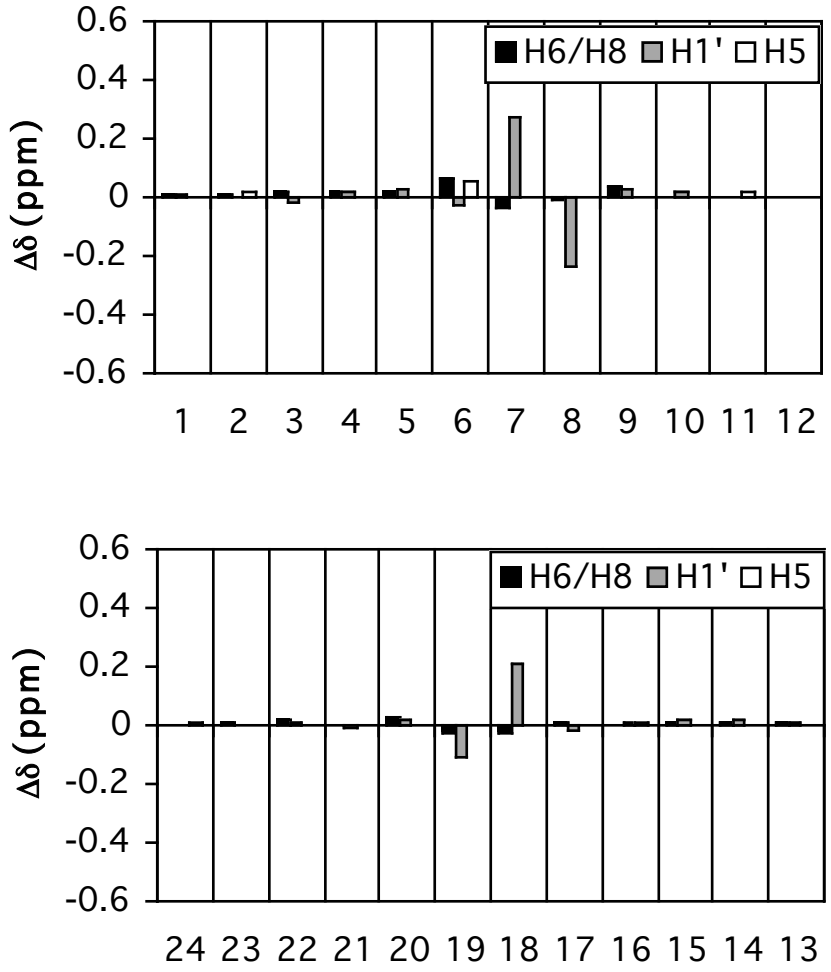

Figure 5-4. Chemical Sifts Differences of nonexchangeable aromatic and sugar protons of the modified and unmodified oligodeoxynucleotides.

Adduct-DNA NOEs. Five NOEs were observed between the N^2-(3-oxo-1(*S*)-methyl-propyl)-dG adduct and non-exchangeable DNA protons, shown in Figure 5-5. The crotonaldehyde-derived methyl protons showed NOEs in the 5' direction to C^{18} H1', G^{19} H1', and G^{19} H4' in the complementary strand of the duplex. The aldehyde proton of the adduct exhibited NOEs in the 3' direction to A^8 H1' and A8 H4' in the modified strand. All of these NOEs involved DNA protons facing the minor groove.

Torsion Angle Measurements. The NOE between the X^7 imidazole and X^7 H1' protons was of normal intensity, indicating that the X^7 glycosyl torsion angle was in the anti conformation, consistent with B type DNA helix (Kim, S. G. et al., 1992). The ^{31}P spectrum showed no unusual chemical shift perturbations, suggesting that the backbone was not significantly perturbed by the N^2-(3-oxo-1(*S*)-methyl-propyl)-dG adduct. The pseudorotation (*P*) of each of the deoxyribose rings, estimated graphically by monitoring the $^3J_{HH}$ couplings of sugar protons (Salazar et al., 1993), was found to be within the C2'-endo conformational range, also consistent with a B type DNA helix.

rMD Calculations. At pH 9.3 the N^2-(3-oxo-1(*S*)-methyl-propyl)-dG adduct represented the major species present in the sample, in equilibrium with diol, and a trace of cyclic adduct. At base pairs C^6•G^{19}, X^7•C^{18}, and A^8•T^{17}, this resulted in the observation of NOE cross-peaks arising from each of these three species. At the remaining base pairs more distal to the adduct, only one set of NOE cross-peaks was observed. To account for the lower intensities of NOE cross-peaks arising from *S*-COPdG adduct at base pairs C^6•G^{19}, X^7•C^{18}, and

$A^8 \bullet T^{17}$, as compared to the remainder of the molecule, these three base pairs were considered separately from the remainder of the oligodeoxynucleotide duplex. At base pairs $C^6 \bullet G^{19}$, $X^7 \bullet C^{18}$, and $A^8 \bullet T^{17}$ a total of 27 NOE cross-peaks specifically arising from *S*-COPdG adduct were identified. The volume integrals of these cross-peaks were utilized for a series of calculations using the program MARDIGRAS, to yield distance restraints for base pairs $C^6 \bullet G^{19}$ and $X^7 \bullet C^{18}$, and $A^8 \bullet T^{17}$. In separate calculations, volume integrals of NOE cross-peaks from base pairs $G^1 \bullet C^{24}$, $C^2 \bullet G^{23}$, $T^3 \bullet A^{22}$, $A^4 \bullet T^{21}$, and $G^5 \bullet C^{20}$, and from base pairs $G^9 \bullet C^{16}$, $T^{10} \bullet A^{15}$, $C^{11} \bullet G^{14}$, and $C^{12} \bullet G^{13}$ were utilized for a series of calculations using the program MARDIGRAS, to yield distance restraints for the remainder of the oligodeoxynucleotide duplex. Utilizing this approach, a total of 308 distance restraints were obtained. Of these, 89 were internucleotide restraints and 219 were intranucleotide restraints. The five NOEs observed between the N^2-(3-oxo-1(*S*)-methyl-propyl)-dG adduct and DNA served to orient the adduct within the minor groove. In addition to the NOE-derived distance restraints, a total of 90 sugar pucker restraints were obtained from the analysis of deoxyribose pseudorotation. These experimental restraints were augmented with 52 empirical hydrogen bonding restraints derived from the AMBER 8.0 force field that were included on the basis of spectroscopic evidence for the presence of Watson-Crick hydrogen bonds (Figure 5-2).

These were used to restrain molecular dynamics calculations that utilized a simulated annealing protocol. The parameterization for the N^2-(3-oxo-1(*S*)-methyl-propyl)-dG adduct was as previously described. Sets of randomly seeded rMD calculations were initiated from two starting structures, in which adduct was oriented in the minor groove. In the IniA starting structure, the

adducted duplex was in the A-DNA conformation, whereas in the IniB starting structure, the adducted duplex was in the B-DNA conformation. The rmsd between the two starting structures was 6.3 Å. The choice of A-form and B-form starting structures, as opposed to initiating the calculations from random coil DNA structures, was based upon the spectroscopic observations that the adducted duplex was relatively unperturbed as compared to its non-adducted counterpart (Figure 5-4).

A stereoview of superimposed structures which emerged from the rMD calculations, beginning either with the A- or B-DNA starting structures, is shown in Figure 5-6. The structural statistics are listed in Table 5-2. Irrespective of starting structure, the rMD calculations yielded right-handed DNA helices with the N^2-(3-oxo-1(*S*)-methyl-propyl)-dG adduct oriented in the minor groove. These structures were more similar to B-form DNA than to A-form DNA, as indicated by rmsd analysis. Thus, the average structure that emerged from the rMD calculations showed a 5.2 Å rmsd as compared to A-form DNA, and a 1.7 Å rmsd as compared to B-form DNA.

The accuracies of the structures that emerged from the rMD calculations with respect to ^{1}H NOEs were assessed using complete relaxation matrix analysis with the program CORMA. This yielded sixth root residuals (R^1_x values) between the theoretical NOE intensities predicted by the calculated structures and the experimental NOE data obtained at a mixing time of 150 ms. The total R^1_x value was 7.94×10^{-2}. The agreement was somewhat better for intra-nucleotide NOEs, with an R^1_x value of 6.65×10^{-2}, whereas for internucleotide NOEs an R^1_x value of 9.00×10^{-2} was obtained. Figure 9 shows R^1_x values for each of the

nucleotides. At base pairs C^{6}•G^{19}, X^{7}•C^{18}, and A^{8}•T^{17} both intra- and inter-nucleotide R_1^x values were about 10% or less, indicative of good agreement with the experimental NOE data.

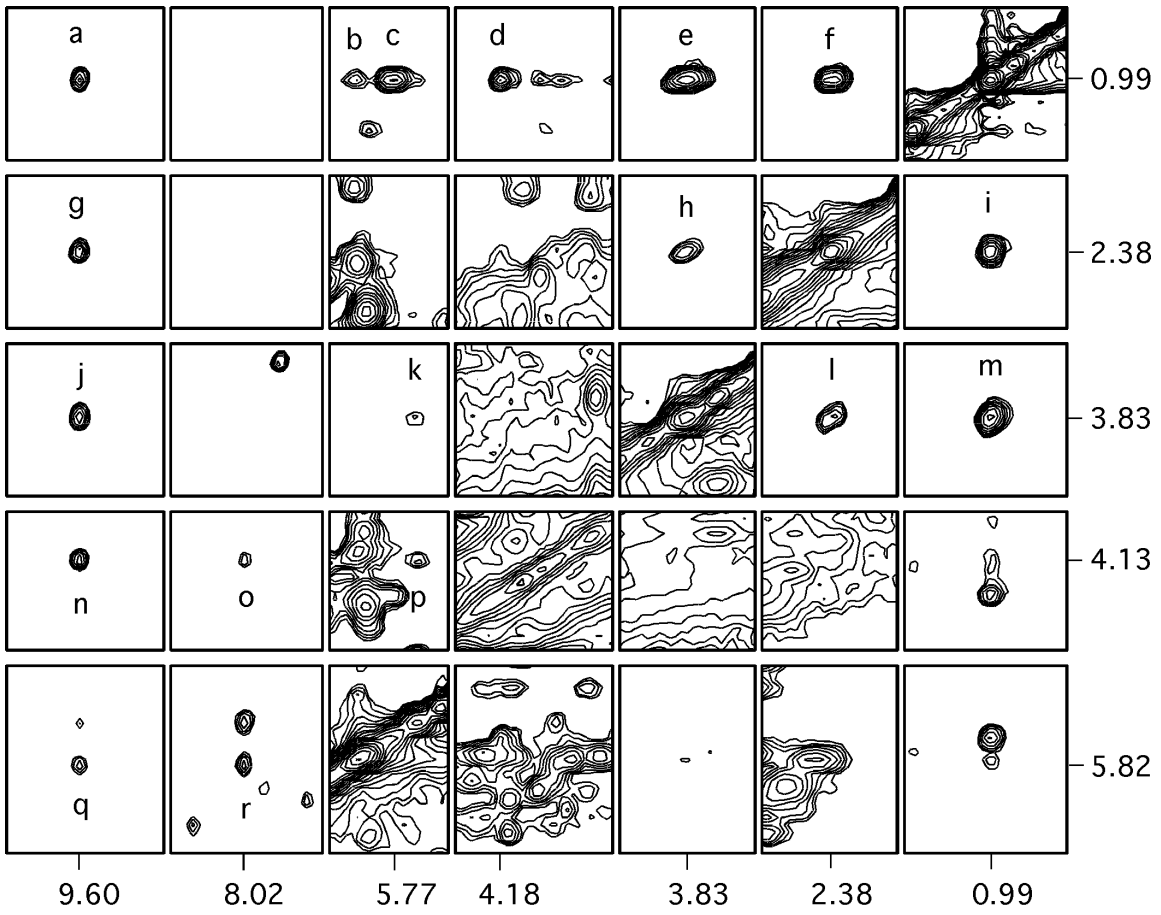

Figure 5-5. Expanded tile plots showing NOEs between the DNA and opened form adduct protons (τ_m= 350 ms). a, $X^7H_\gamma \rightarrow X^7H_{Me}$; b, $C^{18}H1' \rightarrow X^7H_{Me}$; c, $G^{19}H1' \rightarrow X^7H_{Me}$; d, $G^{19}H4' \rightarrow X^7H_{Me}$; e, $X^7H_\alpha \rightarrow X^7H_{Me}$; f, $X^7H_\beta \rightarrow X^7H_{Me}$; g, $X^7H_\gamma \rightarrow X^7H_\beta$; h, $X^7H_\alpha \rightarrow X^7H_\beta$; i, $X^7H_{Me} \rightarrow X^7H_\beta$; j, $X^7H_\gamma \rightarrow X^7H_\alpha$; k, $X^7H1' \rightarrow X^7H_\alpha$; l, $X^7H_\beta \rightarrow X^7H_\alpha$; m, $X^7H_{Me} \rightarrow X^7H_\alpha$; n, $X^7H_\gamma \rightarrow A^8H4'$; o, $A^8H8 \rightarrow A^8H4'$; p, $X^7H1' \rightarrow A^8H4'$; q, $X^7H_\gamma \rightarrow A^8H1'$; r, $A^8H8 \rightarrow A^8H1'$.

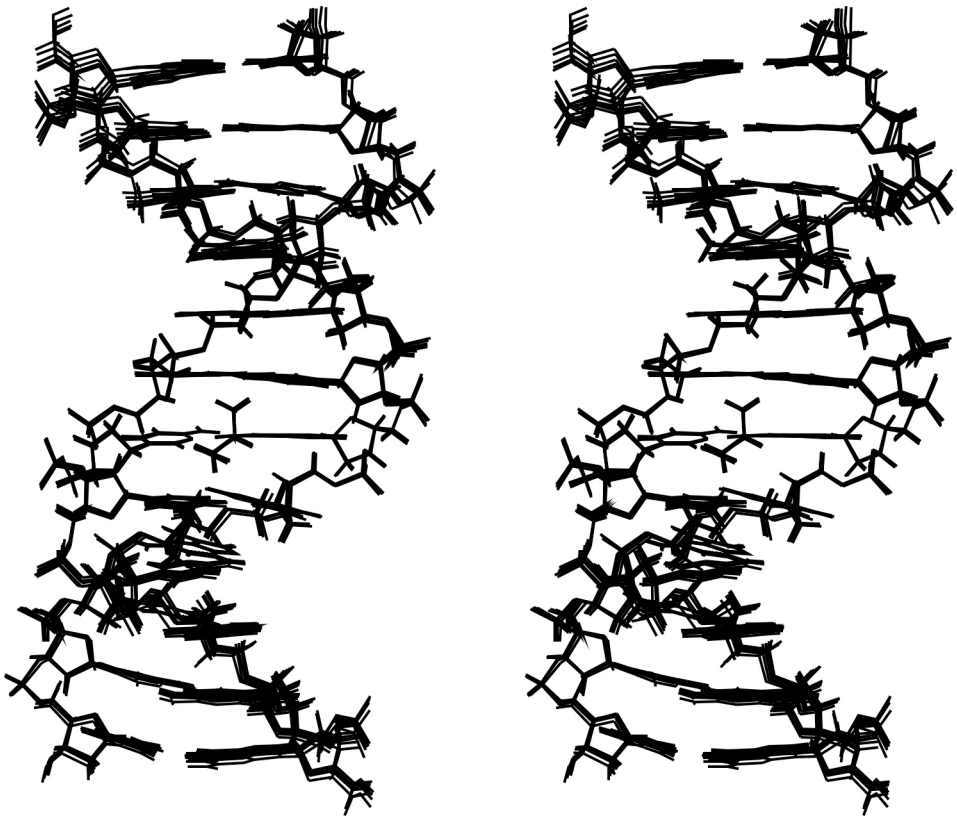

Figure 5-6. Stereoview of five superimposed structures emergent from the simulated annealing rMD protocol of IniA.

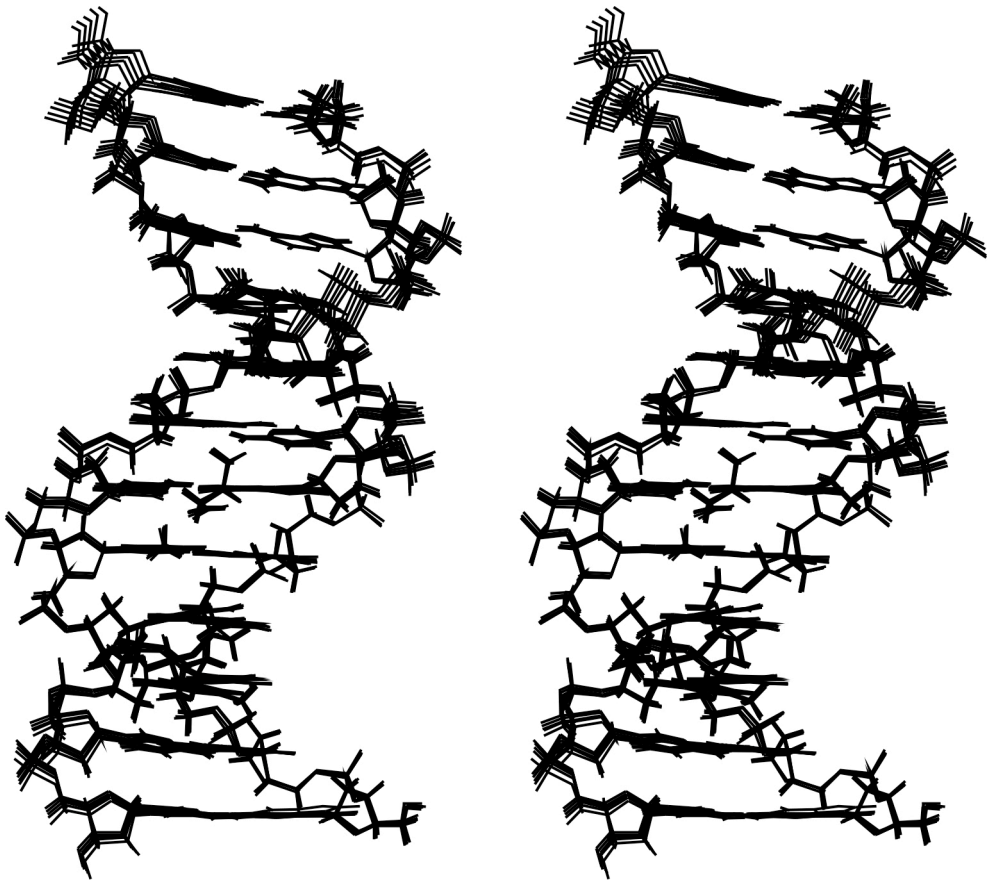

Figure 5-7. Stereoview of five superimposed structures emergent from the simulated annealing rMD protocol of IniB.

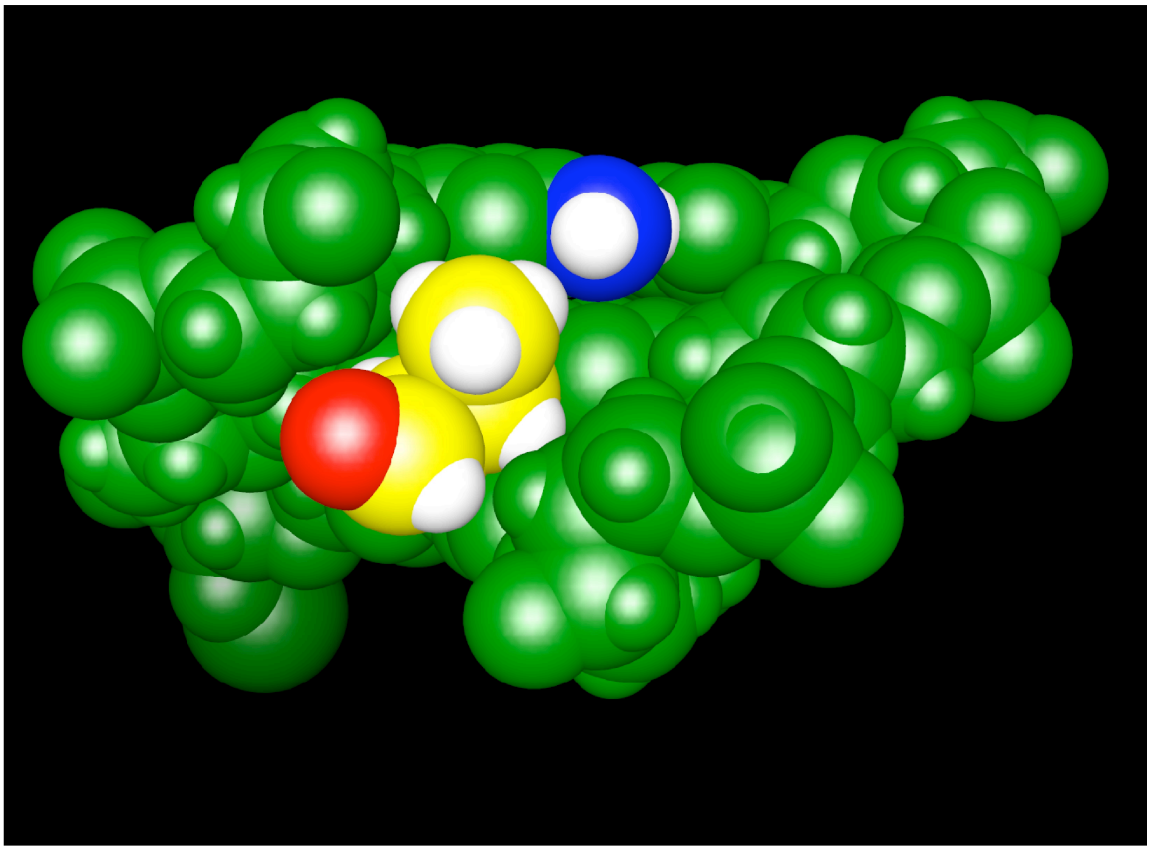

Figure 5-8. A CPK representation of the part of the *S*-COPdG adduct in a duplex. This is the averaged and energy minimized using the conjugate gradients algorithm. The adduct residues are in yellow with protons in white and oxygen in red. The amino nitrogen in an opposite dG is in blue.

Table 5-2. Root Mean Square Deviations (RMSD).

Analysis of the rMD-Genrated Structures of the opened *S*-crotonaldehyde aldehyde adduct in the 5'-CpG-3' sequence	
NMR restraints	
Total number of distance restraints	308
Interresidue distance restraints	89
Intraresidue distance restraints	219
DNA— adduct protons distance restraints	5
Adduct protons distance restraints	5
H-bonding restraints	52
Sugar pucker restraints	90
pairwise rmsd (Å) over all atoms	
IniA vs. IniB	6.316
<rMDA>[a] vs. <rMDA>	0.29 ± 0.14
<rMDB>[b] vs. <rMDB>	0.29 ± 0.14
$rMDA_{avg}$ [c] vs. $rMDB_{avg}$ [d]	1.881
$rMDA_{avg}$ vs. rMD_{avg} [e]	1.81
$rMDB_{avg}$ vs.rMD_{avg}	2.16
IniA vs. rMD_{avg}	5.244
IniB vs. rMD_{avg}	1.679

[a] <rMDA> represents the set of 5 structures that emerged from rMD calculations starting from IniA. [b] <rMDB> represents the set of 5 structures that emerged from rMD calculations starting from IniB. [c] $rMDA_{avg}$ represents the average structure of all five <rMDA>. [d]$rMDB_{avg}$ represents the average structure of all five <rMDB>. [e] rMD_{avg} represents the potential enery minimized average structure of all 10 structures of <rMDA> and <rMDB>.

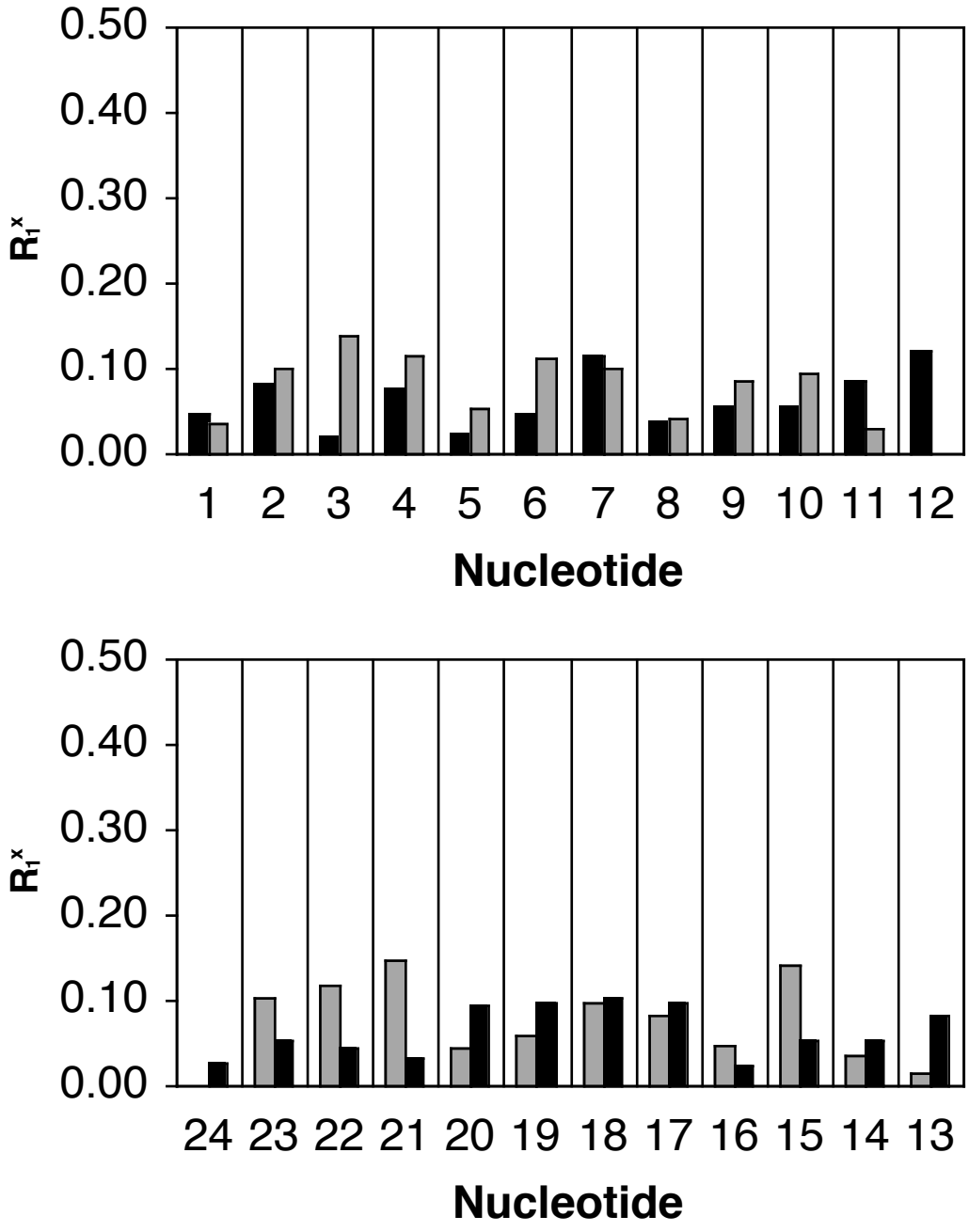

Figure 5-9. Complete relaxation matrix calculations on the average structure emergent from the simulated annealing rMD protocol showing sixth root residuals (R_1^x) for each nucleotide: The adducted strand (top); the complementary strand (bottom). The black bars represent intranucleotide R_1^x values, and the gray bars represent internucleotide R_1^x values.

Discussion

Previously, the two N^2-(3-oxopropyl)-dG aldehyde adducts (*R* and *S*) were modeled in 5'-d(GCTAGCXAGTCC)-3'•5'-d(GGACTCGCTAGC)-3' in Chapter IV. The potential energy minimization predicted that both adducts maintained Watson-Crick hydrogen bonding at both base pairs C^6•Y^{19} and X^7•C^{18}. The modeling studies suggested that the for the *S*-stereoisomer of N^2-(3-oxopropyl)-dG aldehyde, the methyl group oriented within the minor groove in the 5'-direction from the adducted nucleotide X^7. This oriented the aldehyde group in the 3'-direction, placing it distal to the cross-linking target N^2-dG in base pair C^6•Y^{19}. In contrast, the modeling studies suggested that for the *R*-stereoisomer, the methyl group oriented within the minor groove in the 3'-direction from the adducted nucleotide X^7. This oriented the reactive aldehyde in the 5'-direction, placing it proximate to the cross-linking target N^2-dG in base pair C^6•Y^{19}. Significantly, the favored orientation of the corresponding acrolein-derived N^2-(3-oxopropyl)-dG aldehyde also placed the aldehyde in the 5'-direction, proximate to the cross-linking target N^2-dG in base pair C^6•Y^{19}. The present study provides experimental evidence, which corroborate the predictions of the previously conducted modeling studies.

Conformation of the *S*-stereoisomer of N^2-(3-oxopropyl)-dG aldehyde. Several lines of evidence supported the conclusion that the *S*-stereoisomer of N^2-(3-oxopropyl)-dG aldehyde adduct oriented in the minor groove with minimal perturbation of the B-family DNA duplex. The ^{1}H NOE data revealed a complete set of NOE connectivities at base pairs C^6•G^{19}, X^7•C^{18}, and A^8•T^{17} (Figure 5-1). In

addition, the observation of imino ^{1}H resonances at base pairs C^{6}•G^{19}, X^{7}•C^{18}, and A^{8}•T^{17}, and NOEs between the imino protons of each base pair and the C^{6} NH_2, C^{18} NH_2, and A^{18} H2 protons of each base pair, respectively, indicated that the presence of *S*-COPdG adduct did not disrupt Watson-Crick base pairing at the lesion site. Finally, analysis of chemical shift perturbations, deoxyribose pseudorotation, and ^{31}P chemical shift perturbtations, all indicated little adduct-induced perturbation as compared to the unmodified duplex. Within the minor groove, the 3'-orientation of the aldehyde proton of the crotonaldehdye-derived adduct at X^{7} was indicated by the observation of dipolar coupling with A^{8} H1' and A8 H4' in the modified strand. In contrast, the methyl protons of the adduct showed dipolar coupling with C^{18} H1', G^{19} H1', and G^{19} H4' in the complementary strand of the duplex, consistent with their 5'-orientation in the minor groove with respect to X^{7}. The fact that no spectral linebroadening was observed for the adduct protons as compared to the DNA protons, combined with the observed directionality of NOEs between the CH_3 and aldehyde protons with respect to minor groove DNA protons, suggests that the orientation of the *N*^{2}-(3-oxopropyl)-dG aldehyde adduct within the minor groove is fixed at pH 9.3 and 30 ºC.

Structure-Activity Relationships. The 5'-orientation of the crotonaldehdye-derived methyl group as predicted by molecular modeling and now confirmed by NMR spectroscopic analysis provides a plausible rationale for the differential interstrand cross-linking capabilities of the *R*-α-CH_3-γ-OH-PdG adduct and *S*-α-CH_3-γ-OH-PdG adduct in the 5'-CpG-3' sequence context. In this

sequence, the *R*-α-CH_3-γ-OH-PdG adduct generated about 26 % of a carbinolamine cross-link while the *S*-α-CH_3-γ-OH-PdG adduct failed to yield significant levels of the cross-link (Cho, Y.-J. et al., 2006; Kozekov et al., 2003). The present results support the idea that stereochemistry at C_α of the crotonaldehyde adduct plays an important role in facilitating interchain DNA cross-link generation by controlling the positioning of the reactive aldehyde in N^2-(3-oxo-1(*S*)-methyl-propyl)-dG adduct with respect to the exocyclic amine of dG in the complementary strand.

The present results suggest a kinetic basis for the lack of interstrand cross-link formation by N^2-(3-oxo-1(*S*)-methyl-propyl)-dG adduct. In fact, the adduct exists in equilibrium with carbinolamine cross-link. When samples of *S*-α-CH_3-γ-OH-PdG adduct were monitored for periods of several months at 37 °C, presumably allowing sufficient time to reach equilibrium, only small amounts of carbinolamine cross-link arising from the N^2-(3-oxo-1(*S*)-methyl-propyl)-dG adduct were observed. Thus, it can be concluded either that the rate of interstrand cross-linking is extremely slow at pH 7 and 37 °C, or that the cross-link arising from N^2-(3-oxo-1(*S*)-methyl-propyl)-dG adduct must also be thermodynamically disfavored. This question is presently under investigation. Previous molecular modeling suggested that carbinolamine cross-link was of lower stability than that of cross-link, presumably due to the differential orientation of the CH_3 group at the a-carbon of the cross-link. Anecdotally, Lao and Hecht reported conducting molecular dynamics studies of pyrimidopurinone cross-links, formed from adducts **2a** and **2b** (Scheme 1-4), respectively, and reaching a similar conclusion, i.e., that the pyrimidopurinone

cross-link arising from the *R*-α-CH_3-γ-^{13}C-OH-PdG adduct was of greater stability, due to a more favorable orientation of the a-carbon methyl group within the minor groove (Lao and Hecht, 2005).

Formation of Peptide-DNA Conjugates. Peptide trapping experiments demonstrated that both *R*-α-CH_3-γ-OH-PdG adduct and *S*-α-CH_3-γ-OH-PdG adduct formed DNA-peptide conjugates (Kurtz and Lloyd, 2003). The amount of peptide conjugate formed by *S*-α-CH_3-γ-OH-PdG adduct was comparable to that formed by the *R*-α-CH_3-γ-OH-PdG adduct (Kurtz and Lloyd, 2003). Thus, it is concluded that while stereochemistry at C_α modulates interstrand DNA cross-link formation in the 5'-CpG-3' sequence by positioning the aldehyde functionality distal to the exocyclic amine of dG in the complementary strand, it appears to play little role in modulating the formation of peptide-DNA conjugates.

However, the location of an aldehyde group by the methyl stereochemistry of S-CPdG adduct may correlate the interaction with polymerases during replication process. It will be of interest if such biological experiments are designed to investigate the effect of stereochemistry of crotonaldehyde-derived dG adducts in conjunction with enzymes.

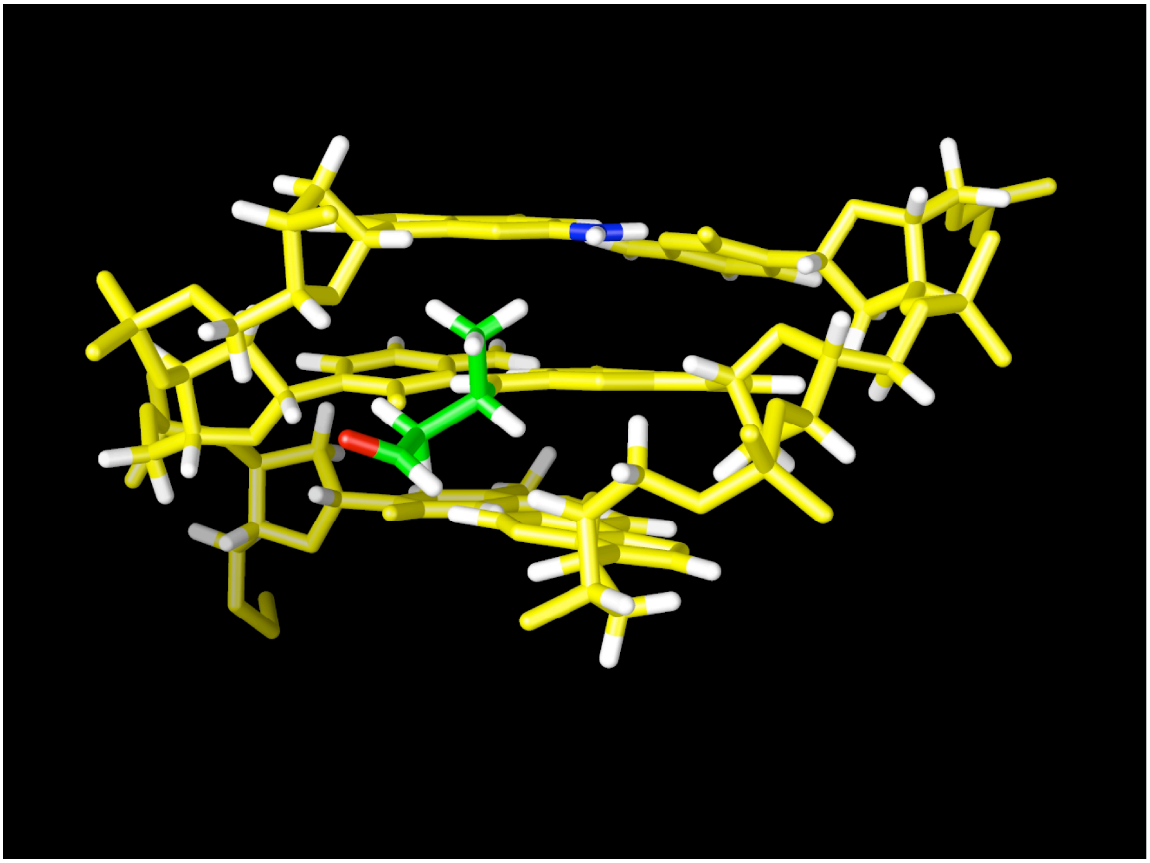

Figure 5-10. A side view of the refined structure, rMD_{avg} from the minor groove.

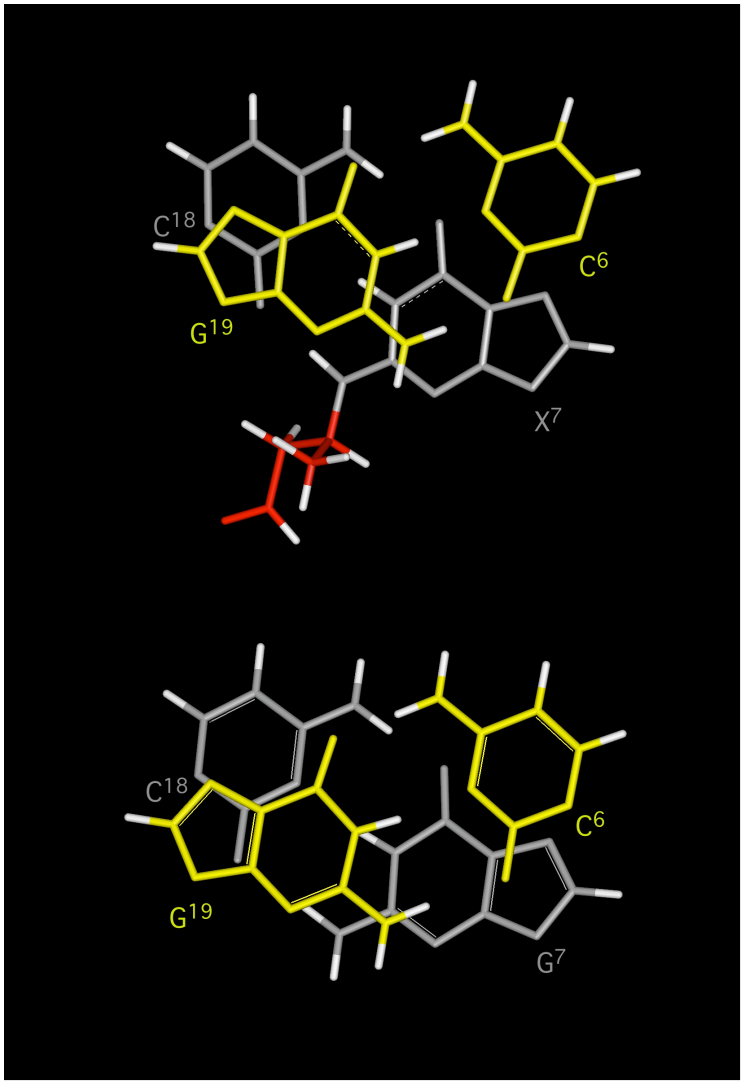

Figure 5-11. The comparison of Base stacking of the base pairs C^{6}•G^{19}, X^{7}•C^{18}, and A^{8}•T^{17} the oligodeoxynucleotide containing the N^{2}-(3-oxo-1(*S*)-methyl-propyl)-dG adduct (Top), and unmodified oligodeoxynucleotide (Bottom).

CHAPTER VI

SOLUTION STRUCTURE OF THE FULLY REDUCED DNA INTERSTRAND CROSS-LINK ARISING FROM RING OPENING OF CROTONALDEHYDE-DERIVED *R*-α-CH_3-γ-OH-1,N^2-PROPANO-2′-DEOXYGUANOSINE ADDUCT IN THE 5′-CpG-3′ SEQUENCE

Introduction

Crotonaldehyde yields the enantiomeric *R*- and *S*-α-CH_3-γ-OH-1,N^2-propano-2′-deoxyguanosine adducts (*R*-CPdG and *S*-CPdG). The ring-opening process via opened aldehyde form in the minor groove facilitated DNA interstrand cross-linking. In the 5′-CpG-3′ sequence context, γ-OH-PdG and *R*-CPdG formed cross-links that were identified as carbinolamines (Chapter III and IV).

A cross-link is a salient phenomenon for DNA replication and repair. To understand the biological effect by a structural changes from crotonaldehyde adduct, such as structural study of cross-link is a sine qua non. However, there were other species to be reckoned with since all species are in equilibrium. It was not possible to single out carbinolamine cross-link for a structural analysis. In complement to monitoring *R*-CPdG adducts by NMR, sodiumborohydride was utilized to fully reduce the carbinolamine cross-link, which can be used as a model of carbinolamine type cross-link. In the case of imine, due to the fact that sp^2 is required on C=N, it is presumed that sp^3 carbon at γ position of this reduced cross-link chain would instead reflect the feature of carbinolamine cross-link than that of imine species. Unmodified 5′-d(GCTAGCGAGTCC)-3′•5′-(GGACTCGCTAGC)-3′ oligodeoxynucleotide was referenced as the control.

In this chapter, I describe structural elucidation by 2D NMR investigations of the fully reduced *R*-crotonaldheyde cross-link (Scheme 6-1) in 5′-d(GCTAGCXAGTCC)-3′•5′-(GGACTCYCTAGC)-3′. The pH was maintained at 6.8. NMR data suggest how such carbinolamine type interchain cross-link can exist in a duplex without disrupting internal base hydrogen bonds.

Scheme 6-1. 5′-CpG-3′ Oligonucleotide and the chemical structure of the fully reduced *R*-crotonaldehyde cross-link. β_1 and γ_1 present left sided protons, and β_2 and γ_2 are right sided protons.

5′-G^1 C^2 T^3 A^4 G^5 C^6 **X^7** A^8 G^9 T^{10} C^{11} C^{12}-3′
3′-$C^{24}$$G^{23}$$A^{22}$$T^{21}$$C^{20}$**$Y^{19}$**$C^{18}$$T^{17}$$C^{16}$$A^{15}$ G^{14} G^{13}-5′

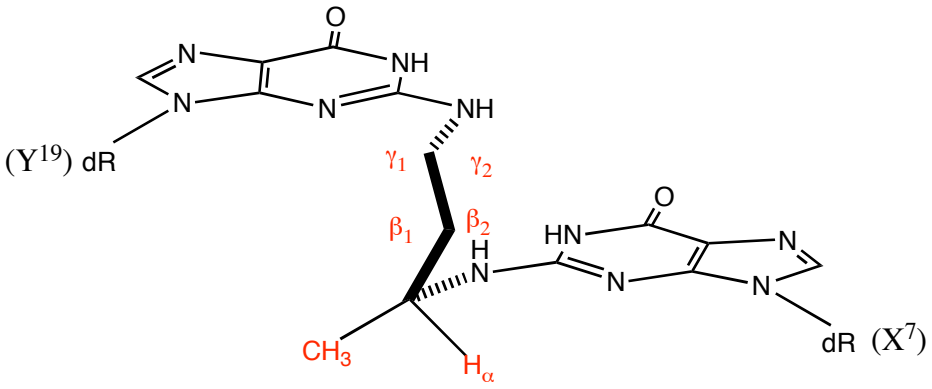

Results

Assignments of non-exchangeable DNA protons. As shown in Figure 6-1, the complete sequential connectivity between the aromatic and the anomeric protons for both strands of the duplex was accomplished in the NOESY walk region. All cytosine H5/H6 cross-peaks were numbered (pink) on each peak. The small numbers (blue) nearby cross-peaks indicate 5'- base proton numbers that have a NOE with 3'-side cytosine H5. Two dimensional NOESY and DQF-COSY spectra were used for further assignments. All data were collected at 30 ^{o}C. A minor overlap occurred for C^{6} and X^{7} H1' resonances, however, other than that, most peaks were well-resolved including adduct protons. Figure 6-2 presents another sequential connectivities between the aromatic and the H3' protons was completed. The completion of NOESY walk in those regions was indicative of a stable and ordered DNA conformation. In addition, these assignments were expanded into other regions of ^{1}H NOESY spectrum to yield complete ^{1}H assignments for the H2', H2'', H3', and H4' protons (Patel, D.J. et al., 1987; Reid, 1987). Table 6-1 details the assignments of the non-exchangeable protons.

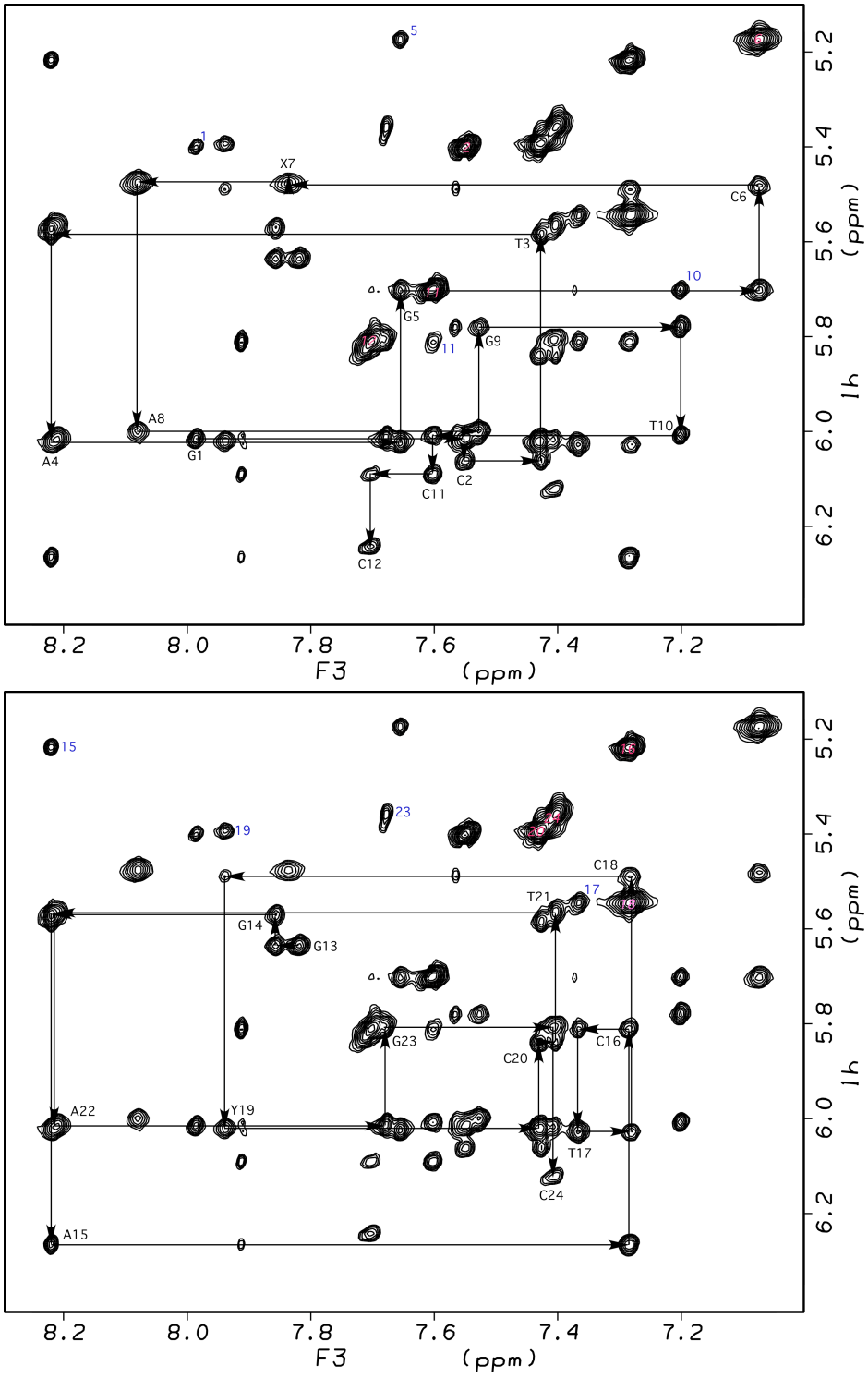

Figure 6-1. Expanded plot of a NOESY spectrum in D_2O buffer at a mixing time of 150 ms showing the sequential NOE connectivities from the aromatic to anomeric protons. The base positions are indicated at the intranucleotide cross-peaks of the aromatic proton to its own anomeric proton. (Top) Sequential NOE connectivities for nucleotides $G^{1}\rightarrow C^{12}$. (Bottom) Sequential NOE connectivities for nucleotides $G^{13}\rightarrow C^{24}$.

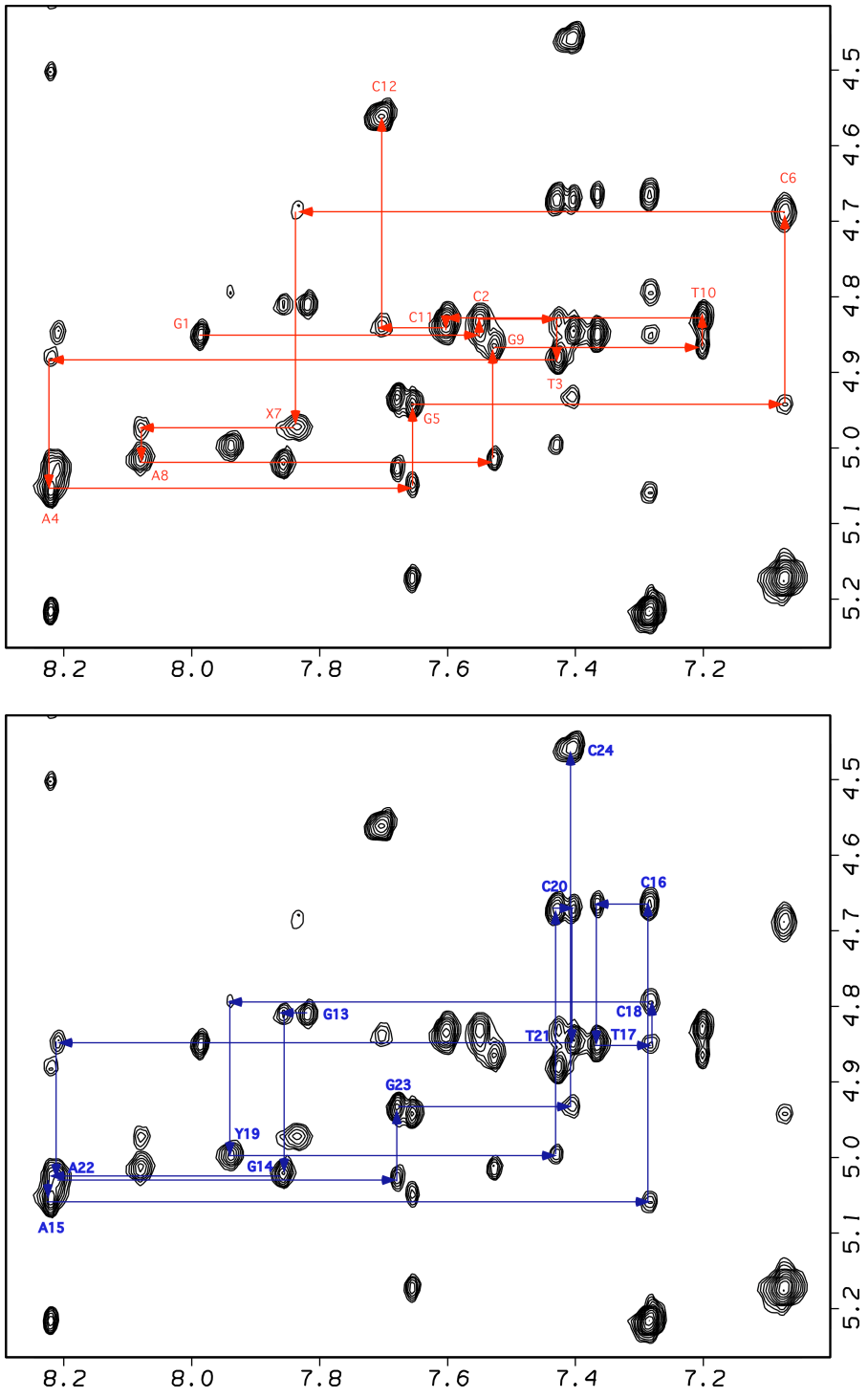

Figure 6-2. Expanded plot of a NOESY spectrum in D_2O buffer at a mixing time of 150 ms showing the sequential NOE connectivities from the aromatic to H3′ protons. The base positions are indicated at the intranucleotide cross-peaks of the aromatic proton to its own H3′ proton. (Top) A sequential NOE connectivities for nucleotides G^{1}→C^{12}. (Bottom) A sequential NOE connectivities for nucleotides G^{13}→C^{24}.

Table 6-1. Chemical shifts (ppm) of non-exchangeable protons in the oligodeoxynucleotide 5′-d(GCTAGCXAGTCC)-3′•5′-(GGACTCYCTAGC)-3′.

BASE	H1′	H2′	H2″	H3′	H4′	H5′	H5″	H6/H8	Me/H5
G^{1}	6.02	2.68	2.79	4.85	4.26	3.75		7.99	
C^{2}	6.06	2.15	2.53	4.83	4.26	4.16	4.21	7.55	5.40
T^{3}	5.58	2.16	2.43	4.88	4.15	4.09	4.10	7.43	1.69
A^{4}	6.03	2.75	2.90	5.05	4.41	4.05	4.15	8.22	
G^{5}	5.70	2.44	2.59	4.95	4.35	4.22	4.18	7.66	
C^{6}	5.48	1.21	1.83	4.69	4.01		4.18	7.07	5.17
X^{7}	5.47	2.78	2.78	4.97	4.32	3.92	4.01	7.84	
A^{8}	6.00	2.66	2.90	5.01	4.34	4.16	4.18	8.08	
G^{9}	5.78	2.42	2.68	4.86	4.33	4.18	4.21	7.53	
T^{10}	6.01	2.11	2.50	4.83	4.20	4.12	4.23	7.20	1.26
C^{11}	6.09	2.24	2.49	4.84	4.17	4.09	4.06	7.60	5.70
C^{12}	6.24	2.29	2.31	4.56	4.06	4.26	4.17	7.70	5.81
G^{13}	5.64	2.47	2.64	4.81	4.17	3.66		7.82	
G^{14}	5.57	2.71	2.79	5.02	4.37	4.06	4.14	7.86	
A^{15}	6.27	2.75	2.92	5.06	4.50	4.20	4.25	8.22	
C^{16}	5.81	1.96	2.47	4.66	4.22	4.18	4.33	7.29	5.22
T^{17}	6.03	2.09	2.43	4.85	4.18	4.06	4.09	7.37	1.50
C^{18}	5.49	1.65	2.10	4.79	4.01	4.03	4.08	7.28	5.54
Y^{19}	6.00	2.81	2.69	5.00	4.39	4.04	4.07	7.94	
C^{20}	5.84	1.98	2.46	4.67	4.17	4.17	4.28	7.43	5.39
T^{21}	5.56	2.08	2.39	4.84	4.11	4.03	4.39	7.40	1.69
A^{22}	6.02	2.73	2.87	5.03	4.38	4.03	4.11	8.21	
G^{23}	5.81	2.47	2.63	4.93	4.35	4.18	4.22	7.68	
C^{24}	6.12	2.13	2.20	4.46	4.22	4.03	4.26	7.40	5.36

X^{7} H_{α} (3.82); Me (1.03); β_1 (1.82); β_2 (1.63); γ_1 (3.71); γ_2 (2.82)

Adduct-DNA NOEs All adduct protons were well resolute and had 10 NOEs with DNA protons shown in Figure 6-3 and Figure 6-4. The adduct protons were assigned from a combination of ^{1}H COSY and NOESY experiments (Figure 6-3). The adduct CH_3 resonance was observed at 1.03 ppm that exhibited a COSY cross-peak to a resonance at 3.82 ppm, assigned as arising from the Hα proton. The H_α proton manifested an additional COSY cross-peak to a resonance at 1.63 ppm, assigned as arising from the β_2. The β_2 proton had a strong geminal coupling to a resonance at 1.82 ppm, the β1, and weak coupling to a resonance at 3.71 ppm, the γ_1. The γ_1 and the Hα were most deshielded, presumably, due to the trans location from the hydrogen-bonded N^2H of deoxyguanosines. All dipolar couplings were observed to other adduct protons. The γ_1 proton also exhibited a geminal coupling to a resonance at 2.82 ppm, the γ_2 proton. The conformation of the adduct protons differentiated the COSY spectrum by the presence of scalar couplings whereas all dipolar couplings were present in the NOESY spectrum as shown in Figure 6-3. The methyl protons gave useful information for the geometry of this cross-link. The methyl protons interacted with A^8 protons in primer strand intensely while left small interactions with Y^{19} and C^{20} protons in the complimentary strand except other adduct protons (Figure 6-4). It indicates that the methyl group in the proximity into 3′ direction of the primer strand, while they showed small cross-peaks to such as H1′ of C^{20} and X^7, and H2 and H4′ of A^8 (Figure 6-4).

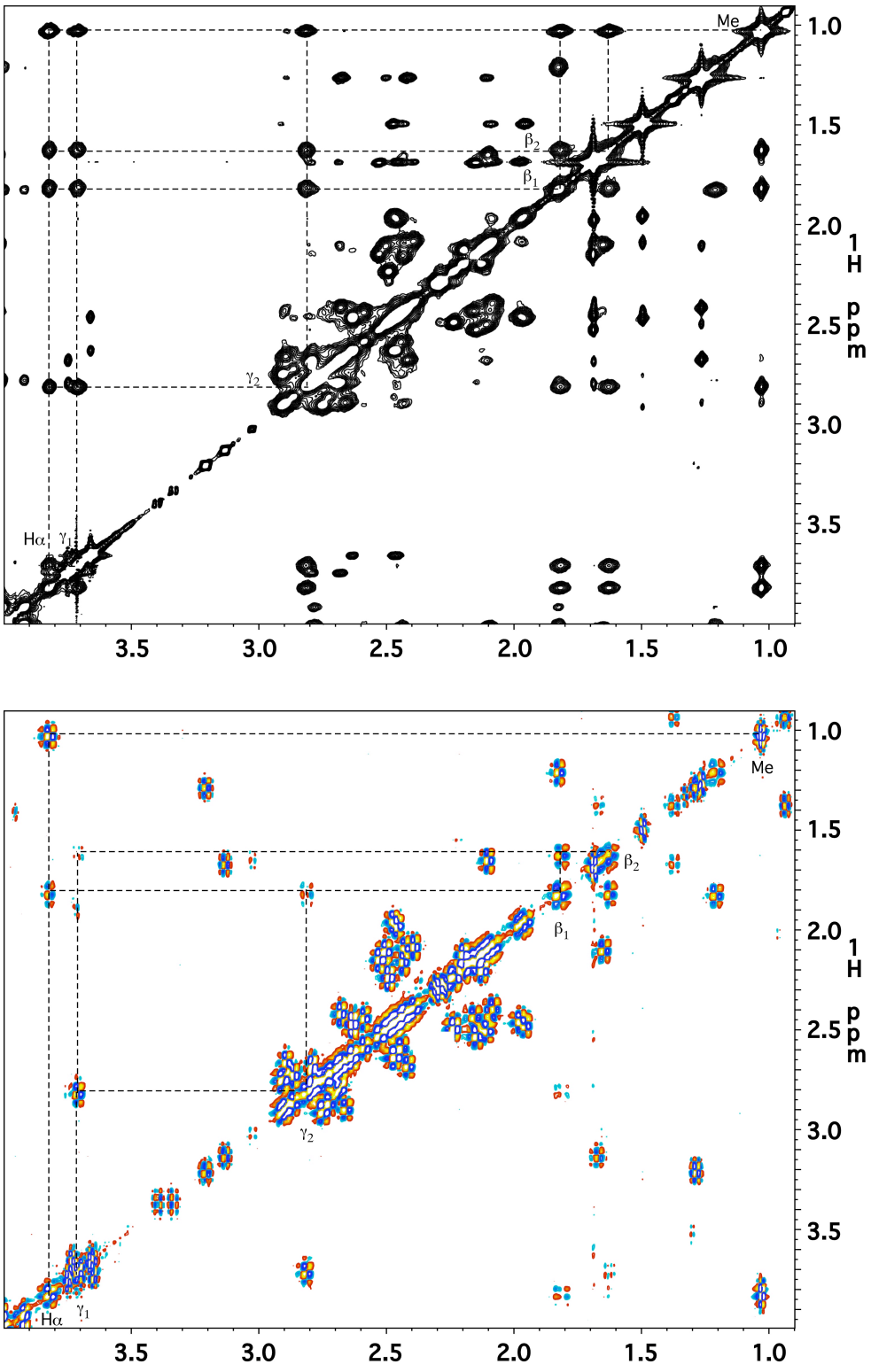

Figure 6-3. Expanded plot of a NOESY and DQF-COSY spectra in D_2O buffer. All adduct protons were assigned.

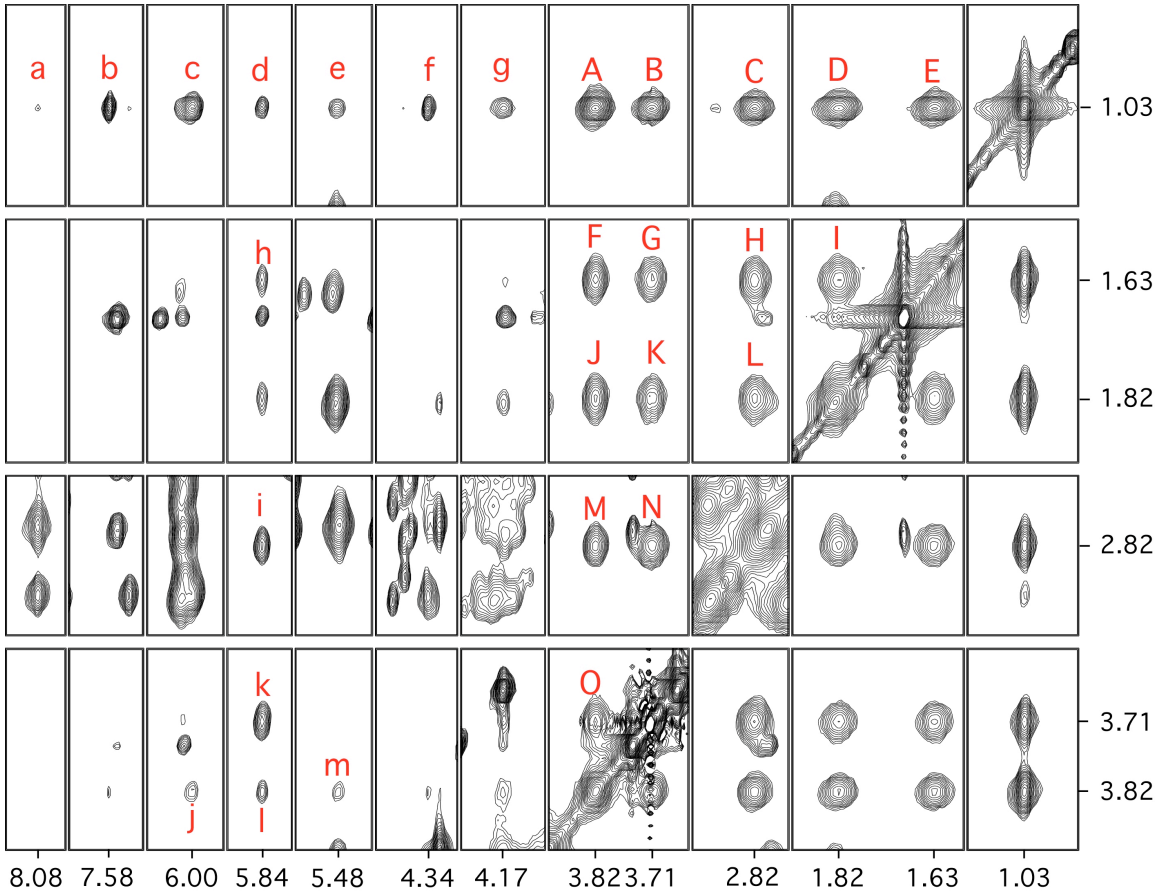

Figure 6-4. Tile plot of a NOESY spectrum in D_2O buffer at a mixing time of 350 ms. a. A^8 H8 → X^7 Me; b. A^8 H2 → X^7 Me; c. A^8 H1′ → X^7 Me; d. C^{20} H1′ → X^7 Me; e. X^7 H1′ → X^7 Me; f. A^8 H4′ → X^7 Me; g. A^8 H5′ → X^7 Me; h. C^{20} H1′ → X^7 β2; i. C^{20} H1′ → X^7 β2; j. A^8 H1′ → X^7 Hα; k. C^{20} H1′ → Y^{19} γ1; l. C^{20} H1′ → X^7 Hα; m. X^7 H1′ → X^7 Hα; A. X^7 Hα → X^7 Me; B. Y^{19} γ1 → X^7 Me; C. Y^{19} γ2 → X^7 Me; D. X^7 β1 → X^7 Me; E. X^7 β2 → X^7 Me; F. X^7 Hα → X^7 β2; G. Y^{19} γ1 → X^7 β2; H. Y^{19} γ2 → X^7 β2; I. X^7 β1 → X^7 β2; J. X^7 Hα → X^7 β1; K. Y^{19} γ1 → X^7 β1; L. Y^{19} γ2 → X^7 β1; M. X^7 Hα → Y^{19} γ2; N. Y^{19} γ1 → Y^{19} γ2; O. X^7 Hα → Y^{19} γ1.

Assignments of exchangeable DNA protons. In the expanded imino proton region of the ^{1}H NOESY spectrum, Figure 6-5 presents the resonances arising from the Watson-Crick hydrogen bonded imino protons: the complete sequential NOE connectivity was observed between imino protons of duplex except terminal bases due to fast exchange between N and H. The imino resonance arising from the $C^{6}\bullet Y^{19}$ base pair was assigned at 12. 6 ppm, the $X^{7}\bullet C^{18}$ base pair was assigned at 12.5 ppm. The conservation of normal Watson-Crick hydrogen bondings is another indicative of the stable duplex DNA in compatible with non-exchangeable NOESY data. The expanded tile plot (Figure 6-6) presents the correlations among base protons in the $X^{7}\bullet C^{18}$ and $C^{6}\bullet Y^{19}$ including NOEs to adduct protons. Each imino proton has a strong NOE to amino proton (peak E and peak C). Further, 4 strong A:T base pairings were present (peak a,b,c, and d).

Chemical Shift Perturbations NMR data suggest that DNA duplex is minimally perturbed by showing locally influenced chemical shifts differences from the unmodified duplex DNA (Figure 6-7). The largest difference was about 0.6 ppm, suggesting that the minimal and localized effect on DNA in the presence of interchain DNA cross-link. Overall, the chemical shifts of 5'- side cytosine protons were shielded in both strands whereas sugar protons of adducted bases were deshielded about 0.2 ppm, of which results are similar to what Dooley et al. observed with there carbon tethered cross-link adduct but with a different sequence (Dooley, P. A. et al., 2001).

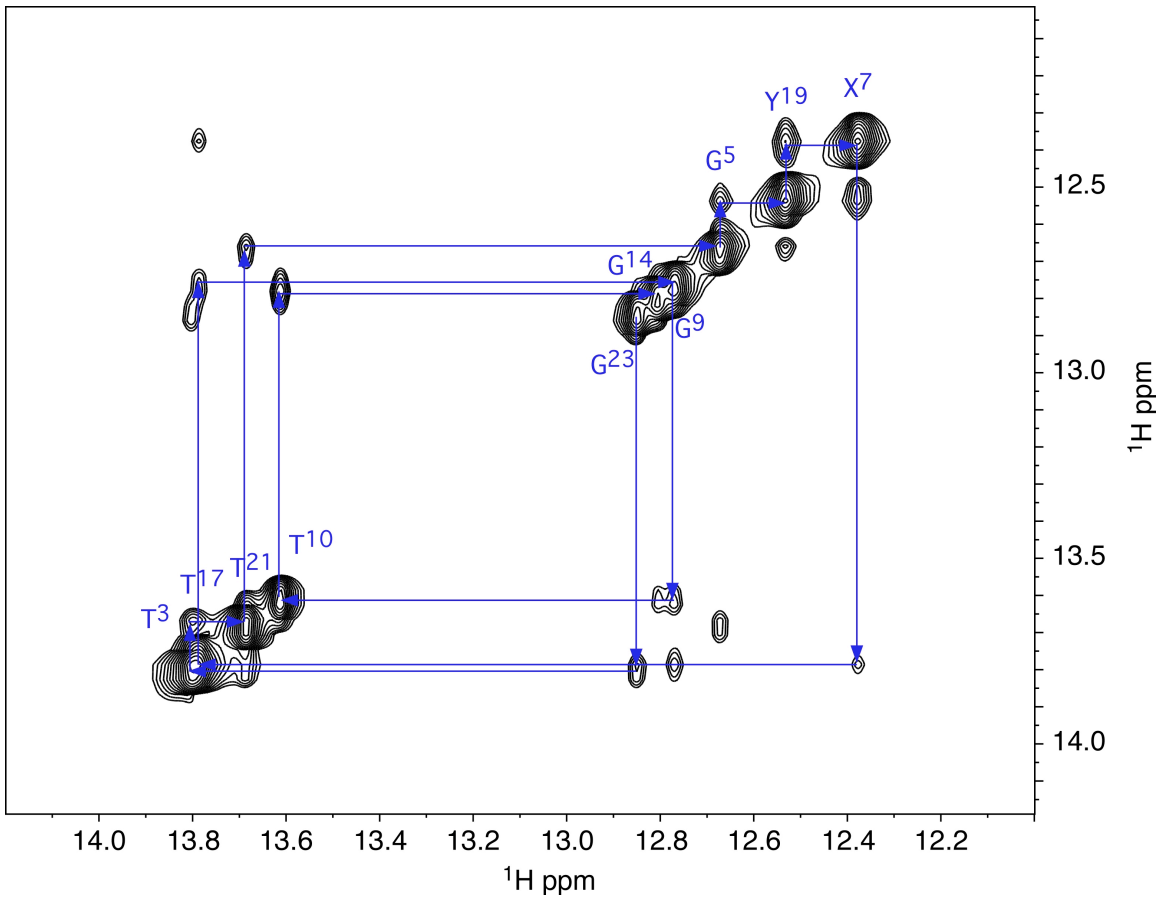

Figure 6-5. Expanded plot of a NOESY spectrum at a mixing time of 200 ms showing NOE connectivities for the imino protons for the base pairs from C^{2}•G^{23} to C^{11}•G^{14}.

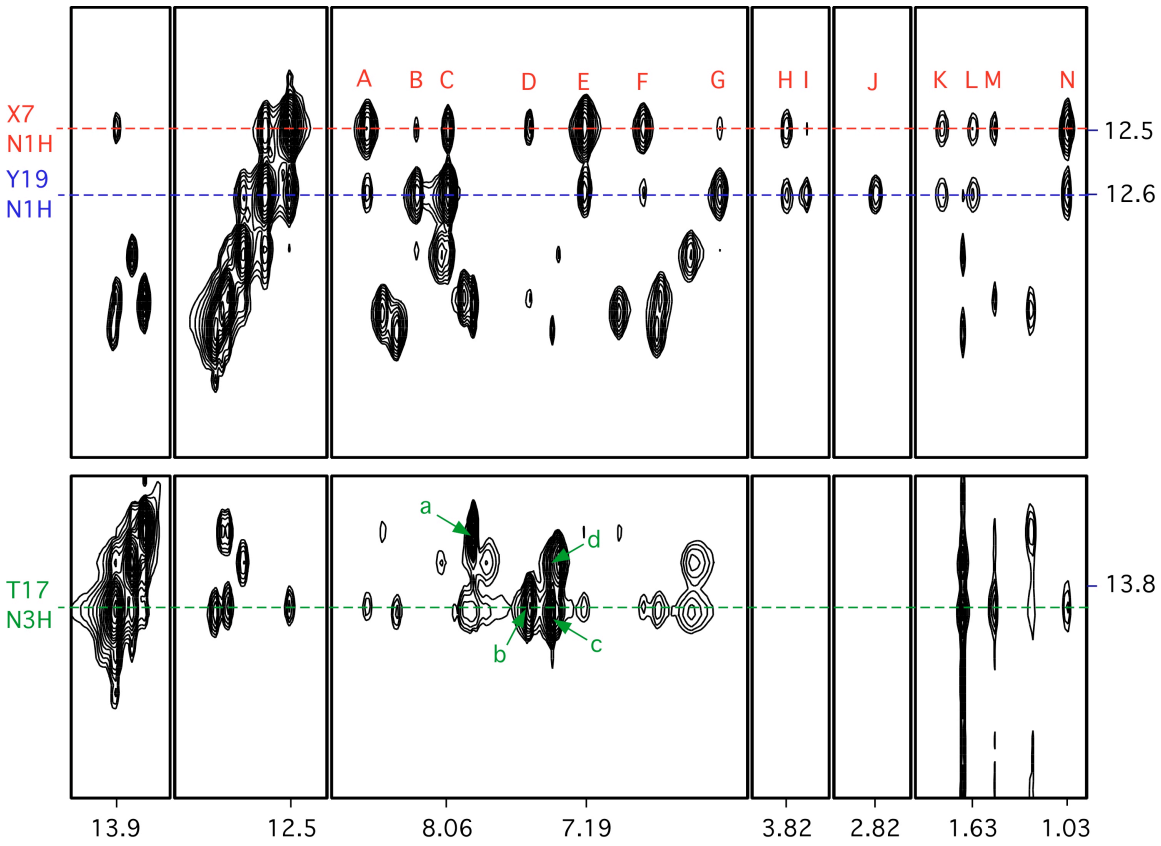

Figure 6-6. Expanded tile plot of a NOESY spectrum at a mixing time of 200 ms showing couplings from selected imino protons to DNA protons. A. C^{18} N4Ha; B. C^{6} N4Ha; C. Y^{19} $N^{2}H$; D. A^{8} H2; E. X^{7} $N^{2}H$; F. C^{18} $N^{4}Hb$; G. C^{6} $N^{4}Hb$; H. X^{7} Hα; I. X^{7} γ1; J. X^{7} γ2; K. X^{7} β1; L. X^{7} β2; M. T^{17} Me; N. X^{7} Me; a. A^{15} H2/T^{10} N3H; b. A^{8} H2/T^{17} N3H; c. A^{22} H2/T^{3} N3H; d. A^{4} H2/T^{21} N3H.

A

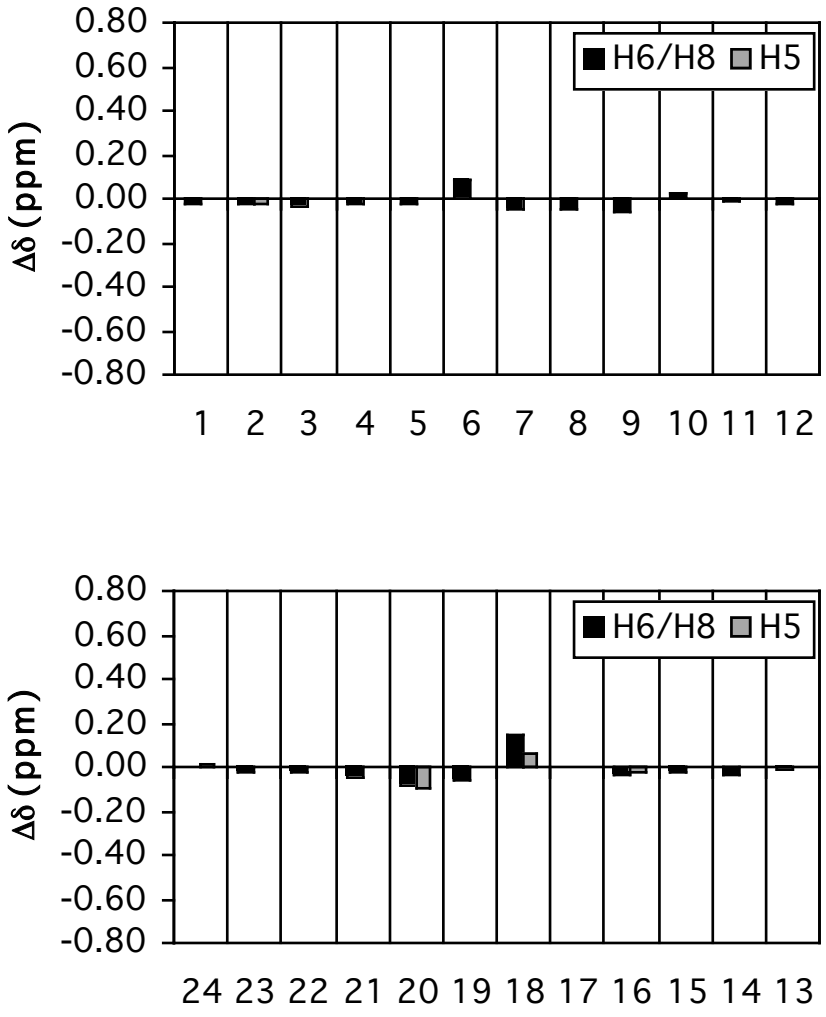

Figure 6-7. Chemical Sifts Differences of non-exchangeable aromatic and sugar protons of the unmodified and cross-liked oligodeoxynucleotides. A: Aromatic H5, H6, and H8 protons. B: Sugar protons (continued on next page)

B

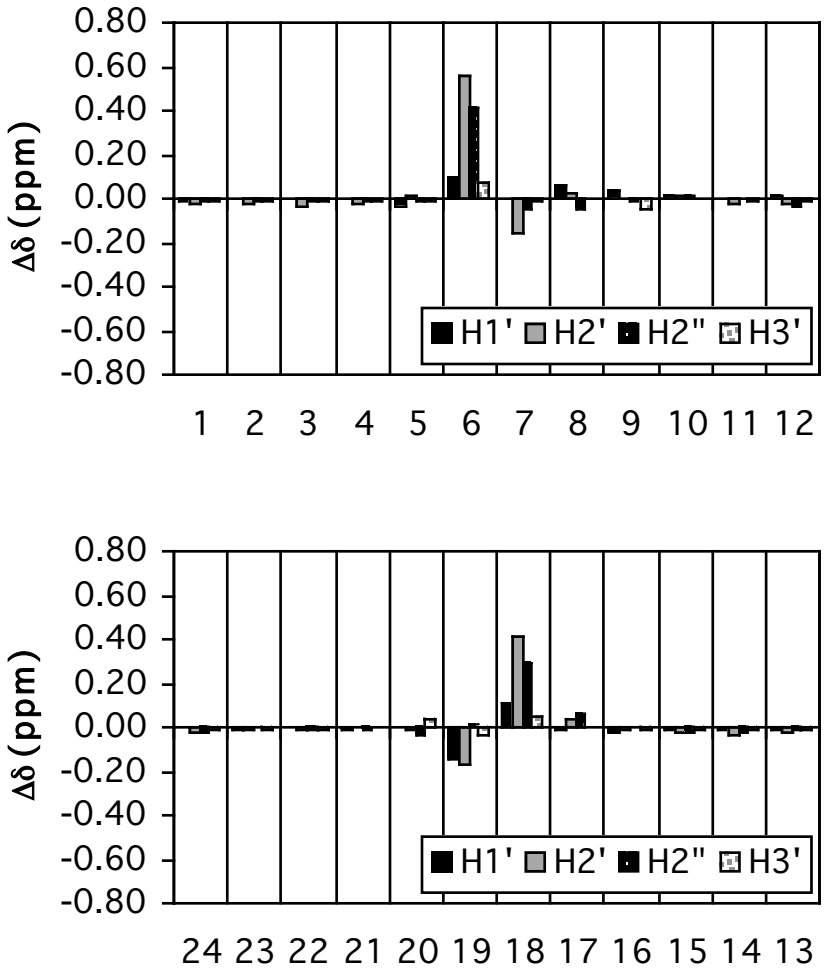

Figure 6-7. Chemical Sifts Differences of non-exchangeable aromatic and sugar protons of the unadducted an dcross-liked oligodeoxynucleotides. A: Aromatic H5, H6, and H8 protons. B: Sugar protons.

Torsion Angle Measurement. All of experimental data were consistent with B-like DNA helix. From NOESY and COSY data, there was no clear evidence of neither syn conformation nor A type DNA helix (Kim, S. G. et al., 1992). The ^{31}P spectrum showed no unusual chemical shifts perturbations (data not shown), suggesting that even the backbone was not significantly perturbed by the existence of the fully reduced *R*-crotonaldehyde interstrand cross-link. In Figure 6-8, the connectivity between H1′ to H2′ and H2′′ to H3′ are present. The chemical shifts of H2′ and H2′′ of Y^{19} were reversed compared to other sugars, however, still suggesting like a B-form DNA.

rMD Calculations. The NOE generated 303 distance restraints and 52 empirical Watson-Crick restraints were incorporated in rMD calculations. Starting structures, IniA and IniB, were built and used in MARDIGRAS calculations (Borgias and James, 1990; Liu, H. et al., 1995 Dec). The stereoview of five convergent structures originating from rMD calculations initiated from a B-form and an A-form starting structures can be viewed in Figure 6-9 and 6-10 respectively. An initial rmsd between starting structures was 6.371 Å, the pairwise rmsd between averaged structures from IniA and IniB was 1.555 Å. The final averaged and energy-minimized structure was compared to starting structure: 2.676 Å between IniB and rMD_{avg}, and 4.067 Å between IniA and rMD_{avg}. Detailed results are listed in Table 6-2. A CPK structure of the averaged structure is shown in Figure 6-11.

Finally, Figure 6-12 presents R_1^x values for each of the nucleotides. The 150 ms intensity data were used for CORMA calculations. The total R_1^x value was 7.04×10^{-2}: 6.47×10^{-2} for intra-residues and 7.72×10^{-2} for inter-residues.

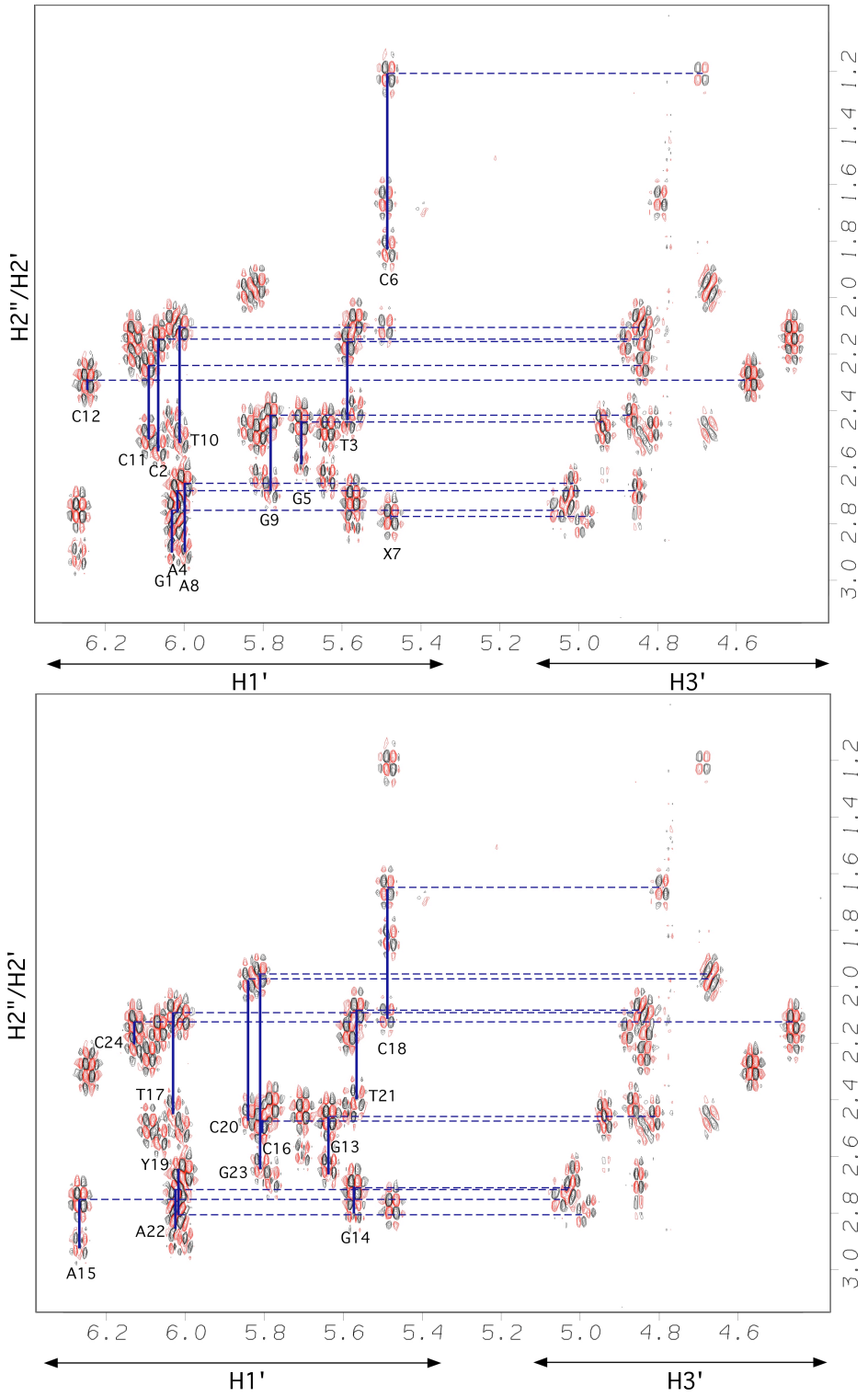

Figure 6-8. Expanded plot of DQF-COSY spectrum. The chemical shift ranges for H1′ and H3′ are indicated by the arrows at the bottom, those for H2′ and H2″ on the left. For each nucleotide the cross-peaks H1′-H2′ and H1′-H2″ are connected by a solid vertical line, and the cross-peaks H1′-H2′ and H2′-H3′ by a broken vertical line.

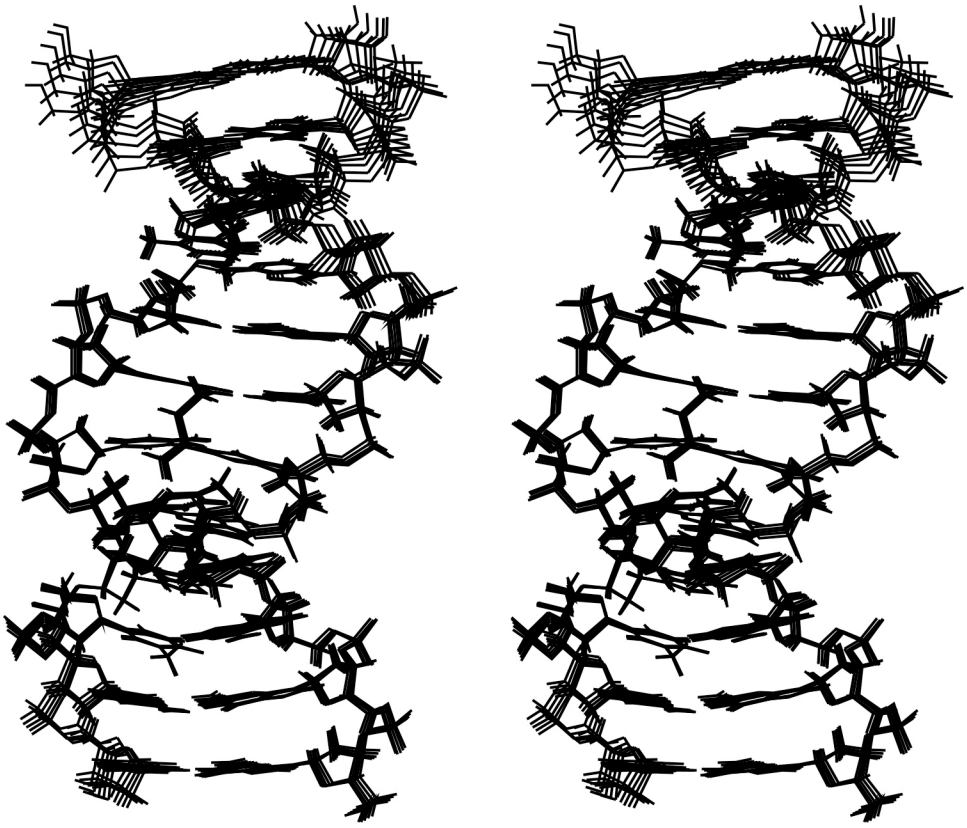

Figure 6-9. Streoview of five superimposed structures emergent from the simulated annealing rMD protocol of IniA.

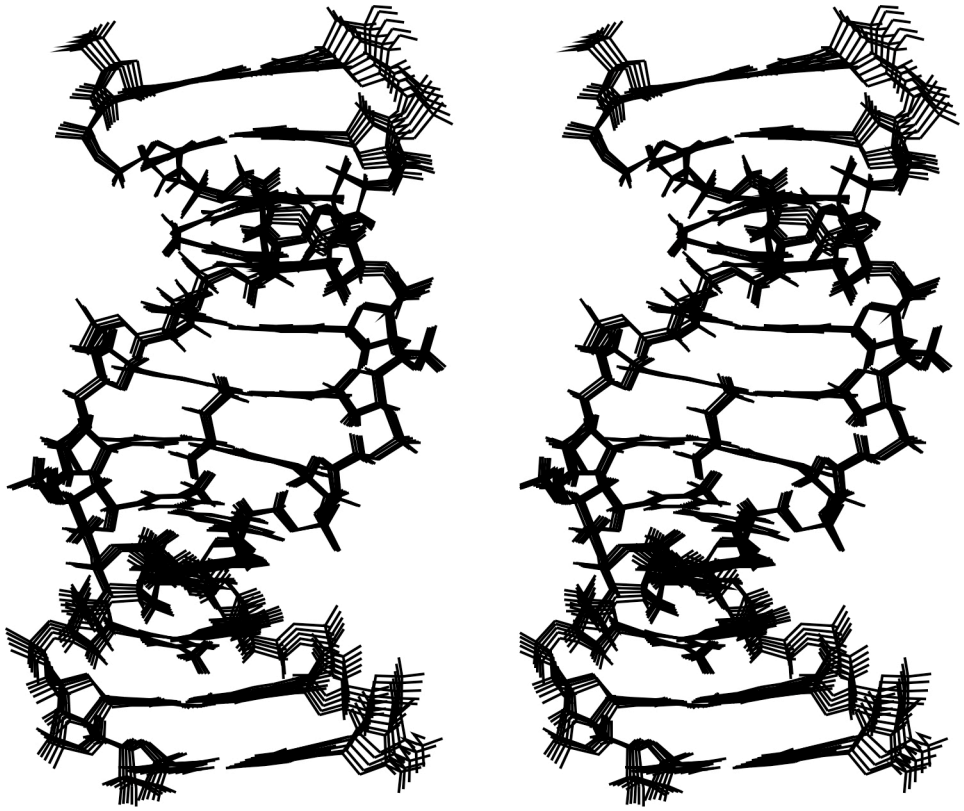

Figure 6-10. Streoview of five superimposed structures emergent from the simulated annealing rMD protocol of IniB.

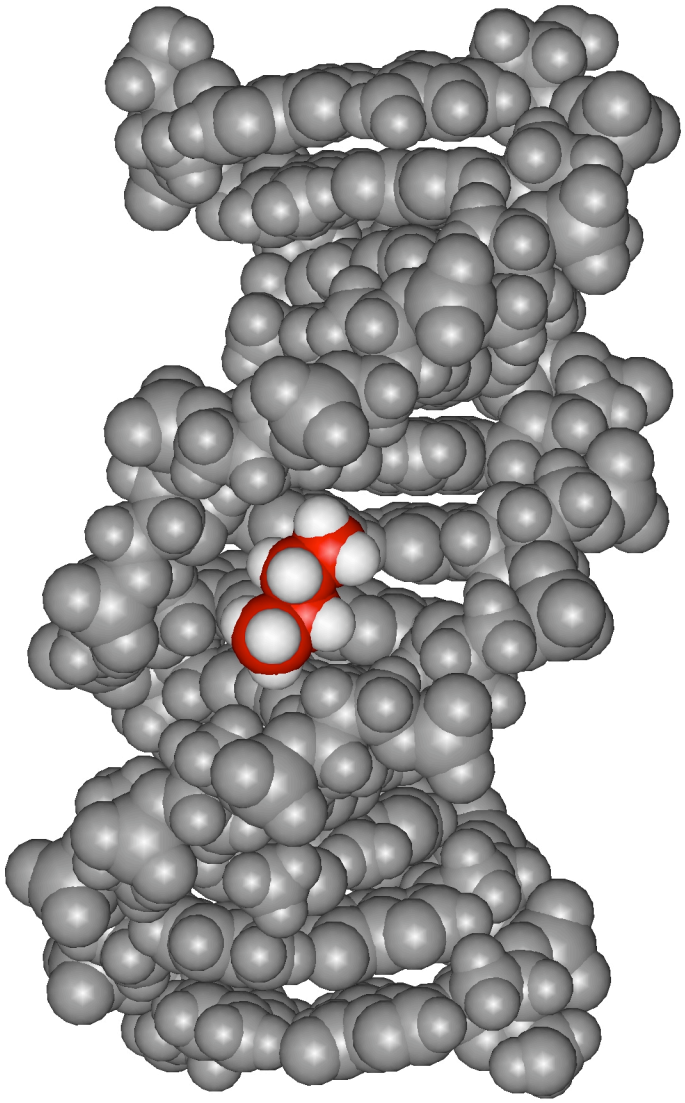

Figure 6-11. A CPK representation of the fully reduced *R*-crotonaldehyde cross-link. This is the averaged and energy minimized using the conjugate gradients algorithm. The cross-linked residues in pink with protons in white.

Table 6-2. Root Mean Square Deviations (RMSD).

Analysis of the rMD-Genrated Structures of the fully reduced *R*-crotonaldehyde cross-link in the 5'-CpG-3' sequence	
NMR restraints	
Total number of distance restraints	246
Interresidue distance restraints	119
Intraresidue distance restraints	127
DNA— adduct protons distance restraints	10
Adduct protons distance restraints	14
H-bonding restraints	52
Backbone torsion angle restraints	0
pairwise rmsd (Å) over all atoms	
IniA vs. IniB	6.371
<rMDA>[a] vs. <rMDA>	0.53 ± 0.27
<rMDB>[b] vs. <rMDB>	0.47 ± 0.24
$rMDA_{avg}$ [c] vs. $rMDB_{avg}$ [d]	1.376
$rMDA_{avg}$ vs. rMD_{avg} [e]	0.795
$rMDB_{avg}$ vs.rMD_{avg}	1.006
IniA vs. rMD_{avg}	4.338
IniB vs. rMD_{avg}	2.623

[a] <rMDA> represents the set of 5 structures that emerged from rMD calculations starting from IniA. [b] <rMDB> represents the set of 5 structures that emerged from rMD calculations starting from IniB. [c] $rMDA_{avg}$ represents the average structure of all five <rMDA>. [d]$rMDB_{avg}$ represents the average structure of all five <rMDB>. [e] rMD_{avg} represents the potential enery minimized average structure of all 10 structures of <rMDA> and <rMDB>.

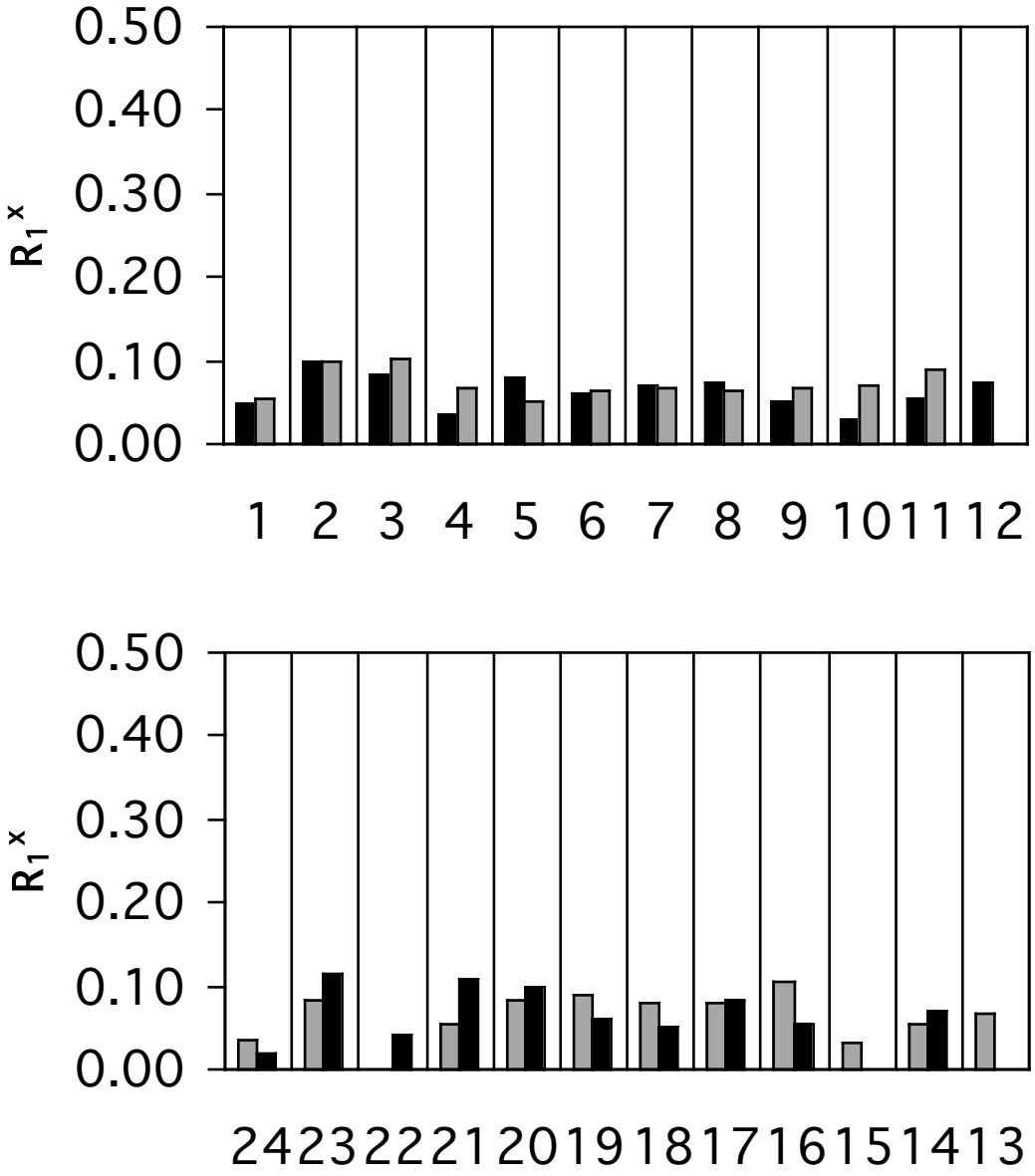

Figure 6-12. Complete relaxation matrix calculations on the average structure emergent from the simulated annealing rMD protocol showing sixth root residuals (R_1^x) for each nucleotide: The adducted strand (top); the complementary strand (bottom). The black bars represent intranucleotide R_1^x values, and the gray bars represent internucleotide R_1^x values.

Discussion

As was expected, the fully reduced *R*-crotonaldehyde-derived cross-link was structurally stable to form a B-form DNA while maintaining Watson-Crick hydrogen bondings (Figure 6-13 and 6-14). This implies that thermodynamically DNA interstrand cross-links are stable which is consistent with a UV melting study (Kozekov et al., 2003). Secondly, carbinolamine type cross-links can exist in a duplex without disrupting Watson-Crick hydrogen bondings. Since other possible cross-links such as imine and pyrimidopurinone require disruption of normal base pairing. It can be inferred that they are not appropriate for duplex environment. On the contrary, the carbinolamine type interstrand cross-links can only satisfy Watson-Crick base pairings between adducts and corresponding opposite bases. Although all 3 possible cross-link forms are in equilibrium, NMR studies of site-specifically labeled APdG and CPdG adducts proved the carbinolamine cross-links predominated as described in the previous chapters. The presence of cross-links increases the melting temperature and thus postulated to interfere with DNA replication and repair process.

This NMR study of the fully reduced cross-linked DNA supports the idea that the chain form of interstrand DNA cross-link, with an sp^3 carbon at γ position, is favored in a duplex environment. With the absence of hydroxyl group at C_γ, this reduced cross-link is regarded as a suitable model for the carbinolamine cross-links. Further, the refined structure strongly supports the involvement of endo-^{1}H of the two amino protons at the exocyclic amino group of guanine (X^7 and Y^{19}) into hydrogen bonding while the cross-linked chain attached onto the exo-^{1}H site. This contrasts the study of the trimethylene cross-

link study by Dooley et al. (Dooley, P. A. et al., 2001; Dooley, P. A. et al., 2003). However, it is believed that the exo-^{1}H displaced structure is more reasonable while it allows the endo-^{1}H to participate in hydrogen bonding. The NMR data support this: the presence of both NOEs between guanosine iminos and cytidine amino protons peaks is indicative of Watson-Crick hydrogen bondings of X:C. Furthermore, the presence of NOEs between thymidine imino and adenosine H2 protons are also support Watson-Crick hydrogen bondings of A:T base pairs are well conserved as shown in Figure 6-6. This indicates the involvement of the amino protons as the endo-^{1}H's. These are consistent with the structural studies of other N^2-dG adducts such as mitomycin, anthramycin and bezo[a]pyrene diol epoxide that leave the endo-^{1}H available to participate in normal Watson-Crick hydrogen bonding (Kopka et al., 1994; Kozack and Loechler, 1997 Aug; Norman et al., 1990). Moreover, the same patterned observances are discovered with the different stereochemistry of the methyl group (Chapter VII).

Additional comparisons with different stereochemistry of the methyl group from *S*-α-CH_3-γ-OH-1,N^2-propano-2'-deoxyguanosine adducts are discussed in the next chapter.

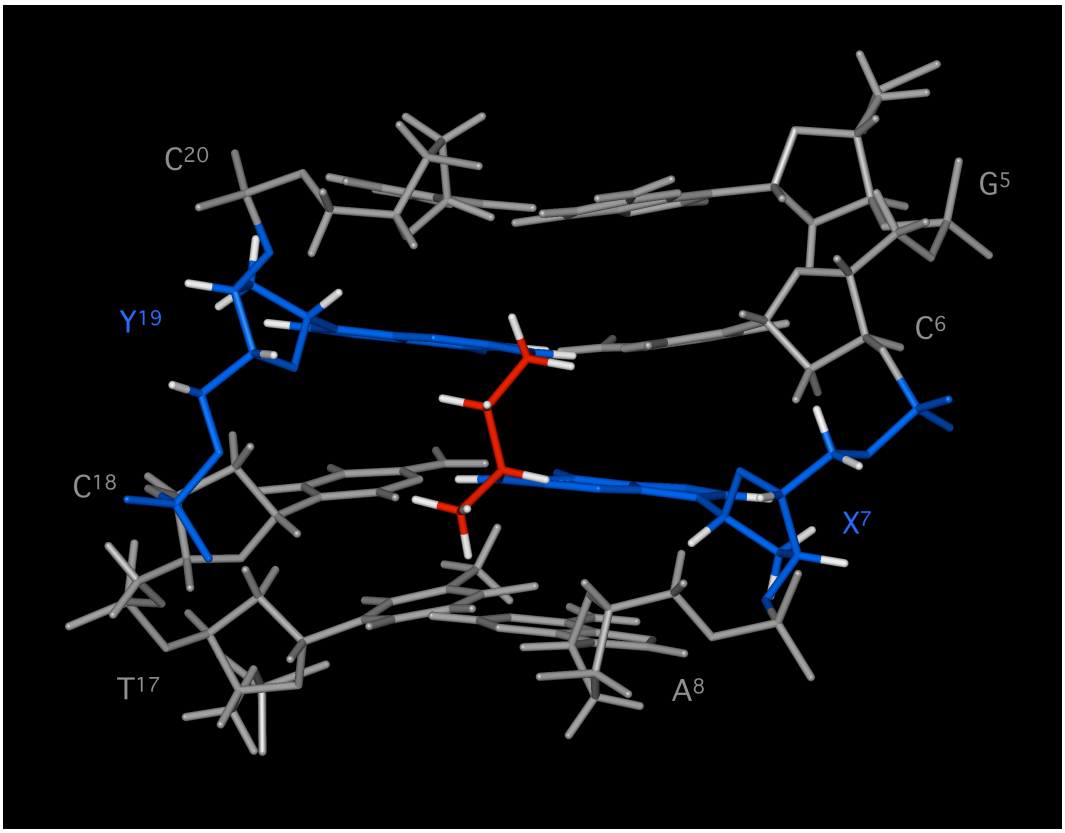

Figure 6-13. A side view of the refined structure rMD_{avg} from the minor groove.

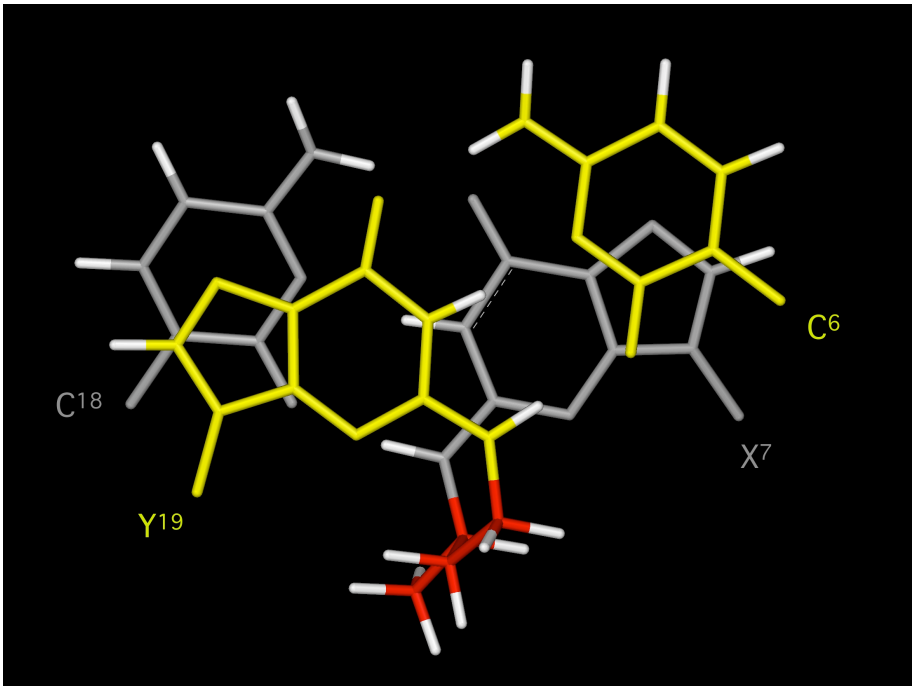

Figure 6-14. A top view of the refined structure, rMD_{avg} for base stacking interaction.

CHAPTER VII

SOLUTION STRUCTURE OF THE FULLY REDUCED DNA INTERSTRAND CROSS-LINK ARISING FROM RING OPENING OF *S*-α- CH_3-γ-OH-1,N^2-PROPANO-2′-DEOXYGUANOSINE ADDUCT IN THE 5′-CpG-3′ SEQUENCE.

Introduction

While the *R*-CPdG adduct formed interstrand carbinolamine cross-links in the 5′-CpG-3′ sequence, the *S*-α-CH_3-γ-OH-1,N^2-propano-2′-deoxyguanosine (*S*-CPdG) did not show as high a tendancy to cross-link. It has been thought that thisis due to hindrance by the methyl stereochemistry of the opened aldehidic form while it also possesses the allylic strain for reacting with the amino group of the targeting dG in the opposite strand, and a possible instability of the cross-link in a duplex that can be issued by the methyl stereochemistry. In the previous Chapter V the structure of the stable aldehyde opened form, *S*-COPdG aldehyde adduct was determined, which supports the hindering effect for generating interstrand cross-link by the methyl group. The fully reduced *R*-CPdG induced interstrand cross-linked structure suggests the stability of the cross-link by *R*-CPdG in the 5′-CpG-3′ sequence. A question remained about the stability of the *S*-CPdG induced cross-links in the same sequence since relatively low amounts of the cross-link was found (Cho, Y.-J. et al., 2006; Kozekov et al., 2003; Lao and Hecht, 2005). Instability of this cross-link may suggest a different amount of cross-link generation by the *R*- and *S*-crotonaldehyde. Otherwise, the kinetic issue is more important that the thermodynamic point for the generation of cross-link. To answer for this question, NMR study has been carried out for the

fully reduced *S*-crotonaldehyde cross-link that was synthesized as shown in Scheme 1-5. Unlike sequence dependent interchain cross-link study, the fully reduced *S*-crotonaldehyde cross-link has a high melting temperature about 2 degree higher than that of *R*-crotonaldehyde cross-link indeed, which may imply the stability of the cross-link.

In this chapter, the NMR studies and the structural refinement of the fully reduced *S*-crotonaldehyde interstrand cross-link is described.

Scheme 7-1. 5′-CpG-3′ Oligonucleotide and the chemical structure of the fully reduced *S*-crotonaldehyde cross-link. β_1 and γ_1 present left sided protons, and β_2 and γ_2 are right sided protons.

5′-G^{1} C^{2} T^{3} A^{4} G^{5} C^{6} **X**^{7} A^{8} G^{9} T^{10} C^{11} C^{12}-3′
3′-C^{24}G^{23}A^{22}T^{21}C^{20}**Y**^{19}C^{18}T^{17}C^{16}A^{15} G^{14} G^{13}-5′

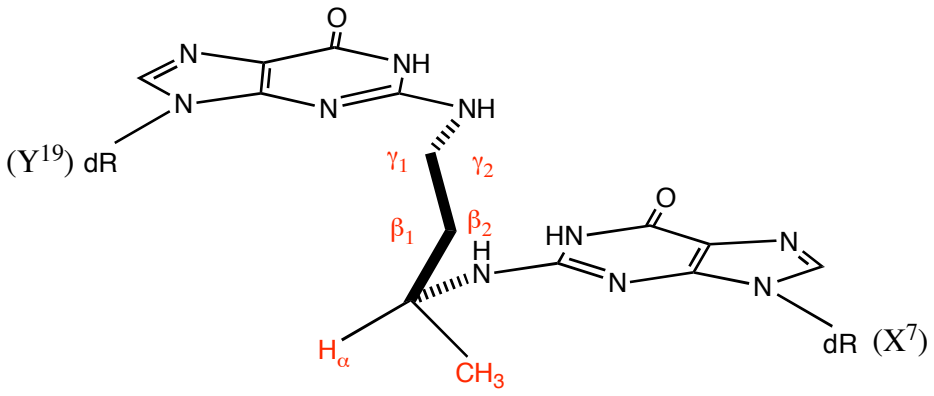

Results

Assignments of nonexchangeable DNA protons. As shown in Figure 7-1, the complete sequential connectivity between the aromatic and the anomeric protons for both strands of the duplex was accomplished in the NOESY walk region. All cytosine H5/H6 cross-peaks were numbered (pink) on each peak. The small numbers (blue) nearby cross-peaks indicate 5'- base proton numbers that have a NOE with 3'-side cytosine H5. Two dimensional NOESY and DQF-COSY spectra were used for further assignments. All data were collected at 30 ^{o}C. In comparison to the fully reduced *R*-crotonaldehyde cross-link adduct, the *S*-cross-link has distinct chemical shifts for C^{6} and X^{7} H1' resonances. The completion of NOESY walk in this region was indicative of a stable and ordered DNA conformation. In addition, these assignments were expanded into other regions of ^{1}H NOESY spectrum to yield complete ^{1}H assignments for the H2', H2'', H3', and H4' protons (Patel, D.J. et al., 1987; Reid, 1987). Table 7-1 details the assignments of the non-exchangeable protons.

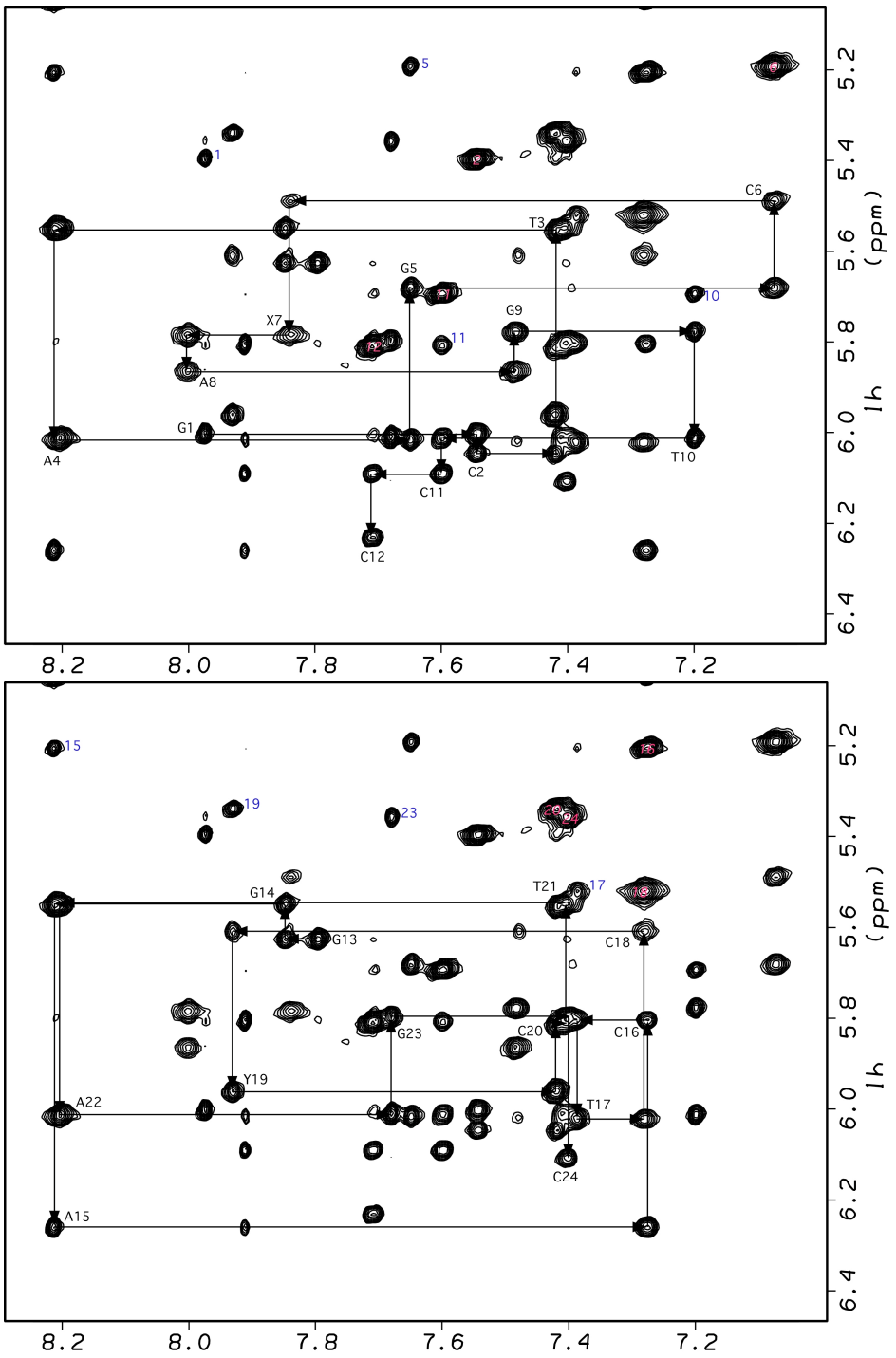

Figure 7-1. Expanded plot of a NOESY spectrum in D_2O buffer at a mixing time of 250ms showing the sequential NOE connectivites from the aromatic to anomeric protons. The base positions are indiceted at the intranucleotide cross-peaks of the aromatic proton to its own anomeric proton. (Top) Sequential NOE connectivities for nucleotides G^{1}→C^{12}. (Bottom) Sequential NOE connectivities for nucleotides G^{13}→C^{24}.

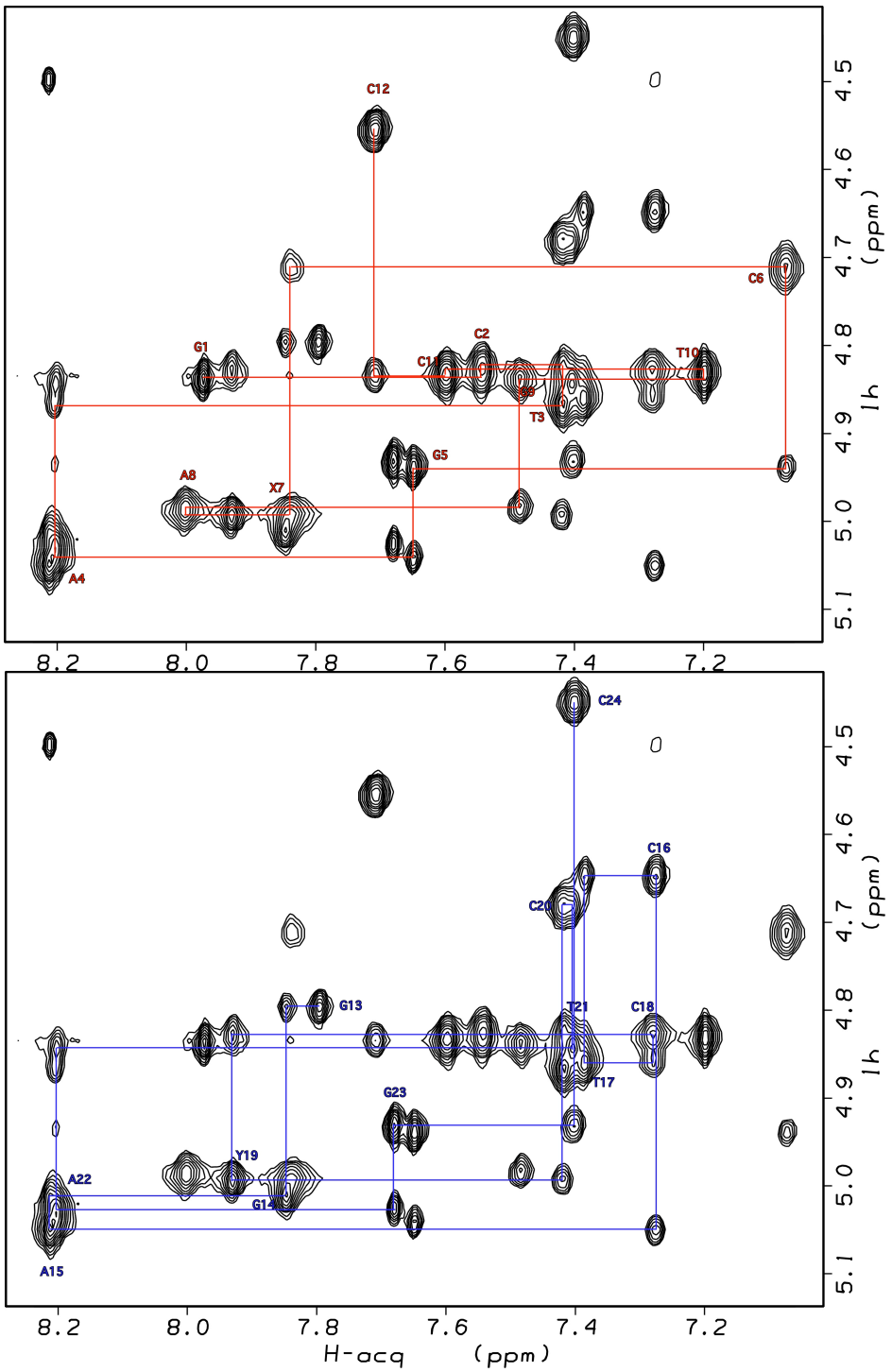

Figure 7-2. Expanded plot of a NOESY spectrum in D_2O buffer at a mixing time of 250ms showing the sequential NOE connectivites from the aromatic to anomeric protons. The base positions are indiceted at the intranucleotide cross-peaks of the aromatic proton to its own anomeric proton. (Top) Sequential NOE connectivities for nucleotides $G^{1}\rightarrow C^{12}$. (Bottom) Sequential NOE connectivities for nucleotides $G^{13}\rightarrow C^{24}$.

Table 7-1. Chemical shifts (ppm) of non-exchangeable protons in the oligodeoxynucleotide 5′-d(GCTAGCXAGTCC)-3′•5′-(GGACTCYCTAGC)-3′.

BASE	H1′	H2′	H2″	H3′	H4′	H5′	H5″	H6/H8	Me/H5
G^{1}	6.00	2.67	2.77	4.84	4.26	3.73		7.98	
C^{2}	6.05	2.14	2.51	4.82	4.25	4.20	4.15	7.54	5.40
T^{3}	5.55	2.15	2.41	4.87	4.13			7.42	1.68
A^{4}	6.01	2.74	2.90	5.04	4.40	4.04	4.14	8.21	
G^{5}	5.68	2.44	2.59	4.94	4.35	4.18		7.65	
C^{6}	5.49	1.33	2.00	4.71	3.99	4.20	4.04	7.07	5.19
X^{7}	5.78	2.73	2.81	4.99	4.33	3.96	4.04	7.84	
A^{8}	5.86	2.51	2.86	4.99	4.19	4.19	4.15	8.00	
G^{9}	5.78	2.39	2.66	4.84	4.33			7.48	
T^{10}	6.01	2.10	2.49	4.82	4.20	4.12		7.20	1.23
C^{11}	6.09	2.23	2.48	4.84	4.17	4.08		7.60	5.70
C^{12}	6.23	2.29		4.55	4.05	4.26	4.17	7.71	5.81
G^{13}	5.63	2.44	2.61	4.80	4.16	3.65		7.80	
G^{14}	5.55	2.70	2.78	5.01	4.36	4.05	4.13	7.85	
A^{15}	6.26	2.75	2.91	5.05	4.50	4.19	4.24	8.22	
C^{16}	5.80	1.99	2.50	4.65	4.23	4.33	4.19	7.27	5.20
T^{17}	6.02	2.14	2.51	4.86	4.20			7.38	1.49
C^{18}	5.61	1.73	2.30	4.83	4.03			7.28	5.52
Y^{19}	5.96	2.76	2.64	4.99	4.39	4.09	4.03	7.93	
C^{20}	5.81	1.94	2.46	4.68	4.16	4.30		7.42	5.34
T^{21}	5.55	2.09	2.39	4.84	4.11			7.40	1.66
A^{22}	6.01	2.72	2.86	5.03	4.38	4.02	4.12	8.20	
G^{23}	5.80	2.47	2.62	4.93	4.34			7.68	
C^{24}	6.11	2.12	2.20	4.45	4.03	4.45		7.40	5.35

X^{7} H_{α} (3.28); Me (1.17); β_1 (1.09); β_2 (2.77); γ_1 (4.06); γ_2 (2.84)

Adduct-DNA NOEs All adduct protons were well resolved and had several NOEs with DNA protons. Unlike the fully reduced *R*-crotonaldehyde cross-link adduct protons, adduct protons exhibit different chemical environment that results in different chemical shifts. The difference is compared in Table 7-2. A major distinct difference is the shielding effect on β protons. In particular the β_1 proton is shielded over the methyl resonances. As listed on Table 7-1, the trans positioned from the hydrogen-bonded N^2H was the most deshielded: Hγ_1 (4.00 ppm) and Me (1.17 ppm, in the case of Me, the deshielding effect is not distinctive due to the higher order of bonds but it is slightly deshielded than that of the fully reduced *R*-crotonaldehyde cross-link). Vice versa, *(E)* positioned proton from N^2H shows upfield chemical shifts: γ_2 (2.84 ppm) and H_α (3.28 ppm) respectively. The DQF-COSY data were helpful for assigning those adduct protons while providing through-bond coupling information (Figure 7-3). Further, TOCSY experiments also provided other clear information for assigning adduct protons (data not shown). It turned out that β protons are most sensitive protons to the configurations of the cross-link: β_1 is the most shielded proton as of 1.09 ppm and β_2 is the most deshielded proton as of 2.77 ppm in comparison to those of the fully reduced *R*-crotonaldehyde cross-link. In Figure 7-4, adduct-DNA cross-peaks were shown. The methyl protons show much intense cross-peaks to the primer strand especially to A^8 H2 and H1'. The β and the γ protons were overlapped with other sugar protons, but β_1, Me and H_α presents relatively well-resolved peaks that were useful for understanding geometry of the cross-link.

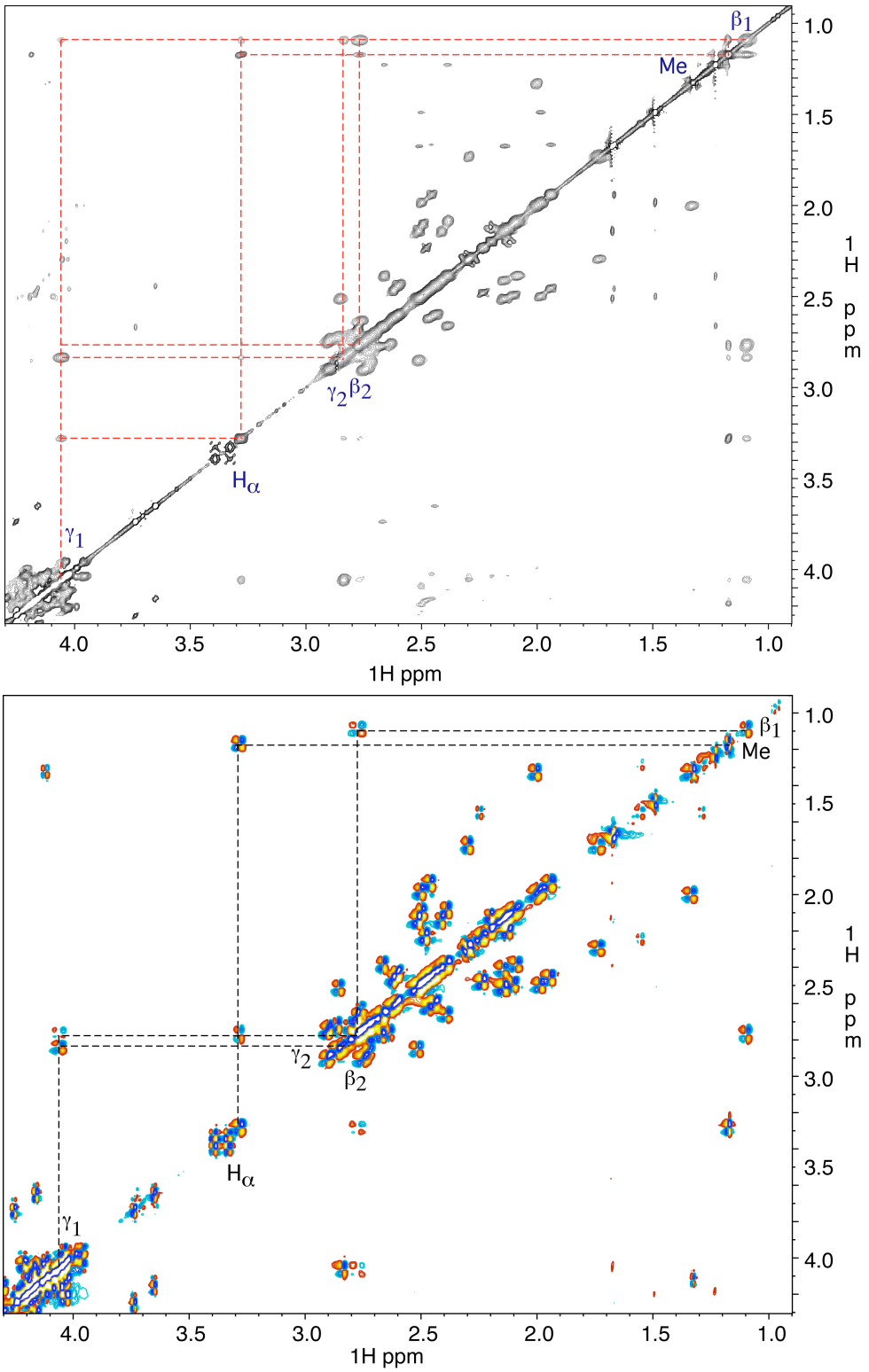

Figure 7-3. Expanded plot of a NOESY (τ_m = 60 ms) and DQF-COSY spectra in D_2O buffer. All adduct protons are assigned.

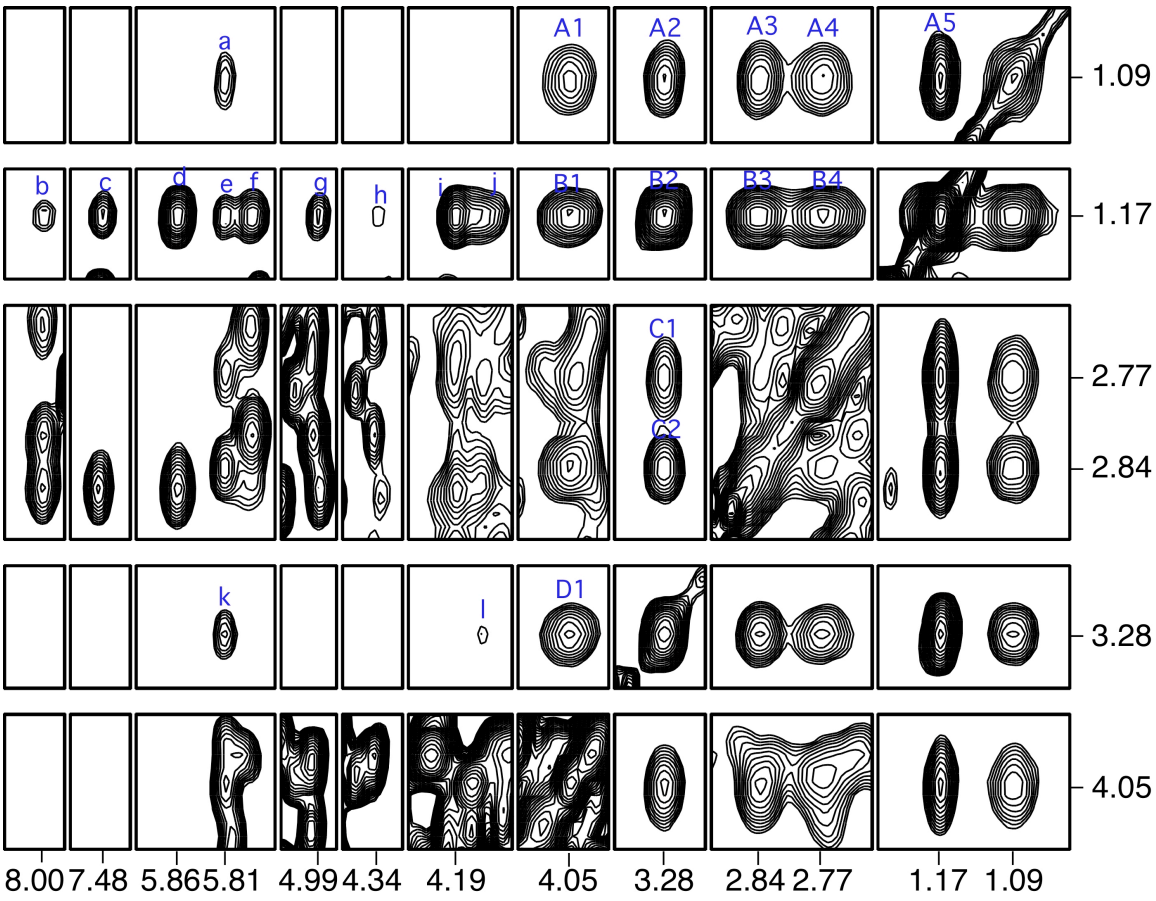

Figure 7-4. Tile plot of a NOESY spectrum in D_2O buffer at a mixing time of 350 ms. Cross-peaks between adduct protons and DNA protons were shown. a. C^{20} H1→ X^7 β_1; b. A^8 H8→ X^7 Me; c. A^8 H2→ X^7 Me; d. A^8 H1′→X^7 Me; e. C^{20} H1→ X^7 Me; f. X^7 H1′→X^7 Me; g. A^8 H3′→X^7 Me; h. X^7 H4′→X^7 Me; i. A^8 H4′→X^7 Me; j. C^{20} H4′→ X^7 Me (overlapped); k. C^{20} H1′→X^7 H_α; l. C^{20} H4′→X^7 H_α; A1. X^7 γ_1→X^7 β_1; A2. X^7 H_α→X^7 β_1; A3. X^7 γ_2→ X^7 β_1; A4. X^7 β_2→X^7 β_1; A5. X^7 Me→X^7 β_1; B1. X^7 γ_1→X^7 Me; B2. X^7 H_α→X^7 Me; B3. X^7 γ_2→X^7 Me; B4. X^7 β_2→X^7 Me; C1. X^7 H_α→ X^7 β_2; C2. X^7 H_α→ X^7 γ_2; D1. X^7 γ_1→ X^7 H_α.

Assignments of exchangeable DNA protons. In the expanded imino proton region from a ^{1}H NOESY experiment, the complete sequential NOE connectivity was observed between imino protons of duplex except terminal bases due to fast exchange between N and H (Figure 7-5). Including NOE to adduct protons, expanded tile plot (Figure 7-6) presents the correlations among base protons in the $X^{7}•C^{18}$ and $C^{6}•Y^{19}$. As pointed out in previous chapters, the conservation of normal Watson-Crick hydrogen bondings is another indicator of the stable duplex DNA. Each imino proton has a strong NOE to amino proton (peak D and peak C). Further, 4 strong A:T base pairings were indicated as peak a,b,c and d.

Chemical Shift Perturbations NMR data suggest that the DNA duplex is minimally perturbed as shown by locally influenced chemical shifts differences from the unmodified duplex DNA (Figure 7-7). The largest difference was about 0.7 ppm, suggesting a minimal effect on DNA in the presence of interchain DNA cross-link. The chemical shifts of 5'- side cytosine protons were shielded in both strands, which is the similar to the fully reduced *R*-crotonaldehyde cross-link study. The peculiar observation is that A^{8} sugar protons were affected by the presence of cross-link that resulted in upfield shifts on H1' and H2' protons. The methyl orientation may be attributed to this.

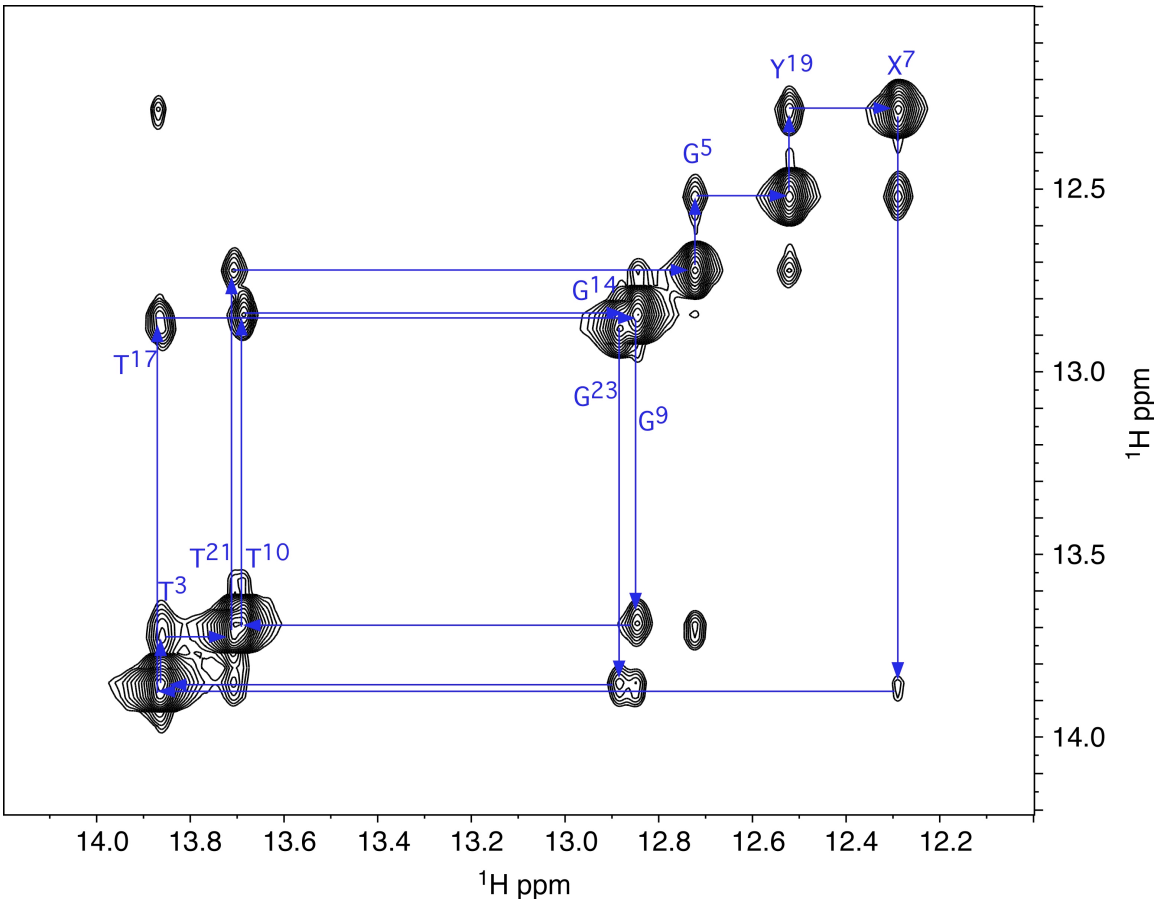

Figure 7-5. Expanded plot of a NOESY spectrum at a mixing time of 250 ms showing NOE connectivities for the imino protons for the base pairs from C^{2}•G^{23} to C^{11}•G^{14}.

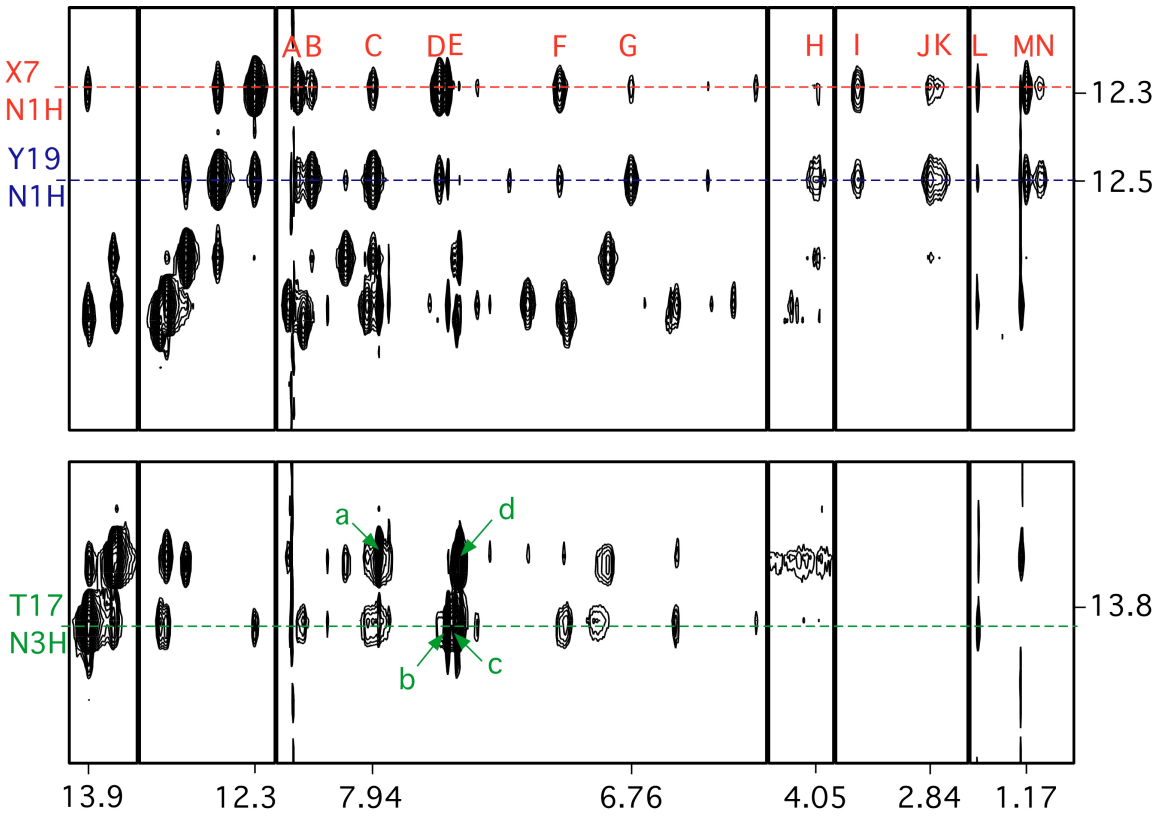

Figure 7-6. Expanded tile plot of a NOESY spectrum at a mixing time of 250 ms showing couplings from selected imino protons to DNA protons. A. C^{18} N^4Ha; B. C^6 N^4Ha; C. Y^{19} N^2H; D. X^7 N^2H; E. A^8 H2; F. C^{18} N^4Hb; G. C^6 N^4Hb; H. X^7 γ_1; I. X^7 H_α; J. X^7 γ_2; K. X^7 β_2; L. T^{17} Me; M. X^7 Me; N. X^7 β_1; a. A^{15} H2/T^{10} N3H; b. A^8 H2/T^{17} N3H; c. A^{22} H2/T^3 N3H; d. A^4 H2/T^{21} N3H.

A

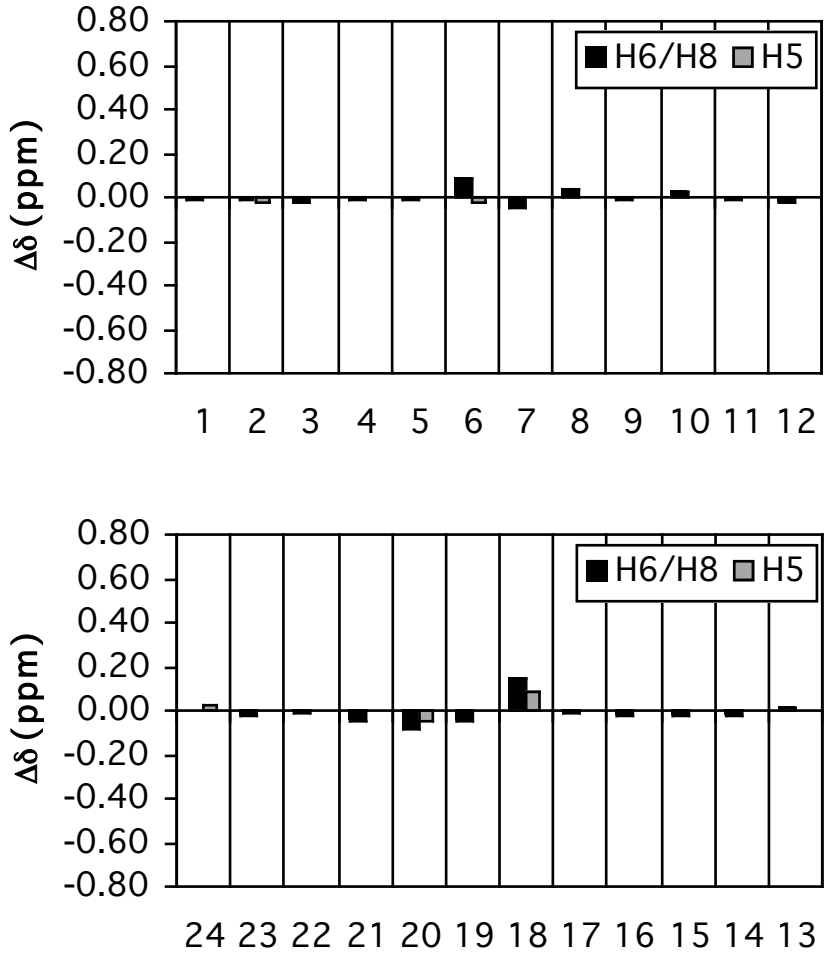

Figure 7-7. Chemical Sifts Differences of non-exchangeable aromatic and sugar protons of the unadducted and cross-liked oligodeoxynucleotides. A: Aromatic H5, H6, and H8 protons. B: Sugar protons (continued on next page).

B

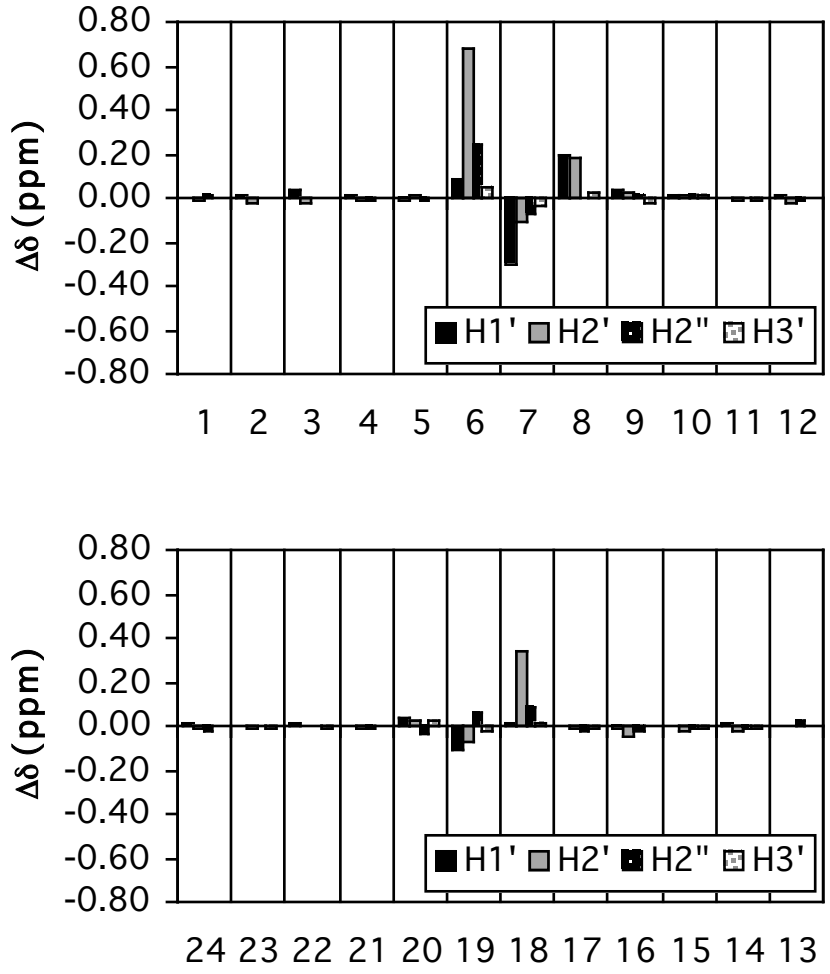

Figure 7-7. (continued) Chemical Sifts Differences of non-exchangeable aromatic and sugar protons of the unadducted and cross-liked oligodeoxynucleotides. A: Aromatic H5, H6, and H8 protons. B: Sugar protons.

rMD Calculations. The NOE generated 270 distance restraints and 52 empirical Watson-Crick restraints were incorporated in rMD calculations (Case, D. A. et al. 2004). Starting structures, IniA and IniB, were built and used in MARDIGRAS calculations (Borgias and James, 1990; Liu, H. et al., 1995 Dec). The stereoview of five convergent structures originating from rMD calculations initiated from a B-form and an A-form starting structures, which were archived each 1 ps over the final 5 ps of the rMD simulation can be viewed in Figure 7-9 and 7-10 respectively. An initial rmsd value between starting structures was 6.39 Å, the pairwise rmsd value between averaged structures from IniA and IniB was 1.555 Å. The final averaged and energy-minimized structure was compared to starting structure: 2.50 Å between IniB and rMD_{avg}, and 4.26 Å between IniA and rMD_{avg}. Detailed results are listed in Table 7-2. A CPK structure of the averaged structures is shown in Figure 7-11.

Finally, Figure 7-12 presents R_1^x values for each of the nucleotides. The 60 ms intensity data were used for CORMA calculations. The total R_1^x value was 5.70×10^{-2}: 5.03×10^{-2} for intra-residues and 7.03×10^{-2} for inter-residues.

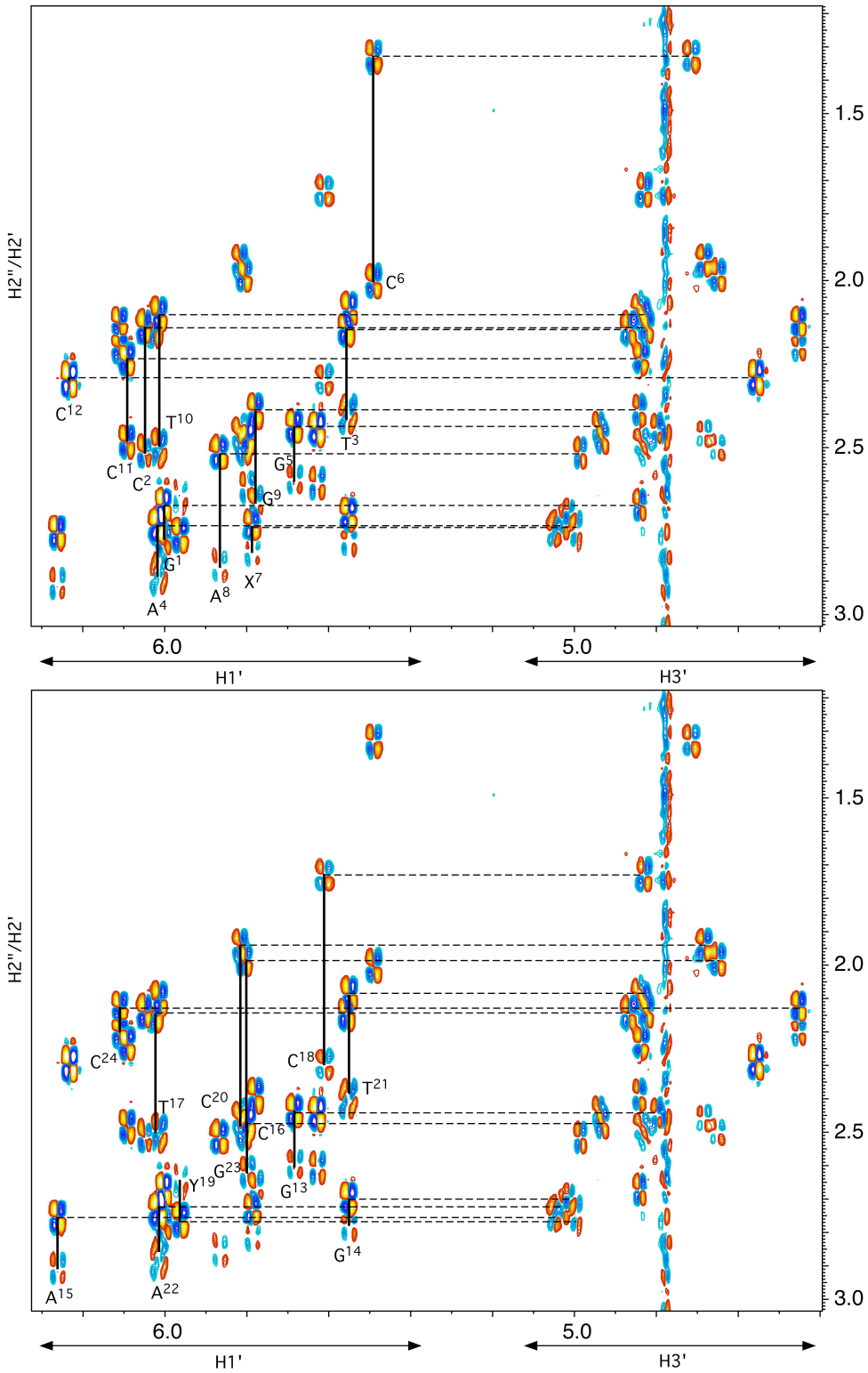

Figure 7-8. Expanded plot of DQF-COSY spectrum. The chemical shift ranges for H1′ and H3′ are indicated by the arrows at the bottom, those for H2′ and H2″ on the left. For each nucleotide the cross-peaks H1′-H2′ and H1′-H2″ are connected by a solid vertical line, and the cross-peaks H1′-H2′ and H2′-H3′ by a broken vertical line.

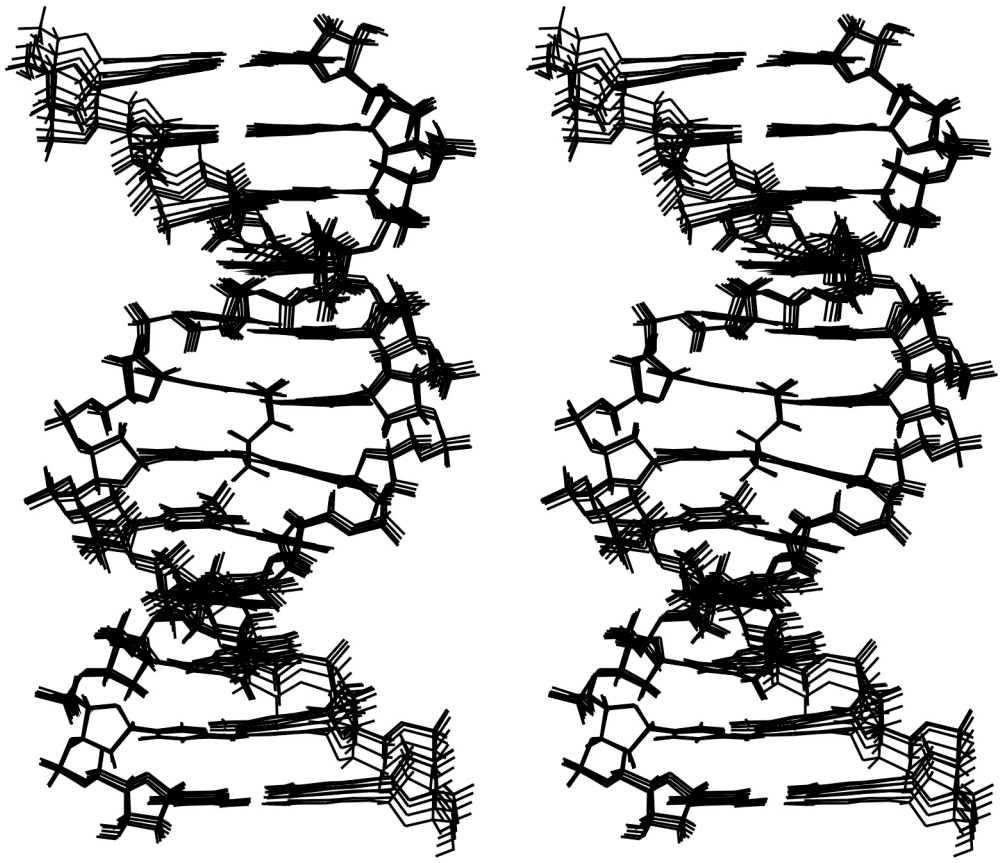

Figure 7-9. Streoview of five superimposed structures emergent from the simulated annealing rMD protocol of IniA.

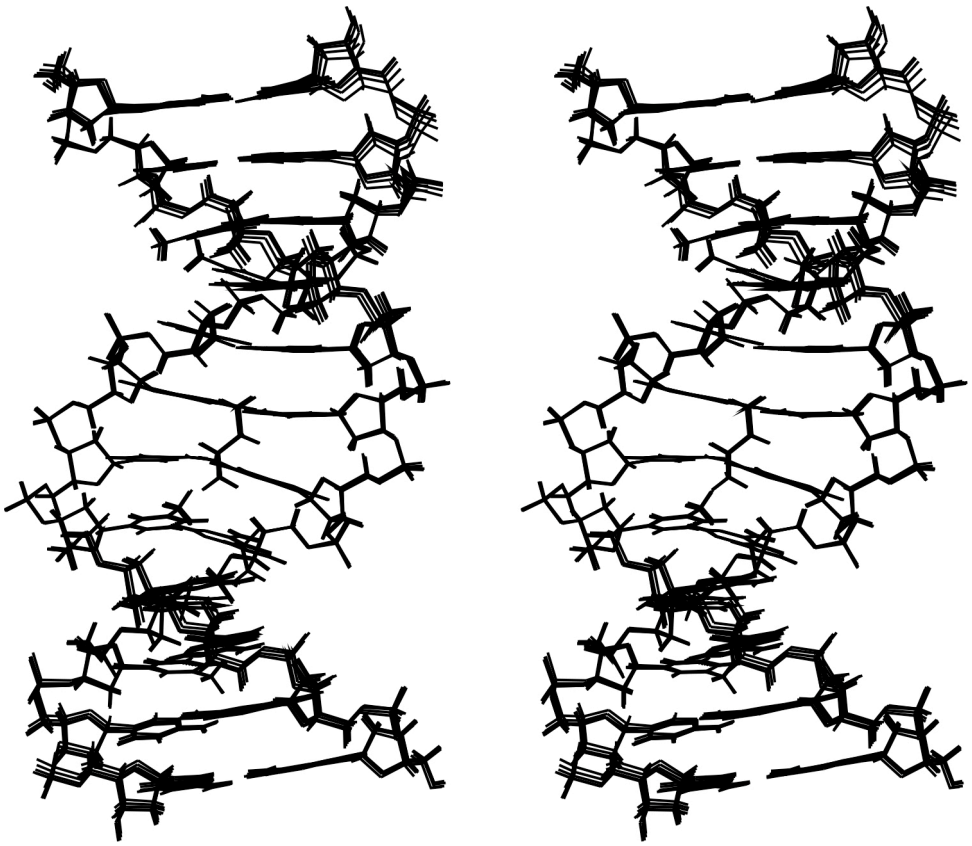

Figure 7-10. Streoview of five superimposed structures emergent from the simulated annealing rMD protocol of IniB.

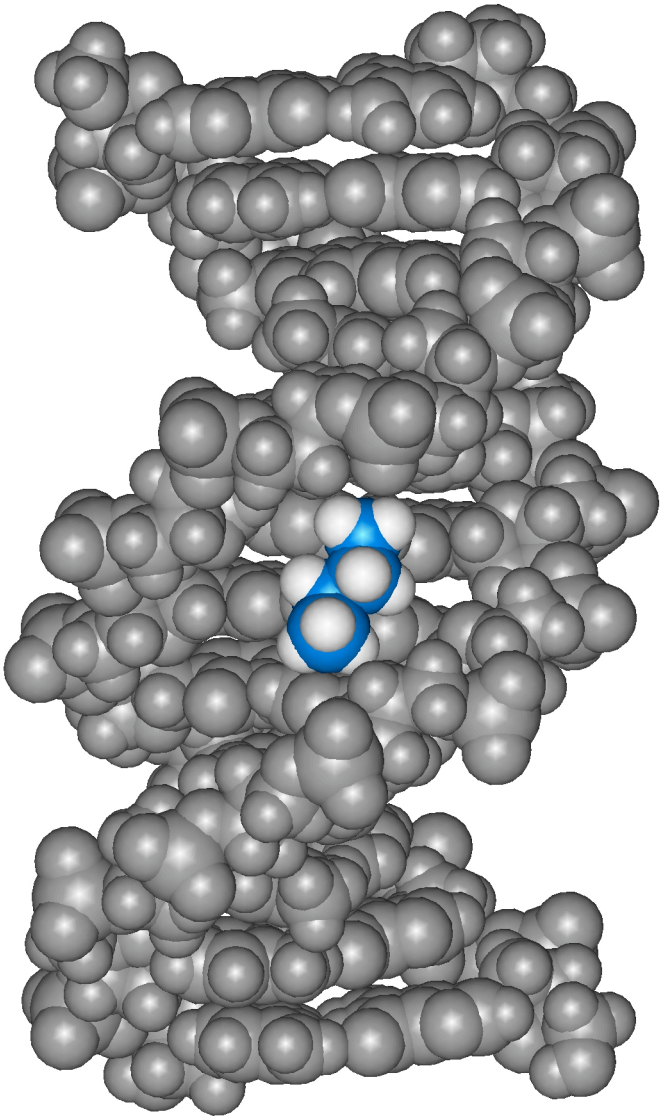

Figure 7-11. A CPK representation of the fully reduced *R*-crotonaldehyde cross-link. This is the averaged and energy minimized using the conjugate gradients algorithm. The cross-linked residues in pink with protons in white.

Table 7-2. Root Mean Square Deviations (RMSD).

Analysis of the rMD-Genrated Structures of the fully reduced *S*-crotonaldehyde cross-link in the 5'-CpG-3' sequence	
NMR restraints	
Total number of distance restraints	362
Interresidue distance restraints	161
Intraresidue distance restraints	201
DNA— adduct protons distance restraints	10
Adduct protons distance restraints	13
H-bonding restraints	52
Backbone torsion angle restraints	0
pairwise rmsd (Å) over all atoms	
IniA vs. IniB	6.39
<rMDA>[a] vs. <rMDA>	0.44 ± 0.23
<rMDB>[b] vs. <rMDB>	0.26 ± 0.14
$rMDA_{avg}$ [c] vs. $rMDB_{avg}$ [d]	1.17
$rMDA_{avg}$ vs. rMD_{avg} [e]	0.77
$rMDB_{avg}$ vs.rMD_{avg}	0.74
IniA vs. rMD_{avg}	4.26
IniB vs. rMD_{avg}	2.50

[a] <rMDA> represents the set of 5 structures that emerged from rMD calculations starting from IniA. [b] <rMDB> represents the set of 5 structures that emerged from rMD calculations starting from IniB. [c] $rMDA_{avg}$ represents the average structure of all five <rMDA>. [d]$rMDB_{avg}$ represents the average structure of all five <rMDB>. [e] rMD_{avg} represents the potential enery minimized average structure of all 10 structures of <rMDA> and <rMDB>.

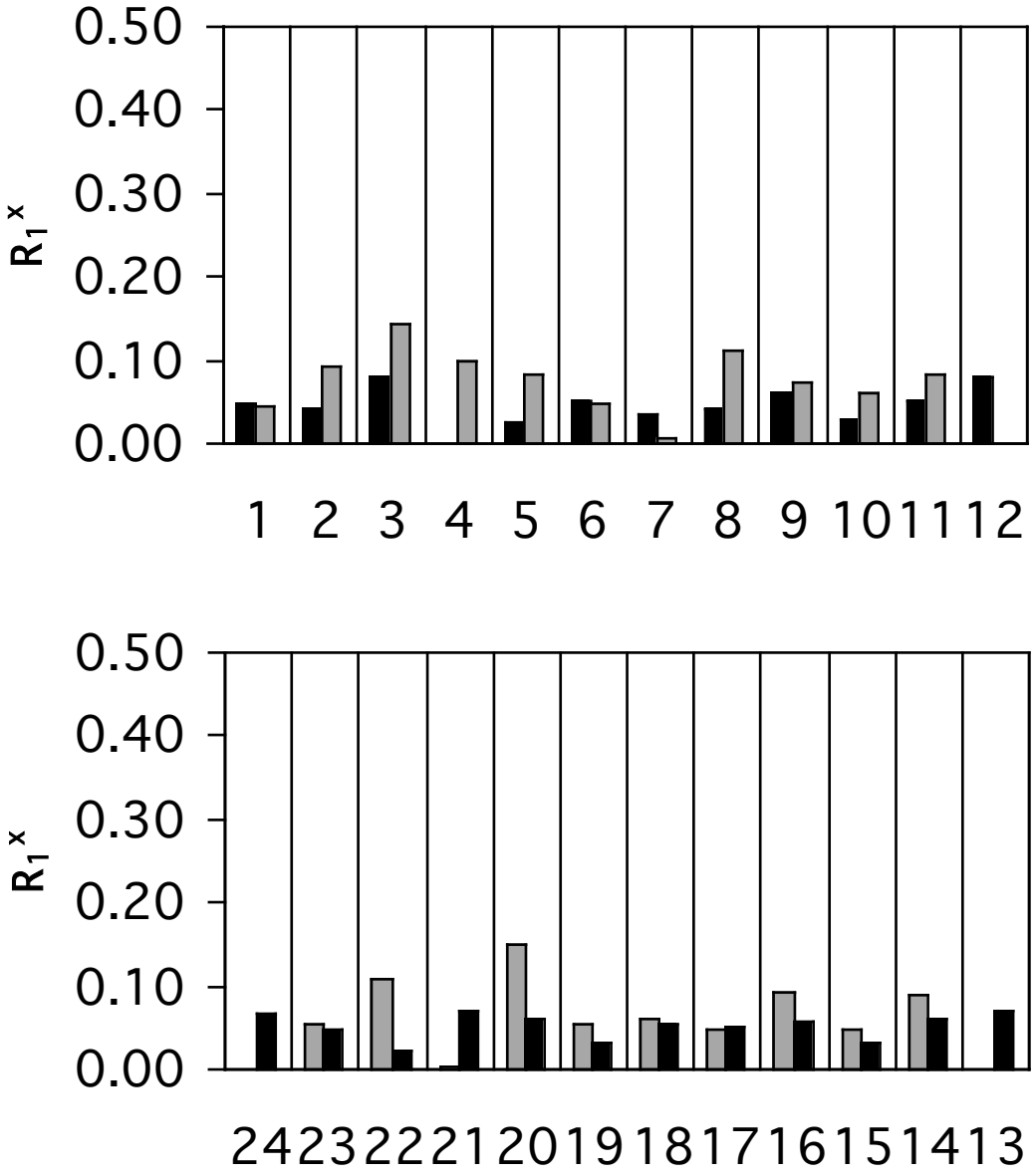

Figure 7-12. Complete relaxation matrix calculations on the average structure emergent from the simulated annealing rMD protocol showing sixth root residuals (R_1^x) for each nucleotide: The adducted strand (top); the complementary strand (bottom). The black bars represent intranucleotide R_1^x values, and the gray bars represent internucleotide R_1^x values.

Discussion

The structural study of the fully reduced *S*-crotonaldehyde-derived cross-link supported the stable B-form-like duplex DNA with containing cross-link (Figure 7-13). The stereochemistry of the methyl group did not cause the absolute instability of duplex DNA nor have two species in equilibrium for the reduced *S*-crotonaldehyde cross-link in a duplex.

At first, the upfielded β_1 proton was mis-interpreted as a possible minor form of the cross-links, which may be caused by instability of the duplex by the *S*-crotonaldehyde cross-link. However, NMR data clearly led to the conclusion that there is a single stable species that enabled the assignment of all adduct protons reasonably, as shown in DQF-COSY (Figure 7-3) and TOCSY data (data not shown). The water NOESY spectrum also supported not only duplex formation with the presence of a single conformation but also the stable base pair alignments by the presence of NOEs between the imino protons of dG and the amino protons of dC, and imino protons of dT and H2 protons of dA. The imino to imino connectivity was completed, which is the indicative of maintenance of Watson-Crick hydrogen bondings (Figure 7-5 and Figure 7-6). The UV melting study also supported the stability of this duplex through oservation of a single T_m = 92ºC. In the case of tethered cross-link studies, 5'-flickering sugar protons are, in general, upfielded, however, the fully reduced *S*-crotonaldehyde cross-link featured additional upfield chemical shift for the β_1 resonance that is even more shielded than that of methyl protons (Table 7-1).

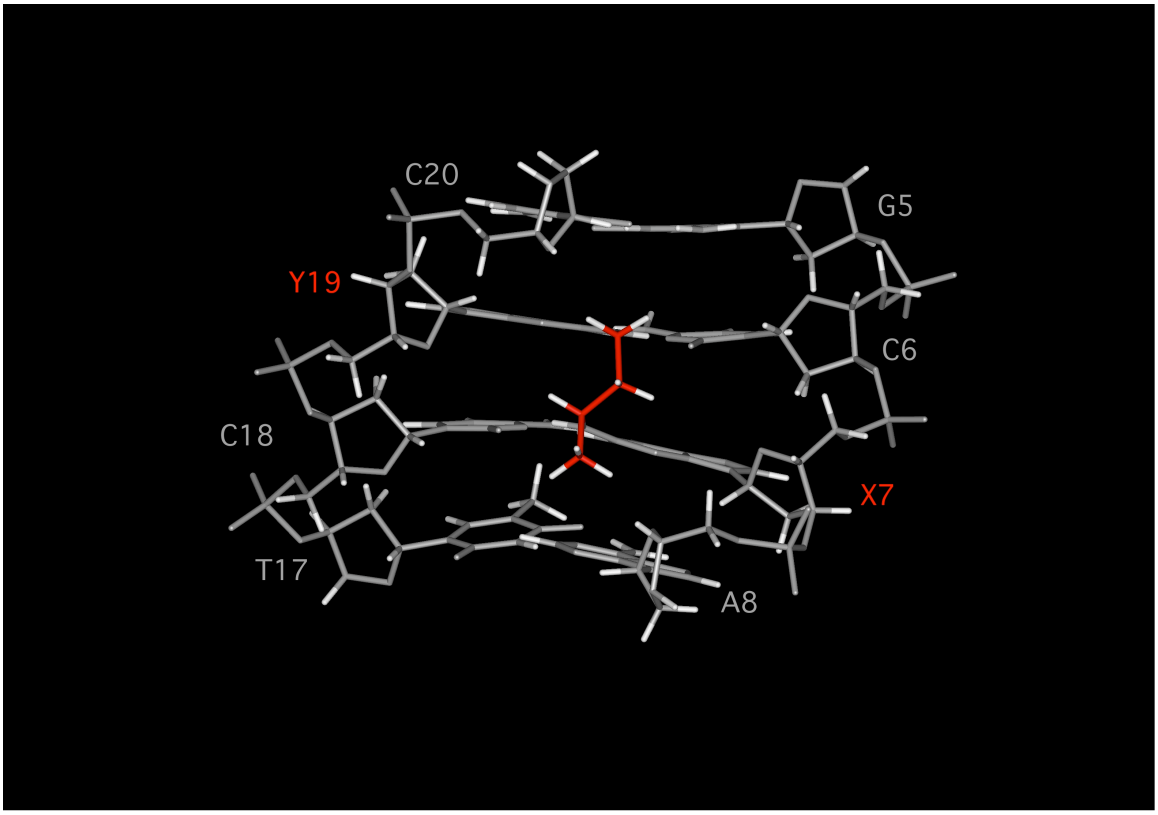

Figure 7-13. A side view of the refined structure, rMD_{avg} from the minor groove.

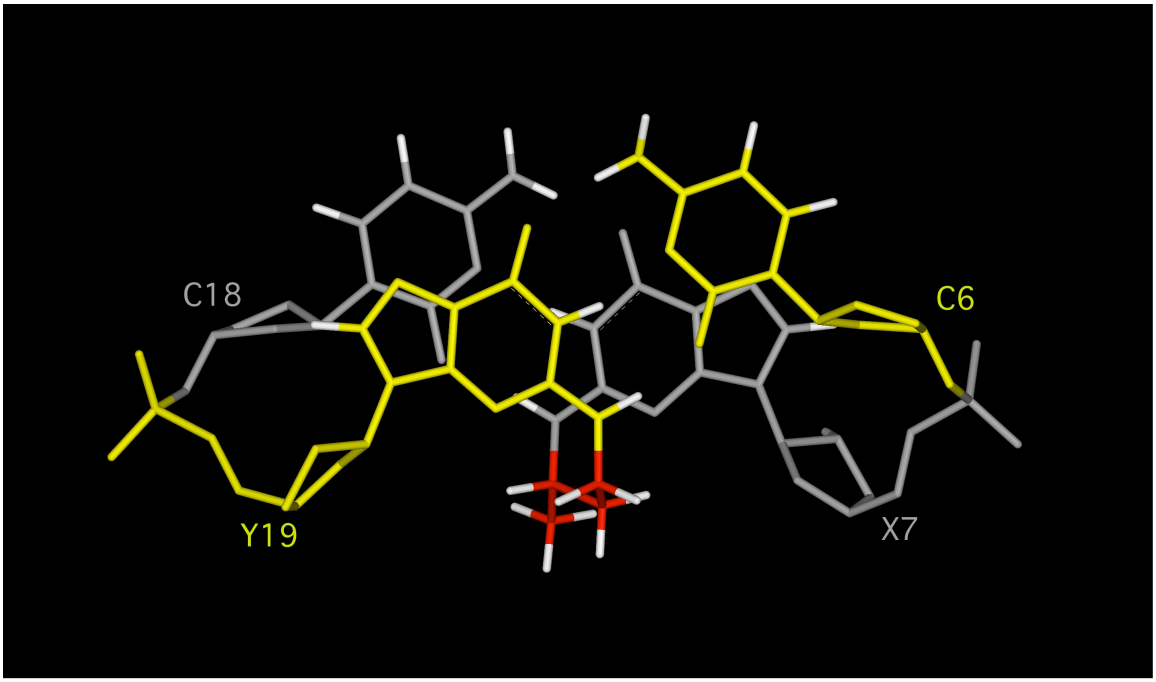

Figure 7-14. A top view of the refined structure, rMD_{avg}, for base stacking interaction.

Based on NMR study and rMD calculated structures, they suggest that the lack of cross-link generation by the *S*-CPdG adduct should come from either a high energy barrier from the aldehidic opened form (*S*-COPdG adduct) to the cross-link due to a steric hindrance in conjunction with allylic strain, or an instability induced by the hydroxyl group into the cross-linked structure. The current data do not allow us to determine which pertains. Since both reduced *R*- and *S*-crotonaldehyde interstrand cross-links were stable in duplex DNA, both refined structures could be achieved. Therefore, the cross-link generation by the methyl stereochemistry issue may need to be considered as a potential kinetic issue rather than a thermodynamic issue. The NMR study in this chapter seemed to support the possibility of the stable cross-link even by the *S*-CPdG adduct that may expel the instability of crotonaldehyde-induced cross-link by methyl stereochemistry. However, it did not consider the effect on stability in conjuction with the hydroxyl group. It may also need to focus the aldehydic species to understand the cross-link generation or hydroxyl group effect on the cross-link combining with the methyl stereochemistry that is not provided by current study. The fact that the reduced *S*-crotonaldehyde cross-link influenced A^8 sugar protons that resulted in chemical shifts changes (Figure 7-7). One question still remains how much hydroxyl group influences the stability of this cross-link in combination with the methyl group.

Additionally, one thing should pointed out is the conformation of the cross-link. In comparison with the fully reduced *R*-crotonaldehyde cross-link, the *S*-crotonaldehdye cross-link presents somewhat different conformation of β protons. Although it can have flexibility on the chain, the averaged-refined structure shows the different preference of β proton location that induced

chemical shift changes. The most shielded proton, β_1, was turned out the most out of helix hydrogen that was not much influenced by neighbor bases. Also the conformation of 5'-side sugars are affected by the cross-link, for instance, the sugar rings of C^6 and C^{18} of the fully reduced cross-link was analized as O4'-endo conformation.

As both reduced cross-links formed stable duplexes, the duplex environment tolerated the interstrand three carbon tethered cross-link with additional methyl group without losing duplex integrity. The conservation of Watson-Crick base pairs also supports the stability of these cross-links. Taken together, the methyl stereochemistry was in conjunction with local conformational changes of the interstrand cross-link chain but did not seem to affect the stability of a whole duplex. The flexibility of methyl in duplex may cause different effects on duplex, which is not spectroscopically observable using NMR. The conformational differences between two cross-link chains are illustrated as following projection pictures in Figure 7-15. The conformations of each reflect the effect of the methyl stereochemistry that allows the conformational changes onto the cross-link chain. All protons about 180° dihedral angle resulted in strong J couplings that are consistent with DQF-COSY data (Figure 7-3). Furthermore this may explain why the β_1 proton chemical shift is most shielded. Therefore, two resonances of β_2/γ_1 and H_α/β_2 in a DQF-COSY spectrum are reflected about 180 ° dihedral angle relationships. Moreover, all geminal couplings also exhibited strong couplings: β_1/β_2, γ_1/γ_2 and Me/H_α (Figure 7-3). Table 7-3 details the comparison of chemical shifts.

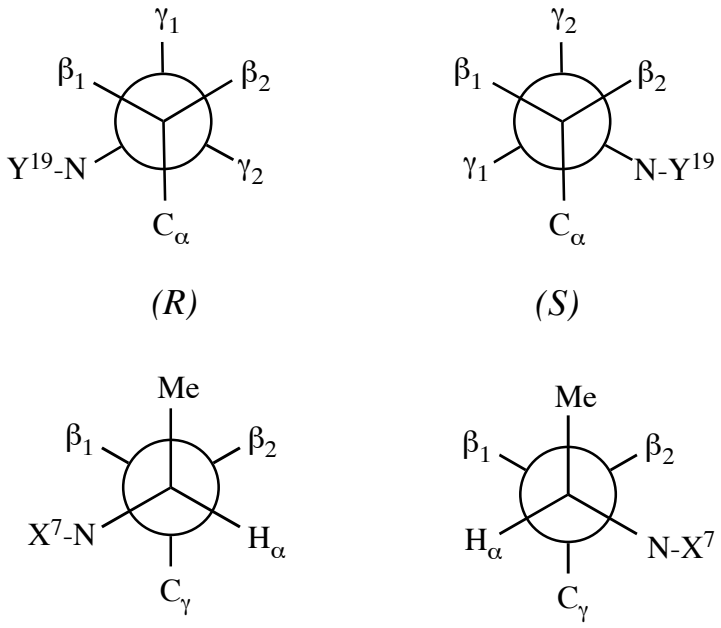

Figure 7-15. Conformational comparison of two cross-link isomers: *R* (left) and *S* (right) reduced cross-links.

Table 7-3. Chemical shifts comparison of two cross-link isomers.

	$X^7N^2H^a$	Me	H_α	β_1	β_2	γ_1	γ_2	$Y^{19}N^2H^a$
R-cross-link	7.19	1.03	3.82	1.82	1.63	3.71	2.82	8.06
S-cross-link	7.47	1.17	3.28	1.09	2.77	4.00	2.84	7.89

[a] chemical shift was measured in water at 13 °C.

It was surmised in previous chapters (Chapter III and Chapter IV) that the major carbinolamine cross-link might possess additional hydrogen bonds between the hydroxyl group and N3 of dG, and O of C^{20}, which corresponds to the γ_1 position. If the hydroxyl group is located in that position, in cases of both the *R*- and the *S*-reduced cross-link conformation, the *R*- may not face with any problem whereas *S*- may conflict with being crowded sterically. The hydroxyl group may crowd with the C_α or vice versa. If hydroxyl group located in γ_2 direction, which was regarded as minor carbinolamine cross-link species, then there will be no clashes with the current conformation. However, this hypothesis may not be well enough to be tested yet. Alternatively, a long time observation for boosting the cross-link reaction may answer for this question. If it can provide the similar amount of cross-links then, it can be explained by slow kinetics for acquiring high yield cross-link by the *S*-crotonaldehyde dG adduct. In this case, it can be an issue of just slow kinetics by the methyl stereochemistry, otherwise, the conformational preference may rule over the cross-linked duplex based on the methyl stereochemistry. A long time experiment was needed to address this question since it may indirectly answer for the cross-link formation differences between two isomers. The NMR investigation was carried out for the *S*-CpdG adduct with long incubation at 37 ºC. At basic condition, the cross-link peak resonance was observed after about 70 days (data not shown). However, the amount was less than 9 %, which implies both thermodynamic and kinetic issues: The methyl direcitionaliy can be attributed to the slow kinetics while the methyl stereochemistry affects the stability of the duplex.

Interstrand cross-links generation is common phenomenon in a biological process. It has been recognized that those cross-links may cause detrimental effect since it requires additional repair process in both strands. Thus, this structural study of crotonaldehyde-induced cross-link may give insights into understanding the interstrand cross-linked DNA adducts by α,β-unsaturated aldehydes.

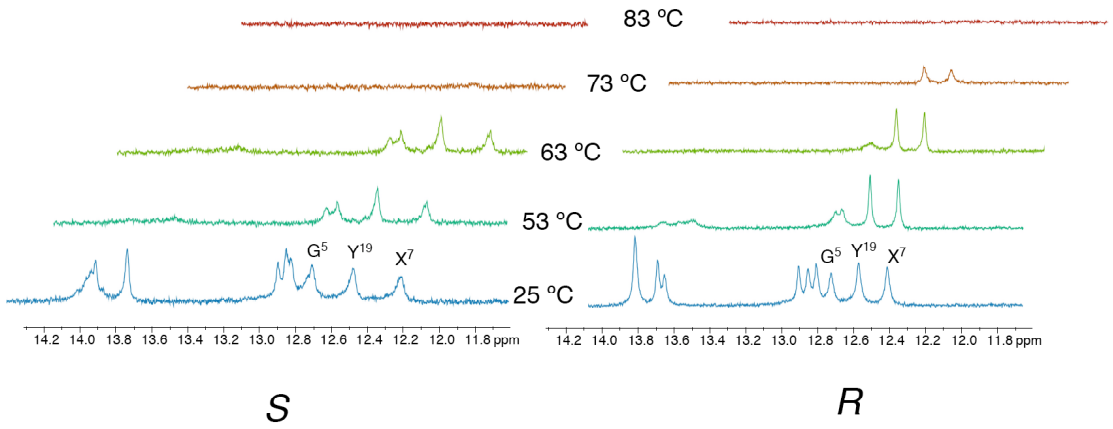

Figure 7-16. Stability of base pairing. The imino peaks were represented in the spectra with different temperatures. At 73 °C, imino peaks of Y^{19} and X^{7} were disappeared in the case of fully reduced *S*-crotonaldehyde cross-link (left) while both were present in the case of fully reduced *R*-crotonaldehyde cross-link (right).

CHAPTER VIII

Conclusion

This dissertation describes the study of monitoring acrolein and crotonaldehyde-derived γ-OH-PdG adducts by NMR in the 5′-CpG-3′ sequence. A spectroscopic characterization of interstrand carbinolamine cross-links was carried out. The reasons for the low amounts of cross-link formation by the S-crotonaldehyde-derived adduct were investigated. Further structural analyses of the fully reduced crotonaldehyde-derived cross-links were conducted as models of interstrand carbinolamine DNA cross-links.

Advances in the preparation of specifically labeled samples have made it possible to trace the chemistry of DNA adducts induced by the α, β-unsaturated family by applying a variety of heteronuclear multidimensional NMR experiments. The site-specifically labeled acrolein and the crotonaldehyde-derived dG adducts, labeled at the gamma carbon by ^{13}C, or the N^2 of the opposite dG or the N^2 of the adducted dG by ^{15}N, were extensively studied by NMR spectroscopy. All adducts were in equilibrium with 3 or 4 different chemical species that were traceable by NMR and could be quantified by ^{13}C direct detection 1D NMR. A carbinolamine was determined by NMR spectroscopy as a dominant interstrand DNA cross-link form in comparison with corresponding other chemical species: the imine species was anticipated to have chemical shifts around 140 ppm but it was below the level of detection. Molecular modeling studies predicted the difference between a carbinolamine and other species by virtue of maintaining Watson-Crick hydrogen bonding. As

postulated, the conservation of and the participation of the N^2 proton in Watson-Crick hydrogen bonding played an important role for the stability of a carbinolamine type cross-link. If the duplex is destabilized by enzyme digestion or deprotonation in mass spectrometry, the carbinolamine cross-link forms, presumably, changed into either imine or pyrimidopurione.

The M_1dG adduct was the first DNA adduct demonstrated to constitute a reactive intermediate within duplex DNA. The presence of a significant amount of aldehyde species was detected in both acrolein and crotonaldehyde-derived dG adducts while conserving hydrogen bonding between pairing bases. Modeling the aldehyde species in a duplex further supported the hypothesis that generating a cross-link form. The structure of the *S*-crotonaldehyde-derived OPdG (*S*-COPdG) adduct rationalized the hindering effect by the methyl group at the α position for enabling a cross-link reaction from the *S*-CPdG adduct in duplex DNA. In addition, the instability of the cross-linked duplex itself was presumed as another reason for the low cross-linking yield not only for the carbinolamine type cross-link but also for the pyrimidopurinone. However, the significance of the aldehyde species should not be underestimated since it can occur in other biological reactions, for instance, making interstrand cross-link and protein-DNA cross-linked complex.

Structural refinement was attempted for the fully reduced *R*- and *S*-crotonaldehyde-derived cross-links as models for carbinolamine cross-links. In the *R*-crotonaldehyde cross-link, without the hydroxyl group, the cross-link was chemically stable and the adduct moiety was located in the minor groove of the DNA. Hydrogen bonding was completely conserved, which was confirmed by NOESY experiment in water. In the *S*-crotonaldehyde cross-link, the cross-link

was also chemically stable and hydrogen bonding was maintained as well. All NMR data agreed with the stable duplex DNA. Therefore, results for the reduced model duplexes for carbinolamine cross-links suggested the possible interstrand cross-link formation in the 5'-CpG-3' sequence, which is independent of the methyl stereochemistry. This finding does not clearly provide an explanation for the lack of cross-link formation by the *S*-crotonaldehyde-dG adduct, but it does illustrate the conformational differences of the cross-link chain results from the methyl stereochemistry, which may lead to a better understanding of the crotonaldehyde-induced interstrand cross-link. As the stability issue of the *S*-crotonaldehyde–derived carbinolamine cross-link remains elusive based on the reduced model study, it may need to be considered in conjunction with the hydroxyl group. Otherwise, the energy barrier between the aldehyde and the cross-link needs to be taken into account. It may be helpful to understand why the *S*-crotonadlehdye-derived dG adduct fails to form a cross-link, in contrast with the *R*-crotonaldehyde adduct.

All of my experimental data and hypotheses explain the difference between acrolein and *R*- and *S*-crotonaldehydes-derived adducts, although all what share the common feature of forming exocyclic γ-OH-PdG adducts initially. Furthermore, the structural aspect of the interstrand cross-link was studied. This work leads to the conclusion that the duplex can accommodate an interstrand dG-dG cross-link without destabilizing the duplex. Additional melting studies have been carried out for both reduced cross-links. While increasing the temperature, it turned out that fully reduced *R*-crotonaldehyde cross-link has thermally stable than that of the *S*-crotonaldehyde cross-link by 10 degrees difference. Therefore, the methyl stereochemistry affects the stability of the

duplex in thermodynamic point, while the study of the ring-opend species explain the slow formation of cross-link by the methyl group in kinetic point of view.

Future Directions

The NMR investigation of acrolein and crotonaldehyde-derived γ-OH-PdG adducts gave insight into the potentially different mutagenic roles of various chemical species via ring-opening. It also indicated the possibility of a stable carbinolamine cross-link in a duplex. Therefore, the mutagenesis to its structure is important in understanding the biological function of these adducts. Importantly, interstrand DNA cross-links arising from α,β-unsaturated aldehydes are believed to be significant sources of genotoxicity and mutagenicity. DNA-peptide cross-links are already known to be another source of toxicity in the cell.

There are other relevant α,β-unsaturated aldehydes such as HNE. The HNE adducts show different stereoselective cross-link formation. It will be of interest to investigate these adducts, and examine the structural differences. Finally, structural studies on these adducts may be of great interest to delineate the mutations associated with α,β-unsaturated aldehydes.

APPENDIX A

ATOM TYPE AND ATOMIC PARTIAL CHARGES

A1. The parameterization of the acrolein-derived carbinolamine cross-link, for the AMBER 8.0 forcefield.

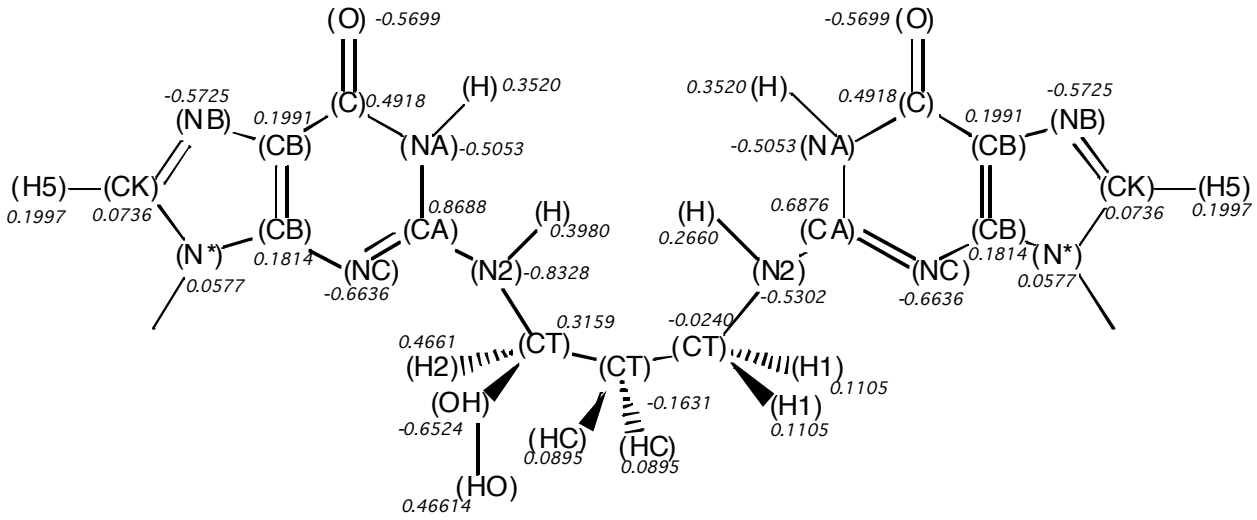

A2. The parameterization of the acrolein-derived pyrimidopurinone cross-link, for the AMBER 8.0 forcefield.

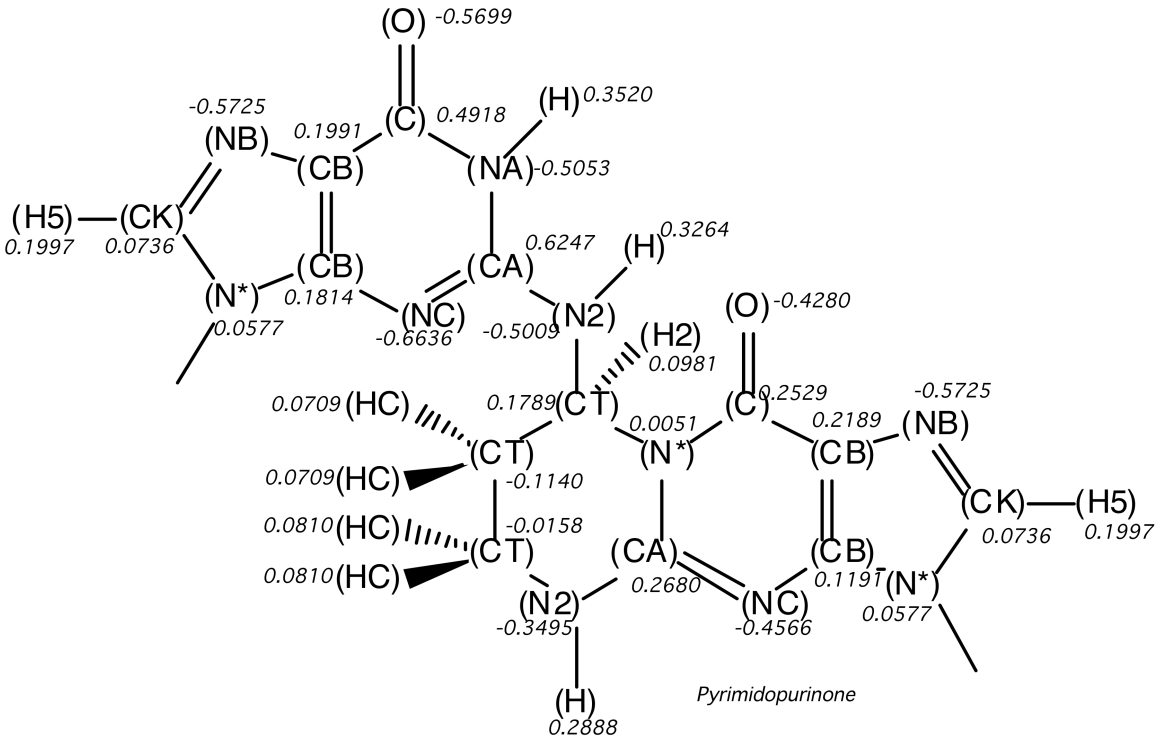

A3. The parameterization of the crotonaldehyde-derived carbinolamine cross-link, for the AMBER 8.0 forcefield.

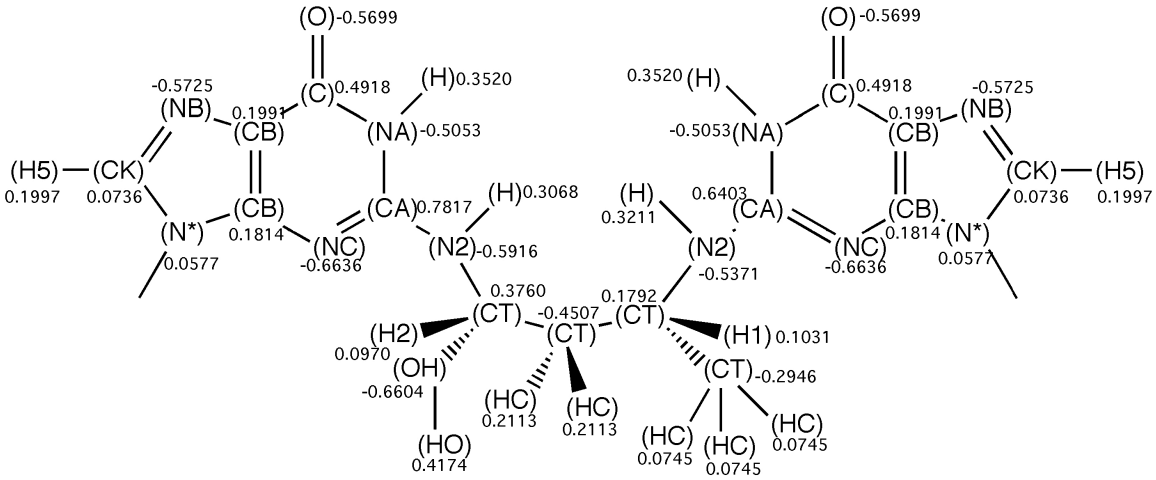

A4. The parameterization of the crotonaldehyde-derived pyrimidopurinone cross-link, for the AMBER 8.0 forcefield.

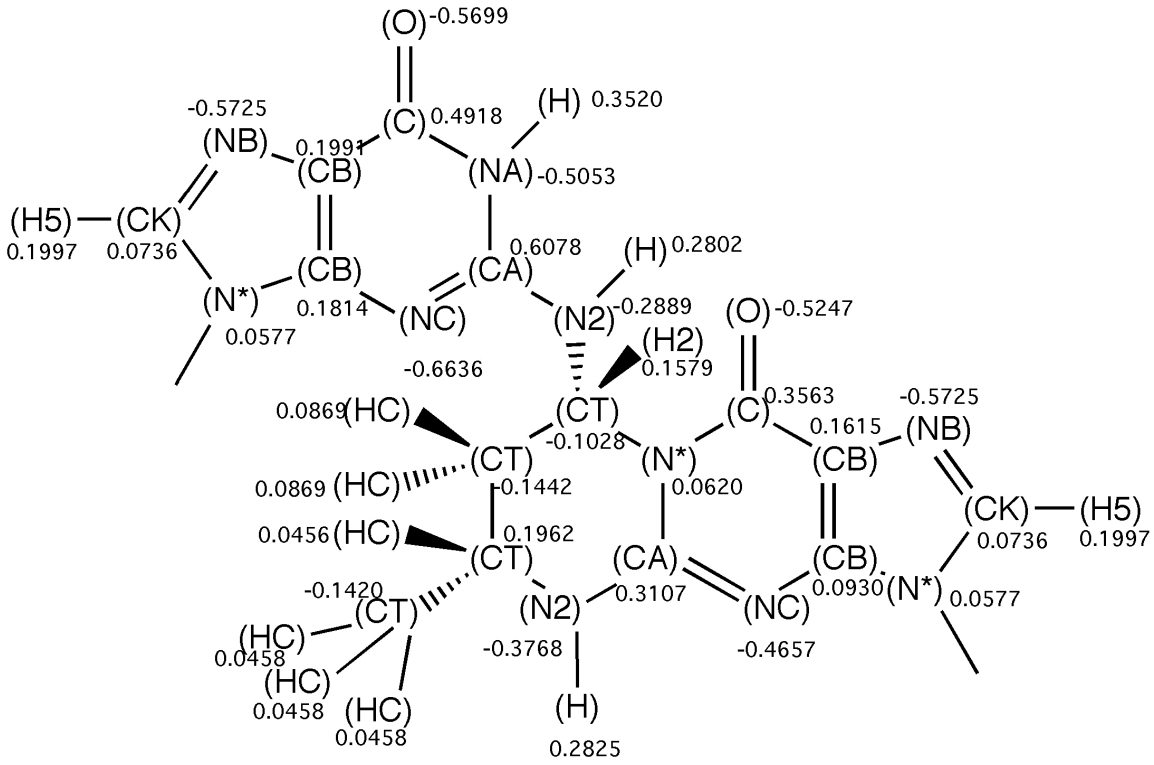

A5. The parameterization of theN2-(3-oxo-1-methyl-propyl)-dG aldehyde for the AMBER 8.0 forcefield.

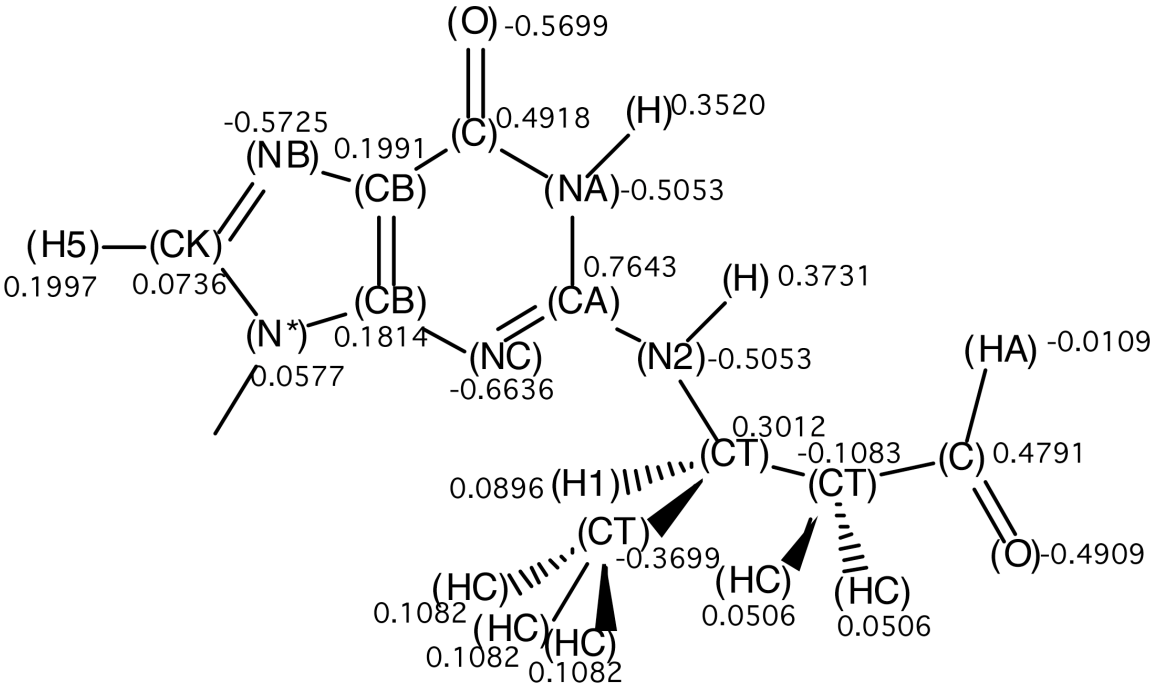

A6. The parameterization of the fully reduced crotonaldehyde cross-link for the AMBER 8.0 forcefield.

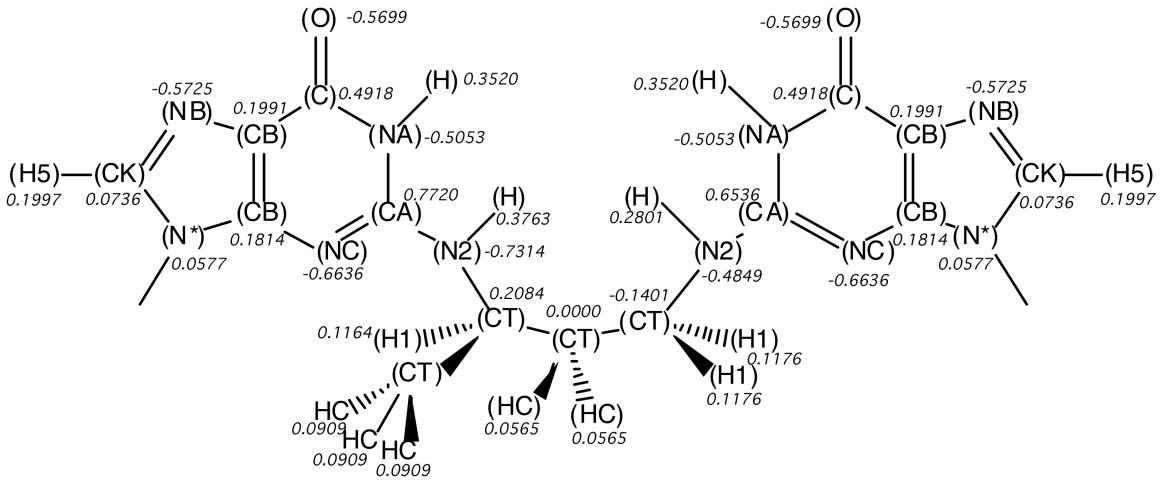

APPENDIX B

DISTANCE RESTRAINTS

B1. NOE Distance Restraints Used in rMD Calculations for the Oligodeoxynucleotide 5'-d(GCTAGCXAGTCC)-3'•5'-(GGACTCGCTAGC)-3', X= N^2-(3-Oxo-1(*S*)-methyl-propyl)-dG Adduct

res_#	res_name	atm_name	res_#	res_name	atm_name	upper_bnd
1	GUA	H2'1	1	GUA	H1'	3.83
1	GUA	H2'1	1	GUA	H3'	2.81
1	GUA	H2'1	1	GUA	H8	2.96
1	GUA	H2'2	1	GUA	H1'	2.38
1	GUA	H2'2	1	GUA	H3'	3.97
1	GUA	H2'2	1	GUA	H8	4.96
1	GUA	H3'	1	GUA	H1'	4.93
1	GUA	H3'	1	GUA	H8	6.26
1	GUA	H4'	1	GUA	H1'	2.88
1	GUA	H4'	1	GUA	H2'1	4.24
1	GUA	H4'	1	GUA	H2'2	4.31
1	GUA	Q5'	1	GUA	H2'1	3.83
1	GUA	Q5'	1	GUA	H2'2	5.67
1	GUA	Q5'	1	GUA	H3'	2.97
1	GUA	Q5'	1	GUA	H8	6.09
2	CYT	H5	1	GUA	H1'	5.1
2	CYT	H5	1	GUA	H2'1	3.4
2	CYT	H5	1	GUA	H2'2	3.18
2	CYT	H6	1	GUA	H1'	3.42
2	CYT	H6	1	GUA	H2'1	4.3
2	CYT	H6	1	GUA	H2'2	2.71
2	CYT	H2'1	2	CYT	H1'	3.97
2	CYT	H2'1	2	CYT	H5	4.48
2	CYT	H2'1	2	CYT	H6	2.34
2	CYT	H2'2	2	CYT	H1'	2.54
2	CYT	H2'2	2	CYT	H6	4.6
2	CYT	H3'	2	CYT	H6	4.14
2	CYT	H4'	2	CYT	H1'	3.88
2	CYT	H4'	2	CYT	H2'1	5.12
2	CYT	H4'	2	CYT	H2'2	4.97
2	CYT	H5	2	CYT	H6	2.49
2	CYT	H6	2	CYT	H1'	4.09
3	THY	H6	2	CYT	H2'2	2.39
3	THY	H6	2	CYT	H3'	4.98
3	THY	M	2	CYT	H1'	6.73
3	THY	M	2	CYT	H2'2	4.27
3	THY	M	2	CYT	H5	4.29
3	THY	M	2	CYT	H6	3.71

3	THY	H1'	3	THY	H2'1	5.45
3	THY	H1'	3	THY	H2'2	2.43
3	THY	H1'	3	THY	H6	4.15
3	THY	H2'2	3	THY	H3'	3.03
3	THY	H3'	3	THY	H6	4.34
3	THY	M	3	THY	H6	2.91
4	ADE	H8	3	THY	H2'1	4.92
4	ADE	H8	3	THY	H2'2	3.04
4	ADE	H8	3	THY	H3'	5.62
4	ADE	H2'1	4	ADE	H1'	3.27
4	ADE	H2'2	4	ADE	H1'	2.43
4	ADE	H3'	4	ADE	H1'	5.38
4	ADE	H3'	4	ADE	H2'1	2.83
4	ADE	H3'	4	ADE	H2'2	2.83
4	ADE	H4'	4	ADE	H1'	3.82
4	ADE	H4'	4	ADE	H2'1	5.75
4	ADE	H4'	4	ADE	H2'2	6.02
4	ADE	H4'	4	ADE	H3'	2.88
4	ADE	H4'	4	ADE	H8	5.76
4	ADE	H5'1	4	ADE	H3'	5.47
4	ADE	H5'1	4	ADE	H8	3.64
4	ADE	H5'2	4	ADE	H3'	2.99
4	ADE	H5'2	4	ADE	H8	5.8
4	ADE	H1'	5	GUA	H8	2.9
4	ADE	H2'1	5	GUA	H8	3.95
4	ADE	H2'2	5	GUA	H8	3.21
5	GUA	H2'1	5	GUA	H1'	3.26
5	GUA	H2'1	5	GUA	H8	2.33
5	GUA	H2'2	5	GUA	H1'	2.36
5	GUA	H2'2	5	GUA	H8	4.85
5	GUA	H3'	5	GUA	H1'	6.11
5	GUA	H3'	5	GUA	H8	5.7
5	GUA	H4'	5	GUA	H1'	4.88
5	GUA	H4'	5	GUA	H2'1	3.99
5	GUA	H4'	5	GUA	H2'2	4.91
5	GUA	H5'1	5	GUA	H1'	4.7
5	GUA	H5'1	5	GUA	H8	4.25
5	GUA	H5'2	5	GUA	H1'	5.38
5	GUA	H8	5	GUA	H1'	4.28
6	CYT	H5	5	GUA	H2'1	4.87
6	CYT	H5	5	GUA	H2'2	3.52
6	CYT	H6	5	GUA	H1'	4.03
6	CYT	H1'	6	CYT	H2'1	3.78
6	CYT	H1'	6	CYT	H2'2	2.48
6	CYT	H1'	6	CYT	H6	5.75
6	CYT	H2'1	6	CYT	H3'	2.53
6	CYT	H2'1	6	CYT	H5	4.97
6	CYT	H2'1	6	CYT	H6	2.26
6	CYT	H2'2	6	CYT	H2'1	2.11

6	CYT	H2'2	6	CYT	H3'	2.99
6	CYT	H2'2	6	CYT	H6	3.69
6	CYT	H3'	6	CYT	H6	5.91
6	CYT	H5	6	CYT	H6	2.45
6	CYT	H5'1	6	CYT	H2'1	4.7
7	S	H8	6	CYT	H2'1	5.38
7	S	H8	6	CYT	H2'2	4.05
7	S	H1'	7	S	H2'1	3.01
7	S	H1'	7	S	H2'2	2.99
7	S	H3'	7	S	H1'	5.09
7	S	H3'	7	S	H2'1	2.72
7	S	H3'	7	S	H8	5.74
7	S	H3g	7	S	H1a	3.63
7	S	H3g	7	S	Qb	4.12
7	S	H4'	7	S	H1'	4.29
7	S	H4'	7	S	H2'1	4.86
7	S	H4'	7	S	H2'2	4.63
7	S	H5'1	7	S	H1'	4.8
7	S	H5'1	7	S	H2'1	4.51
7	S	H5'1	7	S	H2'2	5.32
7	S	H5'2	7	S	H1'	5.53
7	S	H8	7	S	H1'	5.78
7	S	H8	7	S	H2'1	2.65
7	S	H8	7	S	H2'2	4.71
7	S	M	7	S	H1a	2.75
7	S	M	7	S	H3g	4.57
7	S	M	7	S	Qb	3.92
7	S	M	18	CYT	H1'	5.14
7	S	M	19	GUA	H1'	3.41
7	S	M	19	GUA	H4'	3.72
8	ADE	H1'	7	S	H3g	5.1
8	ADE	H4'	7	S	H3g	3.68
8	ADE	H8	7	S	H1'	4.89
8	ADE	H8	7	S	H2'2	3.55
8	ADE	H2'1	8	ADE	H3'	2.67
8	ADE	H2'1	8	ADE	H8	2.53
8	ADE	H2'2	8	ADE	H1'	2.59
8	ADE	H2'2	8	ADE	H8	4.71
8	ADE	H3'	8	ADE	H1'	5.26
8	ADE	H8	8	ADE	H1'	5.17
9	GUA	H8	8	ADE	H2'1	4.69
9	GUA	H8	8	ADE	H2'2	2.89
9	GUA	H1'	9	GUA	H2'2	2.67
9	GUA	H2'1	9	GUA	H8	2.95
9	GUA	H2'2	9	GUA	H8	5.75
9	GUA	H3'	9	GUA	H8	6.29
9	GUA	H1'	10	THY	H6	3.95
10	THY	M	9	GUA	H2'1	4.55
10	THY	M	9	GUA	H2'2	4.03

10	THY	M	9	GUA	H8	4.44
10	THY	H1'	10	THY	H2'1	3.19
10	THY	H1'	10	THY	H2'2	2.49
10	THY	H1'	10	THY	H6	4.49
10	THY	H2'1	10	THY	H6	2.71
10	THY	H2'2	10	THY	H6	4.58
10	THY	H4'	10	THY	H2'1	4.99
10	THY	H5'1	10	THY	H6	3.96
10	THY	M	10	THY	H6	3.64
10	THY	H1'	11	CYT	H5	5.33
11	CYT	H5	10	THY	H2'1	4.33
11	CYT	H5	10	THY	H2'2	2.92
11	CYT	H6	10	THY	H2'1	3.83
11	CYT	H2'1	11	CYT	H1'	3.12
11	CYT	H2'1	11	CYT	H3'	2.75
11	CYT	H2'1	11	CYT	H5	5.53
11	CYT	H2'1	11	CYT	H6	2.31
11	CYT	H2'2	11	CYT	H1'	2.43
11	CYT	H2'2	11	CYT	H6	3.66
11	CYT	H3'	11	CYT	H1'	6.41
11	CYT	H4'	11	CYT	H1'	3.94
11	CYT	H5	11	CYT	H6	2.52
11	CYT	H6	11	CYT	H1'	5.35
12	CYT	H5	11	CYT	H6	6.21
12	CYT	H6	11	CYT	H3'	5.59
12	CYT	H3'	12	CYT	H1'	5.38
12	CYT	H3'	12	CYT	H6	2.91
12	CYT	H4'	12	CYT	H1'	5.2
12	CYT	H4'	12	CYT	H6	6.02
12	CYT	H5	12	CYT	H6	2.43
12	CYT	H6	12	CYT	H1'	4.09
12	CYT	Q5'	12	CYT	H1'	4.84
12	CYT	Q5'	12	CYT	H6	3.62
13	GUA	H2'1	13	GUA	H1'	3.25
13	GUA	H2'1	13	GUA	H3'	2.76
13	GUA	H2'1	13	GUA	H8	2.72
13	GUA	H2'2	13	GUA	H1'	2.46
13	GUA	H2'2	13	GUA	H3'	4.9
13	GUA	H3'	13	GUA	H8	5.79
13	GUA	H8	13	GUA	H1'	3.92
13	GUA	Q5'	13	GUA	H2'1	3.91
13	GUA	Q5'	13	GUA	H2'2	6.4
13	GUA	Q5'	13	GUA	H3'	3.05
13	GUA	Q5'	13	GUA	H8	6.13
14	GUA	H8	13	GUA	H1'	5.58
14	GUA	H8	13	GUA	H2'2	2.77
14	GUA	H8	13	GUA	H3'	5.8
14	GUA	H2'1	14	GUA	H1'	3.93
14	GUA	H2'1	14	GUA	H3'	2.66

14	GUA	H2'1	14	GUA	H8	2.65
14	GUA	H2'2	14	GUA	H1'	2.42
14	GUA	H2'2	14	GUA	H3'	2.81
14	GUA	H2'2	14	GUA	H8	5.64
14	GUA	H3'	14	GUA	H1'	5.31
14	GUA	H3'	14	GUA	H8	5.48
14	GUA	H4'	14	GUA	H1'	4.13
14	GUA	H8	14	GUA	H1'	5.76
15	ADE	H3'	15	ADE	H1'	5.23
15	ADE	H4'	15	ADE	H1'	4.45
15	ADE	H4'	15	ADE	H2'1	4.76
15	ADE	H4'	15	ADE	H2'2	5.43
15	ADE	H4'	15	ADE	H3'	2.88
15	ADE	H5'1	15	ADE	H1'	4.72
15	ADE	H5'1	15	ADE	H3'	3.98
15	ADE	H5'2	15	ADE	H1'	5.03
15	ADE	H8	15	ADE	H1'	4.36
15	ADE	H1'	16	CYT	H6	2.86
15	ADE	H2'1	16	CYT	H5	4.84
15	ADE	H2'1	16	CYT	H6	5.58
15	ADE	H2'2	16	CYT	H5	3.58
15	ADE	H2'2	16	CYT	H6	2.77
15	ADE	H3'	16	CYT	H6	5.93
15	ADE	H8	16	CYT	H5	4.22
15	ADE	H8	16	CYT	H6	5.58
16	CYT	H1'	16	CYT	H2'1	5.04
16	CYT	H2'2	16	CYT	H1'	2.38
16	CYT	H2'2	16	CYT	H2'1	2.1
16	CYT	H2'2	16	CYT	H6	3.81
16	CYT	H4'	16	CYT	H2'1	5.3
16	CYT	H5	16	CYT	H2'1	6.47
16	CYT	H5	16	CYT	H6	2.61
16	CYT	H6	16	CYT	H1'	6.18
16	CYT	H6	16	CYT	H2'1	2.68
16	CYT	H1'	17	THY	M	6.21
16	CYT	H2'1	17	THY	H6	3.7
16	CYT	H2'1	17	THY	M	3.39
16	CYT	H2'2	17	THY	M	3.88
16	CYT	H5	17	THY	M	3.72
16	CYT	H6	17	THY	M	3.64
17	THY	H1'	17	THY	H2'1	4.66
17	THY	H1'	17	THY	H2'2	2.37
17	THY	H1'	17	THY	H6	4.61
17	THY	H2'1	17	THY	M	6.07
17	THY	M	17	THY	H6	3.02
17	THY	H1'	18	CYT	H6	2.95
18	CYT	H5	17	THY	H2'1	4.06
18	CYT	H5	17	THY	H2'2	5.14
18	CYT	H5	17	THY	M	6.14

18	CYT	H6	17	THY	H2'2	2.32
18	CYT	H2'1	18	CYT	H1'	5.32
18	CYT	H2'1	18	CYT	H5	4.95
18	CYT	H2'2	18	CYT	H1'	2.48
18	CYT	H2'2	18	CYT	H6	3.67
18	CYT	H5	18	CYT	H6	2.58
19	GUA	H8	18	CYT	H1'	5.58
19	GUA	H8	18	CYT	H2'1	4.01
19	GUA	H8	18	CYT	H2'2	2.83
19	GUA	H1'	19	GUA	H4'	3.92
19	GUA	H2'1	19	GUA	H3'	2.67
19	GUA	H2'1	19	GUA	H8	2.47
19	GUA	H2'2	19	GUA	H3'	2.98
19	GUA	H2'2	19	GUA	H8	3.76
19	GUA	H3'	19	GUA	H8	5.78
19	GUA	H8	19	GUA	H1'	5.1
20	CYT	H5	19	GUA	H2'1	3.59
20	CYT	H5	19	GUA	H2'2	3.7
20	CYT	H5	19	GUA	H8	5.35
20	CYT	H6	19	GUA	H1'	3.57
20	CYT	H6	19	GUA	H2'1	4.94
20	CYT	H6	19	GUA	H2'2	2.81
20	CYT	H1'	20	CYT	H2'1	7.32
20	CYT	H1'	20	CYT	H2'2	2.49
20	CYT	H2'1	20	CYT	H5	5.2
20	CYT	H2'1	20	CYT	H6	2.4
20	CYT	H5	20	CYT	H6	2.63
21	THY	M	20	CYT	H1'	6.91
21	THY	M	20	CYT	H2'1	3.44
21	THY	M	20	CYT	H2'2	3.4
21	THY	M	20	CYT	H5	4.05
21	THY	H2'1	21	THY	H1'	5.31
21	THY	H2'1	21	THY	M	6.85
21	THY	H2'2	21	THY	H1'	2.53
21	THY	H2'2	21	THY	H2'1	2.17
21	THY	H3'	21	THY	H2'2	2.87
21	THY	H4'	21	THY	H1'	4.43
21	THY	H4'	21	THY	H2'1	3.89
21	THY	H6	21	THY	H2'1	2.56
21	THY	H6	21	THY	H2'2	4.08
22	ADE	H8	21	THY	H2'1	5.82
22	ADE	H8	21	THY	H2'2	3.14
22	ADE	H2'1	22	ADE	H3'	2.8
22	ADE	H2'2	22	ADE	H3'	3.43
22	ADE	H3'	22	ADE	H1'	3.96
22	ADE	H4'	22	ADE	H1'	4.89
22	ADE	H4'	22	ADE	H2'1	3.76
22	ADE	H4'	22	ADE	H2'2	5.04
23	GUA	H8	22	ADE	H1'	6.5

23	GUA	H8	22	ADE	H2'1	3.43
23	GUA	H8	22	ADE	H2'2	2.93
23	GUA	H2'1	23	GUA	H8	2.29
23	GUA	H2'2	23	GUA	H3'	2.82
23	GUA	H2'2	23	GUA	H8	4.98
23	GUA	H3'	23	GUA	H1'	5.12
23	GUA	H3'	23	GUA	H8	4.57
23	GUA	H4'	23	GUA	H1'	4.26
23	GUA	H4'	23	GUA	H2'1	4.44
23	GUA	H4'	23	GUA	H2'2	4.22
24	CYT	H5	23	GUA	H1'	5.46
24	CYT	H5	23	GUA	H2'1	5.79
24	CYT	H5	23	GUA	H2'2	3.92
24	CYT	H5	23	GUA	H8	3.76
24	CYT	H6	23	GUA	H2'2	2.53
24	CYT	H6	23	GUA	H3'	6.28
24	CYT	H6	23	GUA	H8	5.09
24	CYT	H2'1	24	CYT	H1'	5.75
24	CYT	H2'1	24	CYT	H3'	2.55
24	CYT	H2'2	24	CYT	H1'	2.51
24	CYT	H2'2	24	CYT	H3'	6.12
24	CYT	H3'	24	CYT	H6	3.14
24	CYT	H4'	24	CYT	H1'	4
24	CYT	H5	24	CYT	H6	2.51
24	CYT	H6	24	CYT	H1'	3.88

B2. NOE Distance Restraints Used in rMD Calculations for the Oligodeoxynucleotide 5'-d(GCTAGCXAGTCC)-3'•5'-(GGACTCYCTAGC)-3', X and Y = *fully reduced R-crotonaldehyde-derived dG-dG cross-link*

Class1

res_#	res_name	atm_name	res_#	res_name	atm_name	low_bnd	up_bnd
1	GUA	H1'	1	GUA	H8	3.51	4.45
1	GUA	H2'2	1	GUA	H3'	2.61	3.35
1	GUA	H3'	1	GUA	H8	4.03	5.7
2	CYT	H5	1	GUA	H8	3.66	4.97
2	CYT	H2'1	2	CYT	H6	1.88	2.19
2	CYT	H2'2	2	CYT	H6	3.86	6.05
2	CYT	H4'	2	CYT	H2'1	3.76	5.32
2	CYT	H4'	2	CYT	H2'2	3.01	4.28
2	CYT	H5	2	CYT	H6	2.31	2.46
3	THY	M	2	CYT	H6	3.53	4.6
5	GUA	H3'	5	GUA	H1'	3.37	3.68
5	GUA	H8	5	GUA	H1'	3.33	3.98
5	GUA	H2'1	6	CYT	H6	3.62	5.46
6	CYT	H5	5	GUA	H2'2	2.73	2.92
6	CYT	H5	5	GUA	H8	3.51	3.9
6	CYT	H6	5	GUA	H1'	3.02	3.22

6	CYT	H6	5	GUA	H2'2	2.47	2.65
6	CYT	H1'	6	CYT	H2'1	2.76	3.88
6	CYT	H1'	6	CYT	H2'2	2.02	2.25
6	CYT	H1'	6	CYT	H3'	3.7	4.71
6	CYT	H1'	6	CYT	H6	3.17	3.81
6	CYT	H2'1	6	CYT	H3'	2.38	2.58
6	CYT	H2'1	6	CYT	H6	2.21	2.45
6	CYT	H2'2	6	CYT	H3'	2.61	3.2
6	CYT	H2'2	6	CYT	H6	2.95	4.39
6	CYT	H3'	6	CYT	H6	3.17	3.52
6	CYT	H5	6	CYT	H6	2.29	2.42
7	X	H2x1	7	X	H1x	2.16	2.98
7	X	H2x1	7	X	M	2.63	3.79
7	X	H2x2	7	X	H1x	2.3	3.05
7	X	H2x2	7	X	M	2.67	3.78
7	X	M	7	X	H1x	2.15	2.86
8	ADE	H2	7	X	M	4	5.09
8	ADE	H4'	7	X	M	4.11	5.57
8	ADE	H8	7	X	H1'	2.88	3.16
8	ADE	H2'1	8	ADE	H8	2.1	2.42
8	ADE	H2'2	8	ADE	H8	3.3	4.85
8	ADE	H8	8	ADE	H1'	3.42	4.06
9	GUA	H8	9	GUA	H1'	3.38	4
10	THY	H6	9	GUA	H1'	2.67	3.43
10	THY	M	9	GUA	H1'	4.58	6.91
10	THY	M	9	GUA	H2'1	3.47	4.48
10	THY	M	9	GUA	H3'	4.2	5.42
10	THY	M	9	GUA	H8	3.53	4.48
10	THY	H1'	10	THY	H6	3.58	4.35
10	THY	M	10	THY	H6	2.81	3.54
10	THY	H1'	11	CYT	H6	3.41	4.38
11	CYT	H5	10	THY	H2'1	3.18	5.55
11	CYT	H5	10	THY	H6	3.29	3.59
11	CYT	H2'1	11	CYT	H5	4.05	5.89
11	CYT	H5	11	CYT	H6	2.25	2.38
11	CYT	H1'	15	ADE	H2	3.72	4.2
12	CYT	H3'	12	CYT	H1'	3.96	5.79
12	CYT	H4'	12	CYT	H1'	3.06	3.23
12	CYT	H6	12	CYT	H1'	3.47	4.61
13	GUA	H1'	13	GUA	H3'	3.82	5.06
13	GUA	H3'	13	GUA	H8	4.62	7.3
13	GUA	H1'	14	GUA	H8	3.43	3.91
14	GUA	H1'	14	GUA	H8	3.5	5.14
14	GUA	H3'	14	GUA	H8	3.81	5.59
15	ADE	H8	14	GUA	H8	4.54	6.59
15	ADE	H2	15	ADE	H1'	4.03	5.08
15	ADE	H2'1	15	ADE	H1'	2.95	3.45
15	ADE	H2'2	15	ADE	H1'	2.3	2.4
15	ADE	H3'	15	ADE	H1'	3.54	4.41

15	ADE	H4'	15	ADE	H1'	3.07	3.21
15	ADE	H8	15	ADE	H1'	3.47	4.31
16	CYT	H1'	15	ADE	H2	3.32	3.52
16	CYT	H5	15	ADE	H2'2	3.46	4.44
16	CYT	H5	15	ADE	H8	3.4	3.66
16	CYT	H6	15	ADE	H1'	3.15	3.38
16	CYT	H6	15	ADE	H2'1	3.18	3.85
16	CYT	H6	15	ADE	H2'2	2	2.66
16	CYT	H6	15	ADE	H8	3.73	5.1
16	CYT	H2'1	16	CYT	H6	1.82	2.47
16	CYT	H3'	16	CYT	H6	3.31	4.07
16	CYT	H4'	16	CYT	H2'1	3.76	4.81
16	CYT	H5	16	CYT	H6	2.36	2.48
16	CYT	H6	16	CYT	H1'	3.36	3.7
16	CYT	H2'2	17	THY	M	3.9	6.82
17	THY	H6	16	CYT	H1'	4	5.41
17	THY	H6	16	CYT	H3'	4.14	6
17	THY	M	16	CYT	H3'	3.69	4.67
17	THY	M	16	CYT	H5	4.06	5.13
17	THY	M	16	CYT	H6	3.49	4.44
17	THY	H1'	17	THY	H6	3.08	3.79
17	THY	M	17	THY	H6	2.83	3.57
17	THY	H1'	18	CYT	H6	3.79	4.87
18	CYT	H5	17	THY	H6	3.12	3.44
18	CYT	H2'1	18	CYT	H1'	2.92	6.26
18	CYT	H2'2	18	CYT	H1'	2.25	2.35
18	CYT	H3'	18	CYT	H6	3.54	4.48
19	Y	H3x1	7	X	H2x1	2.08	2.92
19	Y	H3x1	7	X	H2x2	2.06	2.81
19	Y	H3x1	7	X	M	3.29	6.38
19	Y	H3x2	7	X	H2x2	2.16	2.88
19	Y	H3x2	7	X	M	2.83	4.59
19	Y	H8	18	CYT	H1'	3.72	4.85
19	Y	H8	18	CYT	H2'2	3.01	3.43
19	Y	H1'	19	Y	H8	3.56	5.13
20	CYT	H1'	19	Y	H3x2	2.26	2.62
20	CYT	H5	19	Y	H8	3.53	4.52
20	CYT	H6	19	Y	H2'1	3.12	3.93
21	THY	H5'1	20	CYT	H1'	3.39	5.13
22	ADE	H8	21	THY	H2'1	4.01	6.51
22	ADE	H3'	23	GUA	H8	3.81	5.02
23	GUA	H1'	23	GUA	H3'	3.58	4.16
24	CYT	H1'	24	CYT	H3'	3.65	4.57

Class2

res_#	res_name	atm_name	res_#	res_name	atm_name	low_bnd	up_bnd
1	GUA	H2'1	1	GUA	H8	2.12	2.3
1	GUA	H2'2	1	GUA	H8	2.97	4.96
1	GUA	H4'	1	GUA	H2'1	2.94	3.96
2	CYT	H6	1	GUA	H2'2	2.4	2.6

2	CYT	H1'	2	CYT	H6	3.19	3.81
3	THY	M	2	CYT	H2'2	3.7	5.24
3	THY	H1'	3	THY	H6	3.14	3.79
3	THY	H2'1	4	ADE	H8	3.07	3.35
4	ADE	H4'	4	ADE	H2'1	3.24	4.01
4	ADE	H4'	4	ADE	H2'2	3.45	4.39
4	ADE	H1'	5	GUA	H8	2.76	3.33
4	ADE	H3'	5	GUA	H8	3.68	4.59
5	GUA	H8	4	ADE	H2'1	2.81	3.38
5	GUA	H8	4	ADE	H2'2	2.37	2.83
5	GUA	H2'2	5	GUA	H8	2.73	4.16
5	GUA	H4'	5	GUA	H1'	2.77	2.97
5	GUA	H2'1	6	CYT	H5	4	6.14
6	CYT	H5	5	GUA	H1'	3.61	4.61
6	CYT	H2'2	6	CYT	H2'1	1.8	2.1
7	X	H8	6	CYT	H2'2	3.09	3.58
7	X	H3'	7	X	H1'	3.13	4.01
7	X	H3'	7	X	H8	3.43	4.71
8	ADE	H3'	8	ADE	H8	3.32	4.66
9	GUA	H8	8	ADE	H3'	4.43	5.72
9	GUA	H8	8	ADE	H8	3.79	5.7
9	GUA	H2'1	9	GUA	H8	2.24	2.4
9	GUA	H3'	9	GUA	H1'	3.51	4.31
9	GUA	H2'2	10	THY	H6	2.06	2.74
9	GUA	H2'2	10	THY	M	3.32	4.52
10	THY	H6	9	GUA	H2'1	2.75	3.49
10	THY	H6	9	GUA	H8	3.72	5.16
10	THY	H2'1	10	THY	H6	2.08	2.28
10	THY	H2'2	10	THY	H6	3	4.63
10	THY	H3'	10	THY	H6	3.17	4.28
11	CYT	H5	10	THY	H3'	3.65	5.42
11	CYT	H5	10	THY	M	4.33	5.84
11	CYT	H6	10	THY	H2'1	3.03	4.45
11	CYT	H6	10	THY	H6	3.67	5.67
11	CYT	H1'	11	CYT	H2'1	2.59	5.47
11	CYT	H1'	11	CYT	H2'2	2.04	2.19
11	CYT	H2'1	11	CYT	H6	2	2.17
11	CYT	H4'	11	CYT	H2'1	3.12	4.04
12	CYT	H5	11	CYT	H6	3.39	4.34
12	CYT	H3'	12	CYT	H6	2.77	3.09
12	CYT	H4'	12	CYT	H3'	2.47	2.92
13	GUA	H1'	13	GUA	H8	3.21	3.91
13	GUA	H2'1	13	GUA	H8	2.1	2.3
13	GUA	H2'2	13	GUA	H8	2.7	4.06
14	GUA	H8	13	GUA	H2'2	2.31	2.52
14	GUA	H1'	14	GUA	H3'	3.26	3.97
14	GUA	H2'1	14	GUA	H8	2	2.29
16	CYT	H5	15	ADE	H2'1	3.29	4.12
16	CYT	H6	15	ADE	H3'	3.84	5.01

17	THY	H6	16	CYT	H2'1	2.87	4.16
17	THY	M	16	CYT	H1'	4.9	7.9
17	THY	M	16	CYT	H2'1	3.02	3.93
17	THY	H2'1	17	THY	H6	1.94	2.09
18	CYT	H1'	8	ADE	H2	3.81	4.48
18	CYT	H2'1	18	CYT	H3'	2.43	2.85
18	CYT	H2'1	18	CYT	H5	3.7	5.24
18	CYT	H2'1	18	CYT	H6	2.1	2.24
18	CYT	H2'2	18	CYT	H3'	2.85	3.35
18	CYT	H6	18	CYT	H1'	3.19	3.96
19	Y	H3x1	7	X	H1x	2.16	2.42
19	Y	H3x2	7	X	H2x1	2.09	2.59
19	Y	H8	18	CYT	H2'1	2.85	3.13
19	Y	H2'1	19	Y	H8	2.1	2.29
19	Y	H2'2	19	Y	H8	2.5	3.54
19	Y	H3'	19	Y	H8	3.53	4.95
20	CYT	H6	19	Y	H2'2	2.05	2.82
20	CYT	H5	20	CYT	H6	2.26	2.42
20	CYT	H2'2	21	THY	M	3.69	6.24
21	THY	M	20	CYT	H2'1	3.07	4.04
21	THY	M	20	CYT	H3'	3.79	4.9
21	THY	H1'	21	THY	H6	3.16	4.65
22	ADE	H1'	23	GUA	H8	3.04	3.34
22	ADE	H2'1	23	GUA	H8	2.77	3.2
22	ADE	H2'2	23	GUA	H8	2.27	2.83
23	GUA	H2'2	23	GUA	H8	2.79	4.05
24	CYT	H1'	24	CYT	H2'1	2.87	4.32
24	CYT	H1'	24	CYT	H2'2	2.12	2.29
24	CYT	H2'1	24	CYT	H3'	2.42	2.64
24	CYT	H3'	24	CYT	H6	2.94	3.29
24	CYT	H5	24	CYT	H6	2.43	2.57

Class3

res_#	res_name	atm_name	res_#	res_name	atm_name	low_bnd	up_bnd
1	GUA	H4'	1	GUA	H2'2	3.21	4.12
2	CYT	H6	1	GUA	H8	3.56	5.01
2	CYT	H2'1	2	CYT	H5	3.66	5.24
5	GUA	H3'	5	GUA	H8	3.33	5.03
6	CYT	H6	5	GUA	H3'	3.7	4.75
7	X	H5'1	6	CYT	H2'2	2.89	3.5
7	X	H8	6	CYT	H2'1	2.97	3.56
7	X	H1x	7	X	H1'	3.29	4.55
8	ADE	H1'	7	X	H1x	3.33	4.96
8	ADE	H1'	7	X	M	2.94	4.35
9	GUA	H1'	8	ADE	H2	3.54	3.93
10	THY	H6	9	GUA	H3'	3.34	4.99
10	THY	H2'1	10	THY	M	4.49	7.47
11	CYT	H1'	11	CYT	H6	3.3	3.81
11	CYT	H1'	12	CYT	H6	3.7	5.93
14	GUA	H8	13	GUA	H2'1	2.88	4.21

14	GUA	H8	13	GUA	H3'	3.52	4.7
15	ADE	H4'	15	ADE	H2'1	3.29	4.66
15	ADE	H4'	15	ADE	H2'2	3.47	4.71
15	ADE	H4'	15	ADE	H8	4.05	5.75
16	CYT	H1'	15	ADE	H1'	3.37	4.7
16	CYT	H5	15	ADE	H1'	3.82	4.79
17	THY	H2'1	17	THY	M	4.31	7.3
17	THY	H3'	18	CYT	H6	4	5.82
18	CYT	H5	17	THY	M	4.82	7.75
19	Y	H3x2	19	Y	H3x1	1.65	1.88
20	CYT	H6	19	Y	H8	3.5	4.98
21	THY	H6	20	CYT	H2'1	2.42	3.8
21	THY	H2'1	21	THY	H6	1.82	2.05
23	GUA	H3'	23	GUA	H8	3.29	5.05
24	CYT	H1'	24	CYT	H6	3.46	4.77

Class4

res_#	res_name	atm_name	res_#	res_name	atm_name	low_bnd	up_bnd
4	ADE	H8	3	THY	H3'	3.98	5.93
6	CYT	H4'	6	CYT	H2'2	2.66	3.02
7	X	H1'	7	X	M	4.04	5.62
7	X	H2x2	7	X	H2x1	1.65	1.84
7	X	H3'	8	ADE	H8	3.89	5.53
11	CYT	H3'	12	CYT	H6	3.5	4.73
12	CYT	H6	11	CYT	H2'1	3.04	5.53
16	CYT	H2'1	16	CYT	H5	3.92	5.32
18	CYT	H4'	18	CYT	H2'1	3.73	5.91
19	Y	H8	18	CYT	H6	3.79	5.26
20	CYT	H1'	7	X	M	5.19	8.54
20	CYT	H6	19	Y	H3'	3.83	5.32
20	CYT	H2'1	20	CYT	H5	4.22	6.6
21	THY	H3'	22	ADE	H8	3.54	5.01
24	CYT	H5	23	GUA	H8	3.46	4.24
24	CYT	H6	23	GUA	H3'	3.92	5.93

Class5

res_#	res_name	atm_name	res_#	res_name	atm_name	low_bnd	up_bnd
2	CYT	H3'	3	THY	H6	3.47	4.83
3	THY	H3'	3	THY	H6	2.86	4.21
6	CYT	H2'1	6	CYT	H5	4.3	5.68
20	CYT	H1'	7	X	H1x	3.54	5.07
20	CYT	H4'	7	X	M	4.91	8.03
20	CYT	H3'	20	CYT	H6	2.94	4.28
21	THY	H6	20	CYT	H3'	3.07	4.38

B3. NOE Distance Restraints Used in rMD Calculations for the Oligodeoxynucleotide 5'-d(GCTAGCXAGTCC)-3'•5'-(GGACTCYCTAGC)-3', X and Y = *fully reduced S-crotonaldehyde-derived dG-dG cross-link*

Class 1

res_#	res_name	atm_name	res_#	res_name	atm_name	low_bnd	up_bnd
1	GUA	H1'	1	GUA	H4'	3.109	3.384
1	GUA	H2'1	1	GUA	H8	2.02	2.435
1	GUA	H2'2	1	GUA	H8	3.032	3.771
1	GUA	H3'	1	GUA	H8	3.382	4.52
1	GUA	H8	1	GUA	H1'	3.2	4.08
2	CYT	H5	1	GUA	H8	3.485	4.012
2	CYT	H5	1	GUA	H2'2	3.104	3.376
2	CYT	H6	1	GUA	H1'	2.933	3.171
2	CYT	H6	1	GUA	H2'2	2.602	2.749
2	CYT	H1'	2	CYT	H4'	2.9	3.089
2	CYT	H2'2	2	CYT	H6	3.047	3.856
2	CYT	H5	2	CYT	H6	2.364	2.468
3	THY	H6	2	CYT	H1'	3.501	4.055
3	THY	M	2	CYT	H6	3.512	3.671
3	THY	M	2	CYT	H5	4.098	4.428
5	GUA	H8	4	ADE	H1'	3.189	3.477
5	GUA	H8	4	ADE	H2'2	2.23	2.93
5	GUA	H1'	5	GUA	H4'	2.992	3.189
5	GUA	H2'1	5	GUA	H8	2.328	2.446
5	GUA	H2'2	5	GUA	H1'	2.378	2.529
5	GUA	H2'2	5	GUA	H8	3.124	3.729
5	GUA	H3'	5	GUA	H8	3.724	4.858
5	GUA	H8	5	GUA	H1'	3.395	3.928
6	CYT	H5	5	GUA	H8	3.441	3.896
6	CYT	H6	5	GUA	H1'	3.027	3.258
6	CYT	H6	5	GUA	H2'2	2.446	2.931
6	CYT	H1'	6	CYT	H4'	2.744	2.94
6	CYT	H2'1	6	CYT	H1'	2.876	3.059
6	CYT	H2'1	6	CYT	H6	2.532	2.648
6	CYT	H2'1	6	CYT	H3'	2.026	2.643
6	CYT	H2'2	6	CYT	H4'	3.094	3.374
6	CYT	H2'2	6	CYT	H1'	2.304	2.413
6	CYT	H2'2	6	CYT	H2'1	1.803	2.189
6	CYT	H3'	6	CYT	H6	3.113	3.399
6	CYT	H5	6	CYT	H6	2.406	2.512
7	X	H3'	7	X	H5'1	2.927	3.849
7	X	H4'	7	X	H5'1	2.418	2.547
8	ADE	H1'	7	X	M	3.129	3.284
8	ADE	H8	7	X	H1'	3.046	3.285
8	ADE	H1'	8	ADE	H4'	2.707	2.857
8	ADE	H2'1	8	ADE	H8	2.455	2.583
8	ADE	H2'1	8	ADE	H3'	2.106	2.538
8	ADE	H2'2	8	ADE	H1'	2.393	2.518

8	ADE	H2'2	8	ADE	H2'1	1.809	2.08
9	GUA	H8	8	ADE	H2'1	2.898	3.097
9	GUA	H8	8	ADE	H2'2	2.15	2.807
9	GUA	H2'1	9	GUA	H8	2.51	2.646
9	GUA	H2'2	9	GUA	H2'1	1.803	2.084
9	GUA	H8	9	GUA	H1'	3.265	4.029
10	THY	H6	9	GUA	H1'	3.236	3.81
10	THY	H6	9	GUA	H2'1	2.939	3.421
10	THY	H6	9	GUA	H2'2	2.296	2.884
10	THY	M	9	GUA	H8	3.647	3.866
10	THY	M	9	GUA	H2'2	3.664	3.945
10	THY	H2'1	10	THY	H6	2.242	2.364
10	THY	H2'2	10	THY	H6	3.095	3.81
10	THY	H6	10	THY	H1'	3.315	3.711
10	THY	M	10	THY	H6	2.671	3.712
11	CYT	H5	10	THY	H6	3.371	3.806
11	CYT	H6	10	THY	H2'1	3.151	3.831
11	CYT	H1'	11	CYT	H4'	2.798	3.001
11	CYT	H2'1	11	CYT	H1'	2.95	3.153
11	CYT	H2'1	11	CYT	H6	2.248	2.366
11	CYT	H2'1	11	CYT	H3'	2.197	2.637
11	CYT	H5	11	CYT	H6	2.415	2.547
12	CYT	H6	11	CYT	H2'2	2.306	3.016
12	CYT	H1'	12	CYT	H4'	2.651	3.186
12	CYT	H3'	12	CYT	H5'2	2.981	3.227
12	CYT	H3'	12	CYT	H6	2.825	2.991
12	CYT	H6	12	CYT	H1'	3.306	3.721
13	GUA	H2'1	13	GUA	H8	2.364	2.491
13	GUA	H2'2	13	GUA	H8	3.233	3.976
13	GUA	H2'2	13	GUA	H3'	2.572	3.074
13	GUA	H8	13	GUA	H1'	3.35	4.323
14	GUA	H8	13	GUA	H2'1	3.161	3.546
14	GUA	H8	13	GUA	H2'2	2.57	3.053
14	GUA	H1'	14	GUA	H4'	3.032	3.252
14	GUA	H8	14	GUA	H1'	3.328	3.998
15	ADE	H3'	15	ADE	H5'2	2.57	2.746
15	ADE	H3'	15	ADE	H4'	2.623	2.761
15	ADE	H4'	15	ADE	H5'1	2.522	2.654
15	ADE	H4'	15	ADE	H5'2	2.42	2.545
15	ADE	H8	15	ADE	H1'	3.452	4.019
16	CYT	H5	15	ADE	H8	3.387	3.881
16	CYT	H6	15	ADE	H1'	2.996	3.269
16	CYT	H6	15	ADE	H2'2	2.585	2.681
16	CYT	H2'1	16	CYT	H6	2.524	2.673
16	CYT	H2'1	16	CYT	H3'	2.008	2.626
16	CYT	H3'	16	CYT	H5'1	3.25	3.647
16	CYT	H3'	16	CYT	H5'2	2.838	2.989
16	CYT	H3'	16	CYT	H6	3.177	3.439
16	CYT	H5	16	CYT	H6	2.443	2.543

16	CYT	H6	16	CYT	H1'	3.257	3.9
17	THY	H6	16	CYT	H2'1	2.85	3.093
17	THY	M	16	CYT	H6	3.56	3.779
17	THY	M	16	CYT	H5	4.094	4.375
17	THY	M	16	CYT	H3'	3.665	3.945
17	THY	M	16	CYT	H2'1	3.161	4.084
17	THY	M	17	THY	H6	2.693	3.751
18	CYT	H5	17	THY	H6	3.252	3.507
18	CYT	H2'1	18	CYT	H1'	2.722	3.524
18	CYT	H2'1	18	CYT	H6	2.093	2.52
18	CYT	H2'2	18	CYT	H1'	2.391	2.518
18	CYT	H2'2	18	CYT	H2'1	1.8	2.221
18	CYT	H3'	18	CYT	H6	3.103	3.552
18	CYT	H5	18	CYT	H6	2.466	2.559
19	Y	H8	18	CYT	H2'1	2.827	2.997
19	Y	H8	18	CYT	H2'2	2.838	3.032
19	Y	H1'	19	Y	H4'	3.089	3.325
19	Y	H2'2	19	Y	H3'	2.696	2.91
19	Y	H3'	19	Y	H4'	2.647	2.791
19	Y	H8	19	Y	H2'2	2.89	3.146
19	Y	H8	19	Y	H2'1	2.28	2.395
20	CYT	H5	19	Y	H8	3.444	3.943
20	CYT	H6	19	Y	H1'	2.673	2.84
20	CYT	H1'	20	CYT	H4'	2.882	3.064
20	CYT	H2'1	20	CYT	H3'	1.974	2.625
21	THY	M	20	CYT	H5	4.086	4.472
21	THY	M	20	CYT	H2'1	2.887	3.415
23	GUA	H8	22	ADE	H1'	2.844	3.363
23	GUA	H8	22	ADE	H2'1	3.094	3.361
23	GUA	H8	22	ADE	H2'2	2.211	2.849
23	GUA	H2'1	23	GUA	H8	2.087	2.419
23	GUA	H2'2	23	GUA	H8	3.084	3.707
23	GUA	H3'	23	GUA	H8	3.453	4.317
24	CYT	H5	23	GUA	H8	3.338	3.794
24	CYT	H1'	24	CYT	H4'	2.88	3.081
24	CYT	H3'	24	CYT	H6	2.999	3.308

Class2

res_#	res_name	atm_name	res_#	res_name	atm_name	low_bnd	up_bnd
2	CYT	H2'1	2	CYT	H6	2.206	2.369
2	CYT	H6	2	CYT	H1'	3.418	4.26
3	THY	M	2	CYT	H3'	4.019	4.513
3	THY	M	2	CYT	H2'1	2.984	3.26
3	THY	M	2	CYT	H2'2	3.663	4.174
3	THY	H2'2	3	THY	H2'1	1.804	2.117
3	THY	H3'	3	THY	H6	3.191	4.152
5	GUA	H8	4	ADE	H2'1	3.104	3.59
6	CYT	H5	5	GUA	H2'2	3.097	3.549
6	CYT	H3'	6	CYT	H4'	2.755	2.974
7	X	H2x1	7	X	H1x	2.587	2.841

7	X	H2x1	7	X	M	2.63	2.891
7	X	H2x1	7	X	H2x2	1.8	2.105
7	X	H2x2	7	X	M	2.761	3.053
7	X	H4'	7	X	H5'2	2.368	2.592
7	X	M	7	X	H1'	3.979	4.442
7	X	M	7	X	H1x	2.208	2.482
8	ADE	H4'	7	X	M	3.282	3.661
8	ADE	H8	7	X	H2'2	2.617	2.864
8	ADE	H2'2	8	ADE	H8	3.111	4.07
9	GUA	H2'1	9	GUA	H1'	2.845	3.201
10	THY	M	9	GUA	H3'	4.176	4.856
10	THY	M	9	GUA	H2'1	3.055	4.377
11	CYT	H6	10	THY	H1'	3.355	4.199
11	CYT	H2'2	11	CYT	H2'1	1.804	2.188
12	CYT	H6	11	CYT	H1'	3.27	3.861
12	CYT	H6	11	CYT	H2'1	2.842	3.155
12	CYT	H3'	12	CYT	H4'	2.481	3.173
12	CYT	H5	12	CYT	H6	2.42	2.635
13	GUA	H1'	13	GUA	H4'	3.281	3.726
13	GUA	H2'1	13	GUA	H3'	2.435	2.689
13	GUA	H2'2	13	GUA	H1'	2.406	2.61
14	GUA	H4'	14	GUA	H5'1	2.388	2.628
14	GUA	H4'	14	GUA	H5'2	2.329	2.523
15	ADE	H1'	15	ADE	H4'	3.081	3.422
15	ADE	H2'2	15	ADE	H1'	2.355	2.575
15	ADE	H3'	15	ADE	H5'1	2.96	3.912
15	ADE	H3'	15	ADE	H1'	3.38	4.185
16	CYT	H6	15	ADE	H2'1	3.195	3.863
16	CYT	H2'2	16	CYT	H3'	3.008	3.304
16	CYT	H2'2	16	CYT	H2'1	1.801	2.18
16	CYT	H3'	16	CYT	H4'	2.491	2.945
17	THY	M	16	CYT	H2'2	3.735	4.212
17	THY	H3'	17	THY	H6	3.232	4.253
17	THY	H6	17	THY	H1'	3.094	3.757
19	Y	H3x1	7	X	H1x	2.371	2.586
19	Y	H3x1	7	X	H2x1	2.375	2.878
19	Y	H3x2	7	X	H2x1	2.316	2.568
19	Y	H1'	19	Y	H2'2	2.443	2.621
19	Y	H3x1	19	Y	H3x2	1.8	2.049
19	Y	H8	19	Y	H3'	3.461	4.625
20	CYT	H6	19	Y	H2'2	2.614	2.863
20	CYT	H2'1	20	CYT	H1'	2.691	2.951
20	CYT	H2'2	20	CYT	H2'1	1.8	2.158
20	CYT	H5	20	CYT	H6	2.302	2.491
21	THY	M	20	CYT	H3'	3.666	4.118
21	THY	H2'2	21	THY	H6	2.945	3.563
23	GUA	H2'2	23	GUA	H1'	2.297	2.49
23	GUA	H8	23	GUA	H1'	3.231	3.956
24	CYT	H6	23	GUA	H2'2	2.278	2.813

24	CYT	H2'2	24	CYT	H1'	2.214	2.398
24	CYT	H2'2	24	CYT	H3'	2.972	3.528
24	CYT	H5	24	CYT	H6	2.409	2.594
24	CYT	H6	24	CYT	H1'	3.304	3.813

Class3

res_#	res_name	atm_name	res_#	res_name	atm_name	low_bnd	up_bnd
2	CYT	H5	1	GUA	H2'1	3.464	5.145
2	CYT	H6	1	GUA	H2'1	3.143	4.035
3	THY	H2'2	3	THY	H4'	3.193	4.277
3	THY	M	3	THY	H6	2.658	2.989
5	GUA	H3'	5	GUA	H1'	3.375	4.385
6	CYT	H5'1	5	GUA	H1'	3.019	3.53
6	CYT	H3'	6	CYT	H5'2	2.684	3.026
7	X	H8	6	CYT	H2'1	2.913	3.417
7	X	H8	6	CYT	H2'2	3.133	3.552
7	X	H1'	7	X	H2'2	2.222	2.526
7	X	H1'	7	X	H2'1	2.751	3.351
8	ADE	H2'1	8	ADE	H1'	2.726	3.131
8	ADE	H3'	8	ADE	H8	3.43	4.369
9	GUA	H8	8	ADE	H1'	2.641	3.648
9	GUA	H2'2	9	GUA	H4'	3.294	4.039
9	GUA	H2'2	9	GUA	H1'	2.208	2.453
9	GUA	H2'2	9	GUA	H8	3.311	4.258
9	GUA	H3'	9	GUA	H8	3.287	4.458
10	THY	H2'2	11	CYT	H5	3.241	4.455
11	CYT	H5	10	THY	H2'1	3.19	4.419
11	CYT	H6	11	CYT	H1'	3.195	3.755
14	GUA	H2'1	14	GUA	H8	2.066	2.328
14	GUA	H3'	14	GUA	H1'	3.394	4.129
18	CYT	H2'2	18	CYT	H6	2.982	3.984
19	Y	H3x2	7	X	H1x	2.623	3.725
19	Y	H3x2	7	X	M	3.372	4.074
19	Y	H1'	19	Y	H3'	3.365	4.206
19	Y	H1'	19	Y	H2'1	2.922	3.561
19	Y	H8	19	Y	H1'	3.451	4.396
20	CYT	H5	19	Y	H2'2	2.414	3.138
20	CYT	H5	19	Y	H1'	3.056	3.593
20	CYT	H3'	20	CYT	H6	3.055	4.057
21	THY	M	20	CYT	H2'2	3.815	4.724
21	THY	H2'2	21	THY	H4'	3.15	4.129
21	THY	H3'	21	THY	H6	3.135	4.212

Class4

res_#	res_name	atm_name	res_#	res_name	atm_name	low_bnd	up_bnd
2	CYT	H5	1	GUA	H1'	3.383	4.379
2	CYT	H2'1	2	CYT	H4'	3.155	4.518
2	CYT	H2'2	2	CYT	H4'	3.077	3.796
3	THY	H2'1	3	THY	H4'	2.877	3.897
3	THY	H2'2	3	THY	H3'	2.499	2.985
4	ADE	H8	3	THY	H2'1	3.531	6.964

6	CYT	H5	5	GUA	H1'	3.365	4.483
6	CYT	H2'2	6	CYT	H6	3.225	4.05
6	CYT	H2'2	6	CYT	H3'	2.792	3.285
6	CYT	H3'	6	CYT	H5'1	3.124	3.942
6	CYT	H6	6	CYT	H1'	3.275	4.356
7	X	H2x2	7	X	H1x	2.712	3.214
7	X	H8	7	X	H3'	3.225	4.534
8	ADE	H2	7	X	M	4.414	6.86
8	ADE	H3'	8	ADE	H1'	3.351	4.763
11	CYT	H5	10	THY	M	4.554	7.459
11	CYT	H2'2	11	CYT	H1'	2.18	2.544
12	CYT	H5	11	CYT	H6	3.351	4.552
13	GUA	H3'	13	GUA	H8	3.581	5.678
14	GUA	H2'2	14	GUA	H8	2.59	3.471
14	GUA	H3'	14	GUA	H8	3.306	4.634
16	CYT	H5	15	ADE	H2'2	3.109	4.032
16	CYT	H6	15	ADE	H8	3.562	5.937
17	THY	H2'2	17	THY	H3'	2.534	3.147
17	THY	H1'	18	CYT	H6	3.271	4.121
18	CYT	H5	17	THY	H2'1	2.933	3.561
18	CYT	H5	17	THY	H2'2	3.309	4.962
18	CYT	H6	17	THY	H2'1	3.221	5.998
19	Y	H3x1	7	X	H2x2	2.707	3.353
20	CYT	H5	19	Y	H2'1	3.416	5.456
20	CYT	H2'2	20	CYT	H1'	2.292	2.71
20	CYT	H2'2	20	CYT	H3'	2.852	3.526
21	THY	H2'1	21	THY	H4'	3.092	3.877
22	ADE	H1'	22	ADE	H3'	3.46	4.478
23	GUA	H8	22	ADE	H8	3.638	5.234

Class5

res_#	res_name	atm_name	res_#	res_name	atm_name	low_bnd	up_bnd
4	ADE	H8	3	THY	H1'	2.5	3.5
7	X	H8	7	X	H1'	3.186	4.06
8	ADE	H2	8	ADE	H1'	3.542	6.33
8	ADE	H8	8	ADE	H1'	3.498	5.439
14	GUA	H8	13	GUA	H1'	3.102	4.299
18	CYT	H6	18	CYT	H1'	3.271	4.437
19	Y	H3x1	7	X	M	3.922	5.725
19	Y	H8	18	CYT	H1'	3.556	6.26

res_#	res_name	atm_name	res_#	res_name	atm_name	low_bnd	up_bnd
1	GUA	H8	1	GUA	H4'	4	5.5
1	GUA	H8	2	CYT	H6	4.5	5.5
2	CYT	H6	1	GUA	H3'	4	5.5
2	CYT	H6	2	CYT	H3'	3.5	5
2	CYT	H1'	3	THY	M	3.5	5
3	THY	H6	2	CYT	H3'	4	5.5
3	THY	H6	3	THY	H3'	3.5	5
3	THY	H6	4	ADE	H8	4.5	5.5

4	ADE	H8	3	THY	H3'	4.5	5.5
4	ADE	H8	3	THY	H2'	3	4
4	ADE	H8	3	THY	H2''	2	3.5
4	ADE	H8	4	ADE	H1'	3.5	4.5
4	ADE	H8	4	ADE	H3'	4	5
4	ADE	H8	4	ADE	H2'	2	4
4	ADE	H8	4	ADE	H2''	3.5	4.5
4	ADE	H8	5	GUA	H8	4.5	5.5
5	GUA	H8	4	ADE	H3'	4.5	5.5
5	GUA	H8	5	GUA	H4'	4	5.5
5	GUA	H8	6	CYT	H6	4.5	5.5
6	CYT	H6	5	GUA	H3'	4.5	5.5
6	CYT	H6	5	GUA	H2'	3	5
6	CYT	H5	6	CYT	H2'	4	5
6	CYT	H6	7	X	H8	4.5	5.5
7	X	H8	6	CYT	H1'	3.5	5
7	X	H8	6	CYT	H3'	4.5	5.5
7	X	H8	8	ADE	H8	4.5	5.5
8	ADE	H1'	7	X	H1x	3	6
8	ADE	H8	7	X	H3'	4.5	5.5
8	ADE	H8	7	X	M	4	5.5
8	ADE	H2	8	ADE	H1'	4	5.5
8	ADE	H2	9	GUA	H1'	4	5.5
8	ADE	H8	9	GUA	H8	4.5	5.5
8	ADE	H2	17	THY	H1'	4	5.5
8	ADE	H2	18	CYT	H1'	4	5.5
9	GUA	H8	8	ADE	H3'	4.5	5.5
9	GUA	H8	9	GUA	H4'	4	5.5
9	GUA	H1'	10	THY	M	3	4.5
9	GUA	H8	10	THY	H6	4.5	5.5
10	THY	H6	9	GUA	H3'	4	5.5
10	THY	H6	10	THY	H3'	3.5	5
10	THY	H6	11	CYT	H6	4.5	5.5
11	CYT	H6	10	THY	H3'	4	5.5
11	CYT	H5	11	CYT	H2'	3.5	5
11	CYT	H6	11	CYT	H3'	3.5	5
11	CYT	H6	12	CYT	H6	4.5	5.5
12	CYT	H6	11	CYT	H3'	4	5.5
13	GUA	H8	13	GUA	H4'	4	5.5
13	GUA	H8	14	GUA	H8	4.5	5.5
14	GUA	H8	13	GUA	H3'	4.5	5.5
14	GUA	H8	15	ADE	H8	4.5	5.5
15	ADE	H2	10	THY	H1'	4	5.5
15	ADE	H2	11	CYT	H1'	4	5.5
15	ADE	H8	14	GUA	H3'	4.5	5.5
15	ADE	H2	15	ADE	H1'	4	5.5
15	ADE	H8	15	ADE	H3'	4	5
15	ADE	H8	15	ADE	H4'	4	5.5
15	ADE	H2	16	CYT	H1'	3.7	5.5

15	ADE	H2	16	CYT	H2''	4	6
16	CYT	H6	15	ADE	H3'	4.5	5.5
16	CYT	H6	16	CYT	H4'	4	5.5
16	CYT	H1'	17	THY	M	3.5	4.5
16	CYT	H6	17	THY	H6	4.5	5.5
17	THY	H6	16	CYT	H3'	4	5.5
18	CYT	H5	17	THY	M	4	5
18	CYT	H6	17	THY	H6	4.5	5.5
18	CYT	H6	17	THY	H3'	4	5.5
19	Y	H1'	7	X	H1x	3	6
19	Y	H8	18	CYT	H6	4.5	5.5
19	Y	H8	18	CYT	H3'	4.5	5.5
19	Y	H8	19	Y	H4'	4	5.5
20	CYT	H1'	7	X	M	3	6
20	CYT	H1'	7	X	H2x1	3	6
20	CYT	H1'	19	Y	H3x1	3	4.5
20	CYT	H1'	19	Y	H3x2	3	4.5
20	CYT	H6	19	Y	H8	4.5	5.5
20	CYT	H6	19	Y	H3'	4.5	5.5
20	CYT	H6	20	CYT	H1'	3.5	4.5
20	CYT	H1'	21	THY	M	3.5	5
21	THY	H6	20	CYT	H1'	2.5	4
21	THY	H6	20	CYT	H3'	4	5.5
21	THY	H6	21	THY	H1'	3.5	4.5
22	ADE	H8	21	THY	H1'	2.5	3.5
22	ADE	H8	21	THY	H6	4.5	5.5
22	ADE	H8	21	THY	H3'	4	5.5
22	ADE	H8	21	THY	H2'	3	4
22	ADE	H8	21	THY	H2''	2	3.5
22	ADE	H8	22	ADE	H1'	3.5	4.5
22	ADE	H8	22	ADE	H3'	4	5
22	ADE	H8	22	ADE	H2'	2	4
22	ADE	H8	22	ADE	H2''	3.5	4.5
23	GUA	H8	22	ADE	H3'	4.5	5.5
23	GUA	H8	23	GUA	H4'	4	5.5
24	CYT	H6	23	GUA	H8	4.5	5.5
24	CYT	H6	23	GUA	H3'	4.5	5.5

APPENDIX C

PDB FILES

C1. PDB File of the S-crotonaldehyde-derived N^2-(3-oxo-1(*S*)-methyl-propyl)-dG containing in d(GCTAGCXAGTCC)•d(GGACTCGCTAGC)

```
REMARK
ATOM      1 H5T  DG5     1       5.907  -7.381  -3.181
ATOM      2 O5'  DG5     1       6.565  -8.008  -2.811
ATOM      3 C5'  DG5     1       6.540  -7.923  -1.388
ATOM      4 H5'1 DG5     1       7.272  -8.624  -0.980
ATOM      5 H5'2 DG5     1       5.553  -8.203  -1.013
ATOM      6 C4'  DG5     1       6.887  -6.507  -0.893
ATOM      7 H4'  DG5     1       7.829  -6.189  -1.339
ATOM      8 O4'  DG5     1       5.848  -5.601  -1.265
ATOM      9 C1'  DG5     1       5.527  -4.841  -0.115
ATOM     10 H1'  DG5     1       6.295  -4.075   0.034
ATOM     11 N9   DG5     1       4.217  -4.160  -0.239
ATOM     12 C8   DG5     1       2.947  -4.669  -0.102
ATOM     13 H8   DG5     1       2.760  -5.718   0.098
ATOM     14 N7   DG5     1       1.995  -3.783  -0.254
ATOM     15 C5   DG5     1       2.691  -2.586  -0.494
ATOM     16 C6   DG5     1       2.236  -1.238  -0.740
ATOM     17 O6   DG5     1       1.086  -0.804  -0.837
ATOM     18 N1   DG5     1       3.264  -0.330  -0.899
ATOM     19 H1   DG5     1       3.009   0.636  -1.047
ATOM     20 C2   DG5     1       4.576  -0.664  -0.870
ATOM     21 N2   DG5     1       5.446   0.292  -1.046
ATOM     22 H21  DG5     1       6.423   0.054  -1.021
ATOM     23 H22  DG5     1       5.135   1.257  -1.135
ATOM     24 N3   DG5     1       5.045  -1.892  -0.671
ATOM     25 C4   DG5     1       4.051  -2.814  -0.483
ATOM     26 C3'  DG5     1       6.984  -6.470   0.651
ATOM     27 H3'  DG5     1       7.101  -7.466   1.086
ATOM     28 C2'  DG5     1       5.635  -5.858   1.019
ATOM     29 H2'1 DG5     1       4.845  -6.608   0.959
ATOM     30 H2'2 DG5     1       5.653  -5.385   2.000
ATOM     31 O3'  DG5     1       7.977  -5.578   1.144
ATOM     32 P    DC      2       9.556  -5.892   1.125
ATOM     33 O1P  DC      2       9.935  -6.519   2.415
ATOM     34 O2P  DC      2       9.926  -6.564  -0.145
ATOM     35 O5'  DC      2      10.124  -4.384   1.075
ATOM     36 C5'  DC      2      10.058  -3.533   2.214
ATOM     37 H5'1 DC      2      11.008  -3.598   2.747
ATOM     38 H5'2 DC      2       9.263  -3.856   2.888
ATOM     39 C4'  DC      2       9.791  -2.073   1.813
ATOM     40 H4'  DC      2      10.443  -1.809   0.978
ATOM     41 O4'  DC      2       8.420  -1.911   1.441
ATOM     42 C1'  DC      2       7.826  -0.890   2.233
ATOM     43 H1'  DC      2       7.944   0.073   1.723
ATOM     44 N1   DC      2       6.381  -1.172   2.481
ATOM     45 C6   DC      2       5.948  -2.444   2.774
ATOM     46 H6   DC      2       6.676  -3.245   2.852
ATOM     47 C5   DC      2       4.622  -2.691   2.938
ATOM     48 H5   DC      2       4.279  -3.690   3.156
ATOM     49 C4   DC      2       3.729  -1.596   2.788
ATOM     50 N4   DC      2       2.443  -1.774   2.855
ATOM     51 H41  DC      2       2.073  -2.690   3.030
ATOM     52 H42  DC      2       1.840  -0.973   2.695
```

```
ATOM     53 N3   DC      2       4.121  -0.364   2.541
ATOM     54 C2   DC      2       5.448  -0.127   2.398
ATOM     55 O2   DC      2       5.782   1.040   2.194
ATOM     56 C3'  DC      2      10.061  -1.122   2.992
ATOM     57 H3'  DC      2      10.669  -1.615   3.754
ATOM     58 C2'  DC      2       8.650  -0.854   3.517
ATOM     59 H2'1 DC      2       8.351  -1.663   4.185
ATOM     60 H2'2 DC      2       8.566   0.107   4.024
ATOM     61 O3'  DC      2      10.723   0.044   2.507
ATOM     62 P    DT      3      11.431   1.119   3.482
ATOM     63 O1P  DT      3      11.816   0.438   4.745
ATOM     64 O2P  DT      3      12.478   1.816   2.697
ATOM     65 O5'  DT      3      10.253   2.178   3.773
ATOM     66 C5'  DT      3       9.952   2.645   5.081
ATOM     67 H5'1 DT      3      10.783   3.251   5.447
ATOM     68 H5'2 DT      3       9.802   1.805   5.760
ATOM     69 C4'  DT      3       8.678   3.500   5.052
ATOM     70 H4'  DT      3       8.801   4.306   4.327
ATOM     71 O4'  DT      3       7.562   2.675   4.704
ATOM     72 C1'  DT      3       6.536   2.925   5.646
ATOM     73 H1'  DT      3       6.043   3.867   5.383
ATOM     74 N1   DT      3       5.525   1.838   5.705
ATOM     75 C6   DT      3       5.894   0.529   5.942
ATOM     76 H6   DT      3       6.945   0.285   6.029
ATOM     77 C5   DT      3       4.955  -0.443   6.090
ATOM     78 C7   DT      3       5.420  -1.864   6.365
ATOM     79 H71  DT      3       5.660  -1.967   7.424
ATOM     80 H72  DT      3       4.628  -2.572   6.119
ATOM     81 H73  DT      3       6.295  -2.100   5.761
ATOM     82 C4   DT      3       3.530  -0.127   5.968
ATOM     83 O4   DT      3       2.585  -0.904   6.093
ATOM     84 N3   DT      3       3.253   1.189   5.684
ATOM     85 H3   DT      3       2.284   1.460   5.603
ATOM     86 C2   DT      3       4.175   2.200   5.594
ATOM     87 O2   DT      3       3.775   3.354   5.449
ATOM     88 C3'  DT      3       8.363   4.100   6.436
ATOM     89 H3'  DT      3       9.232   4.122   7.098
ATOM     90 C2'  DT      3       7.296   3.142   6.951
ATOM     91 H2'1 DT      3       7.751   2.216   7.306
ATOM     92 H2'2 DT      3       6.677   3.602   7.719
ATOM     93 O3'  DT      3       7.743   5.370   6.286
ATOM     94 P    DA      4       8.438   6.759   6.687
ATOM     95 O1P  DA      4       9.557   6.524   7.634
ATOM     96 O2P  DA      4       8.685   7.527   5.442
ATOM     97 O5'  DA      4       7.214   7.446   7.481
ATOM     98 C5'  DA      4       6.827   7.005   8.778
ATOM     99 H5'1 DA      4       7.202   7.728   9.506
ATOM    100 H5'2 DA      4       7.266   6.032   9.006
ATOM    101 C4'  DA      4       5.298   6.895   8.914
ATOM    102 H4'  DA      4       4.833   7.746   8.416
ATOM    103 O4'  DA      4       4.806   5.673   8.345
ATOM    104 C1'  DA      4       3.844   5.163   9.253
ATOM    105 H1'  DA      4       2.937   5.775   9.198
ATOM    106 N9   DA      4       3.459   3.748   9.039
ATOM    107 C8   DA      4       4.235   2.614   9.118
ATOM    108 H8   DA      4       5.307   2.654   9.269
ATOM    109 N7   DA      4       3.569   1.493   8.997
ATOM    110 C5   DA      4       2.239   1.930   8.863
ATOM    111 C6   DA      4       0.979   1.290   8.732
ATOM    112 N6   DA      4       0.805  -0.015   8.663
ATOM    113 H61  DA      4      -0.128  -0.377   8.505
ATOM    114 H62  DA      4       1.610  -0.620   8.660
ATOM    115 N1   DA      4      -0.156   1.992   8.661
ATOM    116 C2   DA      4      -0.066   3.315   8.690
ATOM    117 H2   DA      4      -1.002   3.857   8.624
```

```
ATOM    118 N3   DA      4       1.032   4.057   8.794
ATOM    119 C4   DA      4       2.164   3.297   8.883
ATOM    120 C3'  DA      4       4.886   6.876  10.405
ATOM    121 H3'  DA      4       5.698   7.167  11.074
ATOM    122 C2'  DA      4       4.516   5.410  10.598
ATOM    123 H2'1 DA      4       5.414   4.798  10.706
ATOM    124 H2'2 DA      4       3.840   5.261  11.437
ATOM    125 O3'  DA      4       3.710   7.631  10.664
ATOM    126 P    DG      5       3.713   9.230  10.829
ATOM    127 O1P  DG      5       4.115   9.855   9.546
ATOM    128 O2P  DG      5       4.444   9.582  12.072
ATOM    129 O5'  DG      5       2.138   9.497  11.044
ATOM    130 C5'  DG      5       1.481   9.121  12.249
ATOM    131 H5'1 DG      5       1.410   9.999  12.892
ATOM    132 H5'2 DG      5       2.055   8.354  12.774
ATOM    133 C4'  DG      5       0.073   8.568  11.975
ATOM    134 H4'  DG      5      -0.446   9.232  11.281
ATOM    135 O4'  DG      5       0.167   7.251  11.425
ATOM    136 C1'  DG      5      -0.691   6.384  12.149
ATOM    137 H1'  DG      5      -1.699   6.422  11.727
ATOM    138 N9   DG      5      -0.195   4.986  12.136
ATOM    139 C8   DG      5       1.089   4.532  12.312
ATOM    140 H8   DG      5       1.914   5.214  12.479
ATOM    141 N7   DG      5       1.219   3.231  12.247
ATOM    142 C5   DG      5      -0.093   2.782  12.032
ATOM    143 C6   DG      5      -0.643   1.456  11.873
ATOM    144 O6   DG      5      -0.067   0.367  11.864
ATOM    145 N1   DG      5      -2.014   1.445  11.708
ATOM    146 H1   DG      5      -2.459   0.544  11.615
ATOM    147 C2   DG      5      -2.781   2.562  11.715
ATOM    148 N2   DG      5      -4.075   2.401  11.676
ATOM    149 H21  DG      5      -4.647   3.225  11.731
ATOM    150 H22  DG      5      -4.473   1.469  11.599
ATOM    151 N3   DG      5      -2.321   3.803  11.837
ATOM    152 C4   DG      5      -0.963   3.852  11.987
ATOM    153 C3'  DG      5      -0.734   8.466  13.282
ATOM    154 H3'  DG      5      -0.231   9.006  14.087
ATOM    155 C2'  DG      5      -0.721   6.966  13.556
ATOM    156 H2'1 DG      5       0.186   6.698  14.101
ATOM    157 H2'2 DG      5      -1.606   6.644  14.096
ATOM    158 O3'  DG      5      -2.055   8.972  13.097
ATOM    159 P    DC      6      -3.050   9.278  14.337
ATOM    160 O1P  DC      6      -2.243   9.412  15.575
ATOM    161 O2P  DC      6      -3.927  10.408  13.938
ATOM    162 O5'  DC      6      -3.960   7.954  14.488
ATOM    163 C5'  DC      6      -4.993   7.644  13.556
ATOM    164 H5'1 DC      6      -4.566   7.577  12.554
ATOM    165 H5'2 DC      6      -5.730   8.450  13.555
ATOM    166 C4'  DC      6      -5.726   6.323  13.863
ATOM    167 H4'  DC      6      -6.528   6.202  13.132
ATOM    168 O4'  DC      6      -4.804   5.240  13.737
ATOM    169 C1'  DC      6      -4.858   4.481  14.934
ATOM    170 H1'  DC      6      -5.688   3.771  14.847
ATOM    171 N1   DC      6      -3.592   3.730  15.152
ATOM    172 C6   DC      6      -2.414   4.355  15.475
ATOM    173 H6   DC      6      -2.416   5.422  15.666
ATOM    174 C5   DC      6      -1.260   3.641  15.532
ATOM    175 H5   DC      6      -0.329   4.134  15.768
ATOM    176 C4   DC      6      -1.343   2.245  15.267
ATOM    177 N4   DC      6      -0.277   1.501  15.241
ATOM    178 H41  DC      6       0.624   1.901  15.428
ATOM    179 H42  DC      6      -0.408   0.511  15.057
ATOM    180 N3   DC      6      -2.465   1.621  14.990
ATOM    181 C2   DC      6      -3.607   2.344  14.963
ATOM    182 O2   DC      6      -4.653   1.723  14.778
```

```
ATOM    183 C3'  DC      6      -6.332   6.236  15.278
ATOM    184 H3'  DC      6      -6.519   7.217  15.720
ATOM    185 C2'  DC      6      -5.245   5.477  16.028
ATOM    186 H2'1 DC      6      -4.425   6.144  16.289
ATOM    187 H2'2 DC      6      -5.645   4.984  16.912
ATOM    188 O3'  DC      6      -7.475   5.384  15.298
ATOM    189 O1P  DS      7      -9.034   7.156  16.212
ATOM    190 P    DS      7      -8.990   5.900  15.422
ATOM    191 O2P  DS      7      -9.607   5.864  14.073
ATOM    192 O5'  DS      7      -9.603   4.691  16.313
ATOM    193 C5'  DS      7      -9.316   4.587  17.707
ATOM    194 H5'1 DS      7     -10.161   5.006  18.256
ATOM    195 H5'2 DS      7      -8.438   5.191  17.944
ATOM    196 C4'  DS      7      -9.059   3.144  18.208
ATOM    197 O4'  DS      7      -7.853   2.623  17.633
ATOM    198 H4'  DS      7      -9.907   2.515  17.945
ATOM    199 C3'  DS      7      -8.831   3.178  19.748
ATOM    200 O3'  DS      7      -9.108   1.996  20.516
ATOM    201 H3'  DS      7      -9.286   4.061  20.205
ATOM    202 C2'  DS      7      -7.306   3.259  19.771
ATOM    203 H2'2 DS      7      -6.890   3.006  20.745
ATOM    204 H2'1 DS      7      -6.952   4.237  19.438
ATOM    205 C1'  DS      7      -7.049   2.183  18.713
ATOM    206 H1'  DS      7      -7.450   1.232  19.077
ATOM    207 N9   DS      7      -5.627   1.943  18.387
ATOM    208 C4   DS      7      -5.061   0.698  18.196
ATOM    209 N3   DS      7      -5.705  -0.514  18.183
ATOM    210 C8   DS      7      -4.573   2.825  18.416
ATOM    211 H8   DS      7      -4.704   3.884  18.603
ATOM    212 N7   DS      7      -3.408   2.277  18.202
ATOM    213 C5   DS      7      -3.707   0.914  18.064
ATOM    214 C6   DS      7      -2.859  -0.231  17.867
ATOM    215 O6   DS      7      -1.641  -0.277  17.709
ATOM    216 N1   DS      7      -3.532  -1.434  17.889
ATOM    217 H1   DS      7      -2.972  -2.270  17.822
ATOM    218 C2   DS      7      -4.877  -1.558  18.027
ATOM    219 N2   DS      7      -5.313  -2.807  18.020
ATOM    220 H2   DS      7      -4.614  -3.538  17.937
ATOM    221 C1a  DS      7      -6.689  -3.276  18.134
ATOM    222 C1m  DS      7      -7.031  -4.021  16.845
ATOM    223 H1m  DS      7      -8.058  -4.382  16.869
ATOM    224 H2m  DS      7      -6.921  -3.348  15.996
ATOM    225 H3m  DS      7      -6.354  -4.866  16.713
ATOM    226 H1a  DS      7      -7.379  -2.435  18.260
ATOM    227 C2b  DS      7      -6.816  -4.208  19.343
ATOM    228 H2b  DS      7      -6.473  -3.681  20.230
ATOM    229 H1b  DS      7      -6.192  -5.091  19.202
ATOM    230 C3g  DS      7      -8.257  -4.628  19.589
ATOM    231 H3g  DS      7      -8.995  -3.884  19.843
ATOM    232 O2g  DS      7      -8.592  -5.812  19.496
ATOM    233 P    DA      8     -10.537   1.257  20.634
ATOM    234 O1P  DA      8     -10.957   1.307  22.054
ATOM    235 O2P  DA      8     -11.461   1.789  19.604
ATOM    236 O5'  DA      8     -10.153  -0.275  20.228
ATOM    237 C5'  DA      8     -10.339  -1.411  21.090
ATOM    238 H5'1 DA      8     -10.556  -2.268  20.452
ATOM    239 H5'2 DA      8     -11.227  -1.258  21.706
ATOM    240 C4'  DA      8      -9.160  -1.825  22.008
ATOM    241 H4'  DA      8      -9.268  -2.891  22.182
ATOM    242 O4'  DA      8      -7.894  -1.653  21.378
ATOM    243 C1'  DA      8      -6.924  -1.523  22.401
ATOM    244 H1'  DA      8      -6.680  -2.510  22.813
ATOM    245 N9   DA      8      -5.686  -0.877  21.891
ATOM    246 C8   DA      8      -5.414   0.467  21.763
ATOM    247 H8   DA      8      -6.166   1.229  21.923
```

```
ATOM    248 N7   DA      8      -4.177   0.751  21.455
ATOM    249 C5   DA      8      -3.587  -0.517  21.352
ATOM    250 C6   DA      8      -2.280  -0.985  21.076
ATOM    251 N6   DA      8      -1.239  -0.205  20.849
ATOM    252 H61  DA      8      -0.344  -0.620  20.619
ATOM    253 H62  DA      8      -1.365   0.794  20.864
ATOM    254 N1   DA      8      -2.011  -2.290  21.010
ATOM    255 C2   DA      8      -3.007  -3.141  21.221
ATOM    256 H2   DA      8      -2.755  -4.193  21.160
ATOM    257 N3   DA      8      -4.270  -2.858  21.519
ATOM    258 C4   DA      8      -4.503  -1.514  21.570
ATOM    259 C3'  DA      8      -9.092  -1.114  23.383
ATOM    260 H3'  DA      8      -9.679  -0.203  23.333
ATOM    261 C2'  DA      8      -7.630  -0.693  23.480
ATOM    262 H2'1 DA      8      -7.587   0.371  23.253
ATOM    263 H2'2 DA      8      -7.210  -0.870  24.471
ATOM    264 O3'  DA      8      -9.479  -1.781  24.592
ATOM    265 P    DG      9      -9.565  -3.376  24.845
ATOM    266 O1P  DG      9      -9.792  -3.570  26.298
ATOM    267 O2P  DG      9     -10.560  -3.935  23.898
ATOM    268 O5'  DG      9      -8.105  -3.978  24.510
ATOM    269 C5'  DG      9      -7.956  -5.244  23.870
ATOM    270 H5'1 DG      9      -8.002  -5.114  22.788
ATOM    271 H5'2 DG      9      -8.778  -5.899  24.166
ATOM    272 C4'  DG      9      -6.649  -5.963  24.243
ATOM    273 H4'  DG      9      -6.634  -6.921  23.719
ATOM    274 O4'  DG      9      -5.524  -5.198  23.825
ATOM    275 C1'  DG      9      -4.607  -5.113  24.903
ATOM    276 H1'  DG      9      -3.907  -5.952  24.861
ATOM    277 N9   DG      9      -3.868  -3.834  24.814
ATOM    278 C8   DG      9      -4.367  -2.556  24.831
ATOM    279 H8   DG      9      -5.423  -2.355  24.973
ATOM    280 N7   DG      9      -3.472  -1.623  24.630
ATOM    281 C5   DG      9      -2.275  -2.343  24.495
ATOM    282 C6   DG      9      -0.919  -1.917  24.252
ATOM    283 O6   DG      9      -0.474  -0.786  24.052
ATOM    284 N1   DG      9      -0.009  -2.955  24.257
ATOM    285 H1   DG      9       0.963  -2.714  24.135
ATOM    286 C2   DG      9      -0.347  -4.255  24.429
ATOM    287 N2   DG      9       0.622  -5.125  24.483
ATOM    288 H21  DG      9       0.381  -6.084  24.654
ATOM    289 H22  DG      9       1.590  -4.814  24.447
ATOM    290 N3   DG      9      -1.585  -4.700  24.617
ATOM    291 C4   DG      9      -2.510  -3.694  24.643
ATOM    292 C3'  DG      9      -6.522  -6.233  25.754
ATOM    293 H3'  DG      9      -7.466  -6.019  26.260
ATOM    294 C2'  DG      9      -5.448  -5.230  26.171
ATOM    295 H2'1 DG      9      -5.924  -4.277  26.406
ATOM    296 H2'2 DG      9      -4.854  -5.573  27.016
ATOM    297 O3'  DG      9      -6.137  -7.590  25.968
ATOM    298 P    DT     10      -6.154  -8.287  27.428
ATOM    299 O1P  DT     10      -6.271  -9.753  27.226
ATOM    300 O2P  DT     10      -7.162  -7.605  28.277
ATOM    301 O5'  DT     10      -4.692  -7.972  28.031
ATOM    302 C5'  DT     10      -3.537  -8.621  27.513
ATOM    303 H5'1 DT     10      -3.553  -8.575  26.423
ATOM    304 H5'2 DT     10      -3.551  -9.672  27.809
ATOM    305 C4'  DT     10      -2.223  -7.994  27.995
ATOM    306 H4'  DT     10      -1.407  -8.580  27.566
ATOM    307 O4'  DT     10      -2.091  -6.662  27.523
ATOM    308 C1'  DT     10      -1.244  -5.999  28.437
ATOM    309 H1'  DT     10      -0.216  -6.341  28.283
ATOM    310 N1   DT     10      -1.331  -4.525  28.245
ATOM    311 C6   DT     10      -2.532  -3.852  28.375
ATOM    312 H6   DT     10      -3.415  -4.403  28.673
```

```
ATOM    313 C5   DT     10      -2.618  -2.517  28.122
ATOM    314 C7   DT     10      -3.952  -1.809  28.297
ATOM    315 H71  DT     10      -3.858  -1.055  29.079
ATOM    316 H72  DT     10      -4.222  -1.301  27.372
ATOM    317 H73  DT     10      -4.741  -2.512  28.567
ATOM    318 C4   DT     10      -1.440  -1.768  27.681
ATOM    319 O4   DT     10      -1.389  -0.579  27.372
ATOM    320 N3   DT     10      -0.284  -2.506  27.615
ATOM    321 H3   DT     10       0.568  -2.011  27.393
ATOM    322 C2   DT     10      -0.158  -3.842  27.900
ATOM    323 O2   DT     10       0.955  -4.363  27.848
ATOM    324 C3'  DT     10      -2.028  -7.972  29.523
ATOM    325 H3'  DT     10      -2.947  -8.267  30.033
ATOM    326 C2'  DT     10      -1.710  -6.498  29.803
ATOM    327 H2'1 DT     10      -2.622  -5.990  30.115
ATOM    328 H2'2 DT     10      -0.933  -6.369  30.554
ATOM    329 O3'  DT     10      -0.951  -8.844  29.860
ATOM    330 P    DC     11      -0.569  -9.220  31.384
ATOM    331 O1P  DC     11      -1.762  -9.019  32.243
ATOM    332 O2P  DC     11       0.083 -10.554  31.372
ATOM    333 O5'  DC     11       0.530  -8.117  31.793
ATOM    334 C5'  DC     11       1.867  -8.161  31.299
ATOM    335 H5'1 DC     11       1.856  -8.160  30.207
ATOM    336 H5'2 DC     11       2.347  -9.081  31.635
ATOM    337 C4'  DC     11       2.709  -6.968  31.787
ATOM    338 H4'  DC     11       3.741  -7.142  31.498
ATOM    339 O4'  DC     11       2.250  -5.800  31.111
ATOM    340 C1'  DC     11       2.164  -4.756  32.054
ATOM    341 H1'  DC     11       3.168  -4.340  32.201
ATOM    342 N1   DC     11       1.247  -3.682  31.556
ATOM    343 C6   DC     11      -0.117  -3.733  31.741
ATOM    344 H6   DC     11      -0.579  -4.620  32.155
ATOM    345 C5   DC     11      -0.893  -2.672  31.407
ATOM    346 H5   DC     11      -1.961  -2.713  31.564
ATOM    347 C4   DC     11      -0.246  -1.534  30.862
ATOM    348 N4   DC     11      -0.930  -0.471  30.564
ATOM    349 H41  DC     11      -1.919  -0.442  30.729
ATOM    350 H42  DC     11      -0.426   0.312  30.160
ATOM    351 N3   DC     11       1.045  -1.477  30.624
ATOM    352 C2   DC     11       1.812  -2.545  30.952
ATOM    353 O2   DC     11       3.019  -2.441  30.727
ATOM    354 C3'  DC     11       2.572  -6.746  33.319
ATOM    355 H3'  DC     11       1.963  -7.549  33.738
ATOM    356 C2'  DC     11       1.748  -5.461  33.353
ATOM    357 H2'1 DC     11       0.698  -5.749  33.337
ATOM    358 H2'2 DC     11       1.953  -4.858  34.237
ATOM    359 O3'  DC     11       3.698  -6.601  34.201
ATOM    360 P    DC3    12       5.266  -6.529  33.814
ATOM    361 O1P  DC3    12       5.591  -7.558  32.798
ATOM    362 O2P  DC3    12       6.018  -6.542  35.093
ATOM    363 O5'  DC3    12       5.433  -5.061  33.181
ATOM    364 C5'  DC3    12       6.699  -4.572  32.743
ATOM    365 H5'1 DC3    12       6.765  -4.656  31.657
ATOM    366 H5'2 DC3    12       7.506  -5.169  33.174
ATOM    367 C4'  DC3    12       6.925  -3.105  33.151
ATOM    368 H4'  DC3    12       7.817  -2.744  32.634
ATOM    369 O4'  DC3    12       5.810  -2.305  32.765
ATOM    370 C1'  DC3    12       5.520  -1.408  33.821
ATOM    371 H1'  DC3    12       6.172  -0.533  33.724
ATOM    372 N1   DC3    12       4.087  -0.996  33.780
ATOM    373 C6   DC3    12       3.077  -1.893  34.030
ATOM    374 H6   DC3    12       3.329  -2.930  34.227
ATOM    375 C5   DC3    12       1.782  -1.486  34.019
ATOM    376 H5   DC3    12       0.989  -2.191  34.219
ATOM    377 C4   DC3    12       1.532  -0.120  33.719
```

```
ATOM    378 N4   DC3    12       0.314   0.335  33.666
ATOM    379 H41  DC3    12      -0.459  -0.285  33.824
ATOM    380 H42  DC3    12       0.184   1.299  33.377
ATOM    381 N3   DC3    12       2.481   0.760  33.480
ATOM    382 C2   DC3    12       3.770   0.345  33.522
ATOM    383 O2   DC3    12       4.636   1.202  33.343
ATOM    384 C3'  DC3    12       7.145  -2.922  34.668
ATOM    385 H3'  DC3    12       7.188  -3.888  35.178
ATOM    386 C2'  DC3    12       5.910  -2.144  35.108
ATOM    387 H2'1 DC3    12       5.145  -2.853  35.421
ATOM    388 H2'2 DC3    12       6.121  -1.443  35.917
ATOM    389 O3'  DC3    12       8.314  -2.153  34.940
ATOM    390 H3T  DC3    12       8.459  -2.113  35.908
TER
ATOM    391 H5T  DG5    13       1.770  11.245  32.412
ATOM    392 O5'  DG5    13       2.133  11.932  31.815
ATOM    393 C5'  DG5    13       2.107  11.444  30.475
ATOM    394 H5'1 DG5    13       2.476  12.226  29.808
ATOM    395 H5'2 DG5    13       1.080  11.209  30.186
ATOM    396 C4'  DG5    13       2.985  10.190  30.297
ATOM    397 H4'  DG5    13       3.991  10.403  30.654
ATOM    398 O4'  DG5    13       2.424   9.121  31.052
ATOM    399 C1'  DG5    13       2.318   8.016  30.179
ATOM    400 H1'  DG5    13       3.308   7.560  30.070
ATOM    401 N9   DG5    13       1.400   6.988  30.714
ATOM    402 C8   DG5    13       0.029   6.898  30.654
ATOM    403 H8   DG5    13      -0.584   7.668  30.201
ATOM    404 N7   DG5    13      -0.461   5.813  31.203
ATOM    405 C5   DG5    13       0.681   5.121  31.644
ATOM    406 C6   DG5    13       0.849   3.849  32.306
ATOM    407 O6   DG5    13      -0.004   3.043  32.685
ATOM    408 N1   DG5    13       2.171   3.514  32.532
ATOM    409 H1   DG5    13       2.356   2.614  32.950
ATOM    410 C2   DG5    13       3.216   4.315  32.214
ATOM    411 N2   DG5    13       4.419   3.870  32.450
ATOM    412 H21  DG5    13       5.193   4.444  32.160
ATOM    413 H22  DG5    13       4.559   2.930  32.811
ATOM    414 N3   DG5    13       3.113   5.502  31.632
ATOM    415 C4   DG5    13       1.817   5.848  31.360
ATOM    416 C3'  DG5    13       2.997   9.743  28.809
ATOM    417 H3'  DG5    13       2.701  10.561  28.148
ATOM    418 C2'  DG5    13       1.932   8.646  28.843
ATOM    419 H2'1 DG5    13       0.931   9.079  28.885
ATOM    420 H2'2 DG5    13       2.025   7.952  28.008
ATOM    421 O3'  DG5    13       4.198   9.130  28.322
ATOM    422 P    DG     14       5.671   9.782  28.457
ATOM    423 O1P  DG     14       5.556  11.163  28.987
ATOM    424 O2P  DG     14       6.392   9.582  27.178
ATOM    425 O5'  DG     14       6.308   8.844  29.619
ATOM    426 C5'  DG     14       7.398   7.931  29.434
ATOM    427 H5'1 DG     14       7.844   7.778  30.418
ATOM    428 H5'2 DG     14       8.169   8.397  28.818
ATOM    429 C4'  DG     14       7.103   6.516  28.877
ATOM    430 H4'  DG     14       7.900   5.876  29.246
ATOM    431 O4'  DG     14       5.897   5.930  29.348
ATOM    432 C1'  DG     14       5.691   4.776  28.544
ATOM    433 H1'  DG     14       6.361   3.973  28.870
ATOM    434 N9   DG     14       4.290   4.301  28.625
ATOM    435 C8   DG     14       3.146   4.964  28.253
ATOM    436 H8   DG     14       3.173   5.964  27.839
ATOM    437 N7   DG     14       2.041   4.297  28.463
ATOM    438 C5   DG     14       2.493   3.082  29.000
ATOM    439 C6   DG     14       1.778   1.919  29.458
ATOM    440 O6   DG     14       0.564   1.728  29.518
ATOM    441 N1   DG     14       2.601   0.896  29.882
```

```
ATOM    442 H1   DG     14       2.157   0.034  30.159
ATOM    443 C2   DG     14       3.953   0.972  29.896
ATOM    444 N2   DG     14       4.600  -0.100  30.261
ATOM    445 H21  DG     14       5.604  -0.076  30.232
ATOM    446 H22  DG     14       4.101  -0.962  30.469
ATOM    447 N3   DG     14       4.658   2.035  29.515
ATOM    448 C4   DG     14       3.871   3.066  29.075
ATOM    449 C3'  DG     14       7.050   6.369  27.343
ATOM    450 H3'  DG     14       6.543   7.245  26.951
ATOM    451 C2'  DG     14       6.087   5.201  27.127
ATOM    452 H2'1 DG     14       5.223   5.556  26.564
ATOM    453 H2'2 DG     14       6.553   4.378  26.596
ATOM    454 O3'  DG     14       8.279   6.225  26.611
ATOM    455 P    DA     15       9.515   5.227  26.963
ATOM    456 O1P  DA     15      10.478   5.340  25.840
ATOM    457 O2P  DA     15      10.004   5.538  28.328
ATOM    458 O5'  DA     15       8.948   3.713  26.936
ATOM    459 C5'  DA     15       9.537   2.693  27.739
ATOM    460 H5'1 DA     15       9.337   2.900  28.791
ATOM    461 H5'2 DA     15      10.619   2.707  27.595
ATOM    462 C4'  DA     15       9.036   1.274  27.415
ATOM    463 H4'  DA     15       9.504   0.594  28.130
ATOM    464 O4'  DA     15       7.625   1.180  27.581
ATOM    465 C1'  DA     15       7.111   0.335  26.567
ATOM    466 H1'  DA     15       7.181  -0.713  26.876
ATOM    467 N9   DA     15       5.699   0.702  26.310
ATOM    468 C8   DA     15       5.205   1.873  25.783
ATOM    469 H8   DA     15       5.852   2.665  25.429
ATOM    470 N7   DA     15       3.899   1.959  25.771
ATOM    471 C5   DA     15       3.507   0.723  26.310
ATOM    472 C6   DA     15       2.262   0.114  26.603
ATOM    473 N6   DA     15       1.086   0.687  26.431
ATOM    474 H61  DA     15       0.246   0.188  26.701
ATOM    475 H62  DA     15       1.041   1.614  26.042
ATOM    476 N1   DA     15       2.199  -1.111  27.121
ATOM    477 C2   DA     15       3.337  -1.755  27.350
ATOM    478 H2   DA     15       3.246  -2.751  27.764
ATOM    479 N3   DA     15       4.574  -1.321  27.131
ATOM    480 C4   DA     15       4.592  -0.058  26.614
ATOM    481 C3'  DA     15       9.396   0.784  25.999
ATOM    482 H3'  DA     15       9.952   1.551  25.455
ATOM    483 C2'  DA     15       8.022   0.570  25.363
ATOM    484 H2'1 DA     15       7.740   1.480  24.835
ATOM    485 H2'2 DA     15       8.001  -0.276  24.680
ATOM    486 O3'  DA     15      10.166  -0.413  26.102
ATOM    487 P    DC     16      10.783  -1.189  24.822
ATOM    488 O1P  DC     16      10.875  -0.248  23.679
ATOM    489 O2P  DC     16      12.011  -1.894  25.268
ATOM    490 O5'  DC     16       9.657  -2.294  24.483
ATOM    491 C5'  DC     16       9.382  -3.347  25.400
ATOM    492 H5'1 DC     16       9.314  -2.937  26.410
ATOM    493 H5'2 DC     16      10.201  -4.068  25.384
ATOM    494 C4'  DC     16       8.067  -4.083  25.110
ATOM    495 H4'  DC     16       7.919  -4.801  25.919
ATOM    496 O4'  DC     16       6.962  -3.188  25.127
ATOM    497 C1'  DC     16       5.985  -3.727  24.260
ATOM    498 H1'  DC     16       5.482  -4.566  24.755
ATOM    499 N1   DC     16       4.995  -2.684  23.871
ATOM    500 C6   DC     16       5.401  -1.457  23.403
ATOM    501 H6   DC     16       6.460  -1.269  23.265
ATOM    502 C5   DC     16       4.481  -0.492  23.143
ATOM    503 H5   DC     16       4.798   0.478  22.793
ATOM    504 C4   DC     16       3.114  -0.818  23.356
ATOM    505 N4   DC     16       2.178   0.069  23.191
ATOM    506 H41  DC     16       2.418   1.001  22.906
```

```
ATOM    507 H42  DC     16       1.229  -0.204  23.420
ATOM    508 N3   DC     16       2.704  -1.997  23.770
ATOM    509 C2   DC     16       3.630  -2.947  24.031
ATOM    510 O2   DC     16       3.213  -4.041  24.411
ATOM    511 C3'  DC     16       8.027  -4.867  23.784
ATOM    512 H3'  DC     16       8.925  -4.681  23.190
ATOM    513 C2'  DC     16       6.794  -4.273  23.087
ATOM    514 H2'1 DC     16       7.113  -3.461  22.433
ATOM    515 H2'2 DC     16       6.226  -5.006  22.517
ATOM    516 O3'  DC     16       7.907  -6.254  24.104
ATOM    517 P    DT     17       7.787  -7.422  22.998
ATOM    518 O1P  DT     17       8.355  -8.664  23.578
ATOM    519 O2P  DT     17       8.315  -6.922  21.703
ATOM    520 O5'  DT     17       6.190  -7.607  22.894
ATOM    521 C5'  DT     17       5.571  -8.196  21.759
ATOM    522 H5'1 DT     17       5.848  -9.250  21.700
ATOM    523 H5'2 DT     17       5.908  -7.694  20.851
ATOM    524 C4'  DT     17       4.041  -8.089  21.848
ATOM    525 H4'  DT     17       3.688  -8.675  22.698
ATOM    526 O4'  DT     17       3.640  -6.732  22.008
ATOM    527 C1'  DT     17       2.427  -6.544  21.307
ATOM    528 H1'  DT     17       1.596  -6.946  21.897
ATOM    529 N1   DT     17       2.206  -5.103  21.005
ATOM    530 C6   DT     17       3.264  -4.281  20.667
ATOM    531 H6   DT     17       4.262  -4.700  20.626
ATOM    532 C5   DT     17       3.067  -2.965  20.386
ATOM    533 C7   DT     17       4.264  -2.102  20.020
ATOM    534 H71  DT     17       4.271  -1.928  18.944
ATOM    535 H72  DT     17       4.184  -1.135  20.517
ATOM    536 H73  DT     17       5.198  -2.578  20.323
ATOM    537 C4   DT     17       1.726  -2.383  20.457
ATOM    538 O4   DT     17       1.419  -1.212  20.243
ATOM    539 N3   DT     17       0.730  -3.270  20.794
ATOM    540 H3   DT     17      -0.215  -2.916  20.819
ATOM    541 C2   DT     17       0.894  -4.611  21.041
ATOM    542 O2   DT     17      -0.096  -5.305  21.266
ATOM    543 C3'  DT     17       3.372  -8.608  20.561
ATOM    544 H3'  DT     17       4.135  -8.897  19.835
ATOM    545 C2'  DT     17       2.601  -7.388  20.049
ATOM    546 H2'1 DT     17       3.212  -6.855  19.319
ATOM    547 H2'2 DT     17       1.637  -7.654  19.618
ATOM    548 O3'  DT     17       2.518  -9.709  20.854
ATOM    549 P    DC     18       1.990 -10.719  19.706
ATOM    550 O1P  DC     18       1.631 -11.999  20.363
ATOM    551 O2P  DC     18       2.980 -10.745  18.600
ATOM    552 O5'  DC     18       0.643 -10.032  19.146
ATOM    553 C5'  DC     18      -0.575 -10.086  19.882
ATOM    554 H5'1 DC     18      -0.430  -9.640  20.867
ATOM    555 H5'2 DC     18      -0.864 -11.130  20.018
ATOM    556 C4'  DC     18      -1.730  -9.362  19.176
ATOM    557 H4'  DC     18      -2.652  -9.603  19.710
ATOM    558 O4'  DC     18      -1.543  -7.955  19.238
ATOM    559 C1'  DC     18      -2.038  -7.388  18.042
ATOM    560 H1'  DC     18      -3.126  -7.278  18.108
ATOM    561 N1   DC     18      -1.386  -6.062  17.835
ATOM    562 C6   DC     18      -0.023  -5.962  17.686
ATOM    563 H6   DC     18       0.579  -6.863  17.688
ATOM    564 C5   DC     18       0.561  -4.744  17.561
ATOM    565 H5   DC     18       1.631  -4.667  17.448
ATOM    566 C4   DC     18      -0.292  -3.609  17.585
ATOM    567 N4   DC     18       0.209  -2.415  17.488
ATOM    568 H41  DC     18       1.193  -2.289  17.350
ATOM    569 H42  DC     18      -0.434  -1.632  17.526
ATOM    570 N3   DC     18      -1.598  -3.673  17.742
ATOM    571 C2   DC     18      -2.166  -4.896  17.870
```

```
ATOM    572 O2   DC     18      -3.388  -4.925  18.015
ATOM    573 C3'  DC     18      -1.914  -9.762  17.699
ATOM    574 H3'  DC     18      -1.143 -10.473  17.396
ATOM    575 C2'  DC     18      -1.723  -8.430  16.965
ATOM    576 H2'1 DC     18      -0.685  -8.363  16.643
ATOM    577 H2'2 DC     18      -2.378  -8.320  16.103
ATOM    578 O3'  DC     18      -3.206 -10.338  17.526
ATOM    579 P    DG     19      -3.674 -11.038  16.147
ATOM    580 O1P  DG     19      -4.772 -11.985  16.465
ATOM    581 O2P  DG     19      -2.479 -11.543  15.425
ATOM    582 O5'  DG     19      -4.288  -9.808  15.313
ATOM    583 C5'  DG     19      -5.464  -9.146  15.759
ATOM    584 H5'1 DG     19      -5.383  -8.927  16.825
ATOM    585 H5'2 DG     19      -6.324  -9.801  15.610
ATOM    586 C4'  DG     19      -5.715  -7.827  15.021
ATOM    587 H4'  DG     19      -6.699  -7.463  15.324
ATOM    588 O4'  DG     19      -4.750  -6.846  15.392
ATOM    589 C1'  DG     19      -4.535  -6.058  14.240
ATOM    590 H1'  DG     19      -5.405  -5.413  14.078
ATOM    591 N9   DG     19      -3.333  -5.201  14.357
ATOM    592 C8   DG     19      -1.998  -5.526  14.306
ATOM    593 H8   DG     19      -1.651  -6.548  14.208
ATOM    594 N7   DG     19      -1.192  -4.496  14.395
ATOM    595 C5   DG     19      -2.063  -3.398  14.501
ATOM    596 C6   DG     19      -1.834  -1.975  14.608
ATOM    597 O6   DG     19      -0.773  -1.348  14.653
ATOM    598 N1   DG     19      -2.998  -1.232  14.650
ATOM    599 H1   DG     19      -2.902  -0.230  14.719
ATOM    600 C2   DG     19      -4.238  -1.773  14.596
ATOM    601 N2   DG     19      -5.262  -0.971  14.618
ATOM    602 H21  DG     19      -6.177  -1.377  14.549
ATOM    603 H22  DG     19      -5.124   0.035  14.653
ATOM    604 N3   DG     19      -4.499  -3.067  14.504
ATOM    605 C4   DG     19      -3.371  -3.833  14.467
ATOM    606 C3'  DG     19      -5.699  -7.948  13.483
ATOM    607 H3'  DG     19      -5.556  -8.982  13.164
ATOM    608 C2'  DG     19      -4.490  -7.083  13.115
ATOM    609 H2'1 DG     19      -3.579  -7.680  13.179
ATOM    610 H2'2 DG     19      -4.581  -6.622  12.134
ATOM    611 O3'  DG     19      -6.931  -7.426  12.991
ATOM    612 P    DC     20      -7.385  -7.507  11.444
ATOM    613 O1P  DC     20      -8.729  -8.136  11.391
ATOM    614 O2P  DC     20      -6.289  -8.088  10.629
ATOM    615 O5'  DC     20      -7.526  -5.951  11.052
ATOM    616 C5'  DC     20      -8.550  -5.130  11.614
ATOM    617 H5'1 DC     20      -8.546  -5.241  12.699
ATOM    618 H5'2 DC     20      -9.521  -5.464  11.245
ATOM    619 C4'  DC     20      -8.388  -3.632  11.285
ATOM    620 H4'  DC     20      -9.220  -3.092  11.740
ATOM    621 O4'  DC     20      -7.157  -3.164  11.842
ATOM    622 C1'  DC     20      -6.423  -2.547  10.797
ATOM    623 H1'  DC     20      -6.760  -1.508  10.703
ATOM    624 N1   DC     20      -4.956  -2.573  11.037
ATOM    625 C6   DC     20      -4.248  -3.749  11.002
ATOM    626 H6   DC     20      -4.785  -4.686  10.901
ATOM    627 C5   DC     20      -2.893  -3.728  11.095
ATOM    628 H5   DC     20      -2.335  -4.651  11.067
ATOM    629 C4   DC     20      -2.269  -2.458  11.235
ATOM    630 N4   DC     20      -0.980  -2.354  11.366
ATOM    631 H41  DC     20      -0.408  -3.178  11.380
ATOM    632 H42  DC     20      -0.606  -1.425  11.527
ATOM    633 N3   DC     20      -2.930  -1.325  11.306
ATOM    634 C2   DC     20      -4.278  -1.359  11.210
ATOM    635 O2   DC     20      -4.859  -0.276  11.271
ATOM    636 C3'  DC     20      -8.353  -3.335   9.770
```

```
ATOM    637 H3'  DC     20      -8.836  -4.115   9.176
ATOM    638 C2'  DC     20      -6.855  -3.286   9.527
ATOM    639 H2'1 DC     20      -6.444  -4.292   9.470
ATOM    640 H2'2 DC     20      -6.618  -2.731   8.627
ATOM    641 O3'  DC     20      -8.808  -2.035   9.417
ATOM    642 P    DT     21     -10.348  -1.632   9.257
ATOM    643 O1P  DT     21     -10.903  -2.337   8.075
ATOM    644 O2P  DT     21     -11.035  -1.749  10.567
ATOM    645 O5'  DT     21     -10.164  -0.070   8.885
ATOM    646 C5'  DT     21      -9.712   0.881   9.849
ATOM    647 H5'1 DT     21      -9.389   0.373  10.760
ATOM    648 H5'2 DT     21     -10.552   1.525  10.114
ATOM    649 C4'  DT     21      -8.548   1.771   9.369
ATOM    650 H4'  DT     21      -8.499   2.619  10.054
ATOM    651 O4'  DT     21      -7.290   1.104   9.434
ATOM    652 C1'  DT     21      -6.470   1.706   8.447
ATOM    653 H1'  DT     21      -6.214   2.722   8.764
ATOM    654 N1   DT     21      -5.222   0.927   8.200
ATOM    655 C6   DT     21      -5.269  -0.387   7.781
ATOM    656 H6   DT     21      -6.231  -0.829   7.556
ATOM    657 C5   DT     21      -4.131  -1.126   7.666
ATOM    658 C7   DT     21      -4.207  -2.563   7.178
ATOM    659 H71  DT     21      -3.511  -2.697   6.350
ATOM    660 H72  DT     21      -3.913  -3.236   7.984
ATOM    661 H73  DT     21      -5.209  -2.814   6.831
ATOM    662 C4   DT     21      -2.830  -0.544   7.992
ATOM    663 O4   DT     21      -1.744  -1.119   7.957
ATOM    664 N3   DT     21      -2.862   0.782   8.355
ATOM    665 H3   DT     21      -1.975   1.234   8.524
ATOM    666 C2   DT     21      -3.990   1.567   8.409
ATOM    667 O2   DT     21      -3.864   2.775   8.605
ATOM    668 C3'  DT     21      -8.684   2.335   7.940
ATOM    669 H3'  DT     21      -9.581   1.948   7.450
ATOM    670 C2'  DT     21      -7.418   1.806   7.256
ATOM    671 H2'1 DT     21      -7.622   0.820   6.838
ATOM    672 H2'2 DT     21      -7.034   2.473   6.486
ATOM    673 O3'  DT     21      -8.707   3.760   8.000
ATOM    674 P    DA     22      -9.041   4.679   6.716
ATOM    675 O1P  DA     22      -9.571   5.974   7.212
ATOM    676 O2P  DA     22      -9.870   3.891   5.769
ATOM    677 O5'  DA     22      -7.609   4.937   6.016
ATOM    678 C5'  DA     22      -6.714   5.962   6.448
ATOM    679 H5'1 DA     22      -6.400   5.771   7.476
ATOM    680 H5'2 DA     22      -7.235   6.921   6.425
ATOM    681 C4'  DA     22      -5.465   6.083   5.549
ATOM    682 H4'  DA     22      -5.003   7.047   5.741
ATOM    683 O4'  DA     22      -4.526   5.077   5.915
ATOM    684 C1'  DA     22      -3.992   4.557   4.719
ATOM    685 H1'  DA     22      -3.249   5.257   4.321
ATOM    686 N9   DA     22      -3.352   3.239   4.952
ATOM    687 C8   DA     22      -3.915   1.984   4.904
ATOM    688 H8   DA     22      -4.977   1.826   4.755
ATOM    689 N7   DA     22      -3.065   1.001   5.055
ATOM    690 C5   DA     22      -1.839   1.669   5.205
ATOM    691 C6   DA     22      -0.493   1.259   5.376
ATOM    692 N6   DA     22      -0.100   0.002   5.464
ATOM    693 H61  DA     22       0.871  -0.213   5.651
ATOM    694 H62  DA     22      -0.800  -0.723   5.470
ATOM    695 N1   DA     22       0.499   2.148   5.466
ATOM    696 C2   DA     22       0.182   3.437   5.423
ATOM    697 H2   DA     22       1.007   4.134   5.508
ATOM    698 N3   DA     22      -1.026   3.976   5.285
ATOM    699 C4   DA     22      -2.005   3.029   5.169
ATOM    700 C3'  DA     22      -5.805   5.909   4.039
ATOM    701 H3'  DA     22      -6.887   5.881   3.894
```

```
ATOM    702 C2'  DA     22      -5.206   4.525   3.787
ATOM    703 H2'1 DA     22      -5.919   3.763   4.102
ATOM    704 H2'2 DA     22      -4.919   4.376   2.745
ATOM    705 O3'  DA     22      -5.245   6.759   3.030
ATOM    706 P    DG     23      -4.643   8.239   3.241
ATOM    707 O1P  DG     23      -4.613   8.904   1.916
ATOM    708 O2P  DG     23      -5.311   8.922   4.376
ATOM    709 O5'  DG     23      -3.140   7.833   3.643
ATOM    710 C5'  DG     23      -2.097   8.788   3.792
ATOM    711 H5'1 DG     23      -1.830   8.855   4.848
ATOM    712 H5'2 DG     23      -2.433   9.776   3.469
ATOM    713 C4'  DG     23      -0.838   8.413   2.986
ATOM    714 H4'  DG     23      -0.035   9.078   3.309
ATOM    715 O4'  DG     23      -0.439   7.064   3.243
ATOM    716 C1'  DG     23      -0.090   6.461   2.006
ATOM    717 H1'  DG     23       0.948   6.704   1.763
ATOM    718 N9   DG     23      -0.251   4.984   2.047
ATOM    719 C8   DG     23      -1.401   4.234   1.958
ATOM    720 H8   DG     23      -2.384   4.686   1.883
ATOM    721 N7   DG     23      -1.208   2.941   1.989
ATOM    722 C5   DG     23       0.185   2.820   2.099
ATOM    723 C6   DG     23       1.045   1.664   2.183
ATOM    724 O6   DG     23       0.750   0.469   2.213
ATOM    725 N1   DG     23       2.387   1.977   2.239
ATOM    726 H1   DG     23       3.040   1.210   2.285
ATOM    727 C2   DG     23       2.866   3.243   2.232
ATOM    728 N2   DG     23       4.163   3.388   2.211
ATOM    729 H21  DG     23       4.530   4.323   2.209
ATOM    730 H22  DG     23       4.775   2.575   2.207
ATOM    731 N3   DG     23       2.117   4.341   2.174
ATOM    732 C4   DG     23       0.777   4.067   2.115
ATOM    733 C3'  DG     23      -1.001   8.580   1.461
ATOM    734 H3'  DG     23      -1.947   9.066   1.214
ATOM    735 C2'  DG     23      -1.001   7.130   0.981
ATOM    736 H2'1 DG     23      -2.017   6.742   1.050
ATOM    737 H2'2 DG     23      -0.621   7.012  -0.033
ATOM    738 O3'  DG     23       0.097   9.343   0.965
ATOM    739 P    DC3    24       0.283   9.738  -0.591
ATOM    740 O1P  DC3    24      -0.926   9.344  -1.356
ATOM    741 O2P  DC3    24       0.740  11.149  -0.654
ATOM    742 O5'  DC3    24       1.500   8.776  -1.038
ATOM    743 C5'  DC3    24       2.840   9.062  -0.643
ATOM    744 H5'1 DC3    24       2.889   9.147   0.444
ATOM    745 H5'2 DC3    24       3.139  10.020  -1.071
ATOM    746 C4'  DC3    24       3.858   8.002  -1.094
ATOM    747 H4'  DC3    24       4.859   8.391  -0.893
ATOM    748 O4'  DC3    24       3.710   6.796  -0.356
ATOM    749 C1'  DC3    24       4.057   5.689  -1.178
ATOM    750 H1'  DC3    24       4.947   5.197  -0.770
ATOM    751 N1   DC3    24       2.930   4.712  -1.216
ATOM    752 C6   DC3    24       1.620   5.126  -1.286
ATOM    753 H6   DC3    24       1.401   6.188  -1.318
ATOM    754 C5   DC3    24       0.618   4.209  -1.295
ATOM    755 H5   DC3    24      -0.410   4.532  -1.337
ATOM    756 C4   DC3    24       0.987   2.838  -1.232
ATOM    757 N4   DC3    24       0.084   1.903  -1.182
ATOM    758 H41  DC3    24      -0.890   2.149  -1.159
ATOM    759 H42  DC3    24       0.403   0.945  -1.082
ATOM    760 N3   DC3    24       2.233   2.418  -1.187
ATOM    761 C2   DC3    24       3.223   3.342  -1.195
ATOM    762 O2   DC3    24       4.380   2.918  -1.191
ATOM    763 C3'  DC3    24       3.778   7.632  -2.582
ATOM    764 H3'  DC3    24       2.732   7.572  -2.892
ATOM    765 C2'  DC3    24       4.387   6.234  -2.574
ATOM    766 H2'1 DC3    24       3.968   5.614  -3.368
```

```
ATOM    767 H2'2 DC3    24       5.472   6.289  -2.685
ATOM    768 O3'  DC3    24       4.513   8.506  -3.437
ATOM    769 H3T  DC3    24       5.461   8.494  -3.194
TER
END
```

C2. PDB File of the fully reduced *R*-crotonaldehyde-derived cross-link in d(GCTAGCXAGTCC)•d(GGACTCYCTAGC)

```
REMARK
ATOM      1 H5T  DG5     1       8.496  -3.959  -2.697
ATOM      2 O5'  DG5     1       9.141  -4.676  -2.770
ATOM      3 C5'  DG5     1       9.341  -5.123  -1.441
ATOM      4 H5'1 DG5     1      10.389  -5.392  -1.288
ATOM      5 H5'2 DG5     1       8.718  -5.999  -1.255
ATOM      6 C4'  DG5     1       8.961  -4.008  -0.455
ATOM      7 H4'  DG5     1       9.787  -3.297  -0.367
ATOM      8 O4'  DG5     1       7.788  -3.340  -0.923
ATOM      9 C1'  DG5     1       7.025  -3.016   0.222
ATOM     10 H1'  DG5     1       7.503  -2.184   0.759
ATOM     11 N9   DG5     1       5.638  -2.634  -0.136
ATOM     12 C8   DG5     1       4.517  -3.426  -0.223
ATOM     13 H8   DG5     1       4.541  -4.494  -0.077
ATOM     14 N7   DG5     1       3.418  -2.785  -0.508
ATOM     15 C5   DG5     1       3.840  -1.451  -0.617
ATOM     16 C6   DG5     1       3.120  -0.243  -0.921
ATOM     17 O6   DG5     1       1.929  -0.089  -1.186
ATOM     18 N1   DG5     1       3.917   0.880  -0.940
ATOM     19 H1   DG5     1       3.449   1.761  -1.092
ATOM     20 C2   DG5     1       5.245   0.867  -0.685
ATOM     21 N2   DG5     1       5.861   2.015  -0.693
ATOM     22 H21  DG5     1       6.805   2.013  -0.356
ATOM     23 H22  DG5     1       5.327   2.871  -0.825
ATOM     24 N3   DG5     1       5.959  -0.220  -0.408
ATOM     25 C4   DG5     1       5.198  -1.355  -0.390
ATOM     26 C3'  DG5     1       8.613  -4.577   0.935
ATOM     27 H3'  DG5     1       8.833  -5.643   1.013
ATOM     28 C2'  DG5     1       7.126  -4.291   1.059
ATOM     29 H2'1 DG5     1       6.564  -5.109   0.611
ATOM     30 H2'2 DG5     1       6.826  -4.119   2.093
ATOM     31 O3'  DG5     1       9.204  -3.889   2.010
ATOM     32 P    DC      2      10.779  -3.922   2.292
ATOM     33 O1P  DC      2      10.980  -4.592   3.592
ATOM     34 O2P  DC      2      11.462  -4.409   1.075
ATOM     35 O5'  DC      2      10.989  -2.339   2.442
ATOM     36 C5'  DC      2      10.552  -1.667   3.617
ATOM     37 H5'1 DC      2      11.423  -1.463   4.241
ATOM     38 H5'2 DC      2       9.873  -2.303   4.187
ATOM     39 C4'  DC      2       9.830  -0.348   3.306
ATOM     40 H4'  DC      2      10.453   0.245   2.635
ATOM     41 O4'  DC      2       8.540  -0.556   2.723
ATOM     42 C1'  DC      2       7.660   0.441   3.220
ATOM     43 H1'  DC      2       7.850   1.394   2.714
ATOM     44 N1   DC      2       6.236   0.034   3.066
ATOM     45 C6   DC      2       5.859  -1.268   3.283
ATOM     46 H6   DC      2       6.622  -1.986   3.567
ATOM     47 C5   DC      2       4.561  -1.642   3.130
ATOM     48 H5   DC      2       4.265  -2.665   3.293
ATOM     49 C4   DC      2       3.635  -0.629   2.745
ATOM     50 N4   DC      2       2.395  -0.932   2.515
ATOM     51 H41  DC      2       2.054  -1.851   2.681
ATOM     52 H42  DC      2       1.790  -0.172   2.211
ATOM     53 N3   DC      2       3.975   0.622   2.538
ATOM     54 C2   DC      2       5.271   0.987   2.705
ATOM     55 O2   DC      2       5.544   2.171   2.533
```

```
ATOM     56 C3'  DC      2       9.589   0.452   4.598
ATOM     57 H3'  DC      2       9.981  -0.089   5.464
ATOM     58 C2'  DC      2       8.069   0.576   4.681
ATOM     59 H2'1 DC      2       7.673  -0.249   5.272
ATOM     60 H2'2 DC      2       7.756   1.536   5.093
ATOM     61 O3'  DC      2      10.194   1.729   4.489
ATOM     62 P    DT      3      10.649   2.552   5.793
ATOM     63 O1P  DT      3      11.037   1.575   6.831
ATOM     64 O2P  DT      3      11.612   3.585   5.360
ATOM     65 O5'  DT      3       9.293   3.264   6.266
ATOM     66 C5'  DT      3       8.884   4.526   5.747
ATOM     67 H5'1 DT      3       8.832   4.468   4.656
ATOM     68 H5'2 DT      3       9.632   5.277   6.018
ATOM     69 C4'  DT      3       7.517   4.984   6.293
ATOM     70 H4'  DT      3       7.358   6.018   5.998
ATOM     71 O4'  DT      3       6.497   4.166   5.721
ATOM     72 C1'  DT      3       5.654   3.776   6.786
ATOM     73 H1'  DT      3       5.014   4.630   7.048
ATOM     74 N1   DT      3       4.781   2.618   6.426
ATOM     75 C6   DT      3       5.160   1.313   6.679
ATOM     76 H6   DT      3       6.152   1.118   7.060
ATOM     77 C5   DT      3       4.304   0.281   6.467
ATOM     78 C7   DT      3       4.755  -1.131   6.811
ATOM     79 H71  DT      3       4.119  -1.521   7.607
ATOM     80 H72  DT      3       4.637  -1.772   5.939
ATOM     81 H73  DT      3       5.796  -1.144   7.135
ATOM     82 C4   DT      3       2.964   0.519   5.933
ATOM     83 O4   DT      3       2.130  -0.346   5.671
ATOM     84 N3   DT      3       2.660   1.840   5.710
ATOM     85 H3   DT      3       1.714   2.079   5.440
ATOM     86 C2   DT      3       3.496   2.906   5.941
ATOM     87 O2   DT      3       3.074   4.033   5.728
ATOM     88 C3'  DT      3       7.422   4.857   7.832
ATOM     89 H3'  DT      3       8.413   4.780   8.283
ATOM     90 C2'  DT      3       6.642   3.561   7.944
ATOM     91 H2'1 DT      3       7.310   2.723   7.754
ATOM     92 H2'2 DT      3       6.151   3.447   8.908
ATOM     93 O3'  DT      3       6.640   5.849   8.493
ATOM     94 P    DA      4       6.982   7.421   8.410
ATOM     95 O1P  DA      4       8.366   7.569   7.915
ATOM     96 O2P  DA      4       6.596   8.073   9.676
ATOM     97 O5'  DA      4       5.976   7.872   7.231
ATOM     98 C5'  DA      4       4.920   8.816   7.405
ATOM     99 H5'1 DA      4       4.629   9.142   6.410
ATOM    100 H5'2 DA      4       5.308   9.695   7.917
ATOM    101 C4'  DA      4       3.627   8.354   8.111
ATOM    102 H4'  DA      4       2.809   8.835   7.572
ATOM    103 O4'  DA      4       3.380   6.958   8.038
ATOM    104 C1'  DA      4       2.526   6.634   9.118
ATOM    105 H1'  DA      4       1.495   6.932   8.898
ATOM    106 N9   DA      4       2.598   5.171   9.343
ATOM    107 C8   DA      4       3.703   4.416   9.650
ATOM    108 H8   DA      4       4.661   4.878   9.860
ATOM    109 N7   DA      4       3.511   3.119   9.604
ATOM    110 C5   DA      4       2.148   3.027   9.280
ATOM    111 C6   DA      4       1.248   1.964   9.041
ATOM    112 N6   DA      4       1.550   0.681   9.083
ATOM    113 H61  DA      4       0.834   0.006   8.830
ATOM    114 H62  DA      4       2.468   0.426   9.391
ATOM    115 N1   DA      4      -0.025   2.180   8.733
ATOM    116 C2   DA      4      -0.441   3.437   8.666
ATOM    117 H2   DA      4      -1.486   3.583   8.424
ATOM    118 N3   DA      4       0.278   4.537   8.854
ATOM    119 C4   DA      4       1.579   4.264   9.150
ATOM    120 C3'  DA      4       3.462   8.799   9.575
```

```
ATOM    121 H3'  DA      4       4.399   9.176   9.987
ATOM    122 C2'  DA      4       3.067   7.489  10.265
ATOM    123 H2'1 DA      4       3.968   7.034  10.679
ATOM    124 H2'2 DA      4       2.320   7.638  11.044
ATOM    125 O3'  DA      4       2.453   9.809   9.609
ATOM    126 P    DG      5       2.036  10.614  10.945
ATOM    127 O1P  DG      5       1.503  11.932  10.541
ATOM    128 O2P  DG      5       3.137  10.528  11.926
ATOM    129 O5'  DG      5       0.831   9.715  11.486
ATOM    130 C5'  DG      5      -0.409   9.641  10.801
ATOM    131 H5'1 DG      5      -0.241   9.382   9.756
ATOM    132 H5'2 DG      5      -0.902  10.613  10.846
ATOM    133 C4'  DG      5      -1.320   8.585  11.438
ATOM    134 H4'  DG      5      -2.330   8.702  11.043
ATOM    135 O4'  DG      5      -0.838   7.276  11.127
ATOM    136 C1'  DG      5      -0.927   6.517  12.318
ATOM    137 H1'  DG      5      -1.979   6.260  12.491
ATOM    138 N9   DG      5      -0.140   5.261  12.286
ATOM    139 C8   DG      5       1.194   5.059  12.534
ATOM    140 H8   DG      5       1.882   5.879  12.688
ATOM    141 N7   DG      5       1.555   3.801  12.572
ATOM    142 C5   DG      5       0.362   3.109  12.304
ATOM    143 C6   DG      5       0.059   1.702  12.174
ATOM    144 O6   DG      5       0.810   0.724  12.211
ATOM    145 N1   DG      5      -1.281   1.448  11.955
ATOM    146 H1   DG      5      -1.561   0.490  11.827
ATOM    147 C2   DG      5      -2.224   2.408  11.822
ATOM    148 N2   DG      5      -3.442   2.038  11.547
ATOM    149 H21  DG      5      -4.084   2.769  11.304
ATOM    150 H22  DG      5      -3.686   1.054  11.466
ATOM    151 N3   DG      5      -1.987   3.708  11.906
ATOM    152 C4   DG      5      -0.677   4.002  12.147
ATOM    153 C3'  DG      5      -1.354   8.694  12.975
ATOM    154 H3'  DG      5      -0.965   9.647  13.342
ATOM    155 C2'  DG      5      -0.482   7.515  13.385
ATOM    156 H2'1 DG      5       0.569   7.773  13.267
ATOM    157 H2'2 DG      5      -0.703   7.180  14.396
ATOM    158 O3'  DG      5      -2.631   8.417  13.510
ATOM    159 P    DC      6      -3.809   9.496  13.536
ATOM    160 O1P  DC      6      -3.470  10.544  14.522
ATOM    161 O2P  DC      6      -4.187   9.860  12.154
ATOM    162 O5'  DC      6      -4.930   8.525  14.141
ATOM    163 C5'  DC      6      -5.564   7.531  13.345
ATOM    164 H5'1 DC      6      -5.018   7.393  12.410
ATOM    165 H5'2 DC      6      -6.569   7.876  13.103
ATOM    166 C4'  DC      6      -5.667   6.166  14.044
ATOM    167 H4'  DC      6      -6.469   5.607  13.562
ATOM    168 O4'  DC      6      -4.485   5.394  13.913
ATOM    169 C1'  DC      6      -4.554   4.380  14.897
ATOM    170 H1'  DC      6      -5.226   3.583  14.559
ATOM    171 N1   DC      6      -3.196   3.840  15.150
ATOM    172 C6   DC      6      -2.139   4.692  15.331
ATOM    173 H6   DC      6      -2.329   5.762  15.323
ATOM    174 C5   DC      6      -0.885   4.195  15.471
ATOM    175 H5   DC      6      -0.047   4.858  15.591
ATOM    176 C4   DC      6      -0.743   2.780  15.418
ATOM    177 N4   DC      6       0.447   2.266  15.405
ATOM    178 H41  DC      6       1.246   2.860  15.350
ATOM    179 H42  DC      6       0.510   1.257  15.315
ATOM    180 N3   DC      6      -1.740   1.942  15.249
ATOM    181 C2   DC      6      -2.991   2.454  15.137
ATOM    182 O2   DC      6      -3.923   1.667  15.018
ATOM    183 C3'  DC      6      -5.980   6.218  15.541
ATOM    184 H3'  DC      6      -5.640   7.165  15.966
ATOM    185 C2'  DC      6      -5.164   5.062  16.124
```

```
ATOM    186 H2'1 DC      6      -4.394   5.471  16.776
ATOM    187 H2'2 DC      6      -5.787   4.360  16.675
ATOM    188 O3'  DC      6      -7.371   6.042  15.743
ATOM    189 O1P  X       7      -7.249   7.447  17.817
ATOM    190 P    X       7      -8.059   6.411  17.147
ATOM    191 O2P  X       7      -9.498   6.631  16.894
ATOM    192 O5'  X       7      -7.902   5.068  17.998
ATOM    193 C5'  X       7      -8.678   3.916  17.716
ATOM    194 H5'1 X       7      -8.631   3.703  16.648
ATOM    195 H5'2 X       7      -9.718   4.103  17.990
ATOM    196 C4'  X       7      -8.166   2.693  18.487
ATOM    197 O4'  X       7      -6.919   2.277  17.928
ATOM    198 H4'  X       7      -8.897   1.892  18.382
ATOM    199 C3'  X       7      -7.936   2.988  19.984
ATOM    200 O3'  X       7      -8.260   1.898  20.831
ATOM    201 H3'  X       7      -8.443   3.900  20.306
ATOM    202 C2'  X       7      -6.423   3.139  20.031
ATOM    203 H2'1 X       7      -6.139   4.134  19.690
ATOM    204 H2'2 X       7      -6.024   2.923  21.023
ATOM    205 C1'  X       7      -6.029   2.073  19.009
ATOM    206 H1'  X       7      -6.247   1.093  19.438
ATOM    207 N9   X       7      -4.591   2.085  18.640
ATOM    208 C4   X       7      -3.872   0.967  18.293
ATOM    209 N3   X       7      -4.389  -0.262  18.016
ATOM    210 C8   X       7      -3.650   3.075  18.799
ATOM    211 H8   X       7      -3.916   4.090  19.055
ATOM    212 N7   X       7      -2.414   2.682  18.636
ATOM    213 C5   X       7      -2.539   1.320  18.320
ATOM    214 C6   X       7      -1.558   0.302  18.035
ATOM    215 O6   X       7      -0.329   0.390  17.973
ATOM    216 N1   X       7      -2.116  -0.946  17.814
ATOM    217 H1   X       7      -1.459  -1.704  17.681
ATOM    218 C2   X       7      -3.466  -1.204  17.772
ATOM    219 N2   X       7      -3.816  -2.446  17.427
ATOM    220 H2   X       7      -3.085  -3.145  17.339
ATOM    221 C1x  X       7      -5.169  -2.871  17.065
ATOM    222 H1x  X       7      -5.898  -2.127  17.385
ATOM    223 Cmx  X       7      -5.506  -4.184  17.775
ATOM    224 H1m1 X       7      -5.326  -4.079  18.844
ATOM    225 H1m2 X       7      -4.882  -4.993  17.391
ATOM    226 H1m3 X       7      -6.558  -4.423  17.623
ATOM    227 C2x  X       7      -5.315  -3.078  15.542
ATOM    228 H2x1 X       7      -4.626  -3.861  15.228
ATOM    229 H2x2 X       7      -6.319  -3.461  15.361
ATOM    230 P    DA      8      -9.770   1.512  21.205
ATOM    231 O1P  DA      8     -10.067   2.018  22.560
ATOM    232 O2P  DA      8     -10.656   1.841  20.069
ATOM    233 O5'  DA      8      -9.598  -0.081  21.265
ATOM    234 C5'  DA      8      -9.618  -0.868  20.084
ATOM    235 H5'1 DA      8      -9.102  -0.331  19.287
ATOM    236 H5'2 DA      8     -10.655  -1.008  19.780
ATOM    237 C4'  DA      8      -8.943  -2.242  20.246
ATOM    238 H4'  DA      8      -9.351  -2.914  19.494
ATOM    239 O4'  DA      8      -7.551  -2.108  20.000
ATOM    240 C1'  DA      8      -6.834  -2.478  21.165
ATOM    241 H1'  DA      8      -6.439  -3.493  21.049
ATOM    242 N9   DA      8      -5.726  -1.519  21.335
ATOM    243 C8   DA      8      -5.785  -0.186  21.672
ATOM    244 H8   DA      8      -6.724   0.317  21.871
ATOM    245 N7   DA      8      -4.624   0.420  21.686
ATOM    246 C5   DA      8      -3.737  -0.619  21.360
ATOM    247 C6   DA      8      -2.340  -0.721  21.191
ATOM    248 N6   DA      8      -1.497   0.286  21.293
ATOM    249 H61  DA      8      -0.519   0.141  21.068
ATOM    250 H62  DA      8      -1.871   1.187  21.531
```

```
ATOM    251 N1   DA      8      -1.755  -1.874  20.883
ATOM    252 C2   DA      8      -2.525  -2.943  20.719
ATOM    253 H2   DA      8      -2.022  -3.869  20.475
ATOM    254 N3   DA      8      -3.846  -3.001  20.817
ATOM    255 C4   DA      8      -4.396  -1.797  21.143
ATOM    256 C3'  DA      8      -9.114  -2.891  21.625
ATOM    257 H3'  DA      8      -9.993  -2.504  22.145
ATOM    258 C2'  DA      8      -7.831  -2.460  22.324
ATOM    259 H2'1 DA      8      -7.959  -1.453  22.721
ATOM    260 H2'2 DA      8      -7.549  -3.143  23.122
ATOM    261 O3'  DA      8      -9.205  -4.300  21.454
ATOM    262 P    DG      9      -9.439  -5.306  22.685
ATOM    263 O1P  DG      9      -9.927  -4.531  23.844
ATOM    264 O2P  DG      9     -10.222  -6.456  22.187
ATOM    265 O5'  DG      9      -7.944  -5.791  23.017
ATOM    266 C5'  DG      9      -7.214  -6.604  22.110
ATOM    267 H5'1 DG      9      -7.169  -6.109  21.139
ATOM    268 H5'2 DG      9      -7.731  -7.556  21.992
ATOM    269 C4'  DG      9      -5.779  -6.876  22.588
ATOM    270 H4'  DG      9      -5.332  -7.637  21.945
ATOM    271 O4'  DG      9      -4.998  -5.689  22.480
ATOM    272 C1'  DG      9      -4.170  -5.614  23.623
ATOM    273 H1'  DG      9      -3.288  -6.249  23.497
ATOM    274 N9   DG      9      -3.756  -4.222  23.901
ATOM    275 C8   DG      9      -4.561  -3.143  24.157
ATOM    276 H8   DG      9      -5.639  -3.219  24.156
ATOM    277 N7   DG      9      -3.914  -2.031  24.381
ATOM    278 C5   DG      9      -2.568  -2.407  24.272
ATOM    279 C6   DG      9      -1.347  -1.652  24.391
ATOM    280 O6   DG      9      -1.188  -0.446  24.577
ATOM    281 N1   DG      9      -0.207  -2.417  24.268
ATOM    282 H1   DG      9       0.679  -1.940  24.345
ATOM    283 C2   DG      9      -0.212  -3.743  24.002
ATOM    284 N2   DG      9       0.946  -4.348  23.983
ATOM    285 H21  DG      9       0.925  -5.338  23.807
ATOM    286 H22  DG      9       1.807  -3.839  24.166
ATOM    287 N3   DG      9      -1.311  -4.478  23.874
ATOM    288 C4   DG      9      -2.465  -3.755  24.005
ATOM    289 C3'  DG      9      -5.704  -7.369  24.046
ATOM    290 H3'  DG      9      -6.697  -7.561  24.457
ATOM    291 C2'  DG      9      -5.061  -6.167  24.725
ATOM    292 H2'1 DG      9      -5.844  -5.453  24.978
ATOM    293 H2'2 DG      9      -4.489  -6.440  25.605
ATOM    294 O3'  DG      9      -4.899  -8.539  24.126
ATOM    295 P    DT     10      -4.544  -9.278  25.512
ATOM    296 O1P  DT     10      -5.315  -8.657  26.612
ATOM    297 O2P  DT     10      -4.599 -10.743  25.304
ATOM    298 O5'  DT     10      -3.019  -8.821  25.717
ATOM    299 C5'  DT     10      -2.003  -9.147  24.776
ATOM    300 H5'1 DT     10      -2.169  -8.595  23.847
ATOM    301 H5'2 DT     10      -2.049 -10.216  24.558
ATOM    302 C4'  DT     10      -0.604  -8.820  25.325
ATOM    303 H4'  DT     10       0.144  -9.243  24.654
ATOM    304 O4'  DT     10      -0.428  -7.405  25.389
ATOM    305 C1'  DT     10      -0.069  -7.047  26.710
ATOM    306 H1'  DT     10       1.025  -7.038  26.790
ATOM    307 N1   DT     10      -0.634  -5.710  27.045
ATOM    308 C6   DT     10      -2.002  -5.513  27.120
ATOM    309 H6   DT     10      -2.656  -6.338  26.856
ATOM    310 C5   DT     10      -2.517  -4.310  27.495
ATOM    311 C7   DT     10      -4.020  -4.140  27.640
ATOM    312 H71  DT     10      -4.551  -5.056  27.385
ATOM    313 H72  DT     10      -4.252  -3.871  28.671
ATOM    314 H73  DT     10      -4.352  -3.327  26.995
ATOM    315 C4   DT     10      -1.634  -3.176  27.761
```

```
ATOM    316 O4   DT     10      -1.976  -2.036  28.067
ATOM    317 N3   DT     10      -0.295  -3.456  27.656
ATOM    318 H3   DT     10       0.360  -2.704  27.806
ATOM    319 C2   DT     10       0.255  -4.676  27.357
ATOM    320 O2   DT     10       1.470  -4.806  27.432
ATOM    321 C3'  DT     10      -0.398  -9.401  26.734
ATOM    322 H3'  DT     10      -1.147 -10.165  26.953
ATOM    323 C2'  DT     10      -0.611  -8.168  27.599
ATOM    324 H2'1 DT     10      -1.675  -8.056  27.791
ATOM    325 H2'2 DT     10      -0.077  -8.236  28.537
ATOM    326 O3'  DT     10       0.908  -9.938  26.886
ATOM    327 P    DC     11       1.390 -10.662  28.246
ATOM    328 O1P  DC     11       0.227 -10.869  29.135
ATOM    329 O2P  DC     11       2.265 -11.799  27.895
ATOM    330 O5'  DC     11       2.309  -9.515  28.909
ATOM    331 C5'  DC     11       3.563  -9.181  28.325
ATOM    332 H5'1 DC     11       3.397  -8.789  27.322
ATOM    333 H5'2 DC     11       4.162 -10.088  28.230
ATOM    334 C4'  DC     11       4.372  -8.157  29.134
ATOM    335 H4'  DC     11       5.332  -8.017  28.637
ATOM    336 O4'  DC     11       3.681  -6.914  29.141
ATOM    337 C1'  DC     11       3.526  -6.457  30.467
ATOM    338 H1'  DC     11       4.343  -5.770  30.700
ATOM    339 N1   DC     11       2.207  -5.771  30.582
ATOM    340 C6   DC     11       1.042  -6.481  30.393
ATOM    341 H6   DC     11       1.115  -7.533  30.123
ATOM    342 C5   DC     11      -0.161  -5.869  30.519
ATOM    343 H5   DC     11      -1.066  -6.427  30.346
ATOM    344 C4   DC     11      -0.153  -4.486  30.821
ATOM    345 N4   DC     11      -1.268  -3.829  30.937
ATOM    346 H41  DC     11      -2.140  -4.268  30.734
ATOM    347 H42  DC     11      -1.188  -2.823  31.092
ATOM    348 N3   DC     11       0.945  -3.787  31.016
ATOM    349 C2   DC     11       2.141  -4.407  30.891
ATOM    350 O2   DC     11       3.143  -3.726  31.121
ATOM    351 C3'  DC     11       4.634  -8.591  30.586
ATOM    352 H3'  DC     11       4.386  -9.647  30.723
ATOM    353 C2'  DC     11       3.642  -7.711  31.341
ATOM    354 H2'1 DC     11       2.699  -8.254  31.394
ATOM    355 H2'2 DC     11       3.976  -7.483  32.345
ATOM    356 O3'  DC     11       5.998  -8.364  30.943
ATOM    357 P    DC3    12       6.570  -8.695  32.417
ATOM    358 O1P  DC3    12       7.991  -9.102  32.355
ATOM    359 O2P  DC3    12       5.594  -9.519  33.154
ATOM    360 O5'  DC3    12       6.512  -7.228  33.063
ATOM    361 C5'  DC3    12       7.430  -6.223  32.671
ATOM    362 H5'1 DC3    12       7.276  -5.967  31.620
ATOM    363 H5'2 DC3    12       8.446  -6.604  32.786
ATOM    364 C4'  DC3    12       7.264  -4.970  33.534
ATOM    365 H4'  DC3    12       8.144  -4.340  33.404
ATOM    366 O4'  DC3    12       6.134  -4.223  33.130
ATOM    367 C1'  DC3    12       5.549  -3.590  34.252
ATOM    368 H1'  DC3    12       5.666  -2.507  34.142
ATOM    369 N1   DC3    12       4.098  -3.919  34.300
ATOM    370 C6   DC3    12       3.630  -5.185  34.045
ATOM    371 H6   DC3    12       4.345  -5.972  33.824
ATOM    372 C5   DC3    12       2.292  -5.420  34.027
ATOM    373 H5   DC3    12       1.920  -6.407  33.808
ATOM    374 C4   DC3    12       1.433  -4.315  34.296
ATOM    375 N4   DC3    12       0.143  -4.469  34.319
ATOM    376 H41  DC3    12      -0.261  -5.332  34.023
ATOM    377 H42  DC3    12      -0.411  -3.627  34.468
ATOM    378 N3   DC3    12       1.866  -3.118  34.614
ATOM    379 C2   DC3    12       3.197  -2.895  34.607
ATOM    380 O2   DC3    12       3.585  -1.776  34.928
```

```
ATOM    381 C3'  DC3    12       7.089  -5.270  35.029
ATOM    382 H3'  DC3    12       6.492  -6.173  35.173
ATOM    383 C2'  DC3    12       6.299  -4.061  35.505
ATOM    384 H2'1 DC3    12       5.615  -4.335  36.309
ATOM    385 H2'2 DC3    12       6.977  -3.276  35.842
ATOM    386 O3'  DC3    12       8.330  -5.369  35.704
ATOM    387 H3T  DC3    12       8.748  -6.183  35.399
TER
ATOM    388 H5T  DG5    13      -3.655   5.441  35.367
ATOM    389 O5'  DG5    13      -3.773   6.392  35.263
ATOM    390 C5'  DG5    13      -2.469   6.903  35.026
ATOM    391 H5'1 DG5    13      -1.924   6.955  35.968
ATOM    392 H5'2 DG5    13      -2.524   7.907  34.600
ATOM    393 C4'  DG5    13      -1.691   5.991  34.067
ATOM    394 H4'  DG5    13      -0.646   6.301  34.058
ATOM    395 O4'  DG5    13      -1.772   4.645  34.529
ATOM    396 C1'  DG5    13      -1.756   3.846  33.364
ATOM    397 H1'  DG5    13      -0.759   3.890  32.910
ATOM    398 N9   DG5    13      -2.069   2.427  33.666
ATOM    399 C8   DG5    13      -3.277   1.774  33.706
ATOM    400 H8   DG5    13      -4.212   2.277  33.520
ATOM    401 N7   DG5    13      -3.199   0.505  34.013
ATOM    402 C5   DG5    13      -1.819   0.281  34.145
ATOM    403 C6   DG5    13      -1.047  -0.898  34.466
ATOM    404 O6   DG5    13      -1.411  -2.046  34.739
ATOM    405 N1   DG5    13       0.314  -0.668  34.496
ATOM    406 H1   DG5    13       0.911  -1.468  34.617
ATOM    407 C2   DG5    13       0.884   0.533  34.248
ATOM    408 N2   DG5    13       2.185   0.599  34.237
ATOM    409 H21  DG5    13       2.578   1.454  33.886
ATOM    410 H22  DG5    13       2.750  -0.230  34.398
ATOM    411 N3   DG5    13       0.221   1.648  33.991
ATOM    412 C4   DG5    13      -1.131   1.460  33.940
ATOM    413 C3'  DG5    13      -2.247   6.015  32.623
ATOM    414 H3'  DG5    13      -3.061   6.735  32.528
ATOM    415 C2'  DG5    13      -2.746   4.578  32.460
ATOM    416 H2'1 DG5    13      -3.759   4.491  32.851
ATOM    417 H2'2 DG5    13      -2.696   4.235  31.427
ATOM    418 O3'  DG5    13      -1.274   6.265  31.615
ATOM    419 P    DG     14      -0.286   7.547  31.642
ATOM    420 O1P  DG     14      -0.093   8.023  30.259
ATOM    421 O2P  DG     14      -0.739   8.485  32.694
ATOM    422 O5'  DG     14       1.020   6.756  32.162
ATOM    423 C5'  DG     14       2.360   7.081  31.789
ATOM    424 H5'1 DG     14       2.930   7.186  32.710
ATOM    425 H5'2 DG     14       2.393   8.040  31.272
ATOM    426 C4'  DG     14       3.086   6.017  30.933
ATOM    427 H4'  DG     14       4.148   6.106  31.147
ATOM    428 O4'  DG     14       2.655   4.705  31.293
ATOM    429 C1'  DG     14       2.204   4.072  30.109
ATOM    430 H1'  DG     14       3.058   3.577  29.636
ATOM    431 N9   DG     14       1.157   3.064  30.383
ATOM    432 C8   DG     14      -0.206   3.215  30.358
ATOM    433 H8   DG     14      -0.676   4.178  30.202
ATOM    434 N7   DG     14      -0.877   2.110  30.560
ATOM    435 C5   DG     14       0.129   1.146  30.732
ATOM    436 C6   DG     14       0.073  -0.267  31.014
ATOM    437 O6   DG     14      -0.896  -0.996  31.218
ATOM    438 N1   DG     14       1.310  -0.869  31.094
ATOM    439 H1   DG     14       1.322  -1.873  31.174
ATOM    440 C2   DG     14       2.477  -0.203  30.943
ATOM    441 N2   DG     14       3.571  -0.910  30.958
ATOM    442 H21  DG     14       4.392  -0.433  30.633
ATOM    443 H22  DG     14       3.516  -1.926  30.999
ATOM    444 N3   DG     14       2.587   1.098  30.711
```

```
ATOM    445 C4   DG     14       1.375   1.727  30.618
ATOM    446 C3'  DG     14       2.850   6.197  29.415
ATOM    447 H3'  DG     14       2.539   7.217  29.186
ATOM    448 C2'  DG     14       1.724   5.209  29.202
ATOM    449 H2'1 DG     14       0.792   5.641  29.560
ATOM    450 H2'2 DG     14       1.636   4.906  28.160
ATOM    451 O3'  DG     14       3.899   5.782  28.535
ATOM    452 P    DA     15       5.439   6.182  28.754
ATOM    453 O1P  DA     15       6.150   6.098  27.461
ATOM    454 O2P  DA     15       5.495   7.425  29.550
ATOM    455 O5'  DA     15       5.885   4.965  29.701
ATOM    456 C5'  DA     15       7.158   4.343  29.624
ATOM    457 H5'1 DA     15       7.510   4.214  30.646
ATOM    458 H5'2 DA     15       7.864   4.998  29.114
ATOM    459 C4'  DA     15       7.145   2.951  28.956
ATOM    460 H4'  DA     15       7.823   2.317  29.525
ATOM    461 O4'  DA     15       5.854   2.345  28.976
ATOM    462 C1'  DA     15       5.597   1.845  27.674
ATOM    463 H1'  DA     15       6.031   0.843  27.584
ATOM    464 N9   DA     15       4.145   1.784  27.419
ATOM    465 C8   DA     15       3.265   2.805  27.144
ATOM    466 H8   DA     15       3.588   3.836  27.053
ATOM    467 N7   DA     15       2.013   2.427  27.049
ATOM    468 C5   DA     15       2.092   1.048  27.301
ATOM    469 C6   DA     15       1.148   0.010  27.463
ATOM    470 N6   DA     15      -0.158   0.186  27.482
ATOM    471 H61  DA     15      -0.769  -0.612  27.608
ATOM    472 H62  DA     15      -0.521   1.114  27.349
ATOM    473 N1   DA     15       1.533  -1.244  27.690
ATOM    474 C2   DA     15       2.835  -1.502  27.748
ATOM    475 H2   DA     15       3.114  -2.535  27.904
ATOM    476 N3   DA     15       3.835  -0.633  27.661
ATOM    477 C4   DA     15       3.388   0.641  27.463
ATOM    478 C3'  DA     15       7.638   2.938  27.501
ATOM    479 H3'  DA     15       8.174   3.848  27.229
ATOM    480 C2'  DA     15       6.341   2.783  26.729
ATOM    481 H2'1 DA     15       5.840   3.745  26.646
ATOM    482 H2'2 DA     15       6.512   2.337  25.752
ATOM    483 O3'  DA     15       8.428   1.771  27.328
ATOM    484 P    DC     16       9.517   1.621  26.164
ATOM    485 O1P  DC     16      10.814   2.070  26.708
ATOM    486 O2P  DC     16       8.991   2.238  24.924
ATOM    487 O5'  DC     16       9.560   0.017  25.996
ATOM    488 C5'  DC     16       9.308  -0.613  24.747
ATOM    489 H5'1 DC     16      10.103  -1.340  24.578
ATOM    490 H5'2 DC     16       9.366   0.112  23.936
ATOM    491 C4'  DC     16       7.973  -1.371  24.660
ATOM    492 H4'  DC     16       8.055  -2.304  25.217
ATOM    493 O4'  DC     16       6.805  -0.662  25.079
ATOM    494 C1'  DC     16       5.692  -1.404  24.582
ATOM    495 H1'  DC     16       5.487  -2.238  25.267
ATOM    496 N1   DC     16       4.445  -0.613  24.395
ATOM    497 C6   DC     16       4.482   0.743  24.187
ATOM    498 H6   DC     16       5.440   1.246  24.198
ATOM    499 C5   DC     16       3.325   1.430  23.986
ATOM    500 H5   DC     16       3.342   2.500  23.859
ATOM    501 C4   DC     16       2.112   0.684  23.998
ATOM    502 N4   DC     16       0.954   1.275  23.937
ATOM    503 H41  DC     16       0.907   2.264  24.024
ATOM    504 H42  DC     16       0.143   0.670  24.066
ATOM    505 N3   DC     16       2.071  -0.615  24.150
ATOM    506 C2   DC     16       3.224  -1.296  24.325
ATOM    507 O2   DC     16       3.140  -2.518  24.403
ATOM    508 C3'  DC     16       7.636  -1.623  23.186
ATOM    509 H3'  DC     16       7.698  -0.648  22.704
```

```
ATOM    510 C2'  DC     16       6.157  -1.982  23.244
ATOM    511 H2'1 DC     16       5.648  -1.520  22.406
ATOM    512 H2'2 DC     16       5.986  -3.053  23.261
ATOM    513 O3'  DC     16       8.456  -2.498  22.411
ATOM    514 P    DT     17       8.654  -4.076  22.690
ATOM    515 O1P  DT     17       8.634  -4.301  24.148
ATOM    516 O2P  DT     17       9.812  -4.534  21.895
ATOM    517 O5'  DT     17       7.325  -4.744  22.059
ATOM    518 C5'  DT     17       6.588  -5.720  22.792
ATOM    519 H5'1 DT     17       6.448  -5.377  23.817
ATOM    520 H5'2 DT     17       7.165  -6.643  22.830
ATOM    521 C4'  DT     17       5.200  -6.019  22.215
ATOM    522 H4'  DT     17       4.741  -6.774  22.855
ATOM    523 O4'  DT     17       4.367  -4.869  22.254
ATOM    524 C1'  DT     17       3.462  -4.962  21.173
ATOM    525 H1'  DT     17       2.651  -5.658  21.413
ATOM    526 N1   DT     17       2.930  -3.609  20.872
ATOM    527 C6   DT     17       3.785  -2.541  20.690
ATOM    528 H6   DT     17       4.849  -2.735  20.673
ATOM    529 C5   DT     17       3.308  -1.271  20.592
ATOM    530 C7   DT     17       4.273  -0.116  20.383
ATOM    531 H71  DT     17       4.218   0.562  21.236
ATOM    532 H72  DT     17       5.293  -0.475  20.258
ATOM    533 H73  DT     17       3.969   0.430  19.489
ATOM    534 C4   DT     17       1.872  -1.013  20.681
ATOM    535 O4   DT     17       1.333   0.091  20.664
ATOM    536 N3   DT     17       1.092  -2.142  20.778
ATOM    537 H3   DT     17       0.088  -2.027  20.748
ATOM    538 C2   DT     17       1.544  -3.436  20.819
ATOM    539 O2   DT     17       0.741  -4.358  20.773
ATOM    540 C3'  DT     17       5.188  -6.567  20.779
ATOM    541 H3'  DT     17       6.190  -6.589  20.349
ATOM    542 C2'  DT     17       4.298  -5.560  20.046
ATOM    543 H2'1 DT     17       4.928  -4.800  19.587
ATOM    544 H2'2 DT     17       3.666  -6.033  19.299
ATOM    545 O3'  DT     17       4.648  -7.879  20.856
ATOM    546 P    DC     18       4.289  -8.798  19.585
ATOM    547 O1P  DC     18       4.837  -8.201  18.346
ATOM    548 O2P  DC     18       4.600 -10.201  19.923
ATOM    549 O5'  DC     18       2.706  -8.599  19.577
ATOM    550 C5'  DC     18       1.826  -9.444  18.853
ATOM    551 H5'1 DC     18       1.536 -10.295  19.473
ATOM    552 H5'2 DC     18       2.351  -9.832  17.981
ATOM    553 C4'  DC     18       0.562  -8.671  18.413
ATOM    554 H4'  DC     18      -0.300  -9.031  18.973
ATOM    555 O4'  DC     18       0.701  -7.275  18.647
ATOM    556 C1'  DC     18      -0.104  -6.563  17.737
ATOM    557 H1'  DC     18      -1.139  -6.541  18.106
ATOM    558 N1   DC     18       0.465  -5.198  17.569
ATOM    559 C6   DC     18       1.821  -5.031  17.426
ATOM    560 H6   DC     18       2.451  -5.914  17.401
ATOM    561 C5   DC     18       2.358  -3.785  17.379
ATOM    562 H5   DC     18       3.425  -3.657  17.320
ATOM    563 C4   DC     18       1.452  -2.692  17.463
ATOM    564 N4   DC     18       1.883  -1.465  17.530
ATOM    565 H41  DC     18       2.826  -1.248  17.314
ATOM    566 H42  DC     18       1.153  -0.760  17.619
ATOM    567 N3   DC     18       0.152  -2.829  17.569
ATOM    568 C2   DC     18      -0.372  -4.079  17.614
ATOM    569 O2   DC     18      -1.594  -4.177  17.656
ATOM    570 C3'  DC     18       0.313  -8.799  16.899
ATOM    571 H3'  DC     18       1.268  -9.037  16.433
ATOM    572 C2'  DC     18      -0.027  -7.376  16.449
ATOM    573 H2'1 DC     18       0.768  -7.009  15.804
ATOM    574 H2'2 DC     18      -0.971  -7.311  15.933
```

```
ATOM    575 O3'  DC     18      -0.601  -9.819  16.483
ATOM    576 C3x  X      19      -5.148  -1.839  14.628
ATOM    577 H3x1 X      19      -5.898  -1.097  14.906
ATOM    578 H3x2 X      19      -5.341  -2.141  13.597
ATOM    579 N2y  X      19      -3.823  -1.184  14.677
ATOM    580 H13  X      19      -3.833  -0.196  14.923
ATOM    581 C2y  X      19      -2.627  -1.739  14.453
ATOM    582 N1y  X      19      -1.527  -0.952  14.702
ATOM    583 C6y  X      19      -0.213  -1.397  14.664
ATOM    584 O6y  X      19       0.664  -0.586  14.968
ATOM    585 H15  X      19      -1.674   0.016  14.959
ATOM    586 N3y  X      19      -2.520  -3.019  14.072
ATOM    587 C4y  X      19      -1.242  -3.482  14.002
ATOM    588 C5y  X      19      -0.089  -2.778  14.264
ATOM    589 N7y  X      19       1.026  -3.606  14.049
ATOM    590 C8y  X      19       0.503  -4.747  13.682
ATOM    591 H14  X      19       1.094  -5.615  13.437
ATOM    592 N9y  X      19      -0.871  -4.748  13.634
ATOM    593 C1'y X      19      -1.819  -5.766  13.123
ATOM    594 O4'y X      19      -2.419  -6.525  14.148
ATOM    595 H1'y X      19      -2.619  -5.234  12.601
ATOM    596 C2'y X      19      -1.241  -6.824  12.187
ATOM    597 H6   X      19      -0.971  -6.419  11.212
ATOM    598 H7   X      19      -0.410  -7.350  12.657
ATOM    599 C3'y X      19      -2.467  -7.726  12.110
ATOM    600 O3'y X      19      -3.418  -7.103  11.278
ATOM    601 H9   X      19      -2.233  -8.734  11.767
ATOM    602 C4'y X      19      -2.984  -7.694  13.557
ATOM    603 H10  X      19      -4.073  -7.633  13.558
ATOM    604 C5'y X      19      -2.533  -8.947  14.315
ATOM    605 H11  X      19      -3.048  -9.823  13.918
ATOM    606 H12  X      19      -1.458  -9.072  14.178
ATOM    607 O5'y X      19      -2.812  -8.820  15.696
ATOM    608 Py   X      19      -2.204  -9.849  16.759
ATOM    609 O2Py X      19      -2.676 -11.197  16.381
ATOM    610 O1Py X      19      -2.470  -9.335  18.110
ATOM    611 P    DC     20      -3.696  -7.591   9.784
ATOM    612 O1P  DC     20      -2.515  -7.232   8.969
ATOM    613 O2P  DC     20      -4.196  -8.982   9.833
ATOM    614 O5'  DC     20      -4.888  -6.580   9.425
ATOM    615 C5'  DC     20      -6.056  -6.505  10.239
ATOM    616 H5'1 DC     20      -5.911  -7.061  11.167
ATOM    617 H5'2 DC     20      -6.894  -6.955   9.705
ATOM    618 C4'  DC     20      -6.398  -5.053  10.606
ATOM    619 H4'  DC     20      -7.257  -5.056  11.277
ATOM    620 O4'  DC     20      -5.300  -4.440  11.274
ATOM    621 C1'  DC     20      -5.040  -3.185  10.669
ATOM    622 H1'  DC     20      -5.632  -2.415  11.177
ATOM    623 N1   DC     20      -3.586  -2.874  10.743
ATOM    624 C6   DC     20      -2.646  -3.808  10.387
ATOM    625 H6   DC     20      -2.979  -4.783  10.044
ATOM    626 C5   DC     20      -1.322  -3.503  10.464
ATOM    627 H5   DC     20      -0.590  -4.236  10.170
ATOM    628 C4   DC     20      -0.974  -2.211  10.940
ATOM    629 N4   DC     20       0.276  -1.872  11.074
ATOM    630 H41  DC     20       0.987  -2.527  10.846
ATOM    631 H42  DC     20       0.467  -0.946  11.451
ATOM    632 N3   DC     20      -1.863  -1.292  11.250
ATOM    633 C2   DC     20      -3.177  -1.598  11.137
ATOM    634 O2   DC     20      -3.987  -0.702  11.354
ATOM    635 C3'  DC     20      -6.755  -4.198   9.387
ATOM    636 H3'  DC     20      -6.891  -4.827   8.505
ATOM    637 C2'  DC     20      -5.536  -3.303   9.228
ATOM    638 H2'1 DC     20      -4.801  -3.811   8.606
ATOM    639 H2'2 DC     20      -5.800  -2.331   8.810
```

```
ATOM    640 O3'  DC     20      -7.921  -3.437   9.673
ATOM    641 P    DT     21      -9.006  -3.128   8.535
ATOM    642 O1P  DT     21     -10.239  -2.643   9.190
ATOM    643 O2P  DT     21      -9.071  -4.307   7.648
ATOM    644 O5'  DT     21      -8.346  -1.923   7.712
ATOM    645 C5'  DT     21      -8.571  -0.561   8.059
ATOM    646 H5'1 DT     21      -8.387  -0.415   9.125
ATOM    647 H5'2 DT     21      -9.610  -0.310   7.841
ATOM    648 C4'  DT     21      -7.654   0.379   7.263
ATOM    649 H4'  DT     21      -7.998   1.403   7.391
ATOM    650 O4'  DT     21      -6.336   0.252   7.789
ATOM    651 C1'  DT     21      -5.463   0.159   6.687
ATOM    652 H1'  DT     21      -5.347   1.166   6.270
ATOM    653 N1   DT     21      -4.120  -0.345   7.107
ATOM    654 C6   DT     21      -3.693  -1.639   6.860
ATOM    655 H6   DT     21      -4.383  -2.352   6.436
ATOM    656 C5   DT     21      -2.426  -2.035   7.154
ATOM    657 C7   DT     21      -2.013  -3.463   6.820
ATOM    658 H71  DT     21      -2.710  -3.917   6.115
ATOM    659 H72  DT     21      -1.016  -3.456   6.381
ATOM    660 H73  DT     21      -1.982  -4.066   7.728
ATOM    661 C4   DT     21      -1.466  -1.092   7.732
ATOM    662 O4   DT     21      -0.284  -1.317   7.991
ATOM    663 N3   DT     21      -1.973   0.161   7.974
ATOM    664 H3   DT     21      -1.345   0.872   8.322
ATOM    665 C2   DT     21      -3.240   0.594   7.661
ATOM    666 O2   DT     21      -3.504   1.777   7.831
ATOM    667 C3'  DT     21      -7.611   0.017   5.759
ATOM    668 H3'  DT     21      -8.432  -0.652   5.491
ATOM    669 C2'  DT     21      -6.262  -0.690   5.689
ATOM    670 H2'1 DT     21      -6.376  -1.715   6.041
ATOM    671 H2'2 DT     21      -5.836  -0.661   4.686
ATOM    672 O3'  DT     21      -7.537   1.096   4.832
ATOM    673 P    DA     22      -8.558   2.341   4.805
ATOM    674 O1P  DA     22      -8.767   2.727   3.395
ATOM    675 O2P  DA     22      -9.714   2.080   5.684
ATOM    676 O5'  DA     22      -7.592   3.407   5.509
ATOM    677 C5'  DA     22      -7.756   4.815   5.404
ATOM    678 H5'1 DA     22      -7.803   5.207   6.419
ATOM    679 H5'2 DA     22      -8.695   5.053   4.906
ATOM    680 C4'  DA     22      -6.587   5.532   4.688
ATOM    681 H4'  DA     22      -6.579   6.561   5.031
ATOM    682 O4'  DA     22      -5.361   4.909   5.059
ATOM    683 C1'  DA     22      -4.720   4.441   3.889
ATOM    684 H1'  DA     22      -4.030   5.222   3.548
ATOM    685 N9   DA     22      -3.976   3.190   4.146
ATOM    686 C8   DA     22      -4.383   1.891   3.948
ATOM    687 H8   DA     22      -5.400   1.639   3.672
ATOM    688 N7   DA     22      -3.453   0.989   4.129
ATOM    689 C5   DA     22      -2.355   1.775   4.507
ATOM    690 C6   DA     22      -1.022   1.491   4.863
ATOM    691 N6   DA     22      -0.522   0.274   4.882
ATOM    692 H61  DA     22       0.421   0.131   5.227
ATOM    693 H62  DA     22      -1.132  -0.476   4.619
ATOM    694 N1   DA     22      -0.164   2.445   5.215
ATOM    695 C2   DA     22      -0.606   3.697   5.208
ATOM    696 H2   DA     22       0.106   4.458   5.502
ATOM    697 N3   DA     22      -1.813   4.127   4.862
ATOM    698 C4   DA     22      -2.660   3.107   4.538
ATOM    699 C3'  DA     22      -6.663   5.503   3.143
ATOM    700 H3'  DA     22      -7.686   5.406   2.775
ATOM    701 C2'  DA     22      -5.834   4.268   2.852
ATOM    702 H2'1 DA     22      -6.430   3.380   3.048
ATOM    703 H2'2 DA     22      -5.450   4.256   1.831
ATOM    704 O3'  DA     22      -5.940   6.526   2.465
```

```
ATOM    705 P    DG     23      -6.300   8.090   2.466
ATOM    706 O1P  DG     23      -7.186   8.383   1.321
ATOM    707 O2P  DG     23      -6.665   8.521   3.830
ATOM    708 O5'  DG     23      -4.811   8.599   2.137
ATOM    709 C5'  DG     23      -3.871   8.882   3.168
ATOM    710 H5'1 DG     23      -4.047   8.227   4.023
ATOM    711 H5'2 DG     23      -4.038   9.907   3.502
ATOM    712 C4'  DG     23      -2.403   8.724   2.735
ATOM    713 H4'  DG     23      -1.799   9.383   3.359
ATOM    714 O4'  DG     23      -1.959   7.386   2.965
ATOM    715 C1'  DG     23      -1.051   7.026   1.945
ATOM    716 H1'  DG     23      -0.065   7.453   2.150
ATOM    717 N9   DG     23      -0.955   5.546   1.832
ATOM    718 C8   DG     23      -1.957   4.662   1.517
ATOM    719 H8   DG     23      -2.973   4.993   1.349
ATOM    720 N7   DG     23      -1.581   3.411   1.442
ATOM    721 C5   DG     23      -0.219   3.460   1.780
ATOM    722 C6   DG     23       0.778   2.421   1.899
ATOM    723 O6   DG     23       0.672   1.202   1.749
ATOM    724 N1   DG     23       2.040   2.894   2.191
ATOM    725 H1   DG     23       2.776   2.211   2.279
ATOM    726 C2   DG     23       2.332   4.203   2.367
ATOM    727 N2   DG     23       3.587   4.491   2.590
ATOM    728 H21  DG     23       3.753   5.425   2.918
ATOM    729 H22  DG     23       4.275   3.756   2.723
ATOM    730 N3   DG     23       1.449   5.197   2.264
ATOM    731 C4   DG     23       0.178   4.767   1.985
ATOM    732 C3'  DG     23      -2.111   9.060   1.260
ATOM    733 H3'  DG     23      -3.008   9.413   0.746
ATOM    734 C2'  DG     23      -1.667   7.701   0.718
ATOM    735 H2'1 DG     23      -2.553   7.158   0.392
ATOM    736 H2'2 DG     23      -0.964   7.797  -0.103
ATOM    737 O3'  DG     23      -1.084  10.040   1.175
ATOM    738 P    DC3    24      -0.676  10.751  -0.211
ATOM    739 O1P  DC3    24      -1.751  10.601  -1.210
ATOM    740 O2P  DC3    24      -0.112  12.085   0.087
ATOM    741 O5'  DC3    24       0.538   9.815  -0.680
ATOM    742 C5'  DC3    24       1.818   9.930  -0.087
ATOM    743 H5'1 DC3    24       1.751   9.713   0.981
ATOM    744 H5'2 DC3    24       2.172  10.954  -0.207
ATOM    745 C4'  DC3    24       2.815   8.971  -0.744
ATOM    746 H4'  DC3    24       3.823   9.258  -0.447
ATOM    747 O4'  DC3    24       2.590   7.645  -0.315
ATOM    748 C1'  DC3    24       3.125   6.760  -1.277
ATOM    749 H1'  DC3    24       4.147   6.501  -0.984
ATOM    750 N1   DC3    24       2.281   5.542  -1.327
ATOM    751 C6   DC3    24       0.910   5.641  -1.352
ATOM    752 H6   DC3    24       0.456   6.627  -1.325
ATOM    753 C5   DC3    24       0.153   4.519  -1.366
ATOM    754 H5   DC3    24      -0.924   4.589  -1.348
ATOM    755 C4   DC3    24       0.833   3.270  -1.355
ATOM    756 N4   DC3    24       0.156   2.168  -1.269
ATOM    757 H41  DC3    24      -0.790   2.225  -0.939
ATOM    758 H42  DC3    24       0.710   1.324  -1.134
ATOM    759 N3   DC3    24       2.147   3.157  -1.378
ATOM    760 C2   DC3    24       2.892   4.283  -1.357
ATOM    761 O2   DC3    24       4.116   4.163  -1.388
ATOM    762 C3'  DC3    24       2.742   8.941  -2.277
ATOM    763 H3'  DC3    24       1.718   9.122  -2.613
ATOM    764 C2'  DC3    24       3.135   7.507  -2.619
ATOM    765 H2'1 DC3    24       2.406   7.090  -3.314
ATOM    766 H2'2 DC3    24       4.131   7.464  -3.059
ATOM    767 O3'  DC3    24       3.639   9.860  -2.877
ATOM    768 H3T  DC3    24       3.247  10.736  -2.787
TER
```

```
END
```

C3. PDB File of the fully reduced *S*-crotonaldehyde-derived cross-link in d(GCTAGCXAGTCC)•d(GGACTCYCTAGC)

```
REMARK
ATOM      1 H5T  DG5     1       1.740  -9.135  -2.566
ATOM      2 O5'  DG5     1       2.342  -8.580  -2.066
ATOM      3 C5'  DG5     1       3.599  -8.521  -2.734
ATOM      4 H5'1 DG5     1       3.443  -8.257  -3.781
ATOM      5 H5'2 DG5     1       4.078  -9.501  -2.690
ATOM      6 C4'  DG5     1       4.559  -7.489  -2.121
ATOM      7 H4'  DG5     1       5.514  -7.554  -2.645
ATOM      8 O4'  DG5     1       4.026  -6.186  -2.312
ATOM      9 C1'  DG5     1       3.960  -5.530  -1.056
ATOM     10 H1'  DG5     1       4.851  -4.909  -0.915
ATOM     11 N9   DG5     1       2.745  -4.686  -1.023
ATOM     12 C8   DG5     1       1.430  -5.071  -0.933
ATOM     13 H8   DG5     1       1.139  -6.111  -0.866
ATOM     14 N7   DG5     1       0.573  -4.085  -0.966
ATOM     15 C5   DG5     1       1.388  -2.951  -1.106
ATOM     16 C6   DG5     1       1.078  -1.553  -1.255
ATOM     17 O6   DG5     1      -0.016  -0.994  -1.327
ATOM     18 N1   DG5     1       2.196  -0.752  -1.354
ATOM     19 H1   DG5     1       2.040   0.240  -1.427
ATOM     20 C2   DG5     1       3.465  -1.216  -1.312
ATOM     21 N2   DG5     1       4.431  -0.341  -1.337
ATOM     22 H21  DG5     1       5.354  -0.694  -1.169
ATOM     23 H22  DG5     1       4.226   0.653  -1.422
ATOM     24 N3   DG5     1       3.803  -2.495  -1.222
ATOM     25 C4   DG5     1       2.718  -3.318  -1.122
ATOM     26 C3'  DG5     1       4.825  -7.694  -0.626
ATOM     27 H3'  DG5     1       4.527  -8.689  -0.291
ATOM     28 C2'  DG5     1       3.950  -6.622   0.011
ATOM     29 H2'1 DG5     1       2.953  -7.030   0.160
ATOM     30 H2'2 DG5     1       4.347  -6.262   0.958
ATOM     31 O3'  DG5     1       6.210  -7.504  -0.409
ATOM     32 P    DC      2       6.879  -7.594   1.049
ATOM     33 O1P  DC      2       8.237  -8.150   0.885
ATOM     34 O2P  DC      2       5.907  -8.231   1.964
ATOM     35 O5'  DC      2       6.986  -6.019   1.376
ATOM     36 C5'  DC      2       7.836  -5.194   0.589
ATOM     37 H5'1 DC      2       7.494  -5.215  -0.446
ATOM     38 H5'2 DC      2       8.843  -5.609   0.624
ATOM     39 C4'  DC      2       7.908  -3.733   1.046
ATOM     40 H4'  DC      2       8.671  -3.239   0.443
ATOM     41 O4'  DC      2       6.666  -3.062   0.848
ATOM     42 C1'  DC      2       6.363  -2.320   2.021
ATOM     43 H1'  DC      2       6.853  -1.338   1.983
ATOM     44 N1   DC      2       4.885  -2.174   2.130
ATOM     45 C6   DC      2       4.084  -3.288   2.197
ATOM     46 H6   DC      2       4.554  -4.267   2.200
ATOM     47 C5   DC      2       2.732  -3.156   2.229
ATOM     48 H5   DC      2       2.102  -4.031   2.271
ATOM     49 C4   DC      2       2.205  -1.838   2.164
ATOM     50 N4   DC      2       0.922  -1.631   2.131
ATOM     51 H41  DC      2       0.284  -2.391   2.201
ATOM     52 H42  DC      2       0.611  -0.665   2.075
ATOM     53 N3   DC      2       2.950  -0.760   2.093
ATOM     54 C2   DC      2       4.299  -0.901   2.090
ATOM     55 O2   DC      2       4.969   0.129   2.042
ATOM     56 C3'  DC      2       8.308  -3.571   2.514
ATOM     57 H3'  DC      2       8.683  -4.509   2.939
```

```
ATOM     58 C2'  DC      2       7.001  -3.128   3.155
ATOM     59 H2'1 DC      2       6.421  -4.013   3.411
ATOM     60 H2'2 DC      2       7.191  -2.525   4.037
ATOM     61 O3'  DC      2       9.282  -2.544   2.579
ATOM     62 P    DT      3      10.112  -2.246   3.916
ATOM     63 O1P  DT      3       9.837  -3.297   4.916
ATOM     64 O2P  DT      3      11.496  -1.935   3.509
ATOM     65 O5'  DT      3       9.426  -0.901   4.423
ATOM     66 C5'  DT      3       9.747   0.325   3.800
ATOM     67 H5'1 DT      3       9.507   0.250   2.740
ATOM     68 H5'2 DT      3      10.819   0.515   3.895
ATOM     69 C4'  DT      3       8.979   1.499   4.408
ATOM     70 H4'  DT      3       9.314   2.411   3.918
ATOM     71 O4'  DT      3       7.592   1.318   4.146
ATOM     72 C1'  DT      3       6.882   1.545   5.349
ATOM     73 H1'  DT      3       6.649   2.614   5.425
ATOM     74 N1   DT      3       5.630   0.739   5.353
ATOM     75 C6   DT      3       5.658  -0.630   5.539
ATOM     76 H6   DT      3       6.617  -1.126   5.609
ATOM     77 C5   DT      3       4.509  -1.348   5.634
ATOM     78 C7   DT      3       4.576  -2.847   5.870
ATOM     79 H71  DT      3       4.057  -3.364   5.064
ATOM     80 H72  DT      3       5.610  -3.192   5.923
ATOM     81 H73  DT      3       4.068  -3.079   6.806
ATOM     82 C4   DT      3       3.211  -0.688   5.524
ATOM     83 O4   DT      3       2.115  -1.234   5.625
ATOM     84 N3   DT      3       3.272   0.665   5.280
ATOM     85 H3   DT      3       2.409   1.187   5.220
ATOM     86 C2   DT      3       4.417   1.415   5.190
ATOM     87 O2   DT      3       4.327   2.617   4.972
ATOM     88 C3'  DT      3       9.184   1.659   5.922
ATOM     89 H3'  DT      3      10.003   1.036   6.290
ATOM     90 C2'  DT      3       7.849   1.194   6.485
ATOM     91 H2'1 DT      3       7.914   0.124   6.662
ATOM     92 H2'2 DT      3       7.580   1.703   7.408
ATOM     93 O3'  DT      3       9.446   3.023   6.187
ATOM     94 P    DA      4       9.671   3.593   7.673
ATOM     95 O1P  DA      4       9.883   2.468   8.607
ATOM     96 O2P  DA      4      10.640   4.702   7.582
ATOM     97 O5'  DA      4       8.219   4.203   7.922
ATOM     98 C5'  DA      4       7.774   5.305   7.149
ATOM     99 H5'1 DA      4       7.696   5.012   6.102
ATOM    100 H5'2 DA      4       8.504   6.112   7.233
ATOM    101 C4'  DA      4       6.420   5.823   7.629
ATOM    102 H4'  DA      4       6.191   6.740   7.086
ATOM    103 O4'  DA      4       5.405   4.867   7.364
ATOM    104 C1'  DA      4       4.588   4.764   8.512
ATOM    105 H1'  DA      4       3.806   5.530   8.491
ATOM    106 N9   DA      4       3.985   3.415   8.537
ATOM    107 C8   DA      4       4.618   2.194   8.556
ATOM    108 H8   DA      4       5.696   2.110   8.587
ATOM    109 N7   DA      4       3.814   1.161   8.507
ATOM    110 C5   DA      4       2.545   1.769   8.491
ATOM    111 C6   DA      4       1.210   1.304   8.442
ATOM    112 N6   DA      4       0.862   0.038   8.344
ATOM    113 H61  DA      4      -0.108  -0.199   8.186
ATOM    114 H62  DA      4       1.594  -0.645   8.284
ATOM    115 N1   DA      4       0.175   2.139   8.446
ATOM    116 C2   DA      4       0.431   3.441   8.473
ATOM    117 H2   DA      4      -0.430   4.098   8.472
ATOM    118 N3   DA      4       1.621   4.031   8.495
ATOM    119 C4   DA      4       2.644   3.133   8.505
ATOM    120 C3'  DA      4       6.420   6.134   9.130
ATOM    121 H3'  DA      4       7.425   6.068   9.554
ATOM    122 C2'  DA      4       5.524   5.030   9.687
```

```
ATOM    123 H2'1 DA      4       6.139   4.155   9.897
ATOM    124 H2'2 DA      4       4.987   5.343  10.580
ATOM    125 O3'  DA      4       5.899   7.441   9.303
ATOM    126 P    DG      5       5.840   8.154  10.738
ATOM    127 O1P  DG      5       6.017   9.607  10.545
ATOM    128 O2P  DG      5       6.715   7.421  11.675
ATOM    129 O5'  DG      5       4.316   7.880  11.144
ATOM    130 C5'  DG      5       3.267   8.530  10.445
ATOM    131 H5'1 DG      5       3.267   8.216   9.400
ATOM    132 H5'2 DG      5       3.430   9.607  10.485
ATOM    133 C4'  DG      5       1.897   8.231  11.052
ATOM    134 H4'  DG      5       1.160   8.877  10.574
ATOM    135 O4'  DG      5       1.539   6.880  10.810
ATOM    136 C1'  DG      5       1.070   6.325  12.022
ATOM    137 H1'  DG      5       0.009   6.562  12.145
ATOM    138 N9   DG      5       1.249   4.856  11.982
ATOM    139 C8   DG      5       2.405   4.116  11.979
ATOM    140 H8   DG      5       3.378   4.585  12.002
ATOM    141 N7   DG      5       2.222   2.820  11.922
ATOM    142 C5   DG      5       0.822   2.697  11.842
ATOM    143 C6   DG      5      -0.046   1.547  11.726
ATOM    144 O6   DG      5       0.242   0.354  11.617
ATOM    145 N1   DG      5      -1.389   1.870  11.738
ATOM    146 H1   DG      5      -2.044   1.111  11.642
ATOM    147 C2   DG      5      -1.864   3.132  11.833
ATOM    148 N2   DG      5      -3.155   3.289  11.873
ATOM    149 H21  DG      5      -3.478   4.236  11.847
ATOM    150 H22  DG      5      -3.775   2.494  11.738
ATOM    151 N3   DG      5      -1.106   4.219  11.917
ATOM    152 C4   DG      5       0.230   3.939  11.910
ATOM    153 C3'  DG      5       1.853   8.474  12.568
ATOM    154 H3'  DG      5       2.714   9.049  12.913
ATOM    155 C2'  DG      5       1.871   7.046  13.104
ATOM    156 H2'1 DG      5       2.899   6.689  13.125
ATOM    157 H2'2 DG      5       1.419   6.982  14.090
ATOM    158 O3'  DG      5       0.638   9.150  12.840
ATOM    159 P    DC      6       0.296   9.816  14.255
ATOM    160 O1P  DC      6       1.478   9.726  15.139
ATOM    161 O2P  DC      6      -0.338  11.125  13.986
ATOM    162 O5'  DC      6      -0.832   8.786  14.748
ATOM    163 C5'  DC      6      -2.125   8.813  14.158
ATOM    164 H5'1 DC      6      -2.019   8.730  13.072
ATOM    165 H5'2 DC      6      -2.617   9.754  14.424
ATOM    166 C4'  DC      6      -2.993   7.650  14.648
ATOM    167 H4'  DC      6      -3.988   7.752  14.216
ATOM    168 O4'  DC      6      -2.451   6.415  14.218
ATOM    169 C1'  DC      6      -2.728   5.423  15.187
ATOM    170 H1'  DC      6      -3.655   4.903  14.921
ATOM    171 N1   DC      6      -1.588   4.469  15.245
ATOM    172 C6   DC      6      -0.289   4.918  15.249
ATOM    173 H6   DC      6      -0.120   5.990  15.283
ATOM    174 C5   DC      6       0.741   4.033  15.172
ATOM    175 H5   DC      6       1.759   4.383  15.152
ATOM    176 C4   DC      6       0.400   2.652  15.099
ATOM    177 N4   DC      6       1.310   1.752  14.852
ATOM    178 H41  DC      6       2.163   2.049  14.419
ATOM    179 H42  DC      6       0.934   0.812  14.740
ATOM    180 N3   DC      6      -0.838   2.207  15.129
ATOM    181 C2   DC      6      -1.849   3.098  15.254
ATOM    182 O2   DC      6      -2.987   2.659  15.357
ATOM    183 C3'  DC      6      -3.144   7.612  16.171
ATOM    184 H3'  DC      6      -2.378   8.230  16.644
ATOM    185 C2'  DC      6      -2.918   6.141  16.522
ATOM    186 H2'1 DC      6      -2.026   6.069  17.147
ATOM    187 H2'2 DC      6      -3.769   5.703  17.041
```

```
ATOM    188 O3'  DC      6      -4.437   8.068  16.530
ATOM    189 O1P  X       7      -5.934   9.281  18.132
ATOM    190 P    X       7      -4.845   8.285  18.068
ATOM    191 O2P  X       7      -3.622   8.486  18.875
ATOM    192 O5'  X       7      -5.440   6.866  18.469
ATOM    193 C5'  X       7      -6.775   6.462  18.193
ATOM    194 H5'1 X       7      -6.880   6.204  17.138
ATOM    195 H5'2 X       7      -7.463   7.271  18.439
ATOM    196 C4'  X       7      -7.117   5.242  19.068
ATOM    197 O4'  X       7      -6.272   4.189  18.623
ATOM    198 H4'  X       7      -8.153   4.965  18.905
ATOM    199 C3'  X       7      -6.826   5.568  20.559
ATOM    200 O3'  X       7      -7.619   5.090  21.648
ATOM    201 H3'  X       7      -6.746   6.650  20.672
ATOM    202 C2'  X       7      -5.450   4.937  20.722
ATOM    203 H2'2 X       7      -5.282   4.568  21.732
ATOM    204 H2'1 X       7      -4.711   5.700  20.497
ATOM    205 C1'  X       7      -5.429   3.798  19.687
ATOM    206 H1'  X       7      -5.878   2.904  20.124
ATOM    207 N9   X       7      -4.058   3.450  19.218
ATOM    208 C4   X       7      -3.658   2.215  18.747
ATOM    209 N3   X       7      -4.458   1.144  18.452
ATOM    210 C8   X       7      -2.896   4.186  19.309
ATOM    211 H8   X       7      -2.885   5.224  19.614
ATOM    212 N7   X       7      -1.806   3.531  19.011
ATOM    213 C5   X       7      -2.283   2.262  18.666
ATOM    214 C6   X       7      -1.594   1.061  18.283
ATOM    215 O6   X       7      -0.386   0.847  18.197
ATOM    216 N1   X       7      -2.434   0.007  17.983
ATOM    217 H1   X       7      -1.990  -0.856  17.712
ATOM    218 C2   X       7      -3.794   0.071  18.010
ATOM    219 N2   X       7      -4.404  -0.991  17.488
ATOM    220 H2   X       7      -3.810  -1.793  17.298
ATOM    221 C1x  X       7      -5.808  -1.141  17.060
ATOM    222 H1x  X       7      -5.870  -2.034  16.429
ATOM    223 Cmx  X       7      -6.653  -1.394  18.299
ATOM    224 H1m1 X       7      -7.694  -1.572  18.035
ATOM    225 H1m2 X       7      -6.582  -0.520  18.937
ATOM    226 H1m3 X       7      -6.260  -2.252  18.843
ATOM    227 C2x  X       7      -6.396   0.028  16.218
ATOM    228 H2x2 X       7      -6.260   0.977  16.729
ATOM    229 H2x1 X       7      -7.472  -0.126  16.144
ATOM    230 P    DA      8      -9.108   4.495  21.561
ATOM    231 O1P  DA      8      -9.852   5.102  20.437
ATOM    232 O2P  DA      8      -9.681   4.507  22.923
ATOM    233 O5'  DA      8      -8.704   2.991  21.219
ATOM    234 C5'  DA      8      -9.627   2.029  20.743
ATOM    235 H5'1 DA      8      -9.743   2.157  19.667
ATOM    236 H5'2 DA      8     -10.595   2.169  21.227
ATOM    237 C4'  DA      8      -9.117   0.607  21.043
ATOM    238 H4'  DA      8      -9.667  -0.113  20.435
ATOM    239 O4'  DA      8      -7.722   0.533  20.750
ATOM    240 C1'  DA      8      -7.040   0.046  21.894
ATOM    241 H1'  DA      8      -7.055  -1.049  21.873
ATOM    242 N9   DA      8      -5.636   0.516  21.931
ATOM    243 C8   DA      8      -5.150   1.748  22.293
ATOM    244 H8   DA      8      -5.809   2.557  22.584
ATOM    245 N7   DA      8      -3.848   1.870  22.204
ATOM    246 C5   DA      8      -3.447   0.592  21.783
ATOM    247 C6   DA      8      -2.206  -0.022  21.482
ATOM    248 N6   DA      8      -1.026   0.567  21.505
ATOM    249 H61  DA      8      -0.223   0.058  21.154
ATOM    250 H62  DA      8      -0.979   1.543  21.743
ATOM    251 N1   DA      8      -2.138  -1.295  21.095
ATOM    252 C2   DA      8      -3.273  -1.977  20.999
```

```
ATOM    253 H2   DA      8      -3.181  -3.005  20.680
ATOM    254 N3   DA      8      -4.502  -1.550  21.252
ATOM    255 C4   DA      8      -4.526  -0.238  21.627
ATOM    256 C3'  DA      8      -9.267   0.209  22.519
ATOM    257 H3'  DA      8     -10.056   0.764  23.033
ATOM    258 C2'  DA      8      -7.889   0.531  23.068
ATOM    259 H2'1 DA      8      -7.791   1.605  23.224
ATOM    260 H2'2 DA      8      -7.695  -0.021  23.982
ATOM    261 O3'  DA      8      -9.424  -1.195  22.626
ATOM    262 P    DG      9     -10.776  -1.878  23.117
ATOM    263 O1P  DG      9     -11.152  -1.286  24.419
ATOM    264 O2P  DG      9     -11.742  -1.900  21.999
ATOM    265 O5'  DG      9     -10.205  -3.366  23.375
ATOM    266 C5'  DG      9      -9.512  -3.697  24.578
ATOM    267 H5'1 DG      9     -10.132  -4.410  25.121
ATOM    268 H5'2 DG      9      -9.387  -2.814  25.205
ATOM    269 C4'  DG      9      -8.120  -4.320  24.356
ATOM    270 H4'  DG      9      -8.172  -5.069  23.565
ATOM    271 O4'  DG      9      -7.139  -3.334  24.032
ATOM    272 C1'  DG      9      -5.902  -3.722  24.605
ATOM    273 H1'  DG      9      -5.435  -4.513  24.011
ATOM    274 N9   DG      9      -4.965  -2.579  24.748
ATOM    275 C8   DG      9      -5.257  -1.274  25.043
ATOM    276 H8   DG      9      -6.267  -0.947  25.224
ATOM    277 N7   DG      9      -4.224  -0.477  25.081
ATOM    278 C5   DG      9      -3.142  -1.327  24.815
ATOM    279 C6   DG      9      -1.721  -1.084  24.722
ATOM    280 O6   DG      9      -1.091  -0.030  24.786
ATOM    281 N1   DG      9      -0.979  -2.231  24.533
ATOM    282 H1   DG      9       0.018  -2.119  24.433
ATOM    283 C2   DG      9      -1.516  -3.468  24.434
ATOM    284 N2   DG      9      -0.684  -4.466  24.338
ATOM    285 H21  DG      9      -1.094  -5.370  24.205
ATOM    286 H22  DG      9       0.319  -4.319  24.283
ATOM    287 N3   DG      9      -2.816  -3.739  24.486
ATOM    288 C4   DG      9      -3.587  -2.624  24.664
ATOM    289 C3'  DG      9      -7.630  -4.995  25.653
ATOM    290 H3'  DG      9      -8.345  -4.826  26.462
ATOM    291 C2'  DG      9      -6.322  -4.273  25.957
ATOM    292 H2'1 DG      9      -6.535  -3.460  26.647
ATOM    293 H2'2 DG      9      -5.562  -4.942  26.354
ATOM    294 O3'  DG      9      -7.426  -6.389  25.478
ATOM    295 P    DT     10      -7.276  -7.378  26.747
ATOM    296 O1P  DT     10      -7.891  -6.723  27.924
ATOM    297 O2P  DT     10      -7.718  -8.730  26.354
ATOM    298 O5'  DT     10      -5.689  -7.389  26.997
ATOM    299 C5'  DT     10      -4.780  -8.100  26.163
ATOM    300 H5'1 DT     10      -4.827  -7.705  25.147
ATOM    301 H5'2 DT     10      -5.066  -9.154  26.141
ATOM    302 C4'  DT     10      -3.328  -7.999  26.678
ATOM    303 H4'  DT     10      -2.706  -8.704  26.124
ATOM    304 O4'  DT     10      -2.841  -6.667  26.479
ATOM    305 C1'  DT     10      -2.278  -6.240  27.708
ATOM    306 H1'  DT     10      -1.277  -6.685  27.800
ATOM    307 N1   DT     10      -2.174  -4.757  27.811
ATOM    308 C6   DT     10      -3.293  -3.975  28.030
ATOM    309 H6   DT     10      -4.268  -4.440  28.027
ATOM    310 C5   DT     10      -3.180  -2.639  28.250
ATOM    311 C7   DT     10      -4.428  -1.820  28.530
ATOM    312 H71  DT     10      -4.285  -0.803  28.160
ATOM    313 H72  DT     10      -5.292  -2.248  28.027
ATOM    314 H73  DT     10      -4.602  -1.777  29.604
ATOM    315 C4   DT     10      -1.875  -1.987  28.203
ATOM    316 O4   DT     10      -1.662  -0.797  28.397
ATOM    317 N3   DT     10      -0.817  -2.823  27.948
```

```
ATOM    318 H3   DT     10       0.106  -2.410  27.927
ATOM    319 C2   DT     10      -0.891  -4.188  27.811
ATOM    320 O2   DT     10       0.151  -4.830  27.770
ATOM    321 C3'  DT     10      -3.220  -8.301  28.188
ATOM    322 H3'  DT     10      -4.064  -8.881  28.565
ATOM    323 C2'  DT     10      -3.187  -6.893  28.756
ATOM    324 H2'1 DT     10      -4.188  -6.468  28.756
ATOM    325 H2'2 DT     10      -2.763  -6.878  29.753
ATOM    326 O3'  DT     10      -1.980  -8.866  28.577
ATOM    327 P    DC     11      -1.633 -10.419  28.428
ATOM    328 O1P  DC     11      -1.865 -10.837  27.031
ATOM    329 O2P  DC     11      -2.298 -11.129  29.540
ATOM    330 O5'  DC     11      -0.047 -10.358  28.712
ATOM    331 C5'  DC     11       0.452 -10.187  30.031
ATOM    332 H5'1 DC     11       1.028 -11.075  30.291
ATOM    333 H5'2 DC     11      -0.372 -10.095  30.741
ATOM    334 C4'  DC     11       1.363  -8.962  30.179
ATOM    335 H4'  DC     11       2.183  -9.036  29.462
ATOM    336 O4'  DC     11       0.675  -7.729  29.992
ATOM    337 C1'  DC     11       1.374  -6.736  30.713
ATOM    338 H1'  DC     11       2.295  -6.465  30.183
ATOM    339 N1   DC     11       0.536  -5.523  30.931
ATOM    340 C6   DC     11      -0.809  -5.641  31.176
ATOM    341 H6   DC     11      -1.235  -6.639  31.200
ATOM    342 C5   DC     11      -1.572  -4.531  31.351
ATOM    343 H5   DC     11      -2.635  -4.625  31.502
ATOM    344 C4   DC     11      -0.910  -3.274  31.284
ATOM    345 N4   DC     11      -1.584  -2.171  31.399
ATOM    346 H41  DC     11      -2.580  -2.191  31.373
ATOM    347 H42  DC     11      -1.070  -1.303  31.237
ATOM    348 N3   DC     11       0.383  -3.140  31.110
ATOM    349 C2   DC     11       1.129  -4.254  30.928
ATOM    350 O2   DC     11       2.342  -4.097  30.819
ATOM    351 C3'  DC     11       1.933  -8.910  31.607
ATOM    352 H3'  DC     11       1.361  -9.570  32.264
ATOM    353 C2'  DC     11       1.710  -7.451  32.017
ATOM    354 H2'1 DC     11       0.866  -7.406  32.707
ATOM    355 H2'2 DC     11       2.589  -7.003  32.465
ATOM    356 O3'  DC     11       3.303  -9.283  31.623
ATOM    357 P    DC3    12       4.069  -9.685  32.989
ATOM    358 O1P  DC3    12       5.356 -10.318  32.647
ATOM    359 O2P  DC3    12       3.130 -10.361  33.908
ATOM    360 O5'  DC3    12       4.400  -8.230  33.580
ATOM    361 C5'  DC3    12       5.337  -7.392  32.919
ATOM    362 H5'1 DC3    12       5.074  -7.302  31.863
ATOM    363 H5'2 DC3    12       6.322  -7.856  32.981
ATOM    364 C4'  DC3    12       5.405  -5.989  33.530
ATOM    365 H4'  DC3    12       6.362  -5.544  33.258
ATOM    366 O4'  DC3    12       4.372  -5.141  33.067
ATOM    367 C1'  DC3    12       4.303  -4.029  33.940
ATOM    368 H1'  DC3    12       4.903  -3.212  33.521
ATOM    369 N1   DC3    12       2.899  -3.569  34.103
ATOM    370 C6   DC3    12       1.847  -4.450  34.161
ATOM    371 H6   DC3    12       2.047  -5.510  34.069
ATOM    372 C5   DC3    12       0.577  -3.980  34.299
ATOM    373 H5   DC3    12      -0.257  -4.662  34.311
ATOM    374 C4   DC3    12       0.414  -2.570  34.398
ATOM    375 N4   DC3    12      -0.766  -2.031  34.514
ATOM    376 H41  DC3    12      -1.577  -2.579  34.332
ATOM    377 H42  DC3    12      -0.769  -1.012  34.473
ATOM    378 N3   DC3    12       1.417  -1.724  34.406
ATOM    379 C2   DC3    12       2.670  -2.200  34.249
ATOM    380 O2   DC3    12       3.594  -1.392  34.263
ATOM    381 C3'  DC3    12       5.249  -5.946  35.049
ATOM    382 H3'  DC3    12       4.399  -6.564  35.348
```

```
ATOM    383 C2'  DC3    12       4.917  -4.476  35.275
ATOM    384 H2'1 DC3    12       4.220  -4.367  36.106
ATOM    385 H2'2 DC3    12       5.825  -3.906  35.470
ATOM    386 O3'  DC3    12       6.430  -6.331  35.726
ATOM    387 H3T  DC3    12       6.518  -7.288  35.616
TER
ATOM    388 H5T  DG5    13       0.298   8.166  35.679
ATOM    389 O5'  DG5    13       0.068   9.051  35.365
ATOM    390 C5'  DG5    13       0.614   9.167  34.062
ATOM    391 H5'1 DG5    13       0.750  10.219  33.807
ATOM    392 H5'2 DG5    13      -0.063   8.710  33.340
ATOM    393 C4'  DG5    13       1.969   8.450  34.010
ATOM    394 H4'  DG5    13       2.686   8.971  34.648
ATOM    395 O4'  DG5    13       1.768   7.118  34.472
ATOM    396 C1'  DG5    13       2.076   6.210  33.424
ATOM    397 H1'  DG5    13       3.093   5.825  33.555
ATOM    398 N9   DG5    13       1.108   5.090  33.477
ATOM    399 C8   DG5    13      -0.264   5.129  33.508
ATOM    400 H8   DG5    13      -0.818   6.052  33.402
ATOM    401 N7   DG5    13      -0.834   3.975  33.734
ATOM    402 C5   DG5    13       0.249   3.085  33.817
ATOM    403 C6   DG5    13       0.327   1.669  34.084
ATOM    404 O6   DG5    13      -0.566   0.861  34.350
ATOM    405 N1   DG5    13       1.622   1.184  34.073
ATOM    406 H1   DG5    13       1.731   0.186  34.168
ATOM    407 C2   DG5    13       2.717   1.956  33.863
ATOM    408 N2   DG5    13       3.876   1.372  33.792
ATOM    409 H21  DG5    13       4.621   1.943  33.435
ATOM    410 H22  DG5    13       3.936   0.358  33.855
ATOM    411 N3   DG5    13       2.701   3.267  33.687
ATOM    412 C4   DG5    13       1.435   3.771  33.652
ATOM    413 C3'  DG5    13       2.526   8.372  32.586
ATOM    414 H3'  DG5    13       2.130   9.170  31.955
ATOM    415 C2'  DG5    13       2.032   7.004  32.123
ATOM    416 H2'1 DG5    13       1.010   7.083  31.751
ATOM    417 H2'2 DG5    13       2.681   6.568  31.364
ATOM    418 O3'  DG5    13       3.938   8.464  32.667
ATOM    419 P    DG     14       4.851   8.694  31.360
ATOM    420 O1P  DG     14       3.996   9.299  30.315
ATOM    421 O2P  DG     14       6.087   9.372  31.792
ATOM    422 O5'  DG     14       5.208   7.177  30.954
ATOM    423 C5'  DG     14       6.112   6.412  31.746
ATOM    424 H5'1 DG     14       5.735   6.354  32.767
ATOM    425 H5'2 DG     14       7.070   6.933  31.767
ATOM    426 C4'  DG     14       6.360   4.982  31.237
ATOM    427 H4'  DG     14       7.211   4.577  31.783
ATOM    428 O4'  DG     14       5.232   4.141  31.475
ATOM    429 C1'  DG     14       4.977   3.413  30.283
ATOM    430 H1'  DG     14       5.636   2.540  30.234
ATOM    431 N9   DG     14       3.565   2.959  30.257
ATOM    432 C8   DG     14       2.419   3.698  30.107
ATOM    433 H8   DG     14       2.445   4.757  29.893
ATOM    434 N7   DG     14       1.311   3.024  30.285
ATOM    435 C5   DG     14       1.757   1.718  30.536
ATOM    436 C6   DG     14       1.055   0.492  30.835
ATOM    437 O6   DG     14      -0.146   0.280  31.003
ATOM    438 N1   DG     14       1.886  -0.604  30.956
ATOM    439 H1   DG     14       1.438  -1.502  31.037
ATOM    440 C2   DG     14       3.229  -0.553  30.804
ATOM    441 N2   DG     14       3.872  -1.689  30.797
ATOM    442 H21  DG     14       4.814  -1.643  30.451
ATOM    443 H22  DG     14       3.361  -2.568  30.819
ATOM    444 N3   DG     14       3.928   0.556  30.595
ATOM    445 C4   DG     14       3.135   1.666  30.463
ATOM    446 C3'  DG     14       6.695   4.910  29.743
```

```
ATOM    447 H3'  DG     14       6.949   5.896  29.343
ATOM    448 C2'  DG     14       5.384   4.381  29.173
ATOM    449 H2'1 DG     14       4.668   5.199  29.085
ATOM    450 H2'2 DG     14       5.536   3.888  28.219
ATOM    451 O3'  DG     14       7.764   3.982  29.573
ATOM    452 P    DA     15       8.707   3.983  28.268
ATOM    453 O1P  DA     15      10.109   4.057  28.727
ATOM    454 O2P  DA     15       8.190   4.982  27.308
ATOM    455 O5'  DA     15       8.456   2.533  27.639
ATOM    456 C5'  DA     15       9.185   1.383  28.047
ATOM    457 H5'1 DA     15       9.058   1.246  29.121
ATOM    458 H5'2 DA     15      10.245   1.539  27.842
ATOM    459 C4'  DA     15       8.719   0.106  27.318
ATOM    460 H4'  DA     15       9.367  -0.725  27.603
ATOM    461 O4'  DA     15       7.379  -0.156  27.726
ATOM    462 C1'  DA     15       6.560  -0.119  26.572
ATOM    463 H1'  DA     15       6.472  -1.142  26.191
ATOM    464 N9   DA     15       5.217   0.402  26.877
ATOM    465 C8   DA     15       4.746   1.688  26.774
ATOM    466 H8   DA     15       5.396   2.525  26.557
ATOM    467 N7   DA     15       3.455   1.811  26.941
ATOM    468 C5   DA     15       3.061   0.490  27.211
ATOM    469 C6   DA     15       1.834  -0.140  27.504
ATOM    470 N6   DA     15       0.698   0.504  27.626
ATOM    471 H61  DA     15      -0.151  -0.005  27.836
ATOM    472 H62  DA     15       0.689   1.497  27.485
ATOM    473 N1   DA     15       1.752  -1.451  27.721
ATOM    474 C2   DA     15       2.869  -2.162  27.633
ATOM    475 H2   DA     15       2.769  -3.229  27.793
ATOM    476 N3   DA     15       4.093  -1.722  27.366
ATOM    477 C4   DA     15       4.123  -0.370  27.180
ATOM    478 C3'  DA     15       8.703   0.231  25.779
ATOM    479 H3'  DA     15       9.464   0.916  25.399
ATOM    480 C2'  DA     15       7.296   0.730  25.530
ATOM    481 H2'1 DA     15       7.232   1.794  25.731
ATOM    482 H2'2 DA     15       6.971   0.528  24.515
ATOM    483 O3'  DA     15       8.710  -1.011  25.100
ATOM    484 P    DC     16      10.028  -1.839  24.779
ATOM    485 O1P  DC     16      10.661  -2.247  26.052
ATOM    486 O2P  DC     16      10.800  -1.095  23.765
ATOM    487 O5'  DC     16       9.293  -3.104  24.102
ATOM    488 C5'  DC     16       8.534  -4.031  24.876
ATOM    489 H5'1 DC     16       8.470  -3.695  25.912
ATOM    490 H5'2 DC     16       9.073  -4.979  24.863
ATOM    491 C4'  DC     16       7.098  -4.283  24.367
ATOM    492 H4'  DC     16       6.777  -5.228  24.804
ATOM    493 O4'  DC     16       6.148  -3.297  24.759
ATOM    494 C1'  DC     16       4.983  -3.526  23.979
ATOM    495 H1'  DC     16       4.441  -4.399  24.363
ATOM    496 N1   DC     16       4.078  -2.341  23.934
ATOM    497 C6   DC     16       4.595  -1.086  23.742
ATOM    498 H6   DC     16       5.672  -0.993  23.639
ATOM    499 C5   DC     16       3.775  -0.002  23.702
ATOM    500 H5   DC     16       4.189   0.983  23.570
ATOM    501 C4   DC     16       2.379  -0.235  23.876
ATOM    502 N4   DC     16       1.552   0.767  23.958
ATOM    503 H41  DC     16       1.890   1.704  23.945
ATOM    504 H42  DC     16       0.579   0.529  24.141
ATOM    505 N3   DC     16       1.863  -1.433  24.034
ATOM    506 C2   DC     16       2.688  -2.507  24.034
ATOM    507 O2   DC     16       2.158  -3.614  24.114
ATOM    508 C3'  DC     16       6.942  -4.429  22.852
ATOM    509 H3'  DC     16       7.694  -3.833  22.329
ATOM    510 C2'  DC     16       5.539  -3.868  22.600
ATOM    511 H2'1 DC     16       5.633  -2.981  21.978
```

```
ATOM    512 H2'2 DC     16       4.888  -4.596  22.125
ATOM    513 O3'  DC     16       7.037  -5.791  22.484
ATOM    514 P    DT     17       6.950  -6.258  20.947
ATOM    515 O1P  DT     17       7.800  -7.454  20.789
ATOM    516 O2P  DT     17       7.130  -5.082  20.069
ATOM    517 O5'  DT     17       5.414  -6.695  20.843
ATOM    518 C5'  DT     17       4.897  -7.693  21.704
ATOM    519 H5'1 DT     17       5.126  -7.434  22.737
ATOM    520 H5'2 DT     17       5.369  -8.647  21.468
ATOM    521 C4'  DT     17       3.379  -7.817  21.568
ATOM    522 H4'  DT     17       3.034  -8.563  22.286
ATOM    523 O4'  DT     17       2.768  -6.565  21.866
ATOM    524 C1'  DT     17       1.852  -6.249  20.833
ATOM    525 H1'  DT     17       0.878  -6.685  21.080
ATOM    526 N1   DT     17       1.747  -4.766  20.704
ATOM    527 C6   DT     17       2.842  -4.004  20.340
ATOM    528 H6   DT     17       3.780  -4.507  20.126
ATOM    529 C5   DT     17       2.757  -2.649  20.262
ATOM    530 C7   DT     17       3.975  -1.859  19.815
ATOM    531 H71  DT     17       4.886  -2.451  19.919
ATOM    532 H72  DT     17       3.853  -1.580  18.769
ATOM    533 H73  DT     17       4.060  -0.947  20.407
ATOM    534 C4   DT     17       1.516  -1.957  20.616
ATOM    535 O4   DT     17       1.353  -0.741  20.656
ATOM    536 N3   DT     17       0.462  -2.786  20.925
ATOM    537 H3   DT     17      -0.441  -2.357  21.080
ATOM    538 C2   DT     17       0.510  -4.161  20.963
ATOM    539 O2   DT     17      -0.520  -4.782  21.189
ATOM    540 C3'  DT     17       2.937  -8.257  20.169
ATOM    541 H3'  DT     17       3.784  -8.632  19.587
ATOM    542 C2'  DT     17       2.382  -6.960  19.584
ATOM    543 H2'1 DT     17       3.199  -6.406  19.124
ATOM    544 H2'2 DT     17       1.593  -7.147  18.859
ATOM    545 O3'  DT     17       1.944  -9.256  20.325
ATOM    546 P    DC     18       1.541 -10.263  19.135
ATOM    547 O1P  DC     18       2.715 -10.452  18.257
ATOM    548 O2P  DC     18       0.866 -11.432  19.733
ATOM    549 O5'  DC     18       0.445  -9.372  18.371
ATOM    550 C5'  DC     18      -0.842  -9.187  18.939
ATOM    551 H5'1 DC     18      -0.736  -8.852  19.972
ATOM    552 H5'2 DC     18      -1.358 -10.148  18.944
ATOM    553 C4'  DC     18      -1.705  -8.171  18.180
ATOM    554 H4'  DC     18      -2.720  -8.253  18.570
ATOM    555 O4'  DC     18      -1.271  -6.837  18.398
ATOM    556 C1'  DC     18      -1.801  -6.041  17.359
ATOM    557 H1'  DC     18      -2.842  -5.787  17.581
ATOM    558 N1   DC     18      -0.983  -4.799  17.240
ATOM    559 C6   DC     18       0.386  -4.878  17.153
ATOM    560 H6   DC     18       0.843  -5.860  17.075
ATOM    561 C5   DC     18       1.140  -3.754  17.207
ATOM    562 H5   DC     18       2.212  -3.818  17.161
ATOM    563 C4   DC     18       0.452  -2.515  17.341
ATOM    564 N4   DC     18       1.135  -1.423  17.487
ATOM    565 H41  DC     18       2.126  -1.432  17.408
ATOM    566 H42  DC     18       0.606  -0.567  17.651
ATOM    567 N3   DC     18      -0.855  -2.412  17.423
ATOM    568 C2   DC     18      -1.596  -3.542  17.347
ATOM    569 O2   DC     18      -2.818  -3.412  17.391
ATOM    570 C3'  DC     18      -1.775  -8.389  16.663
ATOM    571 H3'  DC     18      -0.890  -8.928  16.317
ATOM    572 C2'  DC     18      -1.759  -6.950  16.123
ATOM    573 H2'1 DC     18      -0.839  -6.797  15.559
ATOM    574 H2'2 DC     18      -2.617  -6.741  15.490
ATOM    575 O3'  DC     18      -2.956  -9.121  16.349
ATOM    576 O1P  Y      19      -2.018  -9.820  14.109
```

```
ATOM    577 P    Y      19      -3.278  -9.655  14.862
ATOM    578 O2P  Y      19      -4.254 -10.759  14.952
ATOM    579 O5'  Y      19      -4.042  -8.384  14.262
ATOM    580 C5'  Y      19      -5.274  -7.954  14.816
ATOM    581 H5'1 Y      19      -5.162  -7.802  15.891
ATOM    582 H5'2 Y      19      -6.029  -8.723  14.648
ATOM    583 C4'  Y      19      -5.735  -6.642  14.180
ATOM    584 O4'  Y      19      -4.892  -5.576  14.616
ATOM    585 H4'  Y      19      -6.753  -6.438  14.513
ATOM    586 C3'  Y      19      -5.721  -6.686  12.643
ATOM    587 O3'  Y      19      -6.936  -6.113  12.189
ATOM    588 H3'  Y      19      -5.611  -7.704  12.266
ATOM    589 C2'  Y      19      -4.488  -5.844  12.337
ATOM    590 H2'2 Y      19      -4.541  -5.368  11.363
ATOM    591 H2'1 Y      19      -3.613  -6.489  12.397
ATOM    592 C1'  Y      19      -4.495  -4.830  13.481
ATOM    593 H1'  Y      19      -5.251  -4.068  13.273
ATOM    594 N9   Y      19      -3.185  -4.169  13.710
ATOM    595 C4   Y      19      -3.006  -2.842  14.020
ATOM    596 N3   Y      19      -3.992  -1.928  14.232
ATOM    597 C8   Y      19      -1.917  -4.680  13.578
ATOM    598 H8   Y      19      -1.732  -5.725  13.366
ATOM    599 N7   Y      19      -0.960  -3.805  13.744
ATOM    600 C5   Y      19      -1.648  -2.617  14.048
ATOM    601 C6   Y      19      -1.189  -1.286  14.372
ATOM    602 O6   Y      19      -0.036  -0.863  14.500
ATOM    603 N1   Y      19      -2.216  -0.383  14.573
ATOM    604 H1   Y      19      -1.936   0.556  14.824
ATOM    605 C2   Y      19      -3.544  -0.691  14.494
ATOM    606 N2   Y      19      -4.410   0.300  14.709
ATOM    607 H2   Y      19      -4.023   1.220  14.909
ATOM    608 C3x  Y      19      -5.879   0.155  14.773
ATOM    609 H3x2 Y      19      -6.339   1.031  14.312
ATOM    610 H3x1 Y      19      -6.199  -0.714  14.195
ATOM    611 P    DC     20      -7.400  -6.046  10.647
ATOM    612 O1P  DC     20      -6.253  -6.335   9.761
ATOM    613 O2P  DC     20      -8.677  -6.781  10.497
ATOM    614 O5'  DC     20      -7.685  -4.465  10.567
ATOM    615 C5'  DC     20      -8.654  -3.852  11.415
ATOM    616 H5'1 DC     20      -8.479  -4.153  12.449
ATOM    617 H5'2 DC     20      -9.648  -4.190  11.122
ATOM    618 C4'  DC     20      -8.604  -2.319  11.353
ATOM    619 H4'  DC     20      -9.417  -1.923  11.957
ATOM    620 O4'  DC     20      -7.366  -1.877  11.898
ATOM    621 C1'  DC     20      -6.739  -0.957  11.021
ATOM    622 H1'  DC     20      -6.931   0.068  11.367
ATOM    623 N1   DC     20      -5.277  -1.258  10.987
ATOM    624 C6   DC     20      -4.830  -2.519  10.671
ATOM    625 H6   DC     20      -5.558  -3.307  10.494
ATOM    626 C5   DC     20      -3.499  -2.773  10.596
ATOM    627 H5   DC     20      -3.150  -3.761  10.344
ATOM    628 C4   DC     20      -2.621  -1.697  10.887
ATOM    629 N4   DC     20      -1.337  -1.891  10.903
ATOM    630 H41  DC     20      -0.965  -2.809  10.789
ATOM    631 H42  DC     20      -0.764  -1.099  11.187
ATOM    632 N3   DC     20      -3.020  -0.479  11.163
ATOM    633 C2   DC     20      -4.349  -0.235  11.221
ATOM    634 O2   DC     20      -4.685   0.921  11.453
ATOM    635 C3'  DC     20      -8.732  -1.798   9.913
ATOM    636 H3'  DC     20      -8.813  -2.661   9.251
ATOM    637 C2'  DC     20      -7.383  -1.146   9.644
ATOM    638 H2'1 DC     20      -6.797  -1.828   9.033
ATOM    639 H2'2 DC     20      -7.486  -0.194   9.134
ATOM    640 O3'  DC     20      -9.864  -0.974   9.620
ATOM    641 P    DT     21     -10.229   0.446  10.306
```

```
ATOM    642 O1P  DT     21     -11.582   0.829   9.860
ATOM    643 O2P  DT     21      -9.932   0.374  11.750
ATOM    644 O5'  DT     21      -9.189   1.473   9.633
ATOM    645 C5'  DT     21      -8.826   2.675  10.292
ATOM    646 H5'1 DT     21      -8.525   2.446  11.315
ATOM    647 H5'2 DT     21      -9.692   3.335  10.327
ATOM    648 C4'  DT     21      -7.663   3.399   9.600
ATOM    649 H4'  DT     21      -7.454   4.312  10.160
ATOM    650 O4'  DT     21      -6.503   2.573   9.638
ATOM    651 C1'  DT     21      -5.839   2.749   8.408
ATOM    652 H1'  DT     21      -5.360   3.735   8.415
ATOM    653 N1   DT     21      -4.802   1.704   8.174
ATOM    654 C6   DT     21      -5.104   0.449   7.678
ATOM    655 H6   DT     21      -6.128   0.198   7.461
ATOM    656 C5   DT     21      -4.125  -0.463   7.439
ATOM    657 C7   DT     21      -4.500  -1.827   6.885
ATOM    658 H71  DT     21      -3.901  -2.594   7.377
ATOM    659 H72  DT     21      -5.554  -2.042   7.054
ATOM    660 H73  DT     21      -4.284  -1.852   5.817
ATOM    661 C4   DT     21      -2.725  -0.146   7.722
ATOM    662 O4   DT     21      -1.763  -0.888   7.535
ATOM    663 N3   DT     21      -2.514   1.110   8.233
ATOM    664 H3   DT     21      -1.565   1.416   8.389
ATOM    665 C2   DT     21      -3.472   2.073   8.409
ATOM    666 O2   DT     21      -3.122   3.208   8.704
ATOM    667 C3'  DT     21      -7.911   3.792   8.128
ATOM    668 H3'  DT     21      -8.958   3.659   7.844
ATOM    669 C2'  DT     21      -6.993   2.798   7.413
ATOM    670 H2'1 DT     21      -7.505   1.840   7.344
ATOM    671 H2'2 DT     21      -6.664   3.134   6.434
ATOM    672 O3'  DT     21      -7.485   5.140   7.935
ATOM    673 P    DA     22      -7.801   5.977   6.582
ATOM    674 O1P  DA     22      -9.093   6.661   6.772
ATOM    675 O2P  DA     22      -7.613   5.083   5.421
ATOM    676 O5'  DA     22      -6.622   7.080   6.528
ATOM    677 C5'  DA     22      -5.284   6.741   6.867
ATOM    678 H5'1 DA     22      -5.190   5.654   6.834
ATOM    679 H5'2 DA     22      -5.096   7.044   7.897
ATOM    680 C4'  DA     22      -4.172   7.332   5.970
ATOM    681 H4'  DA     22      -3.892   8.328   6.318
ATOM    682 O4'  DA     22      -3.109   6.396   6.135
ATOM    683 C1'  DA     22      -2.961   5.662   4.930
ATOM    684 H1'  DA     22      -2.119   6.112   4.393
ATOM    685 N9   DA     22      -2.662   4.232   5.150
ATOM    686 C8   DA     22      -3.516   3.152   5.153
ATOM    687 H8   DA     22      -4.592   3.265   5.133
ATOM    688 N7   DA     22      -2.920   1.986   5.170
ATOM    689 C5   DA     22      -1.560   2.345   5.201
ATOM    690 C6   DA     22      -0.338   1.634   5.224
ATOM    691 N6   DA     22      -0.243   0.320   5.259
ATOM    692 H61  DA     22       0.668  -0.112   5.341
ATOM    693 H62  DA     22      -1.087  -0.202   5.426
ATOM    694 N1   DA     22       0.838   2.259   5.231
ATOM    695 C2   DA     22       0.834   3.587   5.232
ATOM    696 H2   DA     22       1.800   4.073   5.239
ATOM    697 N3   DA     22      -0.223   4.386   5.197
ATOM    698 C4   DA     22      -1.398   3.700   5.198
ATOM    699 C3'  DA     22      -4.453   7.357   4.450
ATOM    700 H3'  DA     22      -5.463   7.697   4.213
ATOM    701 C2'  DA     22      -4.241   5.893   4.120
ATOM    702 H2'1 DA     22      -5.083   5.311   4.490
ATOM    703 H2'2 DA     22      -4.087   5.730   3.055
ATOM    704 O3'  DA     22      -3.461   8.030   3.678
ATOM    705 P    DG     23      -3.426   9.610   3.462
ATOM    706 O1P  DG     23      -3.378  10.285   4.774
```

```
ATOM    707 O2P  DG     23      -4.473   9.953   2.478
ATOM    708 O5'  DG     23      -1.982   9.737   2.750
ATOM    709 C5'  DG     23      -0.774   9.814   3.507
ATOM    710 H5'1 DG     23      -0.908   9.293   4.459
ATOM    711 H5'2 DG     23      -0.570  10.861   3.726
ATOM    712 C4'  DG     23       0.457   9.195   2.807
ATOM    713 H4'  DG     23       1.348   9.624   3.258
ATOM    714 O4'  DG     23       0.451   7.798   3.079
ATOM    715 C1'  DG     23       0.991   7.094   1.983
ATOM    716 H1'  DG     23       2.085   7.068   2.053
ATOM    717 N9   DG     23       0.422   5.719   1.974
ATOM    718 C8   DG     23      -0.903   5.353   1.967
ATOM    719 H8   DG     23      -1.698   6.089   2.026
ATOM    720 N7   DG     23      -1.111   4.063   1.881
ATOM    721 C5   DG     23       0.183   3.521   1.902
ATOM    722 C6   DG     23       0.661   2.157   1.878
ATOM    723 O6   DG     23       0.038   1.096   1.839
ATOM    724 N1   DG     23       2.035   2.054   1.882
ATOM    725 H1   DG     23       2.424   1.125   1.930
ATOM    726 C2   DG     23       2.869   3.116   1.919
ATOM    727 N2   DG     23       4.146   2.865   1.897
ATOM    728 H21  DG     23       4.725   3.633   2.178
ATOM    729 H22  DG     23       4.481   1.907   1.998
ATOM    730 N3   DG     23       2.484   4.387   1.912
ATOM    731 C4   DG     23       1.124   4.532   1.934
ATOM    732 C3'  DG     23       0.509   9.357   1.268
ATOM    733 H3'  DG     23      -0.442   9.779   0.945
ATOM    734 C2'  DG     23       0.552   7.913   0.767
ATOM    735 H2'1 DG     23      -0.458   7.630   0.472
ATOM    736 H2'2 DG     23       1.237   7.791  -0.068
ATOM    737 O3'  DG     23       1.520  10.185   0.669
ATOM    738 P    DC3    24       3.123  10.124   0.900
ATOM    739 O1P  DC3    24       3.713  11.196   0.067
ATOM    740 O2P  DC3    24       3.418  10.080   2.339
ATOM    741 O5'  DC3    24       3.612   8.732   0.258
ATOM    742 C5'  DC3    24       3.795   8.604  -1.137
ATOM    743 H5'1 DC3    24       4.536   9.335  -1.466
ATOM    744 H5'2 DC3    24       2.849   8.807  -1.639
ATOM    745 C4'  DC3    24       4.293   7.201  -1.491
ATOM    746 H4'  DC3    24       5.312   7.063  -1.127
ATOM    747 O4'  DC3    24       3.461   6.203  -0.946
ATOM    748 C1'  DC3    24       3.658   5.010  -1.672
ATOM    749 H1'  DC3    24       4.481   4.442  -1.223
ATOM    750 N1   DC3    24       2.417   4.194  -1.629
ATOM    751 C6   DC3    24       1.192   4.759  -1.381
ATOM    752 H6   DC3    24       1.120   5.827  -1.224
ATOM    753 C5   DC3    24       0.092   3.971  -1.280
ATOM    754 H5   DC3    24      -0.866   4.407  -1.045
ATOM    755 C4   DC3    24       0.281   2.572  -1.429
ATOM    756 N4   DC3    24      -0.727   1.775  -1.241
ATOM    757 H41  DC3    24      -1.515   2.134  -0.738
ATOM    758 H42  DC3    24      -0.511   0.781  -1.242
ATOM    759 N3   DC3    24       1.445   2.015  -1.696
ATOM    760 C2   DC3    24       2.529   2.813  -1.797
ATOM    761 O2   DC3    24       3.613   2.281  -2.038
ATOM    762 C3'  DC3    24       4.223   6.951  -3.001
ATOM    763 H3'  DC3    24       3.334   7.443  -3.403
ATOM    764 C2'  DC3    24       4.039   5.438  -3.097
ATOM    765 H2'1 DC3    24       3.250   5.204  -3.814
ATOM    766 H2'2 DC3    24       4.968   4.946  -3.391
ATOM    767 O3'  DC3    24       5.391   7.364  -3.689
ATOM    768 H3T  DC3    24       5.510   8.309  -3.545
TER
END
```

REFERENCES

Arnott, S. and Hukins, D. W. L. (1972) *Biochem.Biophys.Res.Comm., 47*, 1504-1509.

Bashford, D. and Case, D. A. (2000) *Annu Rev Phys Chem, 51*, 129-152.

Basu, A. K., O'Hara, S. M., Valladier, P., Stone, K., Mols, O. and Marnett, L. J. (1988) *Chem Res Toxicol, 1*, 53-59.

Benamira, M., Singh, U. and Marnett, L. J. (1992) *J Biol Chem., 267*, 22392-22400.

Boelens, R., Scheek, R. M., Dijkstra, K. and Kaptein, R. (1985) *J Magn Reson, 62*, 378-386.

Borgias, B. A. and James, T. L. (1990) *J Magn Reson, 87*, 475-487.

Brown, T., Kennard, O., Kneale, G. and Rabinovich, D. (1985) *Nature, 315*, 604-606.

Budiawan and Eder, E. (2000) *Carcinogenesis, 21*, 1191-1196.

Burcham, P. C. and Marnett, L. J. (1994) *J.Biol.Chem., 269*, 28844-28850.

Cajelli, E., Ferraris, A. and Brambilla, G. (1987) *Mutat Res, 190*, 169-171.

Case, D. A., Dardden, T.A., Cheatham III, T.E., Simmerling, C.L., Wang, J., Duke, R.E., Luo, R., Merz, K.M., Wang, B., Pearlman, D.A., Crowley, M. Brozell, S., Tsui, V., Gohlke, H., Mongan, J., Hornak, V., Cui, G., berroza, P., Schafmeister, C., Caldwell, J.W., Ross, W.S., and Kollman, P.A., 2004, AMBER 8,

Chemistry, I.-.-I. U. o. P. a. A. (1998) *Pure Appl. Chem., 70*, 117-142.

Cho, Y.-J., Wang, H., Kozekov, I. D., Kurtz, A. J., Jacob, J., Voehler, M., Smith, J., Harris, T. M., Lloyd, R. S., Rizzo, C. J. and Stone, M. P. (2006) *Chem Res Toxicol, 19*, 195-208.

Cho, Y. J., Kim, H. Y., Huang, H., Slutsky, A., Minko, I. G., Wang, H., Nechev, L. V., Kozekov, I. D., Kozekova, A., Tamura, P., Jacob, J., Voehler, M., Harris, T. M., Lloyd, R. S., Rizzo, C. J. and Stone, M. P. (2005) *J Am Chem Soc, 127*, 17686-17696.

Chung, F.-L., Nath, R. G., Nagao, M., Nishikawa, A., Zhou, G.-d. and Randerath, K. (1999) *Mutat Res, 424*, 71-81.

Chung, F. L., Chen, H. J. and Nath, R. G. (1996) *Carcinogenesis, 17*, 2105-2111.

Chung, F. L. and Hecht, S. S. (1983) *Cancer Res, 43*, 1230-1235.

Chung, F. L., Nath, R. G., Nagao, M., Nishikawa, A., Zhou, G. D. and Randerath, K. (1999) *Mutat Res, 424*, 71-81.

Chung, F. L., Tanaka, T. and Hecht, S. S. (1986) *Cancer Res, 46*, 1285-1289.

Chung, F. L., Young, R. and Hecht, S. S. (1984) *Cancer Res, 44*, 990-995.

Chung, F. L., Zhang, L., Ocando, J. E. and Nath, R. G. (1999) *IARC Sci Publ,* 45-54.

Cohen, S. M., Garland, E. M., St John, M., Okamura, T. and Smith, R. A. (1992 Jul 1) *Cancer Res, 52*, 3577-3581.

Crawford, J. L., Kolpak, F. J., Wang, A. H., Quigley, G. J., van Boom, J. H., van der Marel, G. and Rich, A. (1980) *Proc Natl Acad Sci U S A, 77*, 4016-4020.

Curren, R. D., Yang, L. L., Conklin, P. M., Grafstrom, R. C. and Harris, C. C. (1988) *Mutat Res, 209*, 17-22.

Czerny, C., Eder, E. and Runger, T. M. (1998) *Mutat Res, 407*, 125-134.

De Bont, R. and van Larebeke, N. (2004) *Mutagenesis, 19*, 169-185.

de los Santos, C., Zaliznyak, T. and Johnson, F. (2001) *J Biol Chem, 276*, 9077-9082.

DeCorte, B. L., Tsarouhtsis, D., Kuchimanchi, S., Cooper, M. D., Horton, P., Harris, C. M. and Harris,p T. M. (1996) *Chem.Res.Toxicol., 9*, 630-637.

Dedon, P. C., Plastaras, J. P., Rouzer, C. A. and Marnett, L. J. (1998) *Proc Natl Acad Sci U S A, 95. 95*, 11113-11116.

Delaglio, F., Grzesiek, S., Vuister, G. W., Zhu, G., Pfeifer, J. and Bax, A. (1995) *J Biomol NMR, 6*, 277-293.

Dickopf, S., Alexiev, U., Krebs, M. P., Otto, H., Mollaaghababa, R., Khorana, H. G. and Heyn, M. P. (1995) *Proc Natl Acad Sci U S A, 92*, 11519-11523.

Dooley, P. A., Tsarouhtsis, D., Korbel, G. A., Nechev, L. V., Shearer, J., Zegar, I. S., Harris, C. M., Stone, M. P. and Harris, T. M. (2001) *J Am Chem Soc, 123*, 1730-1739.

Dooley, P. A., Zhang, M., Korbel, G. A., Nechev, L. V., Harris, C. M., Stone, M. P. and Harris, T. M. (2003) *J Am Chem Soc, 125*, 62-72.

Eder, E. and Hoffman, C. (1992) *Chem Res Toxicol, 5*, 802-808.

Eder, E. and Hoffman, C. (1993) *Chem Res Toxicol, 6*, 486-494.

Eder, E., Schuler, D. and Budiawan (1999) *IARC Sci Publ,* 219-232.

Erskine, P. T., Newbold, R., Roper, J., Coker, A., Warren, M. J., Shoolingin-Jordan, P. M., Wood, S. P. and Cooper, J. B. (1999) *Protein Sci, 8*, 1250-1256.

Fernandes, P. H., Kanuri, M., Nechev, L. V., Harris, T. M. and Lloyd, R. S. (2005) *Environ Mol Mutagen, 45*, 455-459.

Foster, P. L., Eisenstadt, E. and Miller, J. H. (1983) *Proc Natl Acad Sci USA, 80*, 2695-2698.

Frisch, M. J., Trucks, G. W., Schlegel, H. B., Scuseria, G. E., Robb, M. A., Cheeseman, J. R., Zakrzewski, V. G., Montgomery, J. A., Stratmann, R. E., Burant, J. C., Dapprich, S., Millam, J. M., Daniels, A. D., Kudin, K. N., Strain, M. C., Farkas, O., Tomasi, J., Barone, V., Cossi, M., Cammi, R., Mennucci, B., Pomelli, C., Adamo, C., Clifford, S., Ochterski, J., Petersson, G. A., Ayala, P. Y., Cui, Q., Morokuma, K., Malick, D. K., Rabuck, A. D., Raghavachari, K., Foresman, J. B., Cioslowski, J., Ortiz, J. V., Stefanov, B. B., Liu, A., Liashenko, A., Piskorz, P., Komaromi, I., Gomperts, R., Martin, R. L., Fox, D. J., Keith, T. A., Al-Lham, M. A., Peng, C. Y., Nanayakkara, A., Gonzalez, C., Challacombe, M., Gill, P. M. W., Johnson, B. G., Chen, W., Wong, M. W., Andres, J. L., Head-Gordon, M., Reploge, E. S. and Pople, J. A., 1998, GAUSSIAN98,

Gao, X. and Patel, D. J. (1988) *J Am Chem Soc, 110*, 5178-5182.

Geacintov, N. E., Cosman, M., Hingerty, B. E., Amin, S., Broyde, S. and Patel, D. J. (1997) *Chem.Res.Toxicol., 10*, 111-146.

Gotfredsen, C. H., Spielmann, H. P., Wengel, J. and Jacobsen, J. P. (1996 Nov-Dec) *Bioconjug Chem, 7. 7*, 680-688.

Hare, D., Shapiro, L. and Patel, D. J. (1986) *Biochemistry, 25*, 7445-7456.

Harris, C. M., Zhou, L., Strand, E. A. and Harris, T. M. (1991) *J.Am.Chem.Soc., 113*, 4328-4329.

Hashim, M. F. and Marnett, L. J. (1996) *J.Biol.Chem., 271*, 9160-9165°.

Hecht, S. S., Upadhyaya, P. and Wang, M. (1999) *IARC Sci Publ,* 147-154.

Hunter, W. N., Brown, T. and Kennard, O. (1986) *J Biomol Struct Dyn, 4*, 173-191.

IARC (1999) *IARC Sci Publ, 71*, 109-125.

Izard, C., Valadaud-Barrieu, D., Fayeulle, J. P. and Testa, A. (1980) *Mutat Res, 77*, 341-344.

Kalnik, M. W., Kouchakdjian, M., Li, B. F. L., Swann, P. F. and Patel, D. J. (1988) *Biochemistry, 27*, 108-115.

Kan, L. S., Chandrasegaran, S., Pulford, S. M. and Miller, P. S. (1983 Jul) *Proc Natl Acad Sci U S A, 80*, 4263-4265.

Kanuri, M., Minko, I. G., Nechev, L. V., Harris, T. M., Harris, C. M. and Lloyd, R. S. (2002) *J Biol Chem, 277*, 18257-18265.

Kastan, M. B. and Bartek, J. (2004) *Nature, 432*, 316-323.

Kawanishi, M., Matsuda, T., Nakayama, A., Takebe, H., Matsui, S. and Yagi, T. (1998) *Mutat Res, 417*, 65-73.

Kawanishi, M., Matsuda, T., Sasaki, G., Yagi, T., Matsui, S. and Takebe, H. (1998) *Carcinogenesis, 19*, 69-72.

Keepers, J. W. and James, T. L. (1984) *J.Magn.Reson., 57*, 404-426.

Kennard, O. (1985) *J.Biomol.Struct.Dyn., 3*, 205-226.

Khullar, S., Varaprasad, C. V. and Johnson, F. (1999) *J Med Chem, 42*, 947-950.

Kim, H.-Y. H., Voehler, M., Harris, T. M. and Stone, M. P. (2002) *J Am Chem Soc, 124*, 9324-9325..

Kim, S. G., Lin, L. J. and Reid, B. R. (1992) *Biochemistry, 31*, 3564-3574.

Kneale, G., Brown, T., Kennard, O. and Rabinovich, D. (1985) *J.Mol.Biol., 186*, 805-814.

Kopka, M. L., Goodsell, D. S., Baikalov, I., Grzeskowiak, K., Cascio, D. and Dickerson, R. E. (1994) *Biochemistry, 33*, 13593-13610.

Kouchakdjian, M., Eisenberg, M., Live, D., Marinelli, E., Grollman, A. P. and Patel, D. J. (1990) *Biochemistry, 29*, 4456-4465.

Kozack, R. E. and Loechler, E. L. (1997 Aug) *Carcinogenesis, 18. 18*, 1585-1593.

Kozekov, I. D., Nechev, L. V., Moseley, M. S., Harris, C. M., Rizzo, C. J., Stone, M. P. and Harris, T. M. (2003) *J Am Chem Soc, 125*, 50-61.

Kozekov, I. D., Nechev, L. V., Sanchez, A., Harris, C. M., Lloyd, R. S. and Harris, T. M. (2001) *Chem Res Toxicol, 14*, 1482-1485.

Kurtz, A. J. and Lloyd, R. S. (2003) *J Biol Chem, 278*, 5970-5976.

Lao, Y. and Hecht, S. S. (2005) *Chem Res Toxicol, 18*, 711-721.

Lindahl, T. (2000) *Mutat Res, 462*, 129-135.

Liu, H., Spielmann, H. P., Ulyanov, N. B., Wemmer, D. E. and James, T. L. (1995) *J Biomol NMR, 6. 6*, 390-402.

Liu, H., Tonelli, M. and James, T. L. (1996) *J Magn Reson Series B, 111*, 85-89.

Liu, Y.-S., Zhao, C., Bergbreter, D. E. and Romo, D. J. (1998) *J. Org. Chem., 63*, 3471-3473.

Longstaff, C. and Rando, R. R. (1987) *Biochemistry, 26*, 6107-6113.

Lu, X. J. and Olson, W. K. (2003) *Nucleic Acids Res, 31*, 5108-5121.

Lukin, M. and de Los Santos, C. (2006) *Chem Rev, 106*, 607-686.

Mao, H., Reddy, G. R., Marnett, L. J. and Stone, M. P. (1999) *Biochemistry 38*, 13491-13501.

Mao, H., Schnetz-Boutaud, N. C., Weisenseel, J. P., Marnett, L. J. and Stone, M. P. (1999) *Proc Natl Acad Sci U S A, 96. 96*, 6615-6620.

Markley, J. L., Bax, A., Arata, Y., Hilbers, C. W., Kaptein, R., Sykes, B. D., Wright, P. E. and Wuthrich, K. (1998) *J Mol Biol, 280*, 933-952.

Marnett, L. J. (1999) *Mutat Res, 424. 424*, 83-95.

Marnett, L. J. (2000) *Carcinogenesis, 21*, 361-370.

Marnett, L. J., Basu, A. K., O'Hara, S. M., Weller, P. E., Rahman, A. F. M. M. and Oliver, J. P. (1986) *J Am Chem Soc, 108*, 1348-1350.

Marnett, L. J., Huird, H. K., Hollstein, M. C., Levin, D. E., Esterbauer, H. and Ames, B. N. (1985) *Mutat Res, 148*, 25.

Marnett, L. J., Riggins, J. N. and West, J. D. (2003) *J Clin Invest, 111*, 583-593.

Minko, I. G., Washington, M. T., Kanuri, M., Prakash, L., Prakash, S. and Lloyd, R. S. (2003) *J Biol Chem, 278*, 784-790.

Mori, S., Abeygunawardana, C., Johnson, M. and vanZul, P. C. M. (1995) *J Magn Reson, 108*, 94-98.

Moriya, M., Zhang, W., Johnson, F. and Grollman, A. P. (1994) *Proc Natl Acad Sci U S A, 91*, 11899-11903.

Mu, D., Bessho, T., Nechev, L. V., Chen, D. J., Harris, T. M., Hearst, J. E. and Sancar, A. (2000) *Mol Cell Biol, 20*, 2446-2454.

Nath, R. G., Chen, H. J., Nishikawa, A., Young-Sciame, R. and Chung, F. L. (1994) *Carcinogenesis, 15*, 979-984.

Nath, R. G. and Chung, F.-L. (1994) *Proc. Natl. Acad. Sci. U.S.A., 91*, 7491-7495.

Nath, R. G., Ocando, J. E. and Chung, F. L. (1996) *Cancer Res, 56*, 452-456.

Nechev, L. V., Harris, C. M. and Harris, T. M. (2000) *Chem Res Toxicol, 13*, 421-429.

Nechev, L. V., Kozekov, I. D., Harris, C. M. and Harris, T. M. (2001) *Chem Res Toxicol, 14*, 1506-1512.

Nechev, L. V., Zhang, M., Tsarouhtsis, D., Tamura, P. J., Wilkinson, A. S., Harris, C. M. and Harris, T. M. (2001) *Chem Res Toxicol, 14*, 379-388.

Nelson, D. L. and Cox, M. M. (2000) *Third Edition*,

Norman, D., Live, D., Sastry, M., Lipman, R., Hingerty, B. E., Tomasz, M., Broyde, S. and Patel, D. J. (1990) *Biochemistry, 29*, 2861-2875.

Oliver, S. G. (1996) *Nature, 379*, 597-600.

Patel, D. J., Kozlowski, S. A., Ikuta, S. and Itakura, K. (1984 Jul 3) *Biochemistry, 23*, 3207-3217.

Patel, D. J., Shapiro, L. and Hare, D. (1987) *Q Rev Biophys., 20*, 35-112.

Piotto, M., Saudek, V. and Sklenar, V. (1992) *J Biomol NMR, 2*, 661-665.

Ramu, K., Fraiser, L. H., Mamiya, B., Ahmed, T. and Kehrer, J. P. (1995) *Chem Res Toxicol, 8*, 515-524.

Reddy, G. R. and Marnett, L. J. (1996) *Chem Res Toxicol., 9*, 12-15.

Refolo, L. M., Bennett, C. B. and Humayun, M. Z. (1987) *J Mol Biol., 193*, 609-636.

Reid, B. R. (1987) *Q Rev Biophys., 20*, 2-28.

Riggins, J. N., Daniels, J. S., Rouzer, C. A. and Marnett, L. J. (2004) *J Am Chem Soc, 126*, 8237-8243.

Riggins, J. N., Pratt, D. A., Voehler, M., Daniels, J. S. and Marnett, L. J. (2004) *J Am Chem Soc, 126*, 10571-10581.

Sako, M., Inagaki, S., Esaka, Y. and Deyashiki, Y. (2003) *Bioorg Med Chem Lett, 13*, 3497-3498.

Sako, M., Yaekura, I. and Deyashiki, Y. (2002) *Nucleic Acids Res Suppl,* 21-22.

Salazar, M., Fedoroff, O. Y., Miller, J. M., Ribeiro, N. S. and Reid, B. R. (1993) *Biochemistry, 32*, 4207-4215.

Sanchez, A., Minko, I., Kurtz, A. J., Kanuri, M., Moriya, M. and Lloyd, R. S. (2003) *Chem Res Toxicol., 16*, 1019-1028.

Schnetz-Boutaud, N. C., Saleh, S., Marnett, L. J. and Stone, M. P. (2001) *Adv Exp Med Biol 500*, 513-516.

Schnetz-Boutaud, N. C., Saleh, S., Marnett, L. J. and Stone, M. P. (2001) *Biochemistry, 40*, 15638-15649.

Seto, H., Okuda, T., Takesue, T. and Ikemura, T. (1983) *Bull Chem Soc Jpn, 56*, 1799-1802.

Seto, H., Seto, T., Takesue, T. and Ikemura, T. (1986) *Chem Pharm Bull, 34*, 5079-5085.

Shetty, H. U. and Nelson, W. L. (1985) *J Pharm Sci, 74*, 968-971.

Sklenar, V., Piotto, M. and Leppik, R. a. S., V. (1993) *J Magn Reson, 102*, 241-245.

Smith, J. A., Bifulco, G., Case, D. A., Boger, D. L., Gomez-Paloma, L. and Chazin, W. J. (2000) *J Mol Biol, 300*, 1195-1204.

Smith, R. A., Cohen, S. M. and Lawson, T. A. (1990) *Carcinogenesis, 11*, 497-498.

Smith, R. A., Williamson, D. S., Cerny, R. L. and Cohen, S. M. (1990) *Cancer Res, 50*, 3005-3012.

Sonar, S., Marti, T., Rath, P., Fischer, W., Coleman, M., Nilsson, A., Khorana, H. G. and Rothschild, K. J. (1994) *J Biol Chem, 269*, 28851-28858.

Stryer, L. (1988) *Third Edition*,

Talluri, S. a. W., G. (1996) *J. of Magnetic Resonance, 112*, 200-205.

Theruvathu, J. A., Jaruga, P., Nath, R. G., Dizdaroglu, M. and Brooks, P. J. (2005) *Nucleic Acids Res, 33*, 3513-3520.

Topal, M. D. and Fresco, J. R. (1976) *Nature, 263*, 285-289.

Treitman, R. D., Burgess, W. A. and Gold, A. (1980) *Am Ind Hyg Assoc J, 41*, 796-802.

Tsui, V. and Case, D. A. (2000) *Biopolymers, 56*, 275-291.

Upthagrove, A. L. and Nelson, W. L. (2001) *Drug Metab Dispos, 29*, 1114-1122.

Van De Ven, F. J. M. and Hilbers, C. W. (1988) *Eur.J.Biochem., 178*, 1-38.

VanderVeen, L. A., Hashim, M. F., Nechev, L. V., Harris, T. M., Harris, C. M. and Marnett, L. J. (2001) *J Biol Chem, 276*, 9066-9070.

VanderVeen, L. A., Hashim, M. F., Shyr, Y. and Marnett, L. J. (2003) *Proc Natl Acad Sci U S A, 100*, 14247-14252.

Velez-Cruz, R., Riggins, J. N., Daniels, J. S., Cai, H., Guengerich, F. P., Marnett, L. J. and Osheroff, N. (2005) *Biochemistry, 44*, 3972-3981.

Wang, M., McIntee, E. J., Cheng, G., Shi, Y., Villalta, P. W. and Hecht, S. S. (2000) *Chem Res Toxicol, 13*, 1149-1157.

Washington, M. T., Minko, I. G., Johnson, R. E., Haracska, L., Harris, T. M., Lloyd, R. S., Prakash, S. and Prakash, L. (2004) *Mol Cell Biol, 24*, 6900-6906.

Washington, M. T., Minko, I. G., Johnson, R. E., Wolfle, W. T., Harris, T. M., Lloyd, R. S., Prakash, S. and Prakash, L. (2004) *Mol Cell Biol, 24*, 5687-5693.

Watson, J. D. and Crick, F. H. (1953) *Nature, 171*, 737-738.

Weisenseel, J. P., Moe, J. G., Reddy, G. R., Marnett, L. J. and Stone, M. P. (1995) *Biochemistry, 34*, 50-64.

Weisenseel, J. P., Reddy, G.R., Marnett, L.J., & Stone, M.P. (2002) *Chem Res Toxicol, 15*, 140-152.

Williams, S. D. and David, S. S. (1998) *Nucleic Acids Res, 26*, 5123-5133.

Wishart, D. S., Bigam, C. G., Yao, J., Abildgaard, F., Dyson, H. J., Oldfield, E., Markley, J. L. and Sykes, B. D. (1995) *J Biomol NMR, 6*, 135-140.

Wolfle, W. T., Johnson, R. E., Minko, I. G., Lloyd, R. S., Prakash, S. and Prakash, L. (2005) *Mol Cell Biol, 25*, 8748-8754.

Yang, I.-Y., Johnson, R., Grollman, A.P., & Moriya, M. (2002) *Chem. Res. Toxicol.. 15*, 160-164.

Yang, I. Y., Chan, G., Miller, H., Huang, Y., Torres, M. C., Johnson, F. and Moriya, M. (2002) *Biochemistry, 41*, 13826-13832.

Yang, I. Y., Hossain, M., Miller, H., Khullar, S., Johnson, F., Grollman, A. and Moriya, M. (2001) *J Biol Chem, 276*, 9071-9076.